

*COBE* Diffuse Infrared Background Experiment (*DIRBE*)  
Explanatory Supplement

edited by M. G. Hauser, T. Kelsall, D. Leisawitz, and J. Weiland  
on behalf of the *COBE* Science Working Group

Version 2.3  
14 January 1998

# Preface

This is a “living document.” In order to expedite delivery of an *Explanatory Supplement* that describes the *DIRBE* data products, most of Chapter 4 (Data Processing and Instrument Characterization) was omitted from the present version. The complete *Explanatory Supplement* will be released as soon as possible. A current version of the document will be kept on line at the National Space Science Data Center and may be obtained either by anonymous ftp to `nssdca.gsfc.nasa.gov` in the “cobe” directory or from the *COBE* Home Page at [http://www.gsfc.nasa.gov/astro/cobe/cobe\\_home.html](http://www.gsfc.nasa.gov/astro/cobe/cobe_home.html) on the World Wide Web.

*DIRBE* team members who contributed to the preparation of this document include R. G. Arendt, G. B. Berriman, B. A. Franz, H. T. Freudenreich, C. M. Lisse, K. J. Mitchell, P. M. Mitra, S. H. Moseley, J. S. Newmark, N. P. Odegard, G. L. Rawley, W. T. Reach, R. F. Silverberg, J. A. J. Skard, S. W. Stenwedel, and G. N. Toller.

This document is to be referenced as:

*COBE Diffuse Infrared Background Experiment (DIRBE) Explanatory Supplement*,  
version 2.3,  
ed. M. G. Hauser, T. Kelsall, D. Leisawitz, and J. Weiland,  
COBE Ref. Pub. No. 98-A (Greenbelt, MD: NASA/GSFC),  
available in electronic form from the NSSDC.



# Contributors to *DIRBE*

*This section is in preparation.*



# Contents

<b>Preface</b>	<b>i</b>
<b>Contributors to <i>DIRBE</i></b>	<b>iii</b>
<b>1 Introduction</b>	<b>1</b>
1.1 The Experiment: Objectives and Approach . . . . .	1
1.2 The Explanatory Supplement . . . . .	1
1.3 Overview of Data Products . . . . .	2
<b>2 The <i>DIRBE</i> Instrument</b>	<b>11</b>
2.1 Design Goals . . . . .	11
2.2 Instrument Description . . . . .	11
2.2.1 Optics and Baffling . . . . .	12
2.2.2 Detector Assemblies . . . . .	13
2.2.3 Thermal Control . . . . .	14
2.2.4 Calibration . . . . .	16
2.2.5 Electronics . . . . .	16
2.2.6 <i>DIRBE</i> Operating Modes . . . . .	18
2.3 The Instrument in Context: the <i>COBE</i> Satellite . . . . .	19
2.3.1 Mission Concept . . . . .	19
2.3.2 The Orbit . . . . .	20
2.3.3 Attitude Control . . . . .	22
2.3.4 Sky Scan Strategy . . . . .	23
2.3.5 Power . . . . .	23
2.3.6 Communication . . . . .	26
2.3.7 The Dewar . . . . .	26
2.3.8 The Sun–Earth Shield . . . . .	26
<b>3 Flight Operations</b>	<b>27</b>
3.1 Overview . . . . .	27
3.1.1 Mission Overview . . . . .	27
3.1.2 <i>DIRBE</i> Sky Coverage . . . . .	28
3.2 <i>DIRBE</i> Operations . . . . .	31
3.2.1 Launch to End of Cryogen . . . . .	31
3.2.2 End of Cryogen to End of Mission . . . . .	32
3.3 <i>DIRBE</i> Characterization and Monitoring Tests . . . . .	32
3.3.1 Daily Events . . . . .	32
3.3.2 Special On-orbit Tests . . . . .	32
3.4 Anticipated Environmental Influences . . . . .	35
3.4.1 Nuclear Radiation Effects on Detectors . . . . .	35
3.4.2 Photon-induced Responsivity Enhancement . . . . .	35
3.4.3 Thermal Changes Within the Dewar . . . . .	35
3.4.4 Thermal Changes External to the Dewar . . . . .	35

3.4.5	Atmospheric Glow . . . . .	36
3.5	<i>DIRBE</i> Malfunctions and <i>COBE</i> Influences . . . . .	36
3.5.1	Band 8 Annealing Heater . . . . .	36
3.5.2	Primary IRS . . . . .	36
3.5.3	<i>FIRAS</i> Influences . . . . .	36
<b>4</b>	<b>Data Processing and Instrument Characterization</b> . . . . .	<b>39</b>
4.1	Overview of Data Processing . . . . .	40
4.2	Beam Profile . . . . .	40
4.2.1	Shape . . . . .	40
4.2.2	Centroids . . . . .	40
4.2.3	Solid Angles . . . . .	41
4.3	Attitude Determination . . . . .	41
4.4	Stray Light Rejection . . . . .	41
4.4.1	Near Field . . . . .	41
4.4.2	Far Field . . . . .	41
4.5	Photometry . . . . .	41
4.5.1	The <i>DIRBE</i> Signal Equation . . . . .	41
4.5.2	Offsets . . . . .	41
4.5.3	Gain . . . . .	41
4.5.4	Photometric Calibration Uncertainty . . . . .	41
4.5.5	Sensitivity . . . . .	41
4.5.6	Comparison of <i>DIRBE</i> and <i>FIRAS</i> Calibration . . . . .	41
4.5.7	Comparison of <i>DIRBE</i> and <i>IRAS</i> Calibration . . . . .	41
4.6	Polarimetry . . . . .	41
4.6.1	Method . . . . .	41
4.6.2	Calibration . . . . .	41
4.6.3	Accuracy . . . . .	41
4.7	Exclusion of Low Quality Data . . . . .	42
4.7.1	Pre-optimization Data . . . . .	42
4.7.2	Bright Source Exclusion Zones . . . . .	42
4.7.3	Recovery from Moon Passages . . . . .	42
4.7.4	SAA Passages . . . . .	42
4.7.5	Unusually Noisy Data . . . . .	42
4.7.6	Special Pointing . . . . .	42
4.7.7	Focal Plane Temperature Constraints . . . . .	42
4.7.8	<i>FIRAS</i> Calibrations . . . . .	42
4.7.9	Robust Averaging . . . . .	42
4.8	Known Processing Deficiencies . . . . .	42
4.8.1	AC <i>vs.</i> DC Calibration at 60 and 100 $\mu\text{m}$ . . . . .	42
4.8.2	DC Linearity Uncertainties at 60 and 100 $\mu\text{m}$ . . . . .	42
4.8.3	Limitations of PIRE Correction . . . . .	42
4.8.4	Long-term Photometric Variations . . . . .	42
<b>5</b>	<b><i>DIRBE</i> Data Products</b> . . . . .	<b>45</b>
5.1	Overview . . . . .	45
5.2	Creation of <i>DIRBE</i> Data Products . . . . .	47
5.2.1	Initial Pipeline Processing Stages . . . . .	47
5.2.2	Creation of Calibrated Individual Observations . . . . .	47
5.2.3	Creation of Weekly Sky Maps . . . . .	47
5.2.4	Creation of <i>DIRBE</i> Calibrated Annual File . . . . .	48
5.2.5	Creation of Annual Average Sky Maps . . . . .	48
5.2.6	Creation of $\varepsilon = 90^\circ$ Sky Maps . . . . .	48
5.2.7	Creation of the Galactic Plane Maps . . . . .	50

5.2.8	Creation of <i>DIRBE</i> Sky and Zodi Atlas (DSZA)	51
5.2.9	Creation of Zodi-Subtracted Mission Average (ZSMA) Maps	51
5.3	Pixelization and the Quadrilateralized Spherical Cube Projection	51
5.3.1	Description of the File <i>DIRBE_SKYMAP_INFO.FITS</i>	52
5.4	Data Product Formats	58
5.4.1	FITS Binary Table Extension	58
5.4.2	FITS Image Format	58
5.4.3	Native Binary Format	58
5.4.4	ASCII	58
5.5	Color Corrections	58
5.6	Data Limitations	59
5.6.1	Photometric and Temporal Discontinuities in the Galactic Plane Maps	59
5.6.2	Exclusion of Solar System Objects: Gaps in Sky Coverage	59
5.6.3	Extrapolated Values	59
5.6.4	Regions Where the Statistical Noise is Relatively High	60
5.6.5	Negative Intensities at 140 $\mu\text{m}$ and 240 $\mu\text{m}$	60
5.6.6	Point Source Photometry from the Maps	60
5.6.7	Annual Average Sky Maps	61
5.6.8	4.9 $\mu\text{m}$ Data Excluded from Maps	61
5.6.9	JFET-off Test Periods	61
5.7	The Project Data Sets	61
5.7.1	Time-ordered Data	61
5.7.2	Calibrated Individual Observations and Associated Pixel Index Files	67
5.7.3	Weekly Sky Maps	72
5.7.4	<i>DIRBE</i> Calibrated Annual File and Associated Pixel Index File	74
5.7.5	$\varepsilon = 90^\circ$ Sky Maps	75
5.7.6	Galactic Plane Maps ( $\varepsilon = 90^\circ$ )	76
5.7.7	Annual Average Sky Maps	78
5.8	The Analyzed Science Data Sets	78
5.8.1	<i>DIRBE</i> Sky and Zodi Atlas and associated Pixel Index File	78
5.8.2	Zodi-Subtracted Mission Average Maps (ZSMA)	78
5.8.3	Photometric Standard Values Table	79
5.8.4	Solar System Object Data	86
5.8.5	Faint Source Model (FSM)	87
5.9	Ancillary Data Sets	87
5.9.1	Beam Profile Maps	87
5.9.2	Spectral Response Functions	87
5.9.3	Color Correction Tables	87
<b>6</b>	<b>References</b>	<b>91</b>
<b>A</b>	<b><i>DIRBE</i> System Spectral Response</b>	<b>93</b>
<b>B</b>	<b>Color Correction Tables</b>	<b>113</b>
<b>C</b>	<b><i>DIRBE</i> Cold Mission Events Log</b>	<b>125</b>
<b>D</b>	<b>Data Retrieval</b>	<b>131</b>
D.1	Reading the FITS Data	131
D.1.1	FITS Headers for the <i>DIRBE</i> Data Products	131
D.1.2	FORTRAN Access to the <i>DIRBE</i> Data Products	171
D.1.3	IDL Access to the <i>DIRBE</i> Data Products	189
D.2	Sample Data Plots and Dumps	190
<b>E</b>	<b>Acronyms Used in this Document</b>	<b>193</b>



<b>F</b>	<b>The Faint Source Model</b>	<b>197</b>
F.1	Introduction . . . . .	197
F.2	Calibration . . . . .	198
F.3	Verification . . . . .	198
F.4	Comparison with the <i>DIRBE</i> Data . . . . .	199
F.5	Warnings . . . . .	199
F.6	References . . . . .	199
<b>G</b>	<b>Related <i>COBE</i> Publications</b>	<b>201</b>
G.1	1982 . . . . .	201
G.2	1983 . . . . .	201
G.3	1984 . . . . .	201
G.4	1986 . . . . .	201
G.5	1987 . . . . .	202
G.6	1990 . . . . .	202
G.7	1991 . . . . .	202
G.8	1992 . . . . .	204
G.9	1993 . . . . .	204
G.10	1994 . . . . .	206
G.11	1995 . . . . .	206
G.12	1996 . . . . .	207
G.13	1997 . . . . .	208

# List of Tables

1.3-1 Intensity ranges for Figures 1.3-4–1.3-6 . . . . .	10
2.2-1 Instrument characteristics . . . . .	11
2.2-2 Detector and filter characteristics . . . . .	13
3.1-1 <i>COBE</i> spacecraft and orbital characteristics . . . . .	27
3.1-2 Weekly sky coverage . . . . .	30
3.2-1 Nominal detector operating parameters: cryogenic era . . . . .	31
3.3-1 Non-survey daily operations . . . . .	33
4.2-1 Beam centroids and solid angles . . . . .	40
4.7-1 Interpretation of Sentinel Values . . . . .	43
5.1-1 <i>DIRBE</i> data products . . . . .	46
5.6-1 Photometric discontinuities at $\ell \simeq 102^\circ$ . . . . .	59
5.6-2 <i>FIRAS</i> external calibration times . . . . .	62
5.7-1 Time-Ordered Data files . . . . .	63
5.7-2 Key fields in the Time-Ordered Data record . . . . .	64
5.7-3 Polarization coefficients . . . . .	67
5.7-4 Columns in the Calibrated Individual Observations FITS tables . . . . .	69
5.7-5 Columns in the CIO Pixel Index FITS tables . . . . .	70
5.7-6 Offset corrections for Attack Vectors in CIO files . . . . .	70
5.7-7 Columns in the Weekly Sky Map FITS tables . . . . .	73
5.7-8 Offset values for Weekly Sky Map fields . . . . .	74
5.7-9 Ecliptic coordinate ranges covered by CSC cube faces . . . . .	75
5.7-10 Columns in the DCAF Pixel Index FITS tables . . . . .	75
5.7-11 Columns in the $\varepsilon = 90^\circ$ Sky Map FITS tables . . . . .	76
5.7-12 Columns in the Galactic Plane Maps FITS table . . . . .	77
5.7-13 Offset values for Galactic Plane Map coordinates <sup>a</sup> . . . . .	78
5.7-14 Columns in the Annual Average Sky Map FITS tables . . . . .	79
5.8-1 Columns in the <i>DIRBE</i> Sky and Zodi Atlas . . . . .	80
5.8-2 Columns in the Zodi-Subtracted Mission Average Maps . . . . .	81
5.8-3 Columns in the Photometric Standard Values Table . . . . .	85
5.8-4 Solar System Object Detection Thresholds . . . . .	86
5.8-5 Contents of Solar System Object Dataset . . . . .	88
5.8-6 Orbital elements used to calculate asteroid ephemerides . . . . .	89
5.8-7 Columns in the Faint Source Model FITS tables . . . . .	89
A.0-1 Normalized system responses for the 10 <i>DIRBE</i> bands . . . . .	94
B.0-1 Color correction factors for power law spectra of the form $I_\nu \propto \nu^n$ . . . . .	113
B.0-2 Color correction factors for spectra of the form $I_\nu \propto B_\nu(T)$ . . . . .	114
B.0-3 Color correction factors for spectra of the form $I_\nu \propto \nu^{0.5} B_\nu(T)$ . . . . .	116
B.0-4 Color correction factors for spectra of the form $I_\nu \propto \nu B_\nu(T)$ . . . . .	118

B.0-5	Color correction factors for spectra of the form $I_\nu \propto \nu^{1.5} B_\nu(T)$ . . . . .	120
B.0-6	Color correction factors for spectra of the form $I_\nu \propto \nu^2 B_\nu(T)$ . . . . .	122
C.0-1	Abridged on-orbit events log . . . . .	126
D.1-1	Sample FITS headers for the Calibrated Individual Observations Pixel Index files . . . . .	131
D.1-2	Sample FITS headers for the Calibrated Individual Observations data files . . . . .	133
D.1-3	Sample FITS headers for the <i>DIRBE</i> Calibrated Annual File Index files . . . . .	142
D.1-4	Sample FITS headers for the <i>DIRBE</i> Calibrated Annual File . . . . .	144
D.1-5	Sample Weekly Sky Map FITS header . . . . .	151
D.1-6	Sample $\varepsilon = 90^\circ$ Sky Map FITS header . . . . .	158
D.1-7	The Galactic Plane Maps FITS header . . . . .	162
D.1-8	Sample Annual Average Sky Map FITS header . . . . .	166
D.1-9	Sample Beam Profile FITS header . . . . .	169
D.2-1	Data for pixel 42 in the Galactic Plane Maps . . . . .	190
D.2-2	Data for pixel 42 in Weekly Sky Map 22 . . . . .	191
D.2-3	Data for pixel 42 in the Annual Average Sky Maps . . . . .	191
D.2-4	Data for pixel 42 in the Solar Elongation = $90^\circ$ Sky Maps . . . . .	191
E.0-1	Acronyms . . . . .	194
F.1-1	Faint Source Model Parameters . . . . .	198

# List of Figures

1.3-1 Weekly Sky Map mosaics at $3.5 \mu\text{m}$ . . . . .	3
1.3-2 Weekly Sky Map mosaics at $25 \mu\text{m}$ . . . . .	4
1.3-3 Weekly Sky Map mosaics at $100 \mu\text{m}$ . . . . .	5
1.3-4 Solar elongation = $90^\circ$ Sky Maps at $1.25, 2.2,$ and $3.5 \mu\text{m}$ . . . . .	6
1.3-5 Solar elongation = $90^\circ$ Sky Maps at $4.9, 12, 25,$ and $60 \mu\text{m}$ . . . . .	7
1.3-6 Solar elongation = $90^\circ$ Sky Maps at $100, 140,$ and $240 \mu\text{m}$ . . . . .	8
1.3-7 Comparison of $240 \mu\text{m}$ Solar elongation = $90^\circ$ and Annual Average Sky Maps . . . . .	9
2.2-1 Optics diagram of <i>DIRBE</i> . . . . .	12
2.2-2 Normalized system spectral response . . . . .	15
2.2-3 Electronics block diagram of <i>DIRBE</i> . . . . .	17
2.3-1 Artist cutaway drawing of <i>COBE</i> . . . . .	20
2.3-2 Schematic drawing of <i>COBE</i> in orbit . . . . .	21
2.3-3 Schematic drawing of <i>COBE</i> instrument viewing directions . . . . .	22
2.3-4 <i>DIRBE</i> sky coverage in one orbit . . . . .	24
2.3-5 Sky coverage after various time intervals . . . . .	25
3.1-1 Depth of survey coverage in a typical week and for the whole cryogenic mission . . . . .	29
4.7-1 Glitch counts at $100\mu\text{m}$ as a function of satellite position . . . . .	42
5.2-1 $I_\nu$ vs. $(90/\varepsilon - 1)$ for <i>DIRBE</i> pixel number 247071 . . . . .	49
5.3-1 Internal storage of data using the CSC . . . . .	53
5.3-2 <i>DIRBE</i> pixel numbering scheme . . . . .	54
5.8-1 Calibrator flux density histograms . . . . .	82
5.8-2 Calibrator positions in Galactic coordinates . . . . .	83
5.8-3 Calibrator positions in geocentric ecliptic coordinates . . . . .	84
D.2-1A slice through the $25 \mu\text{m}$ $\varepsilon = 90^\circ$ Sky Map . . . . .	192



# Chapter 1

## Introduction

### 1.1 The Experiment: Objectives and Approach

The Diffuse Infrared Background Experiment (*DIRBE*), one of three instruments aboard the Cosmic Background Explorer (*COBE*) satellite, was designed primarily to search for the isotropic cosmic infrared background (CIB) radiation expected to arise from the cumulative emissions of early luminous objects, and to measure the energy distribution of that radiation. This objective was achieved: the CIB was detected at 140 and 240  $\mu\text{m}$  and limits were placed on the CIB brightness over the spectral range 1–100  $\mu\text{m}$  (Hauser *et al.* 1998). Secondary objectives included studies of foreground astrophysical sources arising in the solar system and Milky Way Galaxy. The observational approach was to make absolute brightness maps of the full sky at 10 wavelengths (1.25, 2.2, 3.5, 4.9, 12, 25, 60, 100, 140, and 240  $\mu\text{m}$ ), and to map linear polarization at 1.25, 2.2, and 3.5  $\mu\text{m}$ .

The *DIRBE* instrument operated at cryogenic temperatures for 10 months, from 1989 November 24 to 1990 September 21, mapping the full sky with high redundancy during the first six months, and covering most of the sky with similar redundancy during the final four months. The data products described in this *Explanatory Supplement* are based upon the high quality data acquired during the cryogenic period.

A more complete description of the *COBE* mission has been given by Boggess *et al.* (1992).

### 1.2 The Explanatory Supplement

This document is intended to provide a complete, self-contained description of the *DIRBE* experiment and the products of the *DIRBE* sky survey. The instrument, its calibration, electronics, operating modes, and context within the *COBE* satellite are described in Chapter 2. Flight operations, instrument monitoring tests, anticipated and actual environmental influences, and malfunctions are described in Chapter 3. Chapter 4 discusses attitude determination and data processing, calibration and quality assurance. Some known processing deficiencies were allowed; these are described at the end of Chapter 4. The *DIRBE* data products, their intended use, formats, and limitations, are given in Chapter 5. Chapter 6 lists the references cited in this document; Appendix G contains a bibliography of related *COBE* publications. The *DIRBE* System Spectral Response is tabulated in Appendix A. Appendix B contains Color Correction Tables. Appendix C gives a chronology of events that took place during the cryogenic mission. Appendix D provides information about data retrieval. Appendix E is a list of acronyms. The *DIRBE* Faint Source Model, which was used by Arendt *et al.* (1998) to subtract stellar emission from the *DIRBE* sky maps as part of the search for the cosmic infrared background, is described in Appendix F; the model is available as a data product.

This version of the *DIRBE Explanatory Supplement* supersedes the version released with the Galactic Plane Maps on July 19, 1993 and version 2.0, which was released on May 4, 1995. The next version will describe additional data products and is likely to be released in mid-1997.

### 1.3 Overview of Data Products

Data from the *DIRBE* sky survey are available in time-ordered and sky map formats. Most of the data products give the sky brightness as observed, including the zodiacal and Galactic components. Some, however, include estimates of the zodiacal light intensity or give residual intensity after zodiacal light subtraction. The data products are described in detail in Chapter 5.

The **Time-Ordered Data (TOD)** product includes calibrated sky brightness values and is the most complete archival record of the *DIRBE* observations. It is necessary to understand the operating modes of the instrument and to recognize various mission events in order to select and interpret the data of interest. The TOD product is not intended for heavy use by the research community. In those rare instances in which individual time-ordered data are needed (*e.g.*, to obtain definitive *DIRBE* point source flux values), the **Calibrated Individual Observations (CIO)** product should be used instead of the TOD. It is expected, however, that one or more of the sky map data products will suffice in most applications.

The maps are distinguished by the time interval over which multiple observations of a single celestial position are coadded. All of the sky maps are presented in FITS binary tables, in which the first column – the independent variable – is pixel number <sup>1</sup>. The following sky map products are available:

**Weekly Sky Maps** provide weekly-averaged intensity values for each pixel and photometric band, plus Stokes Q and U parameters at 1.25, 2.2 and 3.5  $\mu\text{m}$ , for the period of optimized cryogenic operation, 1989 December 11 to 1990 September 21. Each map covers approximately half of the sky. As a set, the 41 Weekly Sky Maps offer an unprecedented view of the interplanetary dust (IPD) cloud, since each celestial direction was observed by the *DIRBE* along a variety of paths through the cloud. The variable zodiacal light signature can be seen in Figures 1.3-1–1.3-3 and is especially pronounced at 25  $\mu\text{m}$  (Figure 1.3-2) where the emission peaks.

**Annual Average Sky Maps** provide a single, ten-month averaged intensity value per pixel for each of the 10 *DIRBE* bands. The effect of coaddition is to improve sensitivity to faint emission. Since these maps average over the variable zodiacal light signal, they are useful primarily at wavelengths at which the IPD signature is weak, particularly 140 and 240  $\mu\text{m}$ . The Annual Average Sky Maps also provide information on the depth of sky coverage over the mission. In many applications, the **Zodi-Subtracted Mission Average (ZSMA) Maps** will supersede the Annual Average Sky Maps.

**Solar Elongation ( $\varepsilon$ ) = 90° Sky Maps** provide an estimate of the infrared intensity for each wavelength at each pixel based on an interpolation of the observations made at various times at  $\varepsilon$  close to 90°. This is the only fixed elongation angle at which the entire sky can be mapped.

**Galactic Plane Maps** are subsets of the  $\varepsilon = 90^\circ$  Sky Maps designed to facilitate studies of the Galaxy. The maps cover Galactic latitudes  $|b| < 10^\circ$  at longitudes  $30^\circ < \ell < 330^\circ$ , and cover  $|b| < 15^\circ$  elsewhere.

Figures 1.3-4–1.3-6 show Mollweide projections, in Galactic coordinates, of the  $\varepsilon = 90^\circ$  Sky Maps for all 10 *DIRBE* intensity bands. The intensity scales are logarithmic and range from the minima (black) to the maxima (white) listed in Table 1.3-1. Zodiacal emission is evident at wavelengths ranging from 4.9 to 100  $\mu\text{m}$  (an ‘S’ pattern is made by the ecliptic plane). The Galactic stellar component is clearly visible in the near-infrared (1.25 – 4.9  $\mu\text{m}$ ), and interstellar dust emission is prominent at  $\lambda \geq 60 \mu\text{m}$ .

To illustrate the better sensitivity available when the data are coadded, the 240  $\mu\text{m}$  Annual Average Sky Map is compared with the 240  $\mu\text{m}$   $\varepsilon = 90^\circ$  Sky Map in Figure 1.3-7.

The *DIRBE* **Calibrated Annual File (DCAF)**, a reorganized form of the Weekly Sky Maps, provides convenient access to the weekly-averaged intensities seen in individual pixels as a function of time, facilitating studies of the zodiacal light.

---

<sup>1</sup>The *DIRBE* convention is to represent the sky as a quadrilateralized spherical cube (see §5.3) in which each cube face ( $4\pi/6$  sr) is divided into  $256 \times 256$  pixels of approximately equal area. The area is equivalent to a square  $0^\circ.32$  on a side. The *DIRBE* beam (instantaneous field of view) is a square  $0^\circ.7$  on a side.

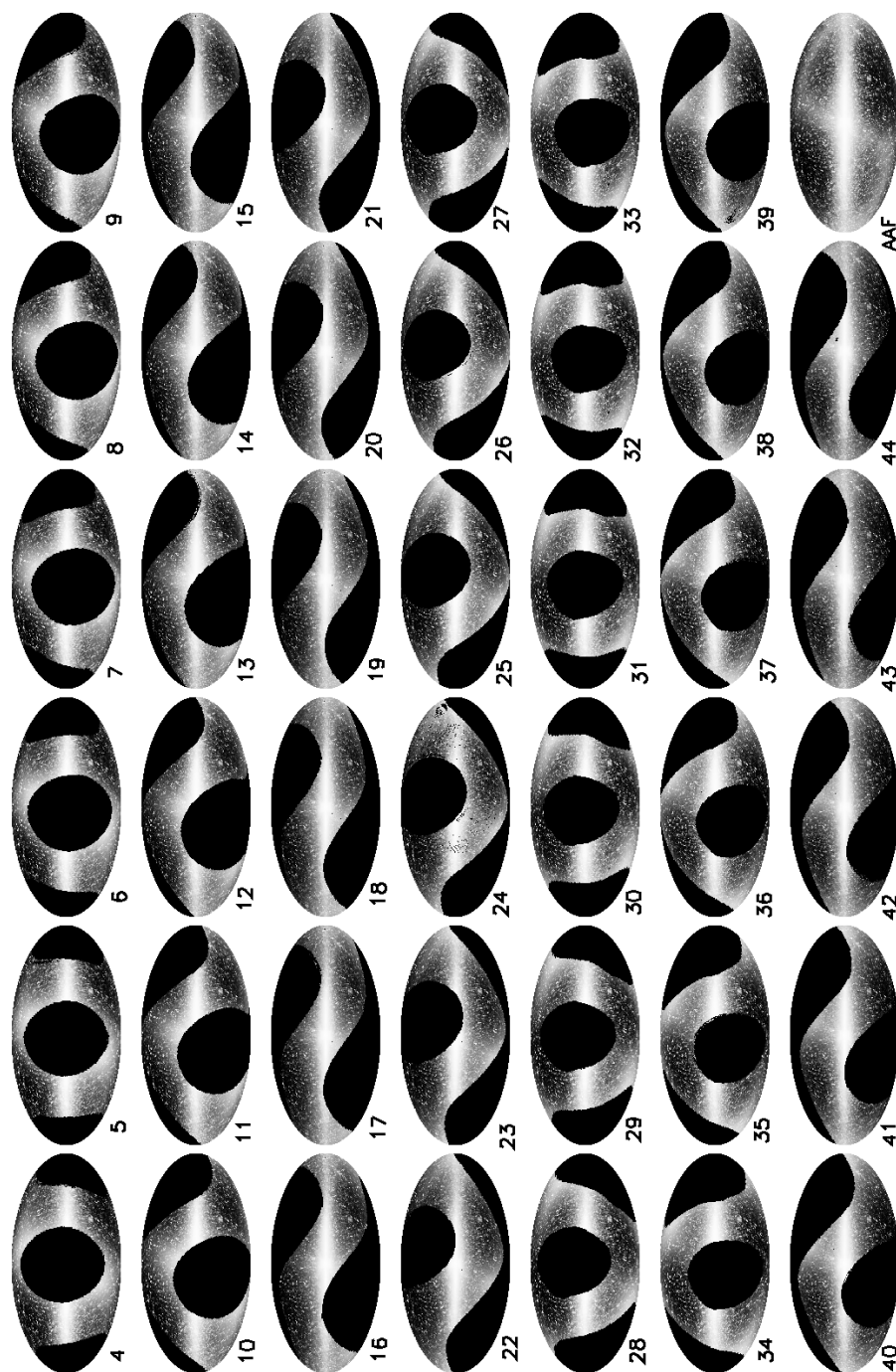


Figure 1.3-1: Weekly Sky Map mosaics at  $3.5 \mu\text{m}$ . Each map is an all-sky Mollweide projection in Galactic coordinates with the Galactic center in the middle. Maps are labeled by mission week number beginning 1989 November 18 (*e.g.*, map 4 shows data from 1989 December 11 – December 17). The map labeled AAF is the Annual Average Sky Map.



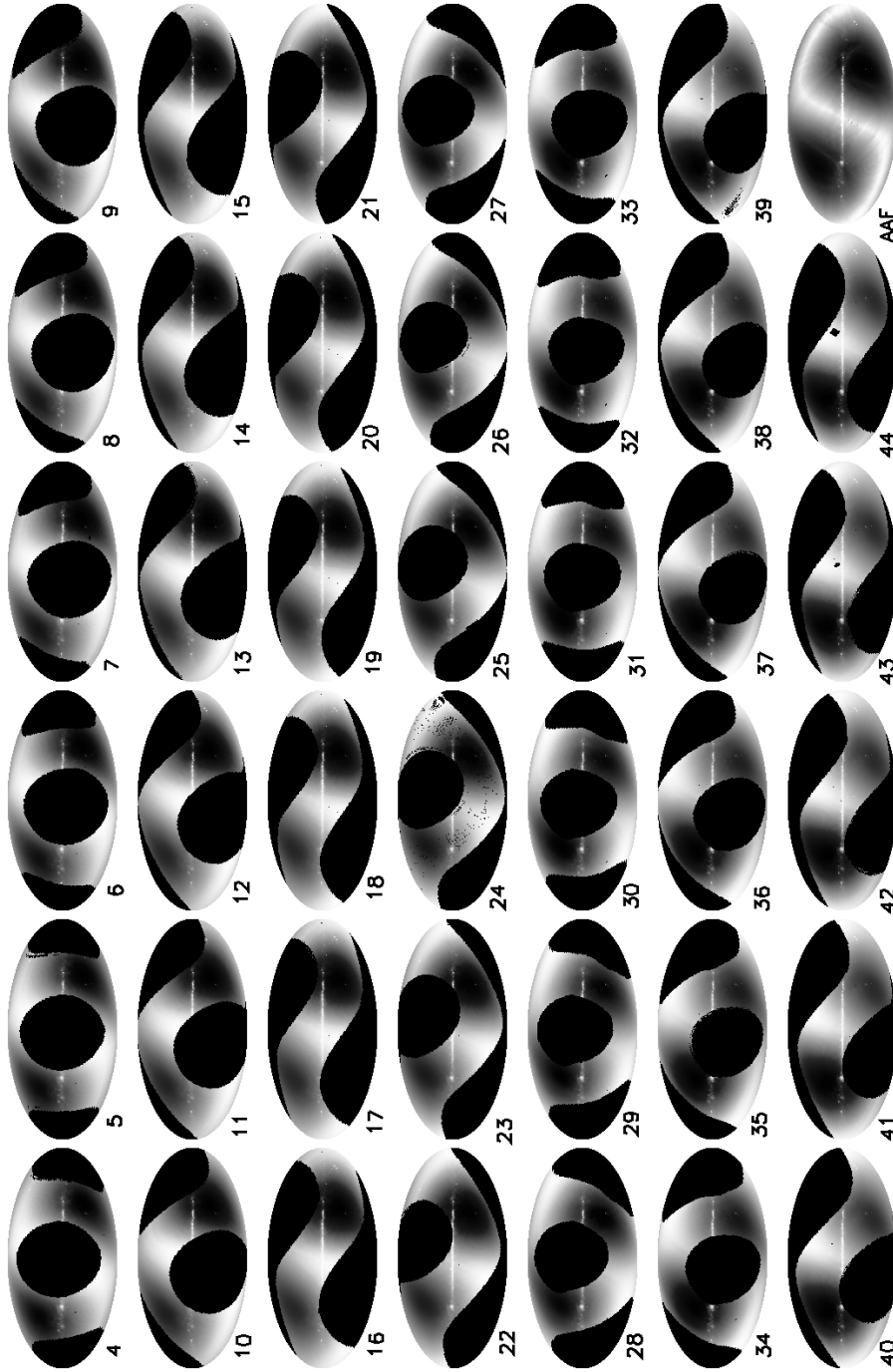


Figure 1.3-2: Same as Fig. 1.3-1 except at  $25 \mu\text{m}$ .

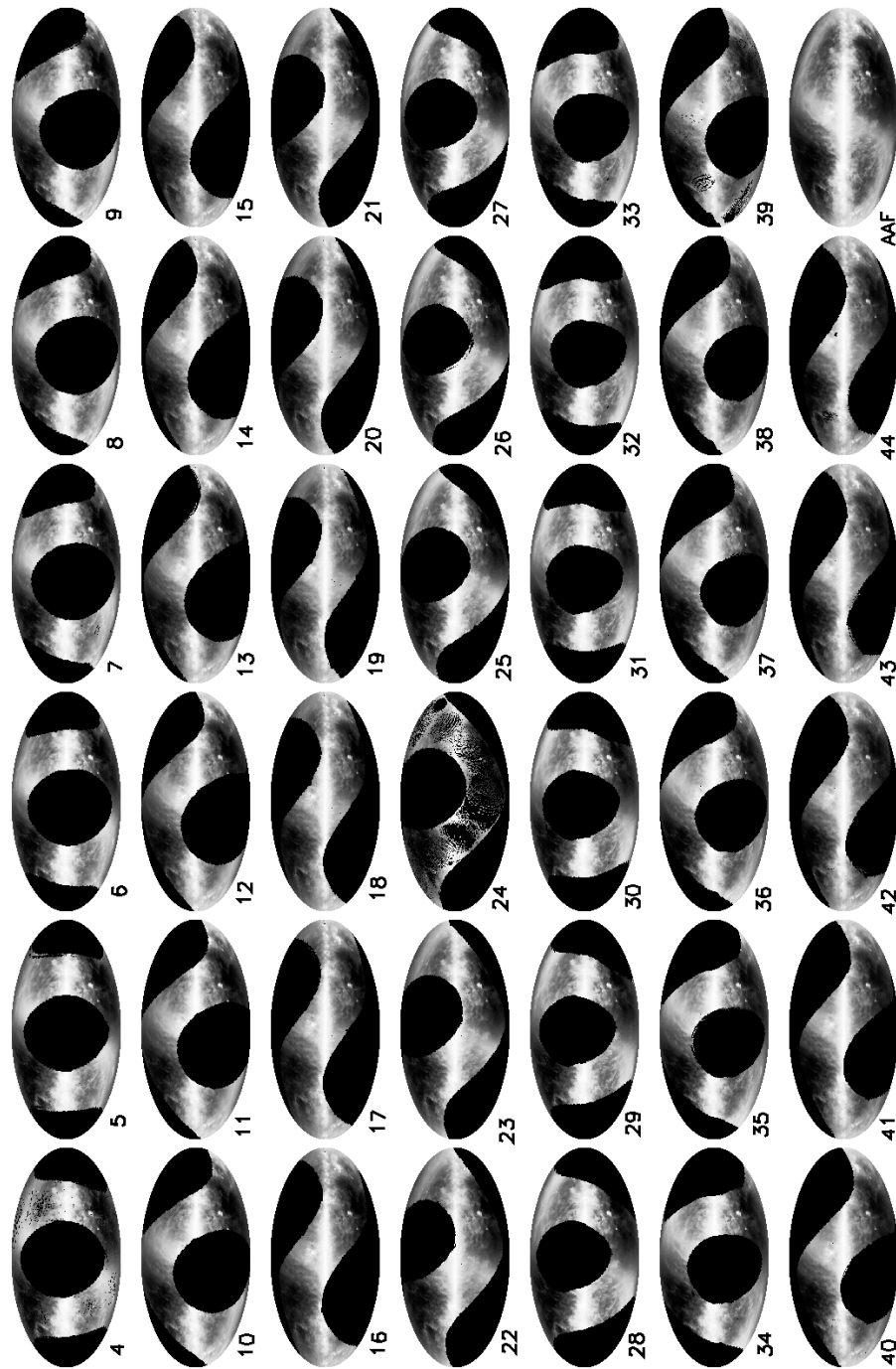


Figure 1.3-3: Same as Fig. 1.3-1 except at 100  $\mu\text{m}$ .

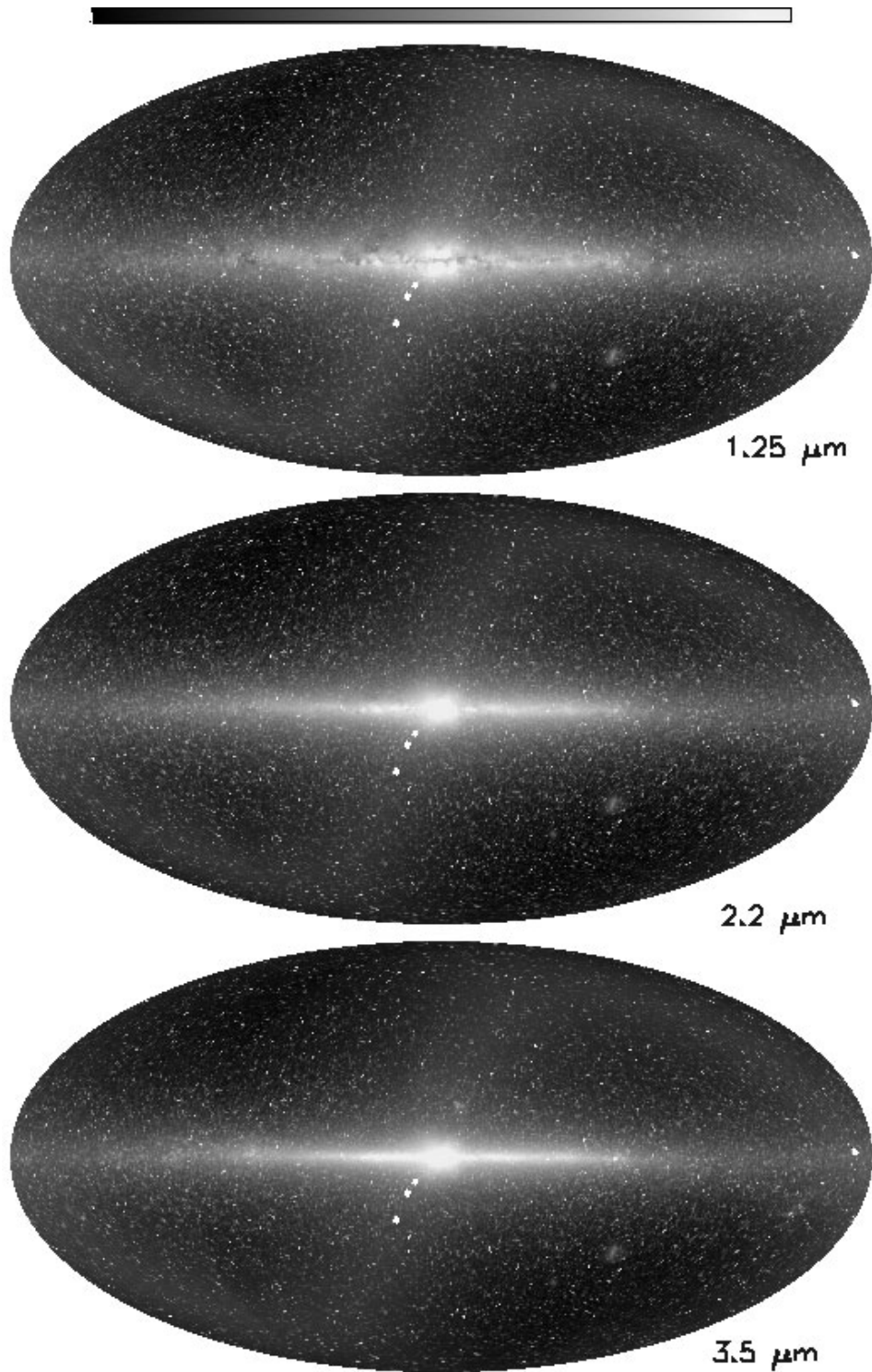


Figure 1.3-4: Solar elongation =  $90^\circ$  Sky Maps at  $1.25$ ,  $2.2$ , and  $3.5 \mu\text{m}$ . Each map is a Mollweide projection in Galactic coordinates with the Galactic center in the middle. Holes in the maps in the ecliptic plane (south of the Galactic center and near the Galactic anti-center) are due to exclusion of data near bright planets (see §5.6.2). The wavelength-dependent intensity scale is given in Table 1.3-1

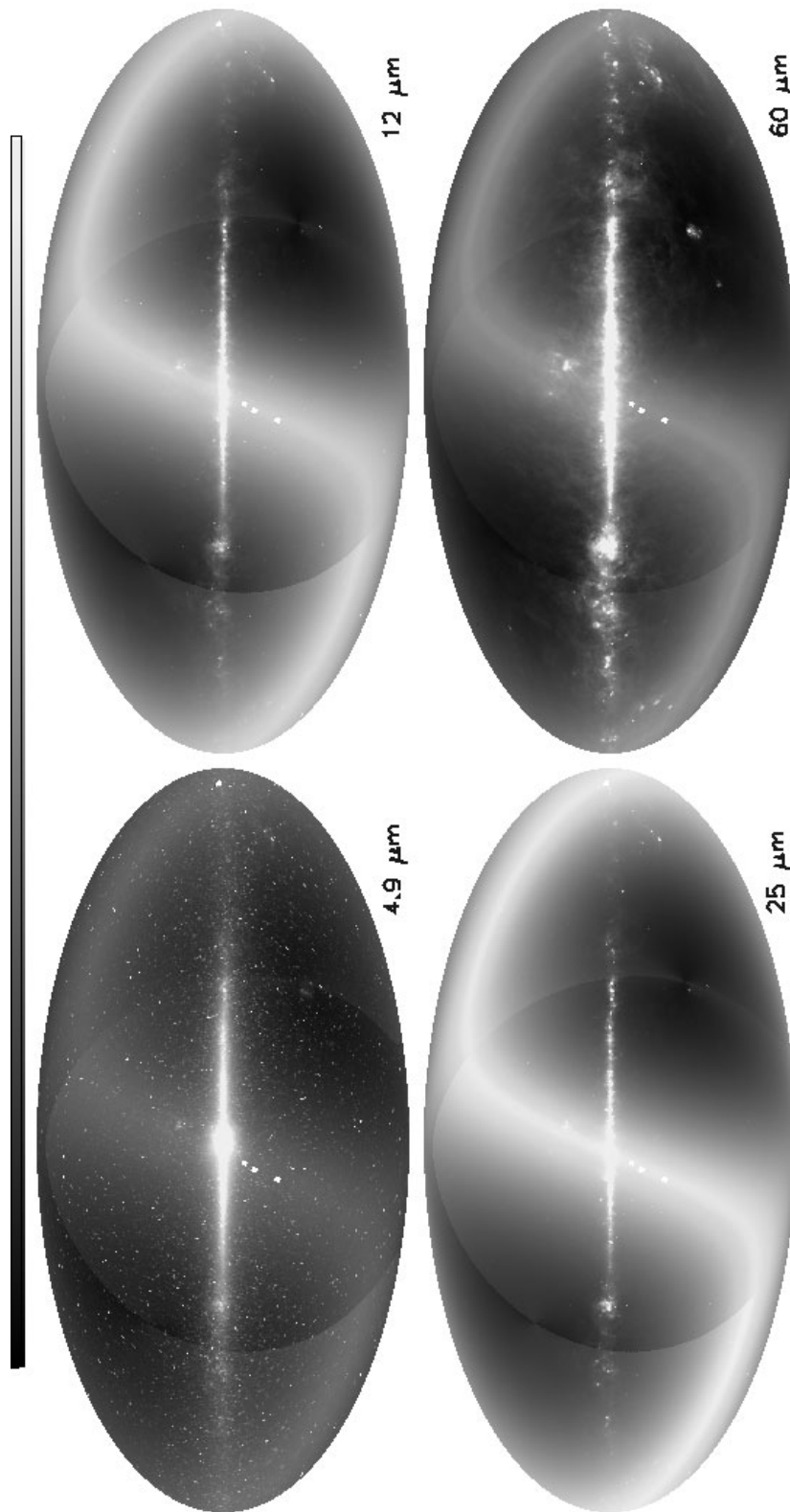


Figure 1.3-5: Same as Fig. 1.3-4 except at 4.9, 12, 25, and 60  $\mu\text{m}$ .

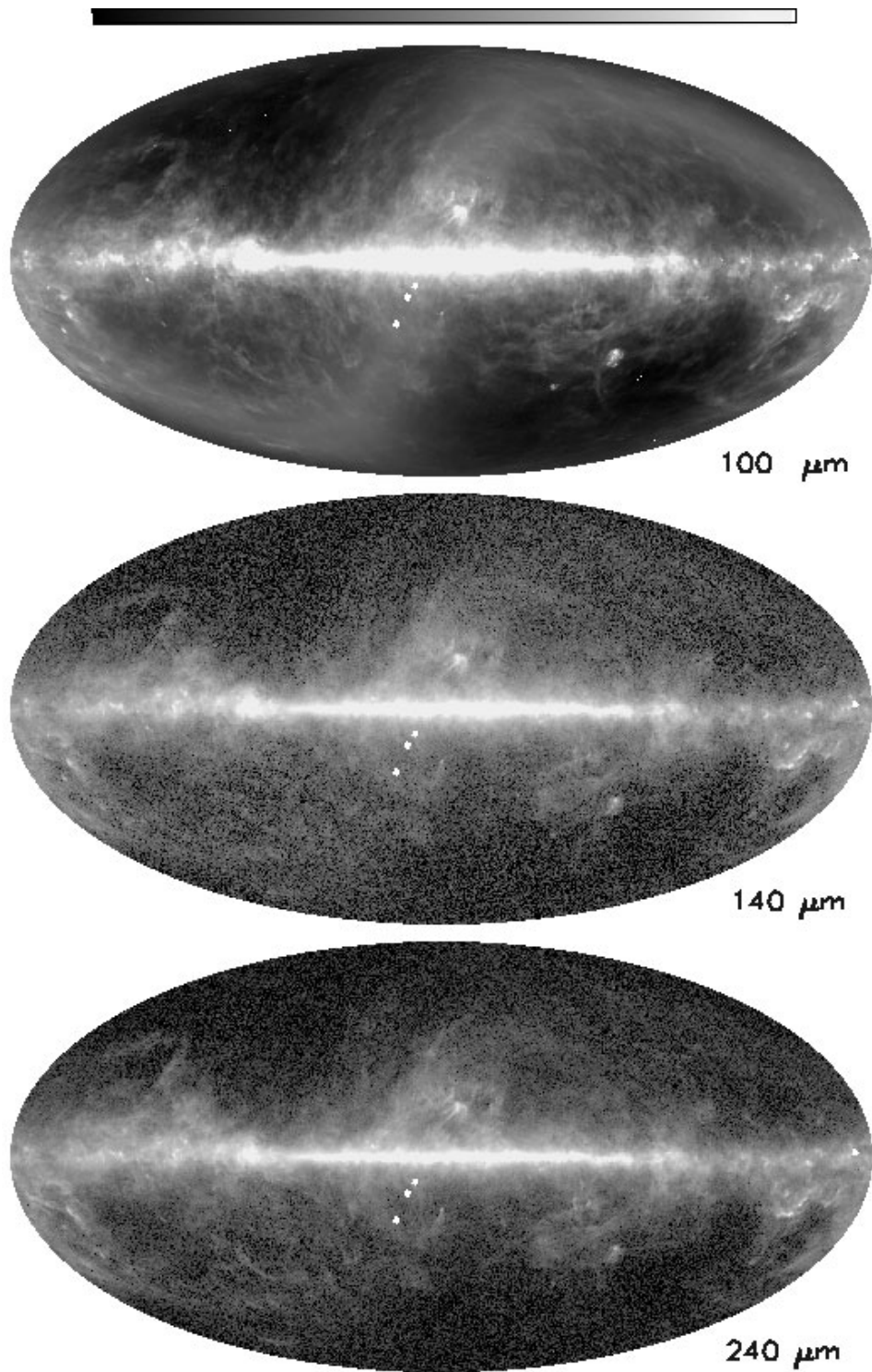


Figure 1.3-6: Same as Fig. 1.3-4 except at 100, 140, and 240  $\mu\text{m}$ .

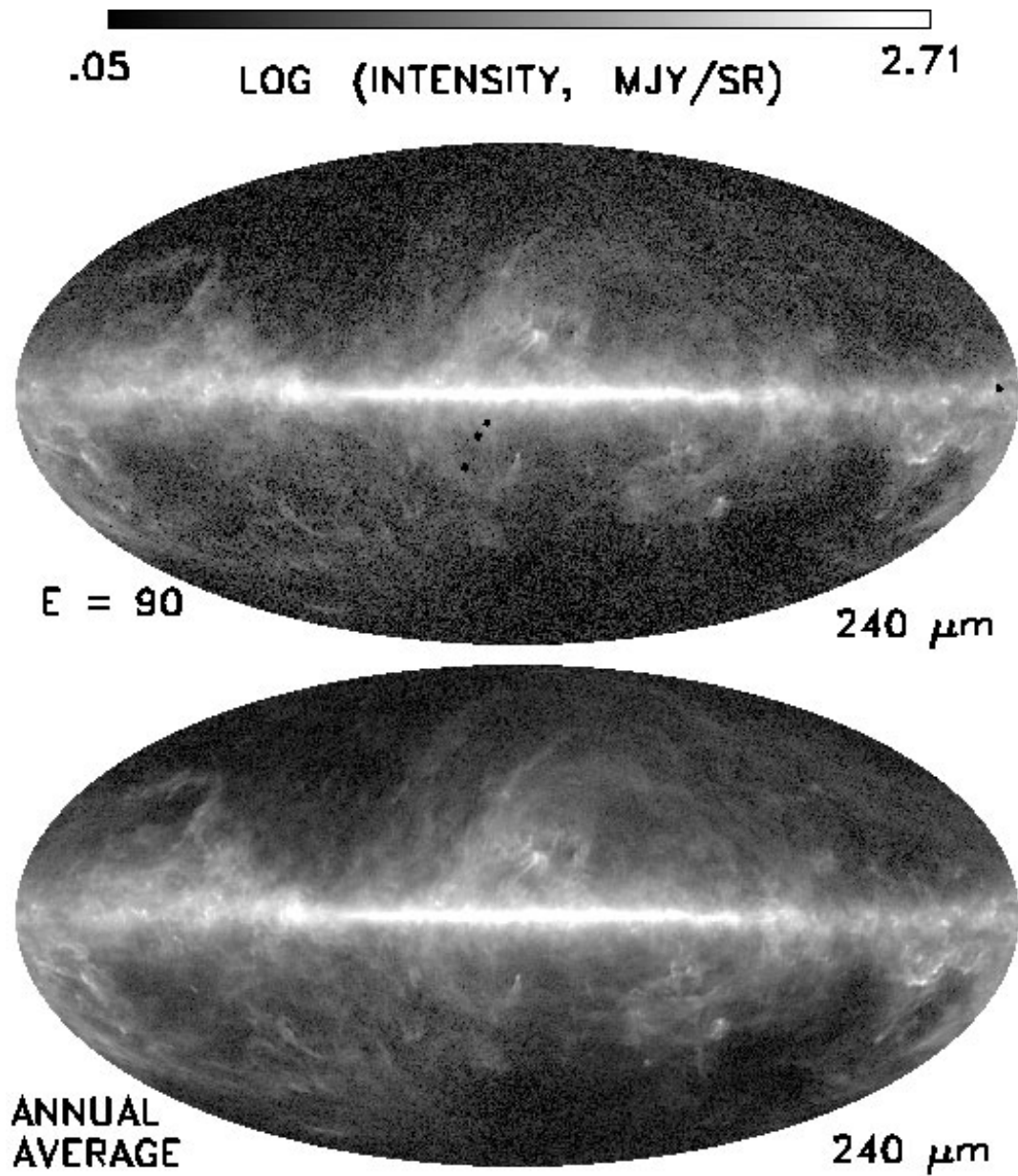


Figure 1.3-7: Comparison of Solar elongation =  $90^\circ$  (*top*) and Annual Average Sky Maps (*bottom*) at  $240\ \mu\text{m}$  illustrating the greater sensitivity in the latter. Both maps are Mollweide projections in Galactic coordinates.

Table 1.3-1: Intensity ranges for Figures 1.3-4–1.3-6

Wavelength ( $\mu\text{m}$ )	log ( $I_\nu$ , MJy/sr) corresponding to	
	black	white
1.25	-0.8	1.1
2.2	-0.95	1.3
3.5	-1.1	1.1
4.9	-0.5	0.75
12	1.0	1.7
25	1.2	1.91
60	0.7	1.91
100	0.42	2.0
140	0.05	2.71
240	0.05	2.71

The highest level *COBE* data products are called Analyzed Science Data Sets (ASDS). The **Photometric Standard Values Table** contains photometric data for the 92 objects which were used to establish the baseline relative celestial calibration system. *DIRBE* observations of Mars, Jupiter, Saturn, Uranus, Ceres, Pallas, and Vesta are reported in the **Solar System Object Dataset**; flux densities and relevant ancillary information are included in this product.

Additional ASDS products include estimates of the zodiacal light (ZL) intensity derived from the *DIRBE* interplanetary dust model (Kelsall *et al.* 1998) or have the zodiacal light subtracted. The *DIRBE Sky and Zodi Atlas (DSZA)* contains most of the data given in the DCAF, as well as an estimate of the ZL contribution to each of the individual weekly averaged photometric measurements. Finally, the ZL intensities were subtracted week by week and the residual intensity values were averaged to create the **Zodi-Subtracted Mission Average Maps (ZSMA)**, which give the best available picture of the Galactic and extragalactic diffuse infrared emission on degree or coarser angular scales.

The following ancillary products are also available:

**Beam Profile Maps** provide the effective two-dimensional shape of the *DIRBE* beam for each wavelength as the *DIRBE* instrument scanned the sky.

**System Response Functions** provide normalized system spectral response functions for each *DIRBE* wavelength band.

**Color Correction Tables** The *DIRBE* spectral intensity data,  $I_\nu$ , are expressed in MJy/sr, assuming the source spectrum is  $\nu I_\nu = \text{constant}$ . Where this is not true, color corrections must be applied to obtain an accurate intensity. These files provide the needed color correction factors for a variety of source spectral shapes.

## Chapter 2

# The *DIRBE* Instrument

### 2.1 Design Goals

The *DIRBE* was designed to make an absolute measurement of the spectrum and angular distribution of the diffuse infrared background. The instrument covers the wavelength range from 1.25  $\mu\text{m}$  to 240  $\mu\text{m}$  in 10 bands with a design sensitivity per field of view on the sky of  $\lambda I_\lambda = 10^{-9} \text{ W m}^{-2} \text{ sr}^{-1}$  in each band after 1 year of observation. The instrument also measures two perpendicular components of linear polarization in its short wavelength bands at 1.25, 2.2, and 3.5  $\mu\text{m}$ . The polarization measurements were included to help distinguish the contribution to the infrared background from sunlight scattered by interplanetary dust and to help in modeling the spatial distribution of the interplanetary dust. Since the *DIRBE* optical axis is oriented  $30^\circ$  from the spin axis of the *COBE* spacecraft, it views half the sky every day at solar elongation angles ranging from  $\varepsilon = 64^\circ$  to  $124^\circ$  with many redundant scans. Over the course of six months, every celestial direction is redundantly sampled at all possible elongation angles in this range.

### 2.2 Instrument Description

The *DIRBE* is a cryogenically-cooled ten band absolute photometer that measures the difference between the sky brightness and a zero-flux internal surface using a tuning-fork chopper running at 32 Hz. The synchronously demodulated signal is averaged for  $\frac{1}{8}$ th of a second before transmission to the ground. A cold shutter can be closed to block the sky signal to measure instrumental offsets. *DIRBE* uses celestial objects and internal thermal reference sources for monitoring response stability, and celestial sources for absolute response calibration. The instrument design, together with the mission and spacecraft capabilities, were chosen to facilitate discrimination of emissions from the solar system and our Galaxy from that of an isotropic cosmic infrared background (CIB). Table 2.2-1 summarizes the instrument characteristics.

Table 2.2-1: Instrument characteristics

Telescope diameter (primary)	19 cm
Telescope type	Cryogenic off-axis folded Gregorian
Telescope effective focal length	14.24 cm
Instantaneous field of view (FOV)	$0^\circ 7 \times 0^\circ 7$
Instrument type	absolute photometer and polarimeter
Photometric bands ( $\mu\text{m}$ )	1.25, 2.2, 3.5, 4.9, 12, 25, 60, 100, 140, 240
Polarimetric bands ( $\mu\text{m}$ )	1.25, 2.2, 3.5



### 2.2.1 Optics and Baffling

The *DIRBE* optics were carefully designed for strong stray light rejection (Magner 1987). The configuration (Figure 2.2-1) includes re-imaging with both a secondary field stop and a Lyot stop, superpolished

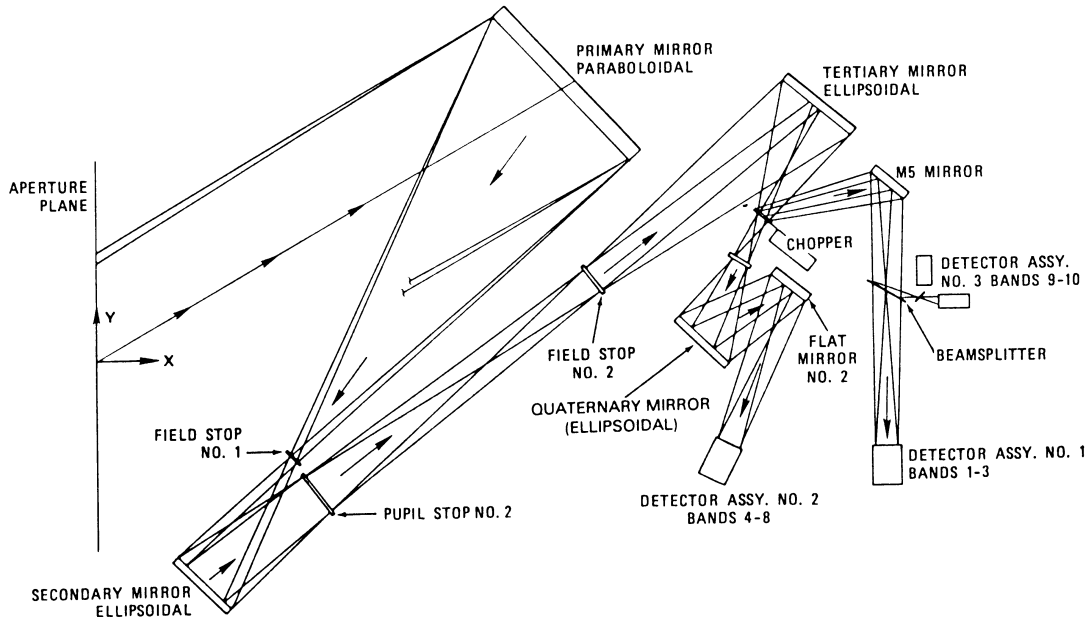


Figure 2.2-1: Optics diagram of *DIRBE*. The full beam shutter (not shown) was located at field stop 1. The cold beam stop (not shown), viewed by all detectors when not exposed to the sky (or shutter), was located to the left of the chopper blades in this Figure.

primary and secondary mirrors to further reduce scattered light, extensive internal baffling as well as a reflective forebaffle, and a complete light-tight enclosure within the *COBE* dewar to eliminate any optical cross-talk from the dewar or the other cryogenic instrument, *FIRAS*. Additional protection from the Earth and Sun are provided by the attitude control system and by the Sun-Earth shade surrounding the *COBE* dewar, which prevent any direct illumination of the dewar or instrument apertures from these omnipresent strong local sources.

The front end of *DIRBE* utilizes an off-axis folded Gregorian telescope with a 19 cm diameter off-axis segment of a parabolic mirror as the primary. There are no structural elements in the optical beam. Collimated incident light is imaged at the first field stop. An off-axis segment of an elliptical secondary forms an image of the primary at a pupil stop. This pupil stop (Lyot stop) is smaller than the image of the primary, blocking radiation diffracted from the primary mirror. The secondary mirror also images the first field stop at a second field stop. The second field stop is smaller than the first, blocking stray radiation scattered or diffracted at the first stop and setting the  $0.7 \times 0.7$  instantaneous field of view. An ellipsoidal tertiary mirror imaged the pupil (Lyot stop) at a tuning fork chopper with mirrored blades. In the chopper open position sky light reaches the elliptical quaternary mirror, which images the pupil via a folding flat onto detector assembly 2. With the chopper closed, the aspheric mirror (M5) reimages the pupil onto detector assemblies 1 and 3.

In this optical arrangement, all detector assemblies are located at a pupil image. Since the required sensitivity could be achieved with modest etendue in the first 8 bands (1–100  $\mu\text{m}$ ), pupil division was employed to divide energy between bands, giving these bands an effective etendue of 0.0044  $\text{cm}^2 \text{sr}$ ; the 140 and 240  $\mu\text{m}$  bands used the entire entrance aperture and have an etendue of 0.044  $\text{cm}^2 \text{sr}$ .

All of the spectral bands view the same instantaneous  $0.7 \times 0.7$  field of view (FOV) simultaneously. Optical testing showed small misalignments of the beam centroids. Corrections for these small pointing

offsets are applied in the ground data processing (see §4.2.2 and Table 4.2-1). With this configuration, each detector assembly received radiation chopped alternately between the sky and the cold beam stop. The cold beam stop was a black enclosure maintained below 3° K, producing no detectable signal at any *DIRBE* wavelength. *DIRBE* sky measurements were thus continuously referenced to zero flux. Instrumental zero point offsets due to electronic pick-up or stray radiation could be measured by closing the full-beam cold shutter located at field stop 1 (see §4.5.2 for discussion of offset determination and correction).

### 2.2.2 Detector Assemblies

The detectors are arranged into three separate mechanical assemblies. Beamsplitters divide the light spectrally to direct the appropriate wavelengths to each detector assembly. The detector and filter characteristics and descriptions are shown in Table 2.2-2. Bands at 1.25, 2.2, and 3.5  $\mu\text{m}$  are each equipped with three detectors, one measuring total intensity and two additional detectors, each of which has a linear polarizer in front of it. Each detector channel in an assembly included a detector element, Winston cone condensing element, spectrally-defining filter, and a cold JFET and load resistor for preamplification.

Each detector element (except the bolometers) was mounted on a low heat capacity substrate which was weakly coupled thermally to the mechanical structure. The substrate included a heater element which was used to set an optimal DC operating temperature for that detector, and, where necessary, to provide thermal annealing of detector response changes due to passage through the South Atlantic Anomaly.

Table 2.2-2: Detector and filter characteristics

Band	$\lambda^a$ ( $\mu\text{m}$ )	$\Delta\nu_e^b$ (Hz)	Detector Type	Filter Construction <sup>c</sup>
1	1.25	$5.95 \times 10^{13}$	InSb <sup>d</sup>	Coated Glass
2	2.2	$2.24 \times 10^{13}$	InSb <sup>d</sup>	Coated Glass
3	3.5	$2.20 \times 10^{13}$	InSb <sup>d</sup>	Coated Germanium
4	4.9	$8.19 \times 10^{12}$	InSb <sup>d</sup>	MLIF/Germanium
5	12	$1.35 \times 10^{13}$	Si:Ga BIB	MLIF/Germanium/ZnSe
6	25	$4.13 \times 10^{12}$	Si:Ga BIB	MLIF/Silicon
7	60	$2.32 \times 10^{12}$	Ge:Ga	MLIF/Sapphire/KRS5/Crystal Quartz
8	100	$9.74 \times 10^{11}$	Ge:Ga	MLIF/KCl/CaF <sub>2</sub> /Sapphire
9	140	$6.05 \times 10^{11}$	Si/diamond bolometer	Sapphire/Mesh Grids/BaF <sub>2</sub> /KBr
10	240	$4.95 \times 10^{11}$	Si/diamond bolometer	Sapphire/Grids/BaF <sub>2</sub> /CsI/AgCl

<sup>a</sup> Nominal wavelength of *DIRBE* band.

<sup>b</sup> Effective bandwidth assuming source spectrum  $\nu I_\nu = \text{constant}$ .

<sup>c</sup> MLIF = multi-layer interference filter.

<sup>d</sup> Anti-reflection coated for the band center wavelength.

#### 2.2.2.1 Detectors

The *DIRBE* detectors are listed by band in Table 2.2-2. All of the detectors were custom-made. The InSb detectors for 1.25 – 4.9  $\mu\text{m}$  (bands 1 – 4) were 1 mm diameter photodiodes obtained from Cincinnati Electronics. The 12 and 25  $\mu\text{m}$  (band 5 and 6) Blocked Impurity Band (BIB) photoconductors each had a  $1 \times 1.75$  mm rectangular active area and were supplied by Rockwell. The Ge:Ga photoconductors used at 60 and 100  $\mu\text{m}$  (bands 7 and 8) had  $1 \times 1 \times 1$  mm dimensions and came from Infrared Labs.

The 140 and 240  $\mu\text{m}$  (band 9 and 10) detectors were fabricated at NASA/Goddard Space Flight Center (GSFC). The bolometers used Cr/Au resistive absorbing films on octagonal diamond substrates (2.75 mm across flats). The 140  $\mu\text{m}$  substrate was 18  $\mu\text{m}$  thick, while the 240  $\mu\text{m}$  substrate was 25  $\mu\text{m}$  thick. The absorbing film impedances were  $\sim 70\Omega$  per square, resulting in  $\sim 80\%$  absorption near band

center. The thermometers were boron-compensated Si cubes 0.25 mm on a side. Electrical contacts were made on two opposite faces using a degenerate As implant with a Cr/Au contact layer.

The detector response functions were measured at GSFC using a Nicolet Michelson Fourier Transform Interferometer Radiometer (FTIR) and a reference detector (a monolithic silicon bolometer). The optimal detector temperatures and bias voltages found in the laboratory were similar to those determined to give the best performance on orbit (see Table 3.2-1).

#### 2.2.2.2 Filters

The *DIRBE* filters are listed by band in Table 2.2-2. Filters for the 1.25 – 4.9  $\mu\text{m}$  bands consisted of multi-layer interference coatings on transparent substrates and were supplied by the AGA Corporation of Sweden (presently Spectrogon, AB). The 12 – 100  $\mu\text{m}$  filters consisted of multi-layer interference coatings stacked atop infrared-active crystals anti-reflection coated with polyethylene (Infrared Labs). The 140 and 240  $\mu\text{m}$  filters were stacked infrared-active crystals with inductive mesh grids (Perkin-Elmer). All of the filters were paralene encapsulated and anti-reflection coated. The filter transmission and beamsplitter characteristics were measured at  $< 10$  K using the Nicolet FTIR at GSFC (Heaney *et al.* 1986).

Not counting the polarizers, there were two beamsplitters. One beamsplitter, consisting of a Cr/Au inductive mesh on a sapphire substrate, reflected long wavelengths and transmitted short wavelengths, and was used to separate the 1.1 – 4.0  $\mu\text{m}$  bands (detector assembly 1; see Figure 2.2-1) from the 120 – 300  $\mu\text{m}$  bands (assembly 3). The second beamsplitter, a mesh filter on a Si substrate, was used to separate the 140 and 240  $\mu\text{m}$  bands.

#### 2.2.2.3 Spectral Response Functions

The *DIRBE* passbands were formed by the convolution of filters, detector response functions, and dichroic beamsplitters. The filter and detector response functions from 1.25 – 100  $\mu\text{m}$  (bands 1 – 8) and the system response functions at 140 and 240  $\mu\text{m}$  (bands 9 and 10) were measured at GSFC. Out-of-band leaks were measured to 1 part in at least  $10^4$  (in some bands to a part in  $10^8$ ) and determined to satisfy the (to-be-provided) requirements.

Though the attempt was made to produce the same spectral response as *IRAS* in the 12 – 100  $\mu\text{m}$  bands, there were several significant differences. The long-wavelength cutoff of the BIB detector used in the *DIRBE* band 6 was  $\sim 27\mu\text{m}$ , as opposed to 30  $\mu\text{m}$  for the Si:Sb photoconductor used in *IRAS* band 2. The *DIRBE* 60  $\mu\text{m}$  response was measured and found to have a long-wavelength cutoff at 70  $\mu\text{m}$  rather than at 78  $\mu\text{m}$  as in the *IRAS* case (see the *IRAS Catalogs and Atlases Explanatory Supplement*, p. II-18).

Normalized system spectral response functions are shown in Figure 2.2-2, tabulated in Appendix A, and delivered as a data product in ASCII form (see §5.9.2).

#### 2.2.2.4 Polarizers

In addition to the full intensity channels (designated ‘A’) in the 1.25, 2.2 and 3.5  $\mu\text{m}$  bands, two detectors were used to make polarization measurements in each of these bands. Channels designated ‘B’ and ‘C’ contain polarizers whose transmission axes are orthogonal and fixed inside the *DIRBE* as well as band-defining spectral filters and detectors like those used in the corresponding A channels. The C channels have axes of maximum transmission aligned along the component of the *DIRBE* scan direction attributable to the spacecraft spin. The polarizing elements are 5000 line/mm aluminum grids etched on sapphire substrates.

### 2.2.3 Thermal Control

Temperatures inside the cryostat (see §2.3.7) were maintained stable and below 1.6 K while the cryogen supply lasted except during occasional transient events (see §3.4.3). The external surfaces of the dewar and surrounding system were designed to minimize the dewar main shell temperature and, therefore, heat loads to the cryogen. A Sun–Earth shield (§2.3.8) protected the *DIRBE* and dewar apertures

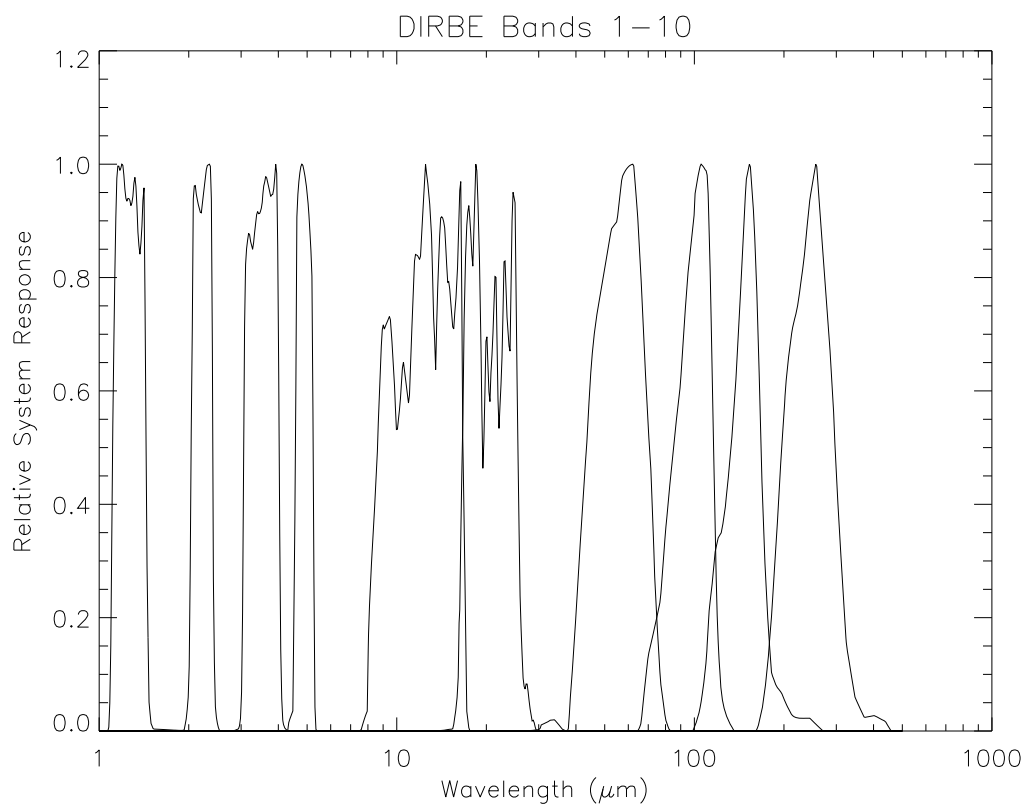


Figure 2.2-2: Normalized system spectral response

from direct solar radiation when the *DIRBE* line of sight was pointed more than  $60^\circ$  from the Sun, a constraint which was maintained throughout the mission.

## 2.2.4 Calibration

### 2.2.4.1 Cold Chopper

Absolute surface brightnesses are measured by chopping between the sky signal and the cold internal beam stop, which is a stable, zero-flux reference at the wavelengths of the *DIRBE*. The cryogenic tuning fork chopper operates at 32 Hz and is located at a pupil image (see Figure 2.2-1).

### 2.2.4.2 Shutter

Instrumental offsets were determined by closing off the sky from the instrument with a cold shutter located at the prime focus (Field Stop No. 1 in Figure 2.2-1; the shutter is not shown in the figure). The shutter was demonstrated to attenuate saturation-level sky signals to well below instrument noise levels at all *DIRBE* wavelengths. The shutter closed condition with the internal reference source (see §2.2.4.3) turned off defined the zero sky brightness signal for *DIRBE* measurements.

### 2.2.4.3 Internal Reference Sources

The back of the shutter has a mirror which allows light from an internal reference source (IRS) system located out of the path of the sky beam to reach the detectors via the secondary and subsequent mirrors only when the shutter is closed. Measuring the instrument signal with the shutter closed and the IRS off permits determination of instrumental noise levels and electrical and radiative offsets. Turning on the IRS at fixed levels permits monitoring of system gain stability. Calibration procedures are described in §3.3.

The IRS system consisted of four thermal sources, only one of which was designated the primary source at any given time. When the source initially used as the primary failed, the source originally designated “secondary” was substituted (see §3.5.2).

## 2.2.5 Electronics

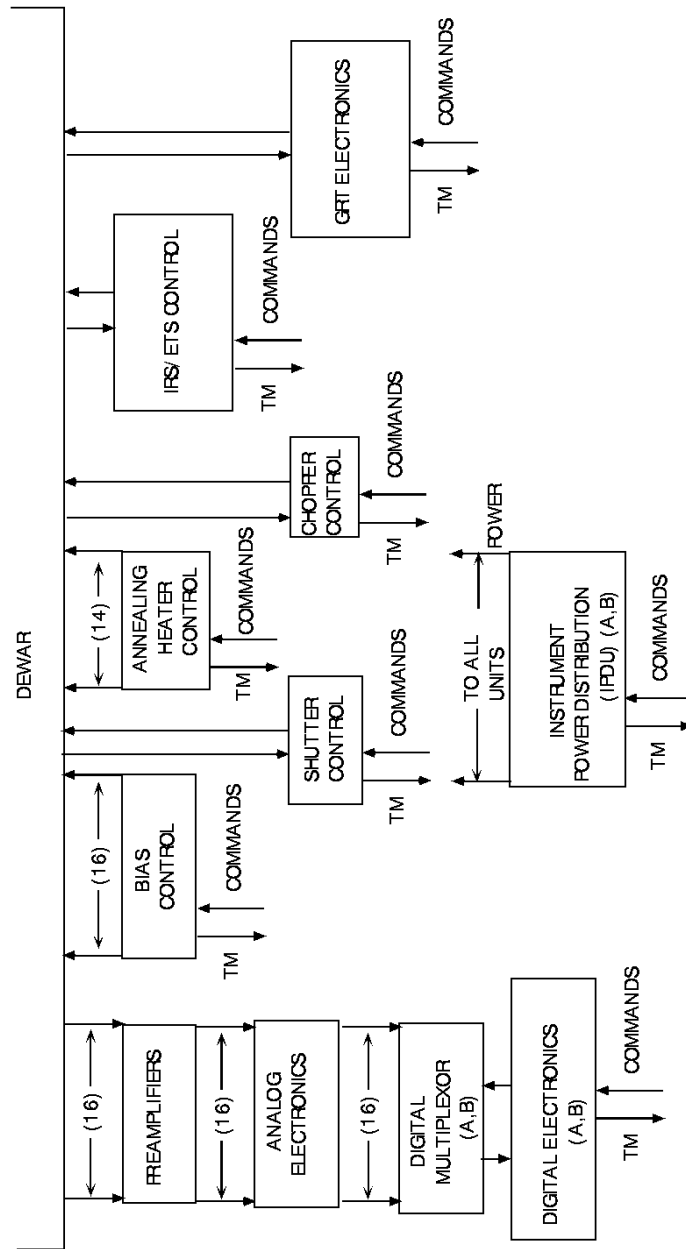
The *DIRBE* instrument electronics consist of the individual detector’s analog electronics and the common electronics for collecting, digitizing, and processing the data (Figure 2.2-3). With the exception of the detector-unique analog electronics, all of the electronic elements were redundant. These units consisted of two duplicate (referred to as unit A or B) instrument power distribution units (IPDU) and two digital electronics units (DEU). Any pair consisting of an IPDU and a DEU was valid and the subsystem was tested on the ground in all possible configurations. Full system performance was tested only using all A units, then all B units. In flight the B units were used; there was never a need to switch to a redundant *DIRBE* electronics unit.

The IPDU conditioned power from the *COBE* solar arrays and from the battery, which was only used during short “eclipse” periods near the June solstices (see §2.3.3). The IPDU electronics also monitored analog and digital electronics and configuration functions, and it provided a command interface for control and monitoring of power functions. All power monitoring signals were inserted into the telemetry stream on a sampled basis, and no signal was sampled less frequently than once per 32 seconds.

Each DEU contained a TI9900 microprocessor which digitized the analog signals from each of the detectors using an analog multiplexer and a 12-bit successive approximation analog-to-digital converter. Advantage was taken of the microprocessor’s inherent flexibility to enable operation of the instrument in a number of modes (see §2.2.6).

A cryogenic JFET source follower on each detector reduced the output impedance. Remaining elements of the transimpedance preamplifiers for the photovoltaic and photoconductive detectors were located outside the dewar; high gain preamplifiers were used for the bolometric detectors.

The electronic gain of each individual detector channel was commandable over a factor of 30. This capability was included to protect against uncertainty in the sky brightness, to allow for possible optical



**DRBE ELECTRONICS BLOCK DIAGRAM**

Figure 2.2-3: Electronics block diagram of *DIRBE*

efficiency degradation, and to permit gain readjustment in some bands after cryogen exhaustion. To achieve the required dynamic range at each commandable gain, each detector output was sampled at 256 Hz at the nominal commanded gain (low) and at 16 times that gain (high). The on-board micro-processor was programmed to choose the highest non-saturated gain for signal processing calculations and insertion into the telemetry. An output bit indicated which gain (high or low) was chosen for each detector's output. Nominal commanded gains were set so that non-saturated signals were produced in the high gain state over most of the sky.

The stability and precise gain ratios of the analog electronics could be determined by injecting an electronic test signal (ETS) into the analog chain in place of the preamplifier output. This test signal was generated in the same unit that provided the drive signals for the IRS.

The shutter and the IRS were controlled by the DEU. For internal calibration and stability monitoring, several programmed sequences of IRS levels were used during flight. The sequences were arranged to assure that each detector was stimulated at several levels in its dynamic range. Programmed sequences were tailored to each of the four IRS sources to produce similar output levels. This was required to account for differences in optical outputs of the sources. Celestial sources provided a long-term monitor of IRS stability and detector performance (see Chapter 4). The IRS and its drive electronics were designed to be highly stable over time scales of at least days.

## 2.2.6 DIRBE Operating Modes

As noted in §2.2.5, the *DIRBE* instrument could be operated in a variety of modes. Most of these modes were used for instrument diagnostics both on the ground and in orbit. Because the mission proceeded nominally, about 95% of the time in orbit was spent in the primary science data-gathering mode (SDM) or in the mode used for calibration and stability monitoring (CAL). In CAL mode, the instrument shutter is closed for internal calibration and offset monitoring; the SDM and CAL modes are otherwise the same.

In SDM, to enhance the signal-to-noise ratio and reduce the bandwidth required to send data for each detector to the ground, data from four chopper cycles were combined on-board. At the chopper oscillation frequency, 32 Hz, four cycles lasted  $\frac{1}{8}$ th of a second, during which time 32 samples were collected. The output signal from the  $i$ th detector,  $S_i$ , was digitally demodulated synchronously with respect to the phase of the chopper and was, specifically,

$$S_i = \sum_{s=1}^{32} D_{i,s} M_{i,s}, \quad (2.1)$$

where  $D_{i,s}$  represents detector sample  $s$  and  $M_{i,s}$  is a mask containing only values of  $\pm 1$ . The phase of the mask was adjusted so that  $M$  would turn out to be  $+1$  for samples obtained when the detector was exposed to the sky signal and to  $-1$  when the chopper was seen. In practice, a phase setting was sought that would maximize the output signal subject to the condition that the mask be symmetrically positioned with respect to the chopper cycles in order to reject to first order the bias inherent in digitizing a smoothly varying sky signal.  $S_i$  represents the average response of the detector to the sky over  $\frac{1}{8}$ th of a second, and these  $\frac{1}{8}$ -second demodulated samples were recorded on the spacecraft tape recorder for telemetry to the ground. To ensure that the wide dynamic range required by some bands could be achieved, data compression to 12 bits was performed on-board and the result was reconstructed on the ground to 0.25% precision or better. Section 4.2.2 describes how the detector sampling time was set to achieve beam alignment.

Complementary to SDM, there were three special data sampling modes in which synchronous demodulation was *not* performed. In snapshot mode (SNAP), either all 8 samples per chopper cycle were telemetered for two selectable detectors, or 16 samples were delivered for one detector. In continuous burst mode (CBM), 4 samples per chopper cycle for two selectable detectors were included in the telemetry. In single channel mode (SNG), data from a single selected detector were telemetered continuously at 4 samples per chopper cycle.

There were two calibration modes in addition to CAL mode. In electronic test signal mode (ETS), the analog electronics were stimulated by the built-in test signal generator. During annealing periods,

special settings of detector heaters and IRS sources were used to remove the effects of nuclear particle bombardment from the detectors (see §§3.4.1 and 3.5.1). In annealing mode (ANL), the normal detector data were replaced by data on the setting of the detector heaters and the DC output from the detectors (see §2.2.2).

A stand-by mode (STM) was included for safety. In this mode, the firmware used by the on-board microprocessor could be dumped into the telemetry stream in place of instrument data.

## 2.3 The Instrument in Context: the COBE Satellite

Boggess *et al.* (1992) described the design of the Cosmic Background Explorer (*COBE*) and its performance two years after launch. This section and section 3.1.1 include *DIRBE*-related parts of the Boggess *et al.* paper. The *COBE* mission design is described here, and spacecraft performance in flight is summarized in Table 3.1-1. The *DIRBE* performance in flight is discussed in Chapters 3 and 4.

### 2.3.1 Mission Concept

To achieve the full benefit of space observations, a goal of the *COBE* mission and instrument design was that measurements would be limited ultimately by our ability to identify and model the various components of the astrophysical foreground sources in order to discriminate between them and the cosmic background emission. This goal drove the design of the mission strategy, the spacecraft and operations, and the choice of instruments. Basic elements in the mission strategy were the requirements for highly redundant full sky coverage and for sufficient time in orbit to achieve necessary sensitivity and evaluate potential sources of systematic errors in the observations. Other elements in the strategy were the needs for on-board instrument calibration and time for frequent checks of calibration stability. To reduce known sources of systematic errors, the mission orbit, spacecraft attitude and instrument enclosures were designed to eliminate direct exposure to Sun and Earth radiation and to maintain a well-controlled thermal environment for the instruments. Instrument and spacecraft design included efforts to minimize radio frequency contamination and interference from sources of stray radiation. Finally, the instruments were chosen to measure specific attributes of the cosmological backgrounds and also, through their complementary spectral coverage, to enable the modeling and subtraction of foreground emissions. Early descriptions of the mission concept were given by Mather (1982) and by Gulkis, Lubin, Meyer, & Silverberg (1990).

The three scientific instruments are the Far Infrared Absolute Spectrophotometer (*FIRAS*), the Differential Microwave Radiometers (*DMR*), and the Diffuse Infrared Background Experiment (*DIRBE*). The *FIRAS* objective is to make a precision measurement of the spectrum of the cosmic microwave background (CMB) from 1 cm to 100  $\mu\text{m}$ . The *DMR* objective is to search for CMB anisotropies on angular scales larger than  $7^\circ$  at frequencies of 31.5, 53, and 90 GHz. The *DIRBE* objective is to search for a CIB by making absolute brightness measurements of the diffuse infrared radiation in 10 photometric bands from 1.25  $\mu\text{m}$  to 240  $\mu\text{m}$  and polarimetric measurements from 1.25  $\mu\text{m}$  to 3.5  $\mu\text{m}$ .

The need to control and measure potential sources of systematic errors required an integrated design and operations concept. It led to the requirements for an all-sky survey and a minimum time in orbit of six months, and imposed constraints on the permitted amount of radiative interference from local sources such as the Earth, Sun, Moon, and radio interference from the ground, *COBE* spacecraft and other satellites. The instruments required temperature stability to maintain gain and offset stability, and a high level of cleanliness to reduce the entry of stray light and thermal emission from particulates. The control of systematic errors in the measurement of the CMB anisotropy and the need for measuring the zodiacal cloud at different solar elongation angles for subsequent modeling required that the satellite rotate. The choice of orbit, within the constraint of available launch vehicles, was also an important consideration in minimizing systematic errors.

The major components of the satellite were the instrument module and the spacecraft module. The instrument module contained the scientific instruments and some of their electronics, a superfluid He dewar, and a Sun-Earth shield. The spacecraft module included most instrument electronics, spacecraft subsystems including the attitude control system, command and data handling system, power system,



solar panels, two omnidirectional antennas, and necessary support structures. These components are shown schematically in Figure 2.3-1.

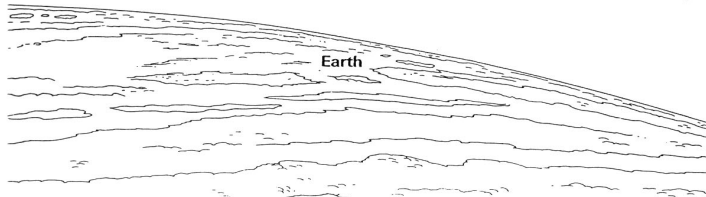
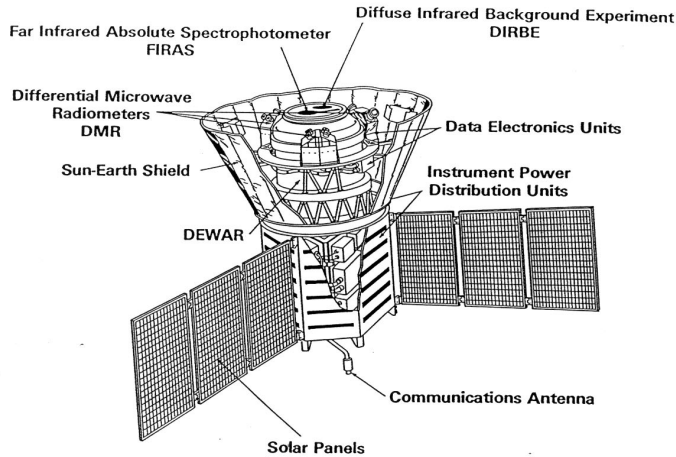


Figure 2.3-1: Artist cutaway drawing of the major components on *COBE*, showing the locations of the three scientific instruments.

### 2.3.2 The Orbit

The overriding considerations in choosing the orbit were the need for full sky coverage, the need to eliminate stray radiation from the instruments, and the need to maintain thermal stability of the dewar and the instruments. In near-Earth orbit, the Sun and Earth are the primary sources of thermal emission and it is necessary to ensure that neither the instruments nor the dewar are exposed to their radiation. A circular Sun-synchronous orbit can satisfy these requirements throughout the year. In a Sun-synchronous orbit, the inclination and altitude are chosen so that the orbital plane precesses  $360^\circ$  in one year due to the Earth's gravitational quadrupole moment. For *COBE*, a 900 km altitude orbit was chosen, requiring a  $99^\circ$  inclination. A 900 km altitude was within the launch capabilities of the Shuttle (with an auxiliary propulsion system on *COBE*) or a Delta rocket. This altitude is a good compromise between contamination from the Earth's residual atmosphere, which increases at lower altitude, and interference due to charged particles in the Earth's radiation belts at higher altitudes. A 6 PM ascending node was chosen for the *COBE* orbital plane; this node follows the terminator (the boundary between sunlight and darkness on the Earth) throughout the year. By continuously reorienting the spacecraft spin axis to about  $94^\circ$  from the Sun and close to the local zenith, the Sun and Earth were kept below the plane of the shield. In this observing mode, the spacecraft central axis scanned the full sky every six months. The orbit is shown schematically in Figure 2.3-2. The orbital period is 103 minutes, giving almost exactly 14 orbits per day.

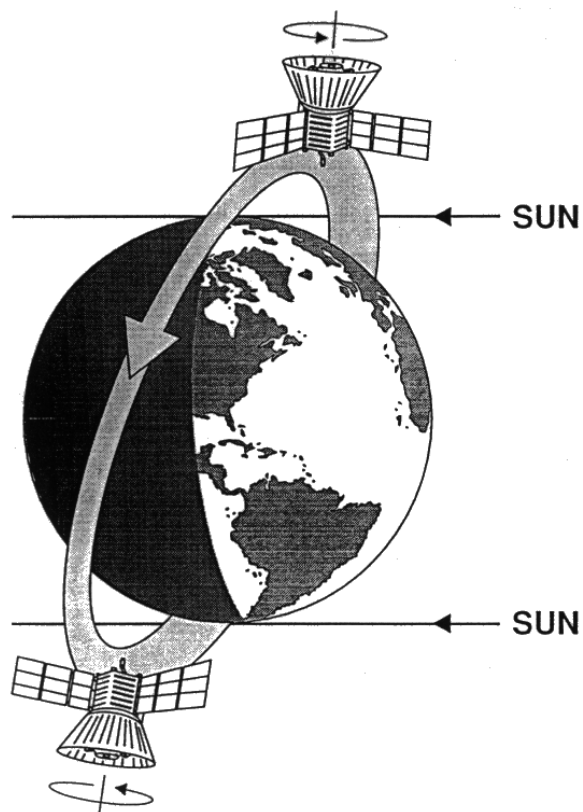


Figure 2.3-2: Schematic drawing of *COBE* in orbit. *COBE* is shown in a high-inclination orbit with its axis of rotation always pointing away from the Earth and about  $90^\circ$  from the Sun.

### 2.3.3 Attitude Control

It was necessary to spin the spacecraft to attain the scientific objectives of measuring the CMB anisotropy and searching for a CIB. As will be discussed in more detail below (and illustrated in Figure 2.3-3), the *FIRAS* optical axis pointed along the spin axis while the *DIRBE* and *DMR* beams

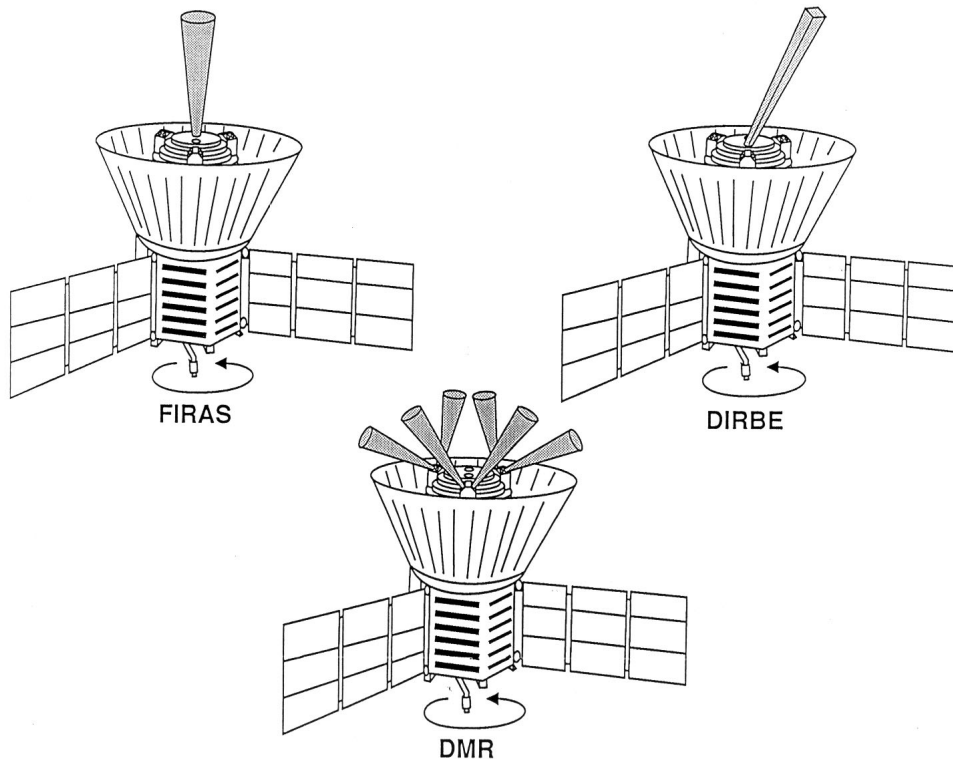


Figure 2.3-3: Schematic drawing of the viewing direction for each of the three *COBE* instruments with respect to the spin axis of the spacecraft.

pointed  $30^\circ$  from the axis. The spin allowed *DIRBE* to measure the emission and scattering by the zodiacal dust cloud over a range of solar elongation angles for each celestial direction, which aids in the discrimination and subsequent modeling of zodiacal radiation. The 0.8 rpm spin rate was chosen to be fast enough to reduce the noise and systematic errors that could otherwise arise from radiometer gain and offset instabilities. The spin axis was tilted back from the orbital velocity vector as a precaution against possible deposition of residual atmospheric gas on the cold optics and against a possible infrared glow that would arise from fast neutral particles hitting surfaces at supersonic speeds. (The tilt-back varied a few degrees about  $96^\circ$  during each orbit.) The axis of the spacecraft was also tipped to angles between  $92^\circ$  and  $94^\circ$  from the Sun to reduce the amount of sunlight reflected or scattered from the edge of the shield into the instrument apertures and dewar.

A sophisticated attitude control system met the unique requirements of slow rotation and 3-axis control. This was implemented by using a pair of inertia wheels (yaw angular momentum wheels), with their axes oriented along the spacecraft spin axis. These wheels carried an angular momentum opposite that of the entire spacecraft to create a zero net angular momentum system. The spacecraft orientation was controlled by three reaction wheels with spin axes  $120^\circ$  apart in the plane perpendicular to the spacecraft spin axis and by electromagnetic coils (torquer bars) that interact with the Earth's magnetic field.

The attitude of the spacecraft was measured and maintained by a redundant set of sensors and servo

systems. Earth and Sun sensors (one of each on each of the three transverse control axes) provided control signals to point the spin axis away from the Earth and at least  $90^\circ$  from the Sun. Rate damping and fine resolution attitude sensing were provided by six gyros, one on each transverse control axis and three on the spin axis. The system was redundant in that stable operation was achievable with one or perhaps two of the transverse control axes disabled, and with only one spin axis gyro operable.

Coarse attitude parameters were calculated by using telemetered data from the attitude control sensors. The Sun and Earth directions were measured in spacecraft body coordinates and transformed to inertial coordinates using the spacecraft ephemeris. These were then used to compute quaternions and rotation matrices describing the spacecraft orientation. The data were smoothed and interpolated using the gyro signals to produce attitude solutions good to  $4'$  ( $1\sigma$ ), adequate to meet the initial requirements for the *FIRAS* and *DMR*. The *DIRBE*, with its smaller beam size ( $0.7^\circ$  rather than  $7^\circ$ ), required a more accurate attitude solution. This fine aspect was determined by using gyro data to interpolate between the positions of known stars detected in the *DIRBE* short wavelength bands. The fine aspect solution was accurate to  $1.5'$  ( $1\sigma$ ) and was used in the analysis of data from all three instruments.

There was an unavoidable radiative perturbation to the instruments from the Earth in the chosen orbit and spacecraft attitude. At 900 km altitude, the Earth's limb is  $118^\circ$  from the zenith. Since the attitude control system maintained the axis of the satellite pointing away from the Earth and  $94^\circ$  from the Sun, the Earth limb did not rise above the plane of the Sun–Earth shield for most of the year. However, since the Earth's axis is tilted  $23.5^\circ$  from the ecliptic pole, the angle between *COBE*'s orbital angular momentum vector and the ecliptic plane varied through the seasons from  $-14.5^\circ$  to  $+32.5^\circ$ . As a consequence, the combination of the tilt of the Earth's axis, the orbit inclination, and the offset of the spacecraft spin axis from the Sun brought the Earth limb above the shield for up to 20 minutes per orbit near the June solstices. During this period the limb of the Earth rose a few degrees above the plane of the shield for part of each orbit, while on the opposite side of the orbit the spacecraft went into the Earth's shadow. To minimize risk, this “eclipse season” was placed as far as possible after launch by locating the ascending node of the orbit over the evening terminator; thus, eclipses occurred near the south pole around the summer solstices.

### 2.3.4 Sky Scan Strategy

The scan strategy was governed by the requirement for all-sky coverage and the need for many scans of each pixel on the sky. Many scans build up the signal-to-noise ratio and allow tests for systematic errors by multiple measurements of the same part of the sky under different environmental conditions, instrument parameters, and observing times.

Each scientific instrument had a unique scan pattern that depended upon its orientation on the satellite (Figure 2.3-3). The *DIRBE*, located inside the dewar, viewed  $30^\circ$  from the spin axis to provide data over solar elongation angles ranging from about  $64^\circ$  to  $124^\circ$  during each spacecraft rotation. Combined with the continuous pitching of the spacecraft to maintain an anti-Earth orientation, the spinning motion caused *DIRBE* to trace out a helical pattern on the sky and to sample half of the sky every day. Figure 2.3-4 shows the coverage achieved in a typical orbit.

Precession of the orbit caused the pattern to move about one degree per day, resulting in complete sky coverage within four months and more uniform sampling in six months. A comparison of the coverage achieved after various time intervals is given in Figure 2.3-5.

### 2.3.5 Power

Three solar array wings, deployed after launch, provided power for the spacecraft and instrument electronics. Each wing consisted of three panels with solar cells on both sides. The arrays were designed for a minimum lifetime of one year to maintain a peak capacity of approximately 1280 W at launch and an average capacity of 750 W at the end of the first year. The actual performance at the end of the first year had diminished by about 3%. The nominal spacecraft and instrument power load was 542 W.

Power generated in the solar arrays was supplied directly to the spacecraft and instrument subsystems through a regulated +28 V bus. The power system operated at close to 100% efficiency by taking

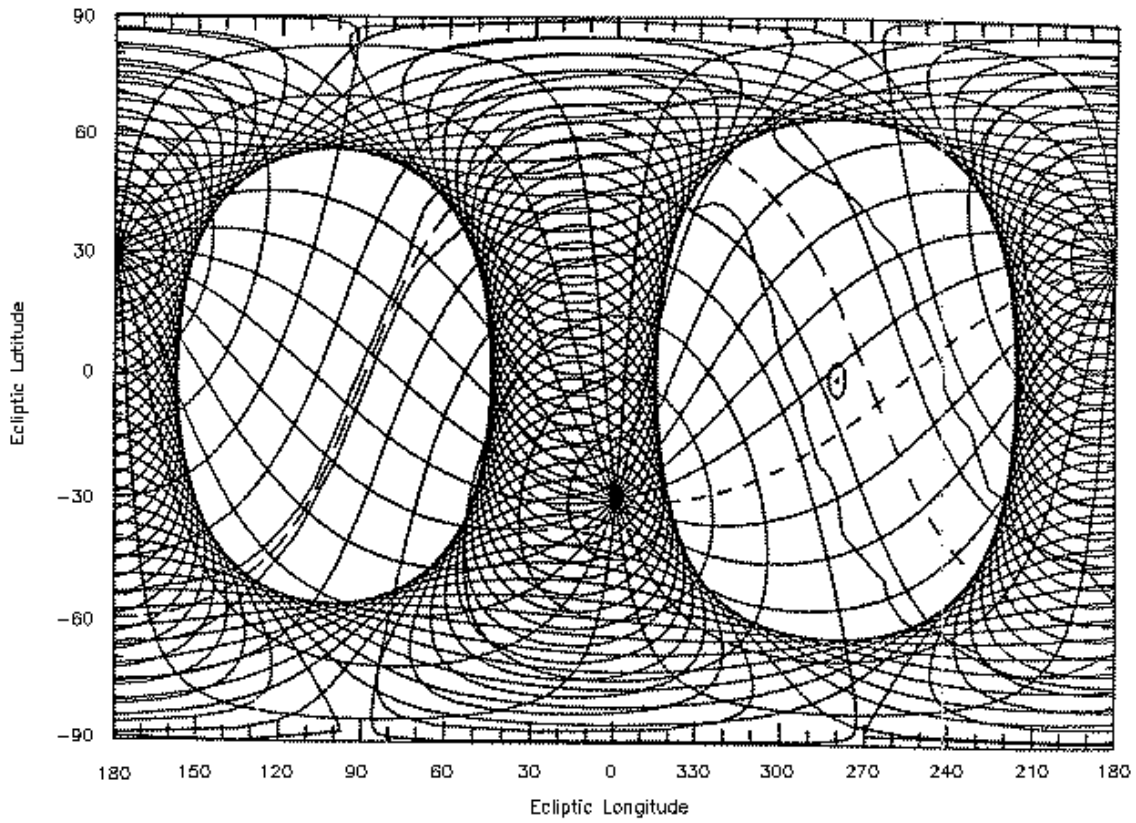


Figure 2.3-4: The track of the *DIRBE* line of sight on the sky over the course of one orbit on 1990 January 1. The sky is presented in ecliptic coordinates, with an overlay grid of Galactic coordinates. The contour lines surrounding the Galactic equator (long dashes) outline the rough appearance of the Milky Way.

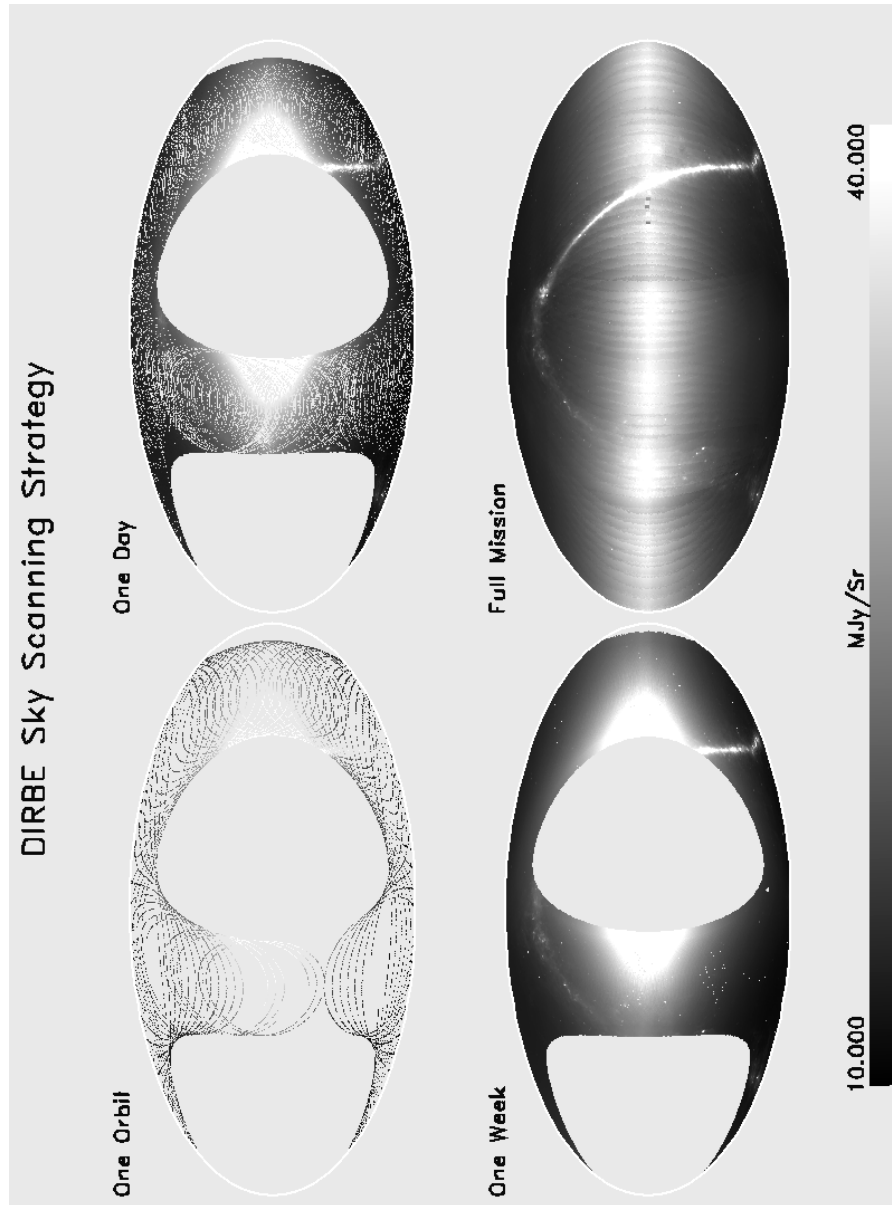


Figure 2.3-5: *DIRBE* sky coverage achieved for a typical orbit, a day, a week, and for the entire cryogenic mission. The maps shown depict  $12 \mu\text{m}$  emission in an Ecliptic Mollweide projection.

advantage of the nearly constant solar illumination provided by the orbit and spacecraft spin. Bus voltages were maintained by shunt regulators which radiated excess power into space. The 20 minute power transients during the eclipse season were smoothed by batteries.

A significant effort was made in developing spaceworthy low noise and RF-free power supplies and power distribution systems for the instruments. The low-noise sections had their own DC-DC power converters with separate grounds, multiple shields, and nested sub-regulators.

### 2.3.6 Communication

*COBE* required a special design for satellite commanding, tracking, and data retrieval. It had two antennas, one to communicate with the Tracking and Data Relay Satellite System (TDRSS), and the other to transmit data stored on tape recorders directly to the ground. The antennas, which were deployed after launch, were located on a mast at the bottom of the spacecraft.

The TDRSS link transmitted commands for tracking, spacecraft attitude maneuvers, and control of the instruments. It was also used to establish a short (10-20 minutes) real-time data flow, approximately every other orbit, from the satellite to the operations control center at the NASA Goddard Space Flight Center (GSFC) via the ground station at White Sands, NM.

The primary data flow was stored on one of two onboard tape recorders and read out daily directly to the NASA receiving station at the Wallops Flight Facility. The *COBE* near-polar orbit provided a minimum of two morning and two evening opportunities for transmission of the stored data. Both the stored and real-time data were relayed to the Payload Operations Control Center at GSFC for satellite health and safety monitoring and engineering trend analysis. The data were also relayed to the analysis center for quick-look processing. An edited tape of the tape recorder dump was received 24-48 hours after contact, and these data were used for final science data processing.

The spacecraft electronics included a command and data handling system that stored and decoded the commands received from the ground, collected data from the instruments and spacecraft at the rate of 4 kbps, and prepared data for transmission to the ground. The onboard tape recorders and data system allowed 24 hours of data to be transmitted to the ground in 9 minutes. Each instrument had a separate data stream located within a fixed part of the telemetry format. The data rate allocations for *DIRBE*, *FIRAS*, and *DMR* are 1716, 1362 and 250 bps, respectively. The remainder of the telemetry was assigned to spacecraft subsystems.

### 2.3.7 The Dewar

The dewar was a 650 liter superfluid helium cryostat designed to keep the *FIRAS* and *DIRBE* instruments cooled to less than 1.8 K for a minimum of six months. The *COBE* dewar was similar to that flown on the *IRAS* mission (Neugebauer *et al.* 1984). An aperture cover, sealing the dewar, permitted calibration and performance testing of the cryogenic instruments prior to launch. A contamination shield attached to the inside of the dewar cover protected the *DIRBE* primary mirror from particulate or gaseous contamination. It also protected *DIRBE* from emission from warm parts of the cryostat during ground testing. In orbit, the helium effluent was vented along the spin axis near the communications antennas.

### 2.3.8 The Sun-Earth Shield

The conical Sun-Earth shield protected the scientific instruments from direct solar and terrestrial radiation and provided thermal isolation for the dewar. The shield also provided the instruments with isolation from Earth-based RFI and from the spacecraft transmitting antenna. The shield was made of 12 honeycomb panels covered with multilayer insulating (MLI) blankets, alternating with flexible MLI segments. The outer layer of the MLI was aluminized Kapton to resist degradation due to the orbital bombardment by monatomic oxygen. The upper portion of the inner surface of the shield was covered with low emissivity aluminum foil to provide a high quality surface viewing the instrumentation. The shield was designed to be flexible and folded to fit within the Delta rocket fairing for launch.

## Chapter 3

# Flight Operations

### 3.1 Overview

#### 3.1.1 Mission Overview

*COBE* was launched aboard Delta rocket No. 189 at 1434 UT on 1989 November 18 from the Western Space and Missile Center at the Vandenberg Air Force Base in California into the desired orbit. The spacecraft and orbital characteristics are given in Table 3.1-1.

Table 3.1-1: *COBE* spacecraft and orbital characteristics

<b>Orbit</b>	
Altitude at insertion	900.2 km
Inclination	99°3
Eccentricity at launch	0.0006
Mean eccentricity over 1 yr	0.0012
Time of ascending node	6 pm
<b>Dimensions of spacecraft</b>	
Total mass	2270 kg
Length	5.49 m
Diameter	8.53 m (with solar panels deployed) 2.44 m (with solar panels folded at launch)
Orbital period	103 minutes (nominal)
Spacecraft rotation rate	0.8 rpm (nominal)
Power available	750 W
Data rate	4 kbps
<b>Dewar</b>	
Capacity available	650 liters
<b>At launch:</b>	
Fill	100%
Fill after pump down	92.7%
Internal temperature	1.7 K
<b>In orbit:</b>	
Internal temperature	1.4 K
Sun-Earth shield inner side temperature	180 K
Lifetime of helium in orbit	307 days

The dewar cover was ejected three days after launch, and the *DIRBE* instrument began to collect science data on the same day. During the first month in orbit, various tests were undertaken to evaluate the performance of the instruments and spacecraft, and to optimize instrument parameters.



All of the spacecraft systems operated well, allowing the mission design requirements to be achieved. According to plan, the satellite spin rate was increased in several small steps (see Table C.0-1) from an initial rate of  $\sim 0.23$  rpm, and the nominal 0.8 rpm spin rate was attained 9 days after launch. One of *COBE*'s transverse control axis gyros failed electrically on the fourth day after launch. However, because of redundancy built into the attitude control system, normal operations continued. The remaining gyros and all other spacecraft systems performed flawlessly during the lifetime of the cryogen. On 1991 September 7, one of the three gyros on the spin axis failed, and, once again, no data were lost. Fine aspect solutions were not carried out for three days while operational changes were made.

The spacecraft altitude decreased at the rate of 30 m per day during the first 10 months of flight, due largely to the thrust from the effluent helium. (The tilt-back of the spacecraft from the velocity vector described in §2.3.3 caused the venting helium to apply a small force opposite to the velocity.) This altitude loss did not pose a problem but had to be considered in the attitude reconstruction.

*COBE* operated in a routine survey mode. During the cryogenic lifetime, the satellite was periodically tilted a few degrees further away from the Sun than the nominal  $94^\circ$ . This maneuver was carried out at the beginning and end of each *FIRAS* calibration to ensure that the *FIRAS* external calibrator would not be exposed to direct sunlight.

The dewar performed thermally better than expected. In flight, the helium temperature inside the main cryogen tank was 1.40 K (the design requirement was 1.6 K). The temperature of the inner surface of the Sun–Earth shield was 180 K (the requirement was 220 K), allowing the outer dewar wall and cryogenic instruments to operate at colder temperatures. As expected, the Earth limb rose a few degrees above the Sun–Earth shield for a part of every orbit during a three month period starting in May. During this period (referred to as “eclipse season” for reasons described in §2.3.3), the Earth’s radiation produced thermal transients in the instruments and adversely affected data for a portion of each orbit. Some of these data were still usable after careful calibration (see §4.7.7). The 10–month lifetime of the cryogen is consistent with the detailed pre–launch model of the cryostat after taking into account Earth limb heating near the summer solstice, anomalous behavior in the *FIRAS* mirror transport mechanism (see §3.5.3.1), and the heat dissipated in normal operation and calibration cycles of the instruments.

The three instruments completed their first full sky coverage by mid–June 1990, and returned high quality data until the liquid helium ran out at 0936 UT on 1990 September 21. Once the cryogen was gone, the six longest wavelength bands of the *DIRBE* were turned off; data acquisition (including polarimetry) continued at 1.25, 2.2, 3.5 and 4.9  $\mu\text{m}$ , albeit at reduced sensitivity. Near–infrared sky maps of the large scale interplanetary dust signals continued to be of adequate quality to permit searching for evidence of temporal changes on annual time scales over a 4 yr period until all *COBE* operations were finally discontinued on 1993 December 23.

### 3.1.2 *DIRBE* Sky Coverage

*DIRBE*'s helical scans (see §2.3.4) covered the sky nonuniformly. Portions of the sky that were observed at the solar elongation extrema ( $\epsilon \sim 94^\circ \pm 30^\circ$ ) were scanned more frequently than regions that lay closer to the center of the viewing swath (at  $\epsilon \sim 94^\circ$ ). Furthermore, unlike directions within  $\sim 30^\circ$  of the ecliptic poles, which were observed year–round, sites along the ecliptic plane were in range for 2 months and then remained inaccessible for 4 months before coming back into view.

Figure 3.1-1 shows the depth of coverage attained (after rejection of low–quality data; see §4.7) during a typical week and for the entire cryogenic mission (10 months). In a week, a typical pixel was observed  $\sim 10$ – $15$  times, and the most densely–surveyed pixels, which delineate two circumpolar annuli at ecliptic latitudes,  $|\beta| \simeq 60^\circ$ , were observed  $\sim 80$ – $100$  times. Over the course of the cryogenic mission, most pixels were observed approximately 200 times, those at  $|\beta| \simeq 60^\circ$  were observed  $\sim 800$ – $1000$  times, and those at the ecliptic polar caps ( $|\beta| > 60^\circ$ ) were observed roughly 400–500 times. Because the cryogenic mission lasted for 10 months rather than a full year, coverage along the ecliptic equator is also uneven. The coverage was relatively sparse at ecliptic longitudes near  $120^\circ$  and  $300^\circ$ .

Table 3.1-2 lists a range of solar elongation angles and two ranges of ecliptic longitudes spanned by the *DIRBE* scan path at the ecliptic equator for each week of the cryogenic mission. Two ecliptic longitude ranges are given. Those denoted “Ascending” refer to ecliptic plane crossings from South to North;

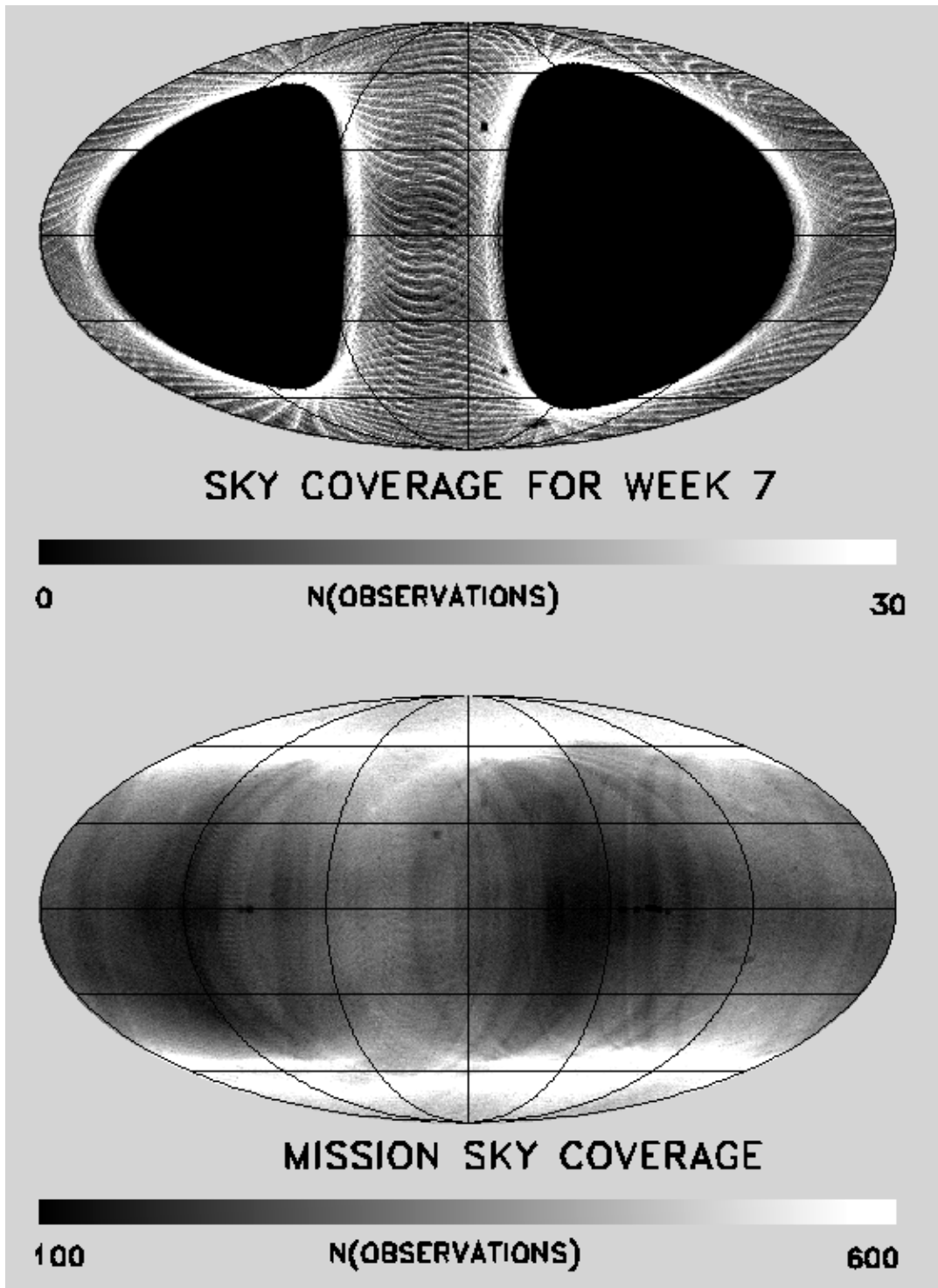


Figure 3.1-1: Number of observations per pixel for (a) week 7 and (b) the entire cryogenic mission. The maps are ecliptic coordinate projections.

Table 3.1-2: Weekly sky coverage

File	Week	Time interval (yyddd)	Elongation range (°)	Ecliptic longitude range (°)	
				Ascending	Descending
1	4	89345 – 89351	63 – 125	323 – 29	201 – 132
2	5	89352 – 89358	63 – 128	329 – 38	209 – 138
3	6	89359 – 89365	65 – 124	338 – 44	216 – 149
4	7	90001 – 90007	65 – 124	346 – 50	223 – 156
5	8	90008 – 90014	65 – 124	353 – 59	230 – 163
6	9	90015 – 90021	65 – 128	0 – 68	237 – 170
7	10	90022 – 90028	65 – 124	7 – 73	244 – 178
8	11	90029 – 90035	65 – 124	14 – 80	251 – 185
9	12	90036 – 90042	65 – 124	21 – 87	258 – 192
10	13	90043 – 90049	65 – 128	28 – 98	265 – 199
11	14	90050 – 90056	65 – 124	35 – 101	272 – 206
12	15	90057 – 90063	65 – 124	42 – 109	277 – 213
13	16	90064 – 90070	65 – 124	49 – 116	286 – 220
14	17	90071 – 90077	65 – 126	56 – 124	292 – 227
15	18	90078 – 90084	65 – 124	63 – 129	295 – 234
16	19	90085 – 90091	62 – 124	69 – 136	305 – 241
17	20	90092 – 90098	65 – 124	77 – 143	314 – 248
18	21	90099 – 90105	65 – 124	84 – 150	321 – 255
19	22	90106 – 90112	63 – 128	94 – 156	330 – 259
20	23	90113 – 90119	63 – 122	99 – 161	337 – 271
21	24	90120 – 90126 <sup>a</sup>	62 – 122	102 – 168	344 – 278
22	25	90127 – 90133	62 – 122	109 – 175	350 – 286
23	26	90134 – 90140	62 – 128	116 – 183	356 – 286
24	27	90141 – 90147	64 – 123	124 – 189	2 – 297
25	28	90148 – 90154	63 – 122	132 – 194	10 – 303
26	29	90155 – 90161	63 – 122	136 – 202	17 – 311
27	30	90162 – 90168	63 – 122	143 – 208	23 – 318
28	31	90169 – 90175	63 – 122	149 – 215	30 – 324
29	32	90176 – 90182	63 – 124	156 – 223	37 – 329
30	33	90183 – 90189	63 – 122	163 – 228	44 – 338
31	34	90190 – 90196	63 – 122	169 – 235	50 – 344
32	35	90197 – 90203	63 – 126	176 – 246	57 – 351
33	36	90204 – 90210	63 – 122	183 – 249	64 – 358
34	37	90211 – 90217	63 – 124	190 – 257	67 – 6
35	38	90218 – 90224	65 – 124	198 – 264	76 – 7
36	39	90225 – 90231 <sup>a</sup>	65 – 124	205 – 271	82 – 14
37	40	90232 – 90238 <sup>a</sup>	65 – 129	212 – 278	89 – 23
38	41	90239 – 90245	65 – 128	218 – 285	95 – 29
39	42	90246 – 90252	65 – 129	225 – 294	102 – 35
40	43	90253 – 90259	65 – 127	232 – 300	109 – 43
41	44	90260 – 90264	65 – 129	239 – 305	113 – 50

<sup>a</sup> coverage reduced due to JFET-off test.

“Descending” scans cross the ecliptic plane from North to South. To first order, the elongation range was constant ( $64^\circ \leq \varepsilon \leq 124^\circ$ ). However, small perturbations in elongation coverage were introduced during the eclipse season (see §2.3.3) and during roll maneuvers (see §3.1.1), and the coverage was extremely sparse during JFET-off test periods (see §3.3.2).

## 3.2 *DIRBE* Operations

### 3.2.1 Launch to End of Cryogen

During the three-week period following launch the *DIRBE* instrument’s functionality was verified and the operating parameters were optimized. The instrument was found to be operating normally, except for the 100  $\mu\text{m}$  annealing heater, which had failed prior to launch (see §3.5.1). As expected, the initial detector operating parameters chosen on the basis of ground tests were not ideally-suited to operation in space. Thus, although the sky was observed, data obtained during the verification period are of limited scientific value. By 1989 November 28 the dewar had stabilized and optimization tests were begun. The objective of these tests was to find detector bias settings, static heater levels, multiplexor (MUX) sampling positions, commandable gains, etc. that provided the highest signal-to-noise ratio for sky signals, and yet maintained detector linearity.

Table 3.2-1: Nominal detector operating parameters: cryogenic era

Detector	MUX position <sup>a</sup>	Data delay <sup>a</sup>	Bias <sup>b</sup> (V)	Heater <sup>b</sup> (V)	Commanded <sup>c</sup> gain	DC <sup>d</sup>	DGL <sup>e</sup>
1A	6	5	.149	.498	G1 (3)	IN	OFF
1B	7	5	.149	.498	G1 (3)	IN	OFF
1C	5	5	.149	.498	G1 (3)	IN	OFF
2A	10	5	.149	.498	G1 (3)	IN	OFF
2B	16	5	.149	.498	G1 (3)	IN	OFF
2C	1	6	.149	.498	G1 (3)	IN	OFF
3A	9	5	.149	.498	G1 (3)	IN	OFF
3B	13	5	.149	.498	G1 (3)	IN	OFF
3C	14	5	.149	.498	G1 (3)	IN	OFF
4	11	1	.149	.498	G1 (3)	IN	OFF
5	3	5	1.103	.23	G0 (1)	IN	OFF
6	15	5	1.103	.23	G0 (1)	IN	OFF
7	2	1	.24	.192	G0 (1)	IN	OFF
8	8	1	.24	broken	G0 (1)	IN	OFF
9	4	4	2.682	N/A	G1 (3)	IN	OFF
10	12	4	1.907	N/A	G1 (3)	IN	OFF

<sup>a</sup> Settings result in optimal phasing of science data samples with respect to chopper cycle at nominal operating temperature (see §2.2.6).

<sup>b</sup> Settings optimize detector linearity and signal-to-noise at nominal operating temperature. The quoted heater settings are those used during normal science data mode, not during thermal annealing (see §2.2.2).

<sup>c</sup> Analog gain chosen to maximize dynamic range in the digitized data without saturating in sky or calibration modes (see §§2.2.5 and 3.3.2.3).

<sup>d</sup> IN indicates “DC offset injected.”

<sup>e</sup> With on-board deglitching (DGL) activated (ON), the microprocessor would reject high and low chopper cycle samples and average the remaining two samples to yield an SDM datum; with DGL OFF, all four chopper cycle samples were combined into an SDM datum.

Routine survey work commenced on 1989 December 11 at 01:04 UT, when the *DIRBE* was configured with the final detector operating parameters chosen for the cryogenic mission (Table 3.2-1). The strategy

ultimately adopted to compensate for the failure of the 100  $\mu\text{m}$  annealing heater (see §3.5.1) was implemented on 1990 January 1. Until then, a variety of annealing “recipes” were tested (see §3.5.1).

Aside from the routine characterization and monitoring tests discussed in §3.3, the *DIRBE* configuration remained stable for the rest of the cryogenic mission, with two exceptions. The first was a test conducted between 1989 December 29 03:22 UT and 1989 December 30 01:57 UT, in which the bias voltage on the 60  $\mu\text{m}$  detector was temporarily changed in order to examine the effect of bias voltage on noise. After the test, the voltage was reset to the value shown in Table 3.2-1. The second configuration change was designed to reduce the lunar-induced noise described in §4.7.5 and involved powering off the band 1B (1.25  $\mu\text{m}$ ) detector twice a month when the Moon came into view. That change was initiated on 1990 August 29. Various possible noise suppression procedures were tested during the period from 1990 July 10 to 16 (see Appendix C). The procedure finally adopted involved reactivating the band 1B detector about 6 days after it was turned off, when the Moon was no longer visible.

### 3.2.2 End of Cryogen to End of Mission

Following cryogen depletion, the 1.25, 2.2, 3.5, and 4.9  $\mu\text{m}$  detectors continued to operate with sensitivity decreased by about an order of magnitude (largely due to the decrease in load resistance). By November 1991, 14 months into the “warm era,” the temperature at the *DIRBE* detectors had climbed to about 50 K. Useful data were obtained over a period that lasted until December 1993. The *DIRBE* warm-era data, which have potential to aid in modeling the zodiacal dust, in particular its evolution and dynamics, may prove useful in the search for the CIB.

## 3.3 *DIRBE* Characterization and Monitoring Tests

On-orbit operations were tailored to produce as much survey data as possible while retaining full knowledge of the performance of the instrument. Some instrument characterization procedures were followed regularly each day while others were carried out occasionally as deemed necessary.

### 3.3.1 Daily Events

The procedures described in Table 3.3-1 were repeated throughout the mission, allowing the system gains and offsets to be monitored as a function of time. To determine electrical and radiative offsets the instrument signal was measured with the shutter closed and the internal reference source (IRS) off. Then the IRS was turned on at various fixed levels to check the system gain. Following each calibration sequence, the *DIRBE* was commanded over to the survey mode and the shutter was opened.

The basic calibration sequence (“IRS run”) shown in the first row of Table 3.3-1 was performed about six times per orbit.<sup>1</sup> Because of the destabilizing effects on detectors of the intense ionizing radiation present in the South Atlantic Anomaly, calibration runs were conducted upon entering and exiting the SAA. The detectors were annealed after each SAA crossing prior to the IRS run. Accounting for routine interruptions, survey data were obtained approximately 82% of the time, yielding 560,000  $\frac{1}{8}$ -second science mode samples per day.

### 3.3.2 Special On-orbit Tests

In addition to the daily calibration activities, special on-orbit tests were conducted to monitor detector linearity, contributions to the instrumental offsets from heat produced by the JFET amplifiers, and stability of the analog commandable gain.

---

<sup>1</sup>Upon entering and exiting the Van Allen belt surrounding the North magnetic pole (NVAB); upon entering and exiting the Van Allen belt surrounding the South magnetic pole (SVAB); upon entering and exiting the South Atlantic Anomaly (SAA); and at a random time in the first and second halves of each day.

Table 3.3-1: Non-survey daily operations

Purpose	Frequency (times/day)	Procedure
<b>Basic calibration sequence</b> <ul style="list-style-type: none"> <li>• Measure detector offsets in science data mode (SDM); and</li> <li>• Measure relative detector gain</li> </ul>	$\sim 75$	<ul style="list-style-type: none"> <li>• Close the shutter and observe the dark response of the detectors for 32 seconds; and</li> <li>• Operate one of the IRS sources under an on-board source-driving program.<sup>a</sup> Following IRS exposure, keep the shutter closed and check for normal detector recovery.</li> </ul>
Measure detector response to redundant Internal Reference Sources in case the primary IRS fails	$\sim 2$	Make back-to-back observations <sup>a</sup> of the sources designated “primary” and “secondary” at least once per day; make additional observations of all four calibration sources back-to-back once per day, either upon exiting the Van Allen belt surrounding the North magnetic pole (NVAB) or upon entering the southern Van Allen belt (SVAB). The primary/secondary source measurements were made more frequently (at every NVAB exit) after 1990 July 7.
Anneal detectors to remove effects of SAA passage	$\sim 11$	Heat 60 $\mu\text{m}$ detector to $\sim 20$ K and simultaneously flood detectors with radiation from a backup IRS bright enough to saturate 60 and 100 $\mu\text{m}$ detectors.
Measure detector offsets and evaluate noise in SNAP mode (see §2.2.6)	$\sim 1$	Observe shutter-closed dark response for every detector at $2\times$ the synchronous demodulation sampling rate <sup>b</sup>

<sup>a</sup> In the standard program the source voltage was ramped up in staircase fashion: the voltage was incremented by a known amount, held constant for 2 seconds, and then incremented again. The process was repeated 32 times.

<sup>b</sup> These data also provide information on the electronics transfer function, since the response to a charged-particle-induced delta function input is seen occasionally.

### 3.3.2.1 Linearity Tests

**Interlocked IRS tests** involved closing the shutter, running a reference source (IRS) through an illumination sequence (step ramp), pausing, running a second IRS through a similar sequence, and then running both sources through the sequence together, with one sequence starting later than the other. Linearity was measured at various levels of illumination by comparing the response of the detectors to the individual sources to the response to the summed intensity.

**“Shutter flutter” tests** involved closing and opening the shutter at several-second intervals while the IRS was on, thus exposing the detectors alternately to an IRS and the sky. These tests measured the time required for the detectors to stabilize following a change in the level of illumination, as well as the linearity in recovery following exposure to a variety of intensities. The Mission Events Log in Appendix C shows when these tests were conducted.

**Absolute differential linearity tests** were designed to determine the response of the detectors to an impulse of fixed brightness seen against various background brightness levels. An IRS staircase ramp sequence was run in which the source voltage was increased by a known increment, held fixed for 32 seconds, and then incremented again to form the background. A second IRS source was activated during each background step for 12 seconds at a fixed voltage.

### 3.3.2.2 JFET-off Test

Normally the JFET amplifiers, which are components of the preamplifiers of all the detectors, are on at all times. Although the JFETs are thermally isolated from the detectors, their thermal radiation could be injected “upstream” of the chopper, modulated, and appear as a component of the 32 Hz signal at the detectors. JFET thermal radiation was detectable at long wavelengths.

A “JFET-off” test was designed to measure the radiative contribution to the detector offsets attributable to the JFETs. The test sequence took a week to execute and consisted of the following steps:

**Day 1:** Turn off JFETs for bands 1–6; take data in bands 7–10;

**Day 2:** additionally turn off band 7 JFET; take data in bands 8–10;

**Day 3:** additionally turn off band 8 JFET; take data in bands 9 and 10;

**Days 4–6:** continue data collection in bands 9 and 10;

**Day 7:** activate JFETs in groups of detectors in the following sequence: bands 4–8, bands 1–3 A and B channels, bands 1–3 C channels.

Normal daily operations continued during the test, except that special monitoring was done with the shutter closed while the JFETs cooled. The JFETs for bands 9 and 10 were not turned off because detector assembly no. 3, which held the 140 and 240  $\mu\text{m}$  detectors, was enclosed in a light-tight environment; these JFETs had no potential to affect any of the detectors.

Two JFET-off tests were performed during the cryogenic mission, one that lasted from 1990 April 30 – May 6 (90120 – 90126), and another from 1990 August 15 – 21 (90227 – 90233). Relatively little science data was obtained during these periods.

### 3.3.2.3 Analog Gain

The relative values of the analog commandable gains were measured prior to launch. Gain stability was checked five times on-orbit during the cryogenic period by closing the shutter and feeding square wave electrical test signals of various amplitudes directly into the analog signal processing electronics. The detectors were bypassed, but the signal propagated through the rest of the electronics as if it had been observed by the detectors.

## 3.4 Anticipated Environmental Influences

### 3.4.1 Nuclear Radiation Effects on Detectors

The effects of ionizing radiation on the detectors were anticipated before launch. Ground tests in proton beams showed that the Ge:Ga detectors became noisier and changed in responsivity when exposed to ionizing radiation doses comparable to the expected one-pass SAA dose.

In flight, there were both short and long term effects. When ionizing particle hits were infrequent, the interactions caused transient events (“glitches”) in the detectors which were recognized by their short duration (shorter than the passage of a point source) and removed from the data stream in the ground data processing. When particle hit rates were very high, such as in the SAA, the data were corrupted and unsalvageable (see §4.7, in which Figure 4.7-1 shows the 100  $\mu\text{m}$  glitch frequency as a function of satellite position over the surface of the Earth).

Some of the detectors, particularly the Ge:Ga photoconductors (60 and 100  $\mu\text{m}$  bands), did not return to nominal operating condition for a long time after exposure to a high dose of ionizing radiation. An overbiasing technique intended to improve detector stability was used on the Infrared Astronomical Satellite (*IRAS*; Neugebauer *et al.* 1984), but the technique was only modestly successful. Prelaunch tests on the *DIRBE* Ge:Ga detectors showed that elevating the temperature of the detectors would produce a much more rapid and reliable return to stable operating conditions. A small resistive heater was attached to a thermally isolated detector mount under each *DIRBE* detector to control the operating temperature and permit thermal annealing for the effects of radiation. Command sequences were developed to provide the short term heating required to anneal the detectors and restore them to nominal operating conditions. Unfortunately, the 100  $\mu\text{m}$  heater was found to be defective late in ground testing, and a modified annealing procedure had to be implemented (see §3.5.1).

### 3.4.2 Photon-induced Responsivity Enhancement

“Photon-induced responsivity enhancement” (PIRE) refers to the effect of *previous* illumination on a detector’s current response to incident light. PIRE was detected and its magnitude estimated by taking advantage of the fact that the photometric history of the instrument before it observed each pixel depended upon the approach direction; the difference in brightness measured at a pixel when it was approached from different scan directions was used to estimate the size of the enhancement. The magnitude of the PIRE effect reached 30–40% at 100  $\mu\text{m}$  and about 5% at 60  $\mu\text{m}$  near the brightest parts of the Galactic plane; the effect was very small (less than a few percent in individual observations) at other wavelengths. Corrections made to mitigate the effect at 100  $\mu\text{m}$  and residual errors will be discussed in Chapter 4.

### 3.4.3 Thermal Changes Within the Dewar

The temperature within the *COBE* dewar varied during the mission as a result of both external and internal influences (*e.g.*, solar eclipses, changes in the instrument operating mode, anomalous behavior of the *FIRAS* mirror transport mechanism). The temperature was monitored at a rate of one reading per 32 seconds by 15 Germanium Resistance Thermometers (GRTs) mounted at various places on the *DIRBE* optical module. There were two GRTs on each of the three detector assemblies. The detector temperature data were used to correct for thermally induced gain variations (see §4.5.3). Thermal effects were further suppressed by disregarding the data obtained with a detector when its temperature exceeded a detector-dependent threshold value (see §4.7.7). Because these measures were taken, the residual errors in the data products due to temperature variations are negligible.

### 3.4.4 Thermal Changes External to the Dewar

With the onset of eclipse season (see §2.3.3) in May 1990, the temperature of the *DIRBE* warm electronics (external to the dewar) began dropping from a nominal value of  $\sim 21$  °C to a minimum of  $\sim 16$  °C at longest eclipse duration. The chopper drive electronics were temperature sensitive and the chopper phase changed as the temperature changed. Depending upon a detector’s sampling position within the



MUX (see §2.2.6 and Table 3.2-1), the detector responsivity was either enhanced or depressed as the chopper phase changed. Smooth, long-term responsivity variations due to this effect were calibrated out through the use of celestial standards (see §4.5).

### 3.4.5 Atmospheric Glow

Constituents of the Earth’s atmosphere at *COBE*’s orbital altitude can be induced to glow by collisions with the spacecraft. Neutral atomic oxygen, for example, has emission lines at 63 and 147  $\mu\text{m}$ . The telltale sign of atmospheric glow is brighter emission in the forward ram direction.

Like PIRE, evidence for atmospheric glow was sought by comparing observations of selected celestial directions made from opposite “approach vectors” along the *DIRBE* scan path, taking advantage of the fact that many pixels approached from one direction were approached and reobserved a short time later from a different direction. The approach vectors are denoted AV1 and AV2, the former vector having a component in the direction of spacecraft motion in which atmospheric glow emission, if present, would have been brighter.

Isolation of atmospheric glow effects from others that contributed to approach vector differences proved difficult. Neither visual inspection of AV1 – AV2 maps nor detailed studies of selected patches of the sky yielded convincing evidence of atmospheric effects distinguishable from residual PIRE, IRS-induced gain changes, or beam offset effects in any photometric band.

## 3.5 *DIRBE* Malfunctions and *COBE* Influences

### 3.5.1 Band 8 Annealing Heater

Shortly before launch the 100  $\mu\text{m}$  (band 8) annealing heater was found to have failed. It was too late to repair the problem. Tests were conducted in flight between 1989 December 11 and 1990 January 1 in order to devise a new annealing strategy. Various combinations and durations of overbiasing and illumination with the internal calibration sources were considered. The annealing procedure adopted on 1990 January 1 consisted of exposing the focal plane to intense light from an IRS for 100 s. The 100  $\mu\text{m}$  data obtained prior to 1990 January 1 are of lower quality than the data obtained later in the mission. A particularly ineffective annealing procedure was used during 1989 December 12 – 17; the band 8 data obtained during that period were excluded from the data products.

The 60  $\mu\text{m}$  (band 7) annealing heater remained functional throughout the cryogenic mission. No other detectors were annealed with their heaters. An analysis of calibration data obtained prior to and following passage through the SAA indicated that response changes in the other detectors were no greater than 1% without heater annealing.

### 3.5.2 Primary IRS

Starting in May 1990 (around day 90135), the detectors began to register an increasing brightness from the primary IRS. This trend continued into the eclipse season, which started a couple of days later. Since the detector response to the secondary IRS, which had been monitored throughout the mission, remained constant, the anomalous behavior was attributed to the primary IRS. On 1990 July 7 (day 90188), the secondary IRS was substituted for the primary as the main internal reference source and thereafter monitored frequently. The original primary source continued to be monitored, but less frequently.

### 3.5.3 *FIRAS* Influences

Two *FIRAS* mechanisms occasionally influenced the performance of the *DIRBE*. According to detector temperature and signal-to-noise constraints described in §§4.7.7 and 4.7.5, respectively, the affected *DIRBE* observations were identified during data processing and excluded from the data products (see §§5.6.4 and 5.6.8).

### 3.5.3.1 *FIRAS* Mirror Transport Mechanism

Early in the mission, especially during passes through the SAA, the *FIRAS* mirror transport mechanism (MTM) driver electronics behaved anomalously and allowed the MTM to continue driving against one of its stops. The *DIRBE* detected these events as thermal spikes triggered by the anomalously high energy delivered to the dewar and as high frequency (microphonic) noise. The precise times of these events are given in the Mission Events Log (Appendix C). At other times the *FIRAS* MTM moved smoothly and was not detected by *DIRBE*. The anomalous behavior of the MTM was eliminated by operational changes instituted after 1990 March 20.

### 3.5.3.2 *FIRAS* External Calibrator

The *FIRAS* external calibrator (XCAL), a temperature-controlled precision blackbody source, was occasionally inserted into the mouth of the *FIRAS* antenna. *FIRAS* calibrations were performed throughout the mission with the XCAL set to different temperatures. These calibrations had two effects on the *DIRBE* instrument. First, the XCAL caused the *COBE* dewar temperature to rise. Second, microphonic noise was triggered by the motion of the XCAL. The microphonics affected *DIRBE* detector assembly 2 (bands 4–8), especially the 4.9 and 60  $\mu\text{m}$  bands, and took  $\sim 75$  s to subside after the XCAL was stowed.



## Chapter 4

# Data Processing and Instrument Characterization

*This chapter is in preparation.*

## 4.1 Overview of Data Processing

### 4.2 Beam Profile

#### 4.2.1 Shape

#### 4.2.2 Centroids

Table 4.2-1: Beam centroids and solid angles

Band	Time range <sup>a</sup>	Centroid position		Solid angle	
		Along-scan ( $\mu$ )	Cross-scan ( $\mu$ )	$\Omega$ ( $10^{-4}$ sr)	Uncertainty (%)
1A	89345–90176	0.86	-1.66	1.198	0.28
	90176–90232	0.88	-2.35		
	90232–90260	1.15	-2.16		
1B	89345–90176	0.40	3.10	1.174	0.56
	90176–90232	0.38	2.48		
	90232–90260	0.58	2.66		
1C	89345–90176	0.06	0.82	1.331	0.26
	90176–90232	0.02	0.16		
	90232–90260	0.30	0.30		
2A	89345–90176	-0.67	1.02	1.420	0.27
	90176–90232	-0.66	0.39		
	90232–90260	-0.40	0.57		
2B	89345–90176	0.22	1.60	1.324	0.35
	90176–90232	0.20	1.02		
	90232–90260	0.48	1.14		
2C	89345–90176	0.14	0.03	1.323	0.34
	90176–90232	0.11	-0.63		
	90232–90260	0.38	-0.46		
3A	89345–90176	-0.61	-0.86	1.285	0.25
	90176–90232	-0.61	-1.56		
	90232–90260	-0.30	-1.32		
3B	89345–90176	-1.62	1.98	1.291	0.22
	90176–90232	-1.63	1.34		
	90232–90260	-1.35	1.58		
3C	89345–90176	-0.65	-0.75	1.282	0.35
	90176–90232	-0.69	-1.46		
	90232–90260	-0.40	-1.19		
4	89345–90176	-2.91	1.37	1.463	0.13
	90176–90232	-2.96	0.68		
	90232–90260	-2.61	0.95		
5	89345–90260	-0.80	1.06	1.427	0.97
6	89345–90260	-0.01	1.05	1.456	1.29
7	89345–90260	-2.97	0.72	1.512	2.69
8	89345–90260	-1.59	0.45	1.425	4.17
9	90046–90116	-1.48	0.73	1.385	2.26
10	90046–90116	-1.27	1.18	1.323	3.41

<sup>a</sup> Time interval over which data were selected for beam profile formation.

4.2.3 Solid Angles

4.3 Attitude Determination

4.4 Stray Light Rejection

4.4.1 Near Field

4.4.2 Far Field

4.5 Photometry

4.5.1 The *DIRBE* Signal Equation

4.5.2 Offsets

4.5.3 Gain

4.5.4 Photometric Calibration Uncertainty

4.5.5 Sensitivity

4.5.6 Comparison of *DIRBE* and *FIRAS* Calibration

4.5.7 Comparison of *DIRBE* and *IRAS* Calibration

4.6 Polarimetry

4.6.1 Method

4.6.2 Calibration

4.6.3 Accuracy

## 4.7 Exclusion of Low Quality Data

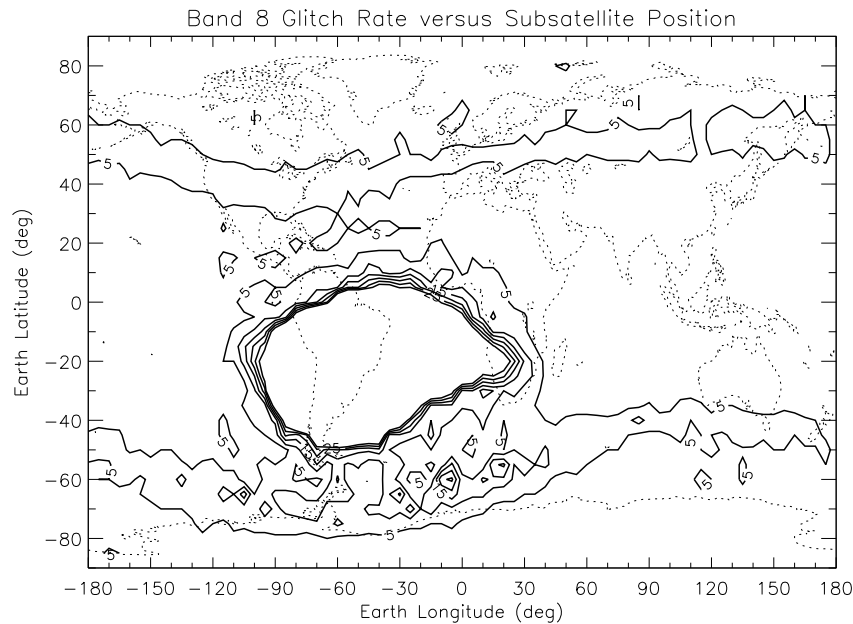


Figure 4.7-1: Number of glitches at  $100\ \mu\text{m}$  as a function of Earth longitude and latitude.

### 4.7.1 Pre-optimization Data

### 4.7.2 Bright Source Exclusion Zones

### 4.7.3 Recovery from Moon Passages

### 4.7.4 SAA Passages

### 4.7.5 Unusually Noisy Data

### 4.7.6 Special Pointing

### 4.7.7 Focal Plane Temperature Constraints

### 4.7.8 *FIRAS* Calibrations

### 4.7.9 Robust Averaging

## 4.8 Known Processing Deficiencies

### 4.8.1 AC *vs.* DC Calibration at $60$ and $100\ \mu\text{m}$

### 4.8.2 DC Linearity Uncertainties at $60$ and $100\ \mu\text{m}$

### 4.8.3 Limitations of PIRE Correction

### 4.8.4 Long-term Photometric Variations

Table 4.7-1: Interpretation of Sentinel Values

Value <sup>a</sup>	Symbol	Interpretation
-16375	BAD_DATA_VALUE	If floating point SDM data value is less than or equal to this value, it is a saturated, missing, or otherwise bad data point.
-16378	DET_OFF_VALUE	If a detector is off in the DARELAYS array then the half minor frame is set to this value.
-16379	QUEST_HMNF_VALUE	If a bit is set in DAMMNFLGS(8) then the minor frame is question- able. Its half minor frame values are set to this value.
-16380	GLITCH_FLAG_VALUE	Value used by BLI to replace photometry values identified as glitches.
-16381	NOT_PROCESSED	Value which replaces original photometry values for detectors not processed, in floating- point TOD data.
-16382	SAT_SIGNATURE	Marks a saturated point in floating-point TOD data.
sat_signature	SKY_SAT_SIGNATURE	Marks a saturated point in skymap data
-16383	TRASHED_SIGNATURE	Data trashed by command
-16384	TEMP_OUT_OF_RANGE	Temperature outside correctable range
-16385	PHASE_OUT_OF_RANGE	Phase outside correctable range
-16386	BIAS_OUT_OF_RANGE	Detector bias outside correctable range
-16387	ATH_OUT_OF_RANGE	ATH (heater) setting outside correctable range
-16388	BAD_IRSCC_FLAG	Value used by BLI to flag the SDM data, if IRS calibration coefficients are bad
-16389	MNF_PARITY_MISMATCH	MNF has parity of detector words disagreeing with parity defining T/M bits.
-16390	NO_ROBUST_AVERAGE	Value used in sky maps to flag where a robust average has been rejected.
-16391	EXCLUDED_DATA	Value used to flag data falling within excluded time ranges. (See BEX_ED)
-16392	INTERPOLATION_SKIPPED	Data did not satisfy criteria for interpolation/extrapolation by BCS
-16393	INTERPOLATION_FAILED	Numerical failures for both methods of elongation interpolation in BCS
-16394	NO_CEL_CALIB	Failure for celestial calibration of photometry
-16395	NO_ABS_CALIB	Failure for absolute calibration of photometry
-16396	NO_POLARIZ_RATIOS	No valid polarization ratios available to form Stokes
-16397	BAD_ORIENTATION	Failure to form Stokes due to bad polarization orientation
-16398	NO_POLARIZ_SOLUTION	Failure to form Stokes due to insoluble simultaneous eqns.
-16399	GRT_NOT_SAMPLED	GRT was not sampled during this half minor frame
-16400	TOO_CLOSE_IRS_OR_ANL	The time since IRS or Anneal was too close (script specified) to processing time for the Time since IRS gain correction.
-16401	NO_HYST_CORRECTION	Could not correct for hysteresis.
-16402	BAD_OR_NO_RAD_OFFSETS	Radiative offsets were bad or not available.
-16403	EXCLUDED_ZONE	Data falling within excluded zone (set by BPW).
-16404	GLITCHY_MF	When the flags for BLI glitch detection red limits exceeded. (set by BPW).

<sup>a</sup> If the DADRBSCI2 value reported in the Time-Ordered Data (see Table 5.7-2) is less than -28358, add 11985 to derive the corresponding sentinel value.





# Chapter 5

## *DIRBE* Data Products

### 5.1 Overview

Brief descriptions of the *DIRBE* data products were given in §1.3. To make the Annual Average Sky Maps and Solar Elongation ( $\epsilon$ ) = 90° Sky Maps network-accessible and easy to use, they were broken up into files containing data for individual wavelength bands. The Weekly Sky Maps, which are designed to preserve information about the temporal variation of sky brightness stemming from a variable viewing perspective relative to the interplanetary dust (IPD) cloud, and other relatively large files are available from the NSSDC on CD-ROMs or tape. The network-accessible data products may be obtained by anonymous ftp from [cobe.gsfc.nasa.gov](http://cobe.gsfc.nasa.gov), or through the World Wide Web from the COBE Home Page ([http://www.gsfc.nasa.gov/astro/cobe/cobe\\_home.html](http://www.gsfc.nasa.gov/astro/cobe/cobe_home.html)). Table 5.1-1 lists the data products, shows how they are divided into files, and indicates how the files may be obtained.

Final (“Pass 3B”) versions of the Project Data Sets <sup>1</sup> described in §5.7 were released in March 1997. These **supersede the “Pass 2B” versions** and include calibration and data quality improvements. The most notable change compensates for an error made in our application of the Sirius spectrum to calibrate the Pass 2B products, Sirius being the source used for absolute calibration at the five shortest *DIRBE* wavelengths (see §4.5.3): Pass 3B 1.25 - 12  $\mu\text{m}$  intensity values are 5% lower than the corresponding Pass 2B values. Further changes designed to improve the stability of the relative calibration as a function of time affected mainly the long wavelength photometry. Finally, a better algorithm was used to calculate weekly-averaged intensity values (see §4.7.9), yielding more reliable photometry. The resulting improvement can be seen in a small number of sparsely sampled pixels where the Pass 2B data were anomalous, especially at 60 and 100  $\mu\text{m}$ .

In addition to the calibration and data processing refinements noted above, slight changes were made in the data file formats. Standard FITS readers will now properly interpret the “binned quantities” and  $\Delta$ Time values in the Weekly Sky Maps, and the sky coordinates recorded in the Galactic Plane Maps, rendering sections 5.7.2.1, 5.7.2.2 and 5.7.4.1 obsolete. Also, the Beam Profile Maps are normalized and sampled differently.

---

<sup>1</sup>The version is specified in the FITS primary header.

Table 5.1-1: *DIRBE* data products

Product	Contents	# files	MB/file	Format	Distrib. <sup>a</sup> medium
Time-Ordered Data	Calibrated time-ordered data; 1 file per week of optimized cryogenic operation	41	190	Native	t
Calibrated Individual Observations (CIO)	$\frac{1}{8}$ th sec sampled sky survey data listed in pixel order for each day of the cryogenic mission	285	60	FITS binary table	n,c,t
CIO Pixel Index	Specifies which pixels are covered in each daily CIO file, and which rows in the CIO file contain data for a given pixel	285	1	FITS binary table	n,c,t
Weekly Sky Maps	Weekly-averaged intensities for 10 bands and Stokes Q and U parameters for 1.25, 2.2, and 3.5 $\mu\text{m}$ bands; 1 file per week	41	28	FITS binary table	n,c,t
<i>DIRBE</i> Calibrated Annual File (DCAF)	Merged, pixel-ordered, weekly-averaged intensities for cryogenic mission. One file per face of the skycube.	6	$\sim 200$	FITS binary table	n,c,t
DCAF Pixel Index	Specifies which rows in the DCAF file contain data for each <i>DIRBE</i> pixel, and for which weeks of the mission	6	1	FITS binary table	n,c,t
Annual Average Sky Maps	Average of intensities for all 10 bands over the entire cryogenic mission; 1 file per band	10	11	FITS binary table	n,c,t
$\varepsilon = 90^\circ$ Sky Maps	Intensities for all 10 bands for the special case of $\varepsilon = 90^\circ$ ; 1 file per band	10	13	FITS binary table	n,c,t
Galactic Plane Maps	Galactic Plane subset of the $\varepsilon = 90^\circ$ Sky Maps; limited to a 6 month interval	1	6	FITS binary table	n,c,t
<i>DIRBE</i> Sky And Zodi Atlas (DSZA)	Augmented form of the DCAF; includes a modeled IPD intensity for each week and each wavelength.	6	$\sim 200$	FITS binary table	n,c,t
Pixel Index to DSZA	Analogous to the DCAF Pixel Index, but for the DSZA.	6	1	FITS binary table	n,c,t
Zodi-Subtracted Mission Average Maps (ZSMA)	Average sky brightness after removal of the <i>DIRBE</i> IPD model for each of the 10 wavelength bands	10	6.3	FITS binary table	n,c,t
Photometric Standard Values	Names, positions, and photometric data for the 92 objects used to establish the baseline relative celestial calibration system	1	0.01	FITS binary table	n,c,t
Solar System Objects Data	<i>DIRBE</i> observations of Mars, Jupiter, Saturn, Uranus, Ceres, Pallas, and Vesta, including flux density measurements and ancillary data	7	0.05	FITS binary table	n,c,t

Faint Source Model	Predicted contribution to the diffuse sky brightness due to (faint) stars and other discrete Galactic sources. Model sky maps at 1.25, 2.2, 3.5, 4.9, 12 and 25 $\mu\text{m}$ .	6	5	FITS binary table	n,c,t
Beam Profiles	Effective two-dimensional shape of <i>DIRBE</i> beam for each detector	16	0.5	FITS image	n,c,t
Color Corrections	Color correction factors needed in case source spectrum is not $\nu I_\nu = \text{constant}$	1	0.04	ASCII	n,c,t
System Responses	Normalized system spectral response functions for each wavelength band	1	0.06	ASCII	n,c,t

<sup>a</sup> Data available from the NSSDC on tape (t), CD-ROM (c), or by anonymous ftp over the network (n).

## 5.2 Creation of *DIRBE* Data Products

Telemetry data from the *DIRBE* instrument were calibrated and converted to useful data products via the sequentially executed set of programs described in Chapter 4. This section briefly describes the processing steps that led to the creation of the individual data products.

### 5.2.1 Initial Pipeline Processing Stages

The unprocessed *DIRBE* science data consisted of consecutive  $\frac{1}{8}$ -second sampled observations of the sky brightness. At the survey scan rate, point sources were visible in the field of view for 0.3 s, during which time 2.4 samples were obtained. The attitude solution used to determine the line-of-sight for each sample was based upon data from the spacecraft Sun and Earth sensors and gyros, with fine corrections based upon the locations of isolated bright stars detected in the *DIRBE* 2.2  $\mu\text{m}$  band. The rms accuracy of the attitude solution is approximately 1.5'. Sky observations were routinely interrupted when the *COBE* spacecraft passed through the South Atlantic Anomaly (SAA) or when the instrument calibration stability was checked. The time-ordered sky observations had instrument offset signals removed and were calibrated photometrically relative to the *DIRBE* Internal Reference Source (IRS) (see §4.5). They were then made into daily sky maps by associating each sample with a pixel on the sky. Pixel area and location were determined according to the adopted map projection, the *COBE* Quadrilaterized Spherical Cube (CSC) in ecliptic J2000 coordinates (see §5.3). On average, in that half of the sky covered, each pixel in a daily sky map was observed about 2.4 times, but the sampling was much denser for pixels near the edges of the viewing swath (solar elongation angles near 64° and 124°) than for those near the middle (see §3.1.2).

### 5.2.2 Creation of Calibrated Individual Observations

The photometric data in the daily sky maps described in §5.2.1 were corrected for the subsequently determined long-term response trends and absolute calibration factors in order to create the Calibrated Individual Observations (CIO) files. Observations made while the *COBE* was in the SAA, or when the data from *all* detectors are of low quality, were omitted. The photometric and ancillary data are organized in wavelength band order rather than in the original MUX sequence, and are presented in FITS binary tables (see §5.4). A pixel index file was prepared for each CIO file to facilitate retrieval of desired data.

### 5.2.3 Creation of Weekly Sky Maps

The *DIRBE* daily sky maps were averaged to make Weekly Sky Maps as follows. First, long-term gain stabilization corrections based upon repeated observations of stable celestial sources were applied,

and the data were converted from instrumental units to calibrated specific intensities in MJy/sr (see §4.5.3.3). Data collected when the *COBE* spacecraft was in the SAA or when the *DIRBE* line-of-sight was close to the Moon, Mars, Jupiter, Saturn, Neptune, Uranus, or a bright comet or asteroid were excluded (see §4.7). Consequently, there are small holes in the *DIRBE* Weekly Sky Maps corresponding to these times. The remaining observations were then averaged to derive the quoted intensity at each pixel and wavelength; a robust averaging technique was employed (§4.7.9) to reduce the effects of outliers. The polarization channel intensities were converted to Stokes Parameters, Q and U, using the algorithm described in §4.6. If for some reason it was not possible to derive a reliable average intensity or Stokes parameter value for a given pixel, then a standard value less than -16375 was substituted for the real data. The mean time of observation and the mean solar elongation angle for each pixel were also recorded in the Weekly Sky Maps.

### 5.2.4 Creation of DIRBE Calibrated Annual File

One of the last steps in the *DIRBE* processing pipeline is to merge all weekly-averaged photometry into a single master file, and sort the data in ascending pixel-number order. This file, referred to as the *DIRBE* Calibrated Annual File, or DCAF, gives a pixel-by-pixel view of the intensity variations seen as a function of time. To create a DCAF data product, the master file was divided into six segments, one for each face of the *COBE* Sky Cube (see §5.3), and presented in FITS binary table format (see §5.4).

Each DCAF FITS file is accompanied by a pixel index file, which can be used to access the data corresponding to specific pixels without scrolling through the entire DCAF file.

### 5.2.5 Creation of Annual Average Sky Maps

At each wavelength, an Annual Average Sky Map was made by averaging the 41 Weekly Sky Maps that covered the cryogenic mission. In calculating the average, each Weekly Sky Map pixel (at each wavelength) was assigned a weight based on the number of times the pixel was observed. Information about the depth of sky coverage over the whole cryogenic mission is included in the Annual Average Sky Maps.

### 5.2.6 Creation of $\varepsilon = 90^\circ$ Sky Maps

At the ecliptic equator, solar elongations angles,  $\varepsilon$ , ranging from  $64^\circ$  to  $124^\circ$  were observed. In principle (except for gaps in coverage due to SAA passages, instrument calibration, etc.), every celestial line of sight was viewed by the *DIRBE* through the IPD cloud at  $90^\circ$  solar elongation once every 6 months, and hence once or twice during the 10-month cryogenic mission. When two  $\varepsilon = 90^\circ$  observations were made, different foreground brightness values were observed at the two epochs since generally the Earth was not at the same heliocentric distance at these times, and also because the IPD cloud is not perfectly symmetric around the Sun or the ecliptic plane. The  $\varepsilon = 90^\circ$  Sky Maps provide the 10 intensity values for each  $\varepsilon = 90^\circ$  epoch observed for each pixel.

To be precise, few pixels were observed when the solar elongation angle was *exactly*  $90^\circ$ . To create the  $\varepsilon = 90^\circ$  Sky Maps, the weekly-averaged intensities were monitored as a function of  $\varepsilon$  as time progressed and then interpolated to  $\varepsilon = 90^\circ$ . Specifically, a straight line was fitted to  $I_\nu(\varepsilon; \lambda, \beta)$  vs.  $[\frac{90}{\varepsilon} - 1]$  and the y-intercept was adopted as the  $\varepsilon = 90^\circ$  intensity at nominal frequency  $\nu$  and ecliptic coordinates  $(\lambda, \beta)$ . Figure 5.2-1 shows the variation of brightness with  $\varepsilon$  for a representative pixel. The quantity  $[\frac{90}{\varepsilon} - 1]$  was used instead of  $\varepsilon$  as the independent variable because the brightness was found to vary more linearly with the former than with the latter. Only observations made within  $\pm 19$  days of the  $\varepsilon = 90^\circ$  point at each pixel were fitted, a restriction that also ensured a more linear trend; the effect was to exclude data obtained when the line of sight came close to the Sun ( $\varepsilon \sim 64^\circ$ ), where  $\frac{\partial^2 I_\nu}{\partial \varepsilon^2}$  was relatively large. The weight assigned to each weekly-averaged intensity was based on the standard deviation of the weekly-averaged value,  $\sigma_{I_\nu}$ . When the weekly-averaged intensity value resulted from 5 or fewer observations, then the weight for that observation was based on  $0.01I_\nu$  or  $\sigma_{I_\nu}$ , whichever was greater.

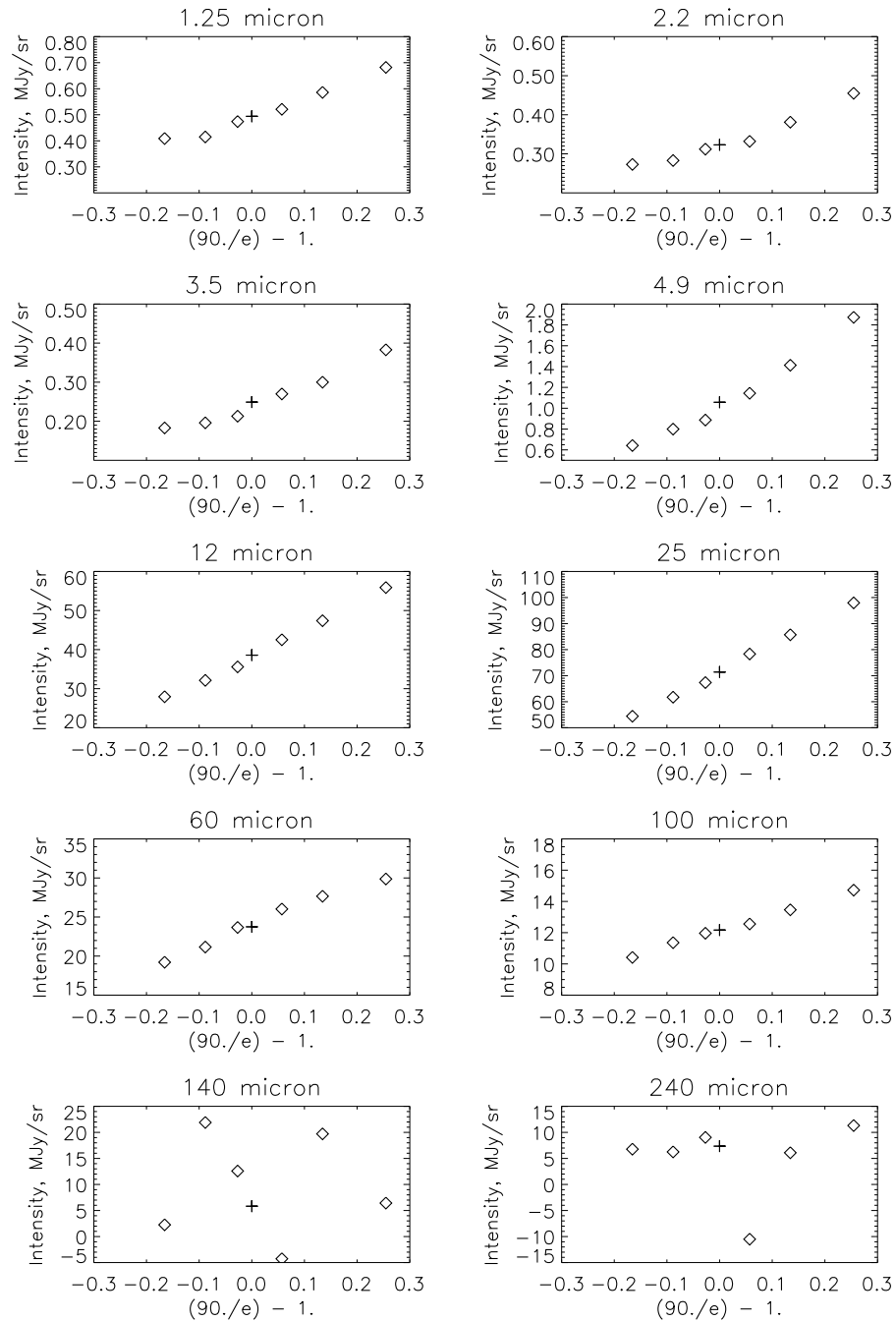


Figure 5.2-1:  $I_\nu$  vs.  $(90/\varepsilon - 1)$  for *DIRBE* pixel number 247071 at  $(\lambda, \beta) \approx (198^\circ, 1^\circ)$ . The  $\diamond$  symbols designate weekly-averaged *DIRBE* observations and the  $+$  symbols represent the interpolated intensities.

The standard deviation assigned to the interpolated intensity was the formal statistical error in the intercept at  $\varepsilon = 90^\circ$ . The model error used to calculate the quoted  $\chi^2$  did not take into account sources of systematic error such as uncorrected nonlinearity or confusion noise. Hence, the quoted  $\chi^2$  values do not always accurately reflect the goodness of fit.

When the interpolated value was negative, which sometimes occurred in regions of low brightness (particularly at 140 and 240  $\mu\text{m}$ , where the signal-to-noise ratio was low in a single week), the weighted average intensity was quoted instead of the interpolated value.

In some cases, weekly-averaged data were not available (either because of data processing constraints or the observational strategy), and the  $\varepsilon = 90^\circ$  intensity was obtained by extrapolating outside the range of elongation angles observed. Such cases include:

- pixels that would have been observed at  $\varepsilon = 90^\circ$  during the very beginning or very end of the cryogenic mission;
- a small number of pixels near the ecliptic plane where observations made at a solar elongation angle close to  $90^\circ$  were discarded due to close proximity of the Moon or Jupiter to the line of sight;
- pixels for which several weeks of observations were discarded because they consistently fell within SAA passages or instrument calibration periods; and
- pixels that would have been observed at  $\varepsilon = 90^\circ$  during the days (yyddd) 90110 – 90135 and 90217 – 90242 but were undersampled due to a suspension of normal observations while JFET-off tests were conducted (see §3.3.2.2).

Extrapolated values were included in the  $\varepsilon = 90^\circ$  Sky Maps only if two conditions were met:

1. intensity measurements were available for elongation angles within  $5^\circ$  of  $\varepsilon = 90^\circ$ ; and
2. the extrapolation interval in  $\varepsilon$  did not exceed one-third of the interval over which intensity measurements were available.

For the special case of an extrapolation within  $1^\circ$  of either ecliptic pole, the weighted average intensity was quoted.

Pixels with extrapolated intensities are flagged in the Photometric Quality field (FITQUAL for the  $\varepsilon = 90^\circ$  Sky Maps; the first byte of PHOTQUAL for the Galactic Plane Maps; see §5.7). Note that, because extrapolation was permitted, some of the times recorded in the  $\varepsilon = 90^\circ$  Sky Maps lie outside the temporal boundaries of the actual *DIRBE* mission.

In a limited number of cases, neither an interpolated nor a reliable extrapolated value could be computed. These cases include:

- pixels that would have been observed at  $\varepsilon = 90^\circ$  during the very beginning or very end of the cryogenic mission; and
- pixels for which photometry was unavailable or flagged as “bad” in a particular band for three or four successive weeks. This condition had the greatest impact at 100  $\mu\text{m}$  (see §3.5.1).

In these cases, the  $\varepsilon = 90^\circ$  Sky Map value was set to a number less than or equal to -16375.

### 5.2.7 Creation of the Galactic Plane Maps

The Galactic Plane Maps are subsets of the  $\varepsilon = 90^\circ$  Sky Maps constrained spatially and temporally as follows:

- only pixels whose Galactic coordinates satisfy the conditions  $-10^\circ < b < +10^\circ$  for  $30^\circ < \ell < 330^\circ$ , and  $-15^\circ < b < +15^\circ$  at Galactic longitudes within  $30^\circ$  of the Galactic center are included; and

- only  $\varepsilon = 90^\circ$  intensity values applicable to the 6-month interval between 1990 January 1 and 1990 July 2 inclusive are provided; thus, a single intensity value is recorded per pixel (unlike the  $\varepsilon = 90^\circ$  Sky Maps; see §5.2.4). The time range was chosen to assure that map discontinuities in the foreground brightness due to differences in the Earth’s orbital position at the time of observation would occur only along two boundaries (see §5.6.1).

### 5.2.8 Creation of *DIRBE* Sky and Zodi Atlas (DSZA)

An abridged version of the *DIRBE* Calibrated Annual File (DCAF) data set was merged with model zodiacal brightness values to create the *DIRBE* Sky and Zodi Atlas (DSZA). The zodiacal light intensity was computed using the *DIRBE* Interplanetary Dust (IPD) model (Kelsall *et al.* 1998). Data and model intensities from all 10 full-intensity wavelength bands appear in the DSZA.

To create the DSZA, selected fields were copied from each row of the DCAF table, and, if the quality of the copied photometry met certain specifications, then the corresponding zodiacal light contribution was computed and attached. Data obtained during certain time intervals with particular detectors were deemed to be of low quality. This includes weekly averaged photometry from Bands 1 through 8 for weeks 24 (90120–90126), 39 (90225–90231) and 40 (90232–90238), owing to the instrument testing that was done during these periods (see §3.3.2). The Band 8 photometry was also poor during week 4 (89345–89351), as the procedure for annealing the  $100\mu\text{m}$  detector following SAA passages had not yet been finalized. In these cases, the photometry was recorded in the DSZA, but the zodiacal light contribution was not computed, as is indicated by the sentinel value -16999 in the table. For all other weeks and wavelengths, and in all pixels, a model zodiacal light intensity was recorded in the DSZA, even if the photometry was considered deficient.

To calculate the zodiacal light intensity, the *DIRBE* IPD Model was evaluated at a spatial position corresponding to the pixel number at the time that position was observed (**Time + Delta-Time**), and at each wavelength. The *DIRBE* IPD Model, a semi-physical parameterized model, is described in detail by Kelsall *et al.* (1998). Thermal and scattering source terms were integrated along each line of sight to compute the model intensities. The computed model brightness is color corrected (see §5.5 and Chapter 4) (*i.e.*, evaluated as if observed with the appropriate *DIRBE* bandpass, assuming an energy distribution  $\nu I_\nu = \text{constant}$ ), putting it on an equal footing with the observations. Thus the model intensities and photometry values listed in the DSZA can be compared directly.

### 5.2.9 Creation of Zodi-Subtracted Mission Average (ZSMA) Maps

The ZSMA Maps are derived from the *DIRBE* Sky and Zodi Atlas (DSZA). For each pixel and wavelength, the tabulated zodiacal light (ZL) contribution is subtracted from each valid weekly photometric measure. To a good approximation, this has the effect of removing apparent time variations from the observed sky brightness. The individual weekly ZL-subtracted intensity values are then averaged over the entire cryogenic mission, yielding ten zodiacal light subtracted maps, one for each of the *DIRBE* full-intensity wavelength bands.

All of the weekly ZL-subtracted intensity values included in the average were assigned equal weights, however certain high-quality observations were excluded from the ZSMA to mitigate the effects of known imperfections in the IPD Model at extreme solar elongation angles. At  $|\beta| \lesssim 60^\circ$  the observations for which  $\varepsilon < 68^\circ$  or  $\varepsilon > 120^\circ$  were excluded. At higher ecliptic latitudes, in order to avoid discontinuities at  $|\beta| \sim 60^\circ$ , the clipping at extreme solar elongation angles was gradually tapered to “zero clipping” at the poles.

## 5.3 Pixelization and the Quadrilateralized Spherical Cube Projection

A quadrilateralized spherical projection and a quad-tree pixelization scheme were adopted for all *COBE* sky maps, including the *DIRBE* maps. The so-called “*COBE* Quadrilateralized Spherical Cube” (CSC) is an approximately equal-area projection (to within a few percent) in which the celestial sphere is



projected onto an inscribed cube. An advantage of the CSC over the Aitoff, Mollweide and Global-Sinusoidal projections is that polar singularities are avoided. A disadvantage is that there is no standard way to present data in the quad-cube projection in a FITS file. To maintain the best possible photometric integrity, the data products should be kept in their native projection for analysis. If reprojection is desired, it is recommended that quantities such as color temperatures be derived first.

Figure 5.3-1 depicts the CSC projection. The coordinate system is Geocentric Ecliptic J2000. The ecliptic plane runs horizontally through the middle of the unfolded cube. The North Ecliptic Pole is centered on “face 0” and the South Ecliptic Pole is centered on “face 5.” The *DIRBE* convention is to divide each cube face into  $256 \times 256$  pixels; thus, all-sky maps have  $256^2 \times 6 = 393216$  pixels. Each pixel is approximately  $0.32^\circ$  on a side. Figure 5.3-2 illustrates the pixel numbering scheme.

CSC pixel numbers are used in the *DIRBE* Sky Map FITS files to convey spatial pointing information. Except for the Galactic Plane Maps, which provide sky coordinates as well as pixel numbers, the pixel number is the *only* pointing information provided in the map products. FORTRAN and IDL programs that convert pixel numbers to ecliptic, Galactic, or equatorial coordinates are described in Appendix D (see §§D.1.2 and D.1.3) and available on line through the *COBE* Home Page ([http://www.gsfc.nasa.gov/astro/cobe/cobe\\_home.html](http://www.gsfc.nasa.gov/astro/cobe/cobe_home.html)). A related ancillary information file called `DIRBE_SKYMAP_INFO.FITS` is described in §5.3.1.

The Weekly Sky Maps and Annual Average Sky Maps give more precise pointing information in the form of a “pixel subposition” (see Tables 5.7-7 and 5.7-14). The subposition specifies a location within a  $16 \times 16$  element grid superposed on a pixel. Numbers ranging from 0 to 255 are assigned to the grid positions according to the standard quad-tree rules described below.

### 5.3.1 Description of the File `DIRBE_SKYMAP_INFO.FITS`

An ancillary information file called `DIRBE_SKYMAP_INFO.FITS` explains the quad-tree scheme that relates CSC pixel numbers to (x,y) positions within the quad-sphere cube faces and tabulates the ecliptic J2000, Galactic ( $\ell_{II}$ ,  $b_{II}$ ) and equatorial J2000 coordinates corresponding to the *DIRBE* pixel centers. This file may be obtained from the directory `cobe/general_information/skymap_info` at the anonymous ftp site `nssdca.gsfc.nasa.gov`.

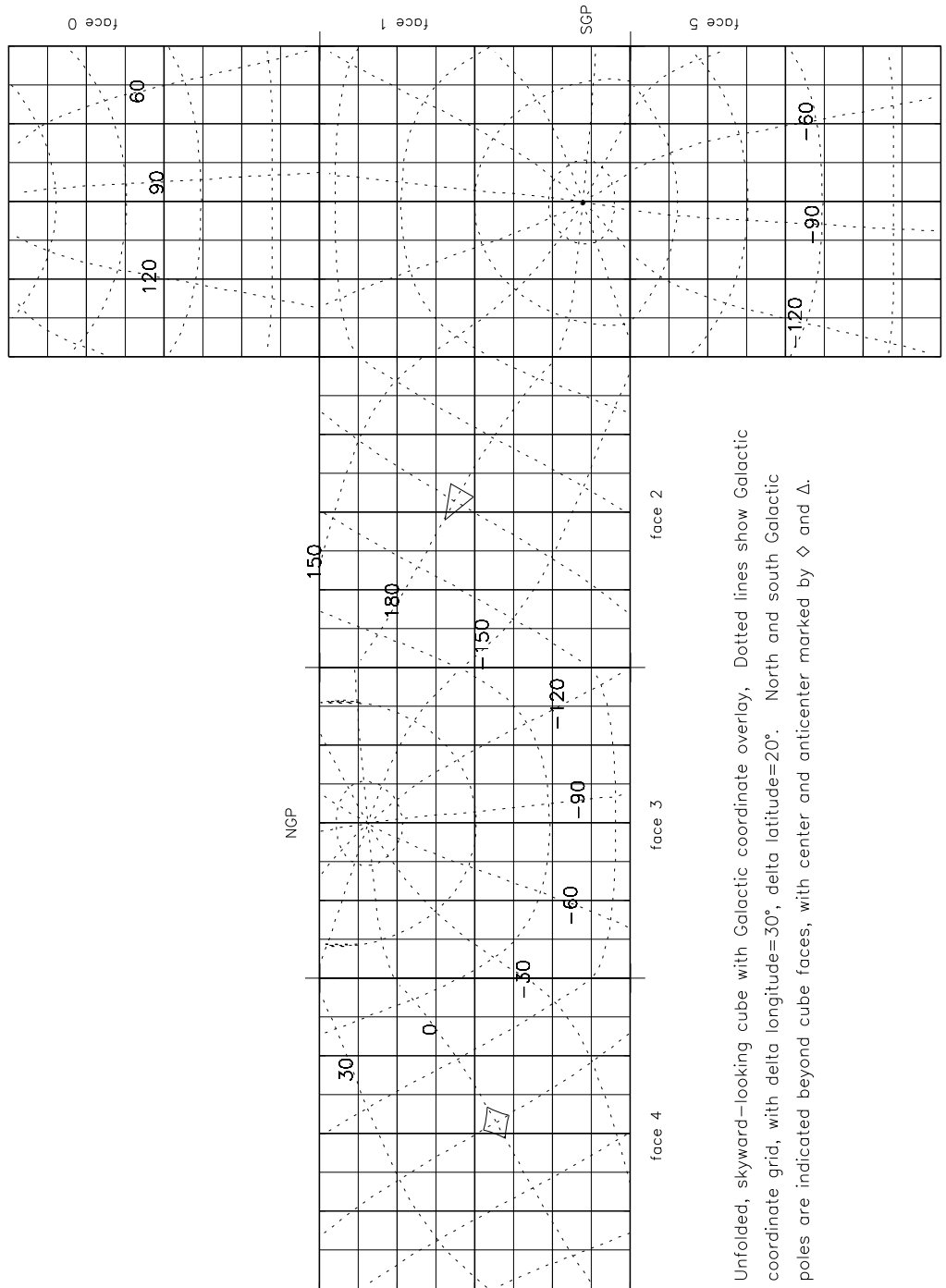
The file has two parts: (1) a primary data array which is stored as a standard FITS image, and (2) a binary table extension. The 3-dimensional primary data array gives a rasterized  $256 \times 256$  pixel image of each of the six CSC cube faces showing the *DIRBE* pixel numbers. The binary table lists the sky coordinates corresponding to the center of each *DIRBE* pixel and can substitute for the software described above.

Key elements of the quad-sphere projection and quad-tree pixelization scheme are explained in COMMENT lines in the main and extension FITS headers. For convenience, the remainder of this section contains excerpts from the header documentation.

Quadrilateralized spherical cube faces are tangent plane projections of the celestial sphere. In the quad-sphere projection, pixels are equally spaced and have approximately equal area on the cube and on the sky. The COBE quadrilateralized spherical cube (CSC) projection conserves area to approximately 1% across the whole cube with a maximum discrepancy from equal area of only a few percent at the edges of the cube. Furthermore, the projection distorts shapes minimally. Beam shapes or point response functions will differ only slightly depending upon location on the quad-cube face.

In the quad-tree nearest neighbor pixel numbering scheme, which is hierarchical, the pixel numbers are not sequential along a row or column. As presented in the primary data array, the first row of pixel numbers on a face is at the bottom, the last row is at the top, and the first pixel per face is in the lower right corner. The cube faces are numbered 0 through 5 corresponding to planes 1 through 6 (NAXIS3) in the primary data array, respectively. The *COBE* FITS keyword `PIXINDEX` is a CSC resolution index. It is defined such that  $2^{(\text{PIXINDEX}-1)}$  specifies the dimension of a side of each square face, 256 pixels in the case of *DIRBE*. The dimension implied by `PIXINDEX` is recorded in the primary header keywords `NAXIS1` and `NAXIS2`.

An all-sky, skyward-looking, unfolded cube can be constructed by arranging the cube faces as follows (also see Figure 5.3-1):



Unfolded, skyward-looking cube with Galactic coordinate overlay. Dotted lines show Galactic coordinate grid, with delta longitude=30°, delta latitude=20°. North and south Galactic poles are indicated beyond cube faces, with center and anticenter marked by  $\diamond$  and  $\Delta$ .

Figure 5.3-1: Unfolded, skyward-looking cube in ecliptic coordinates with Galactic coordinate overlay.

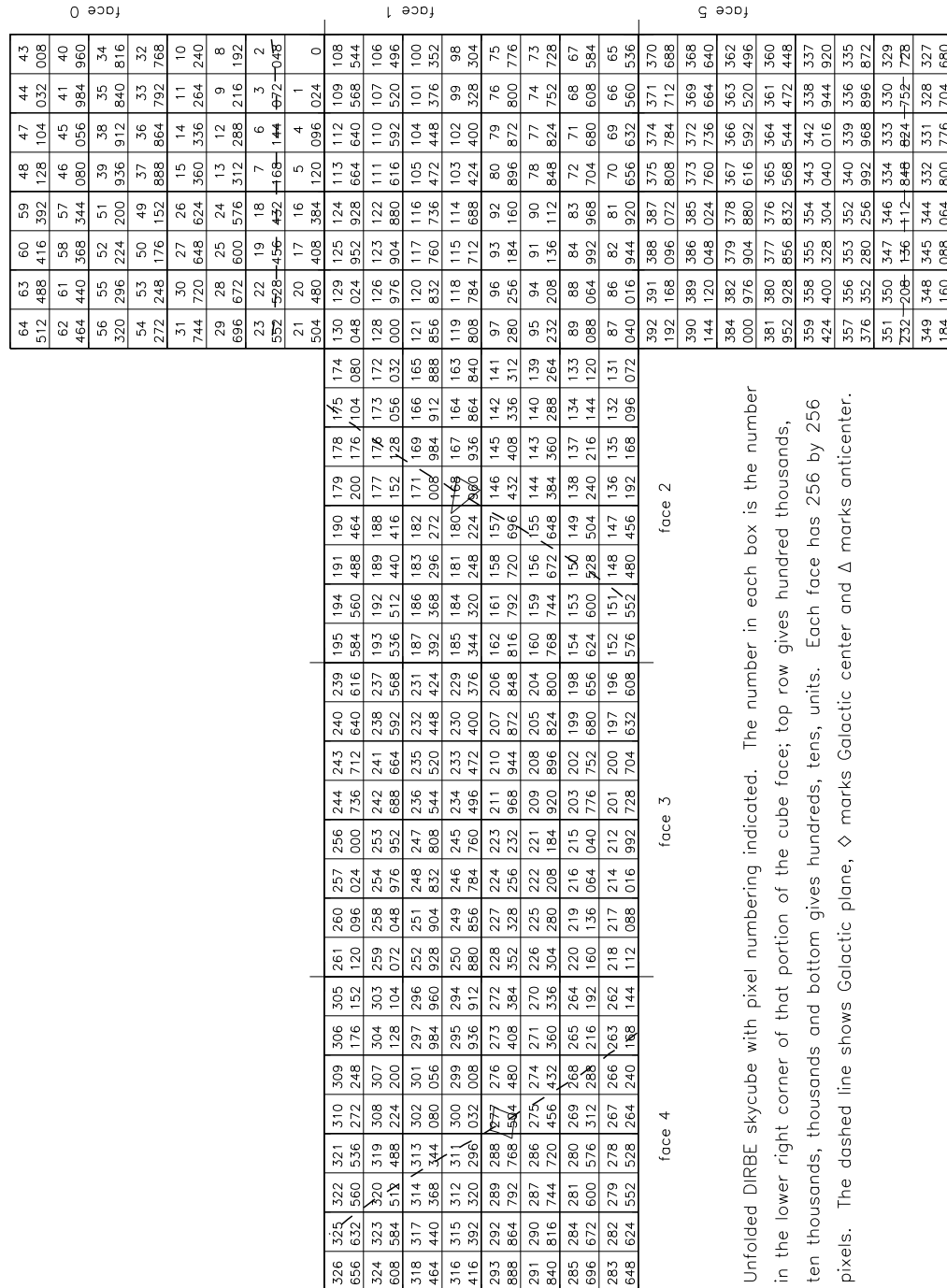
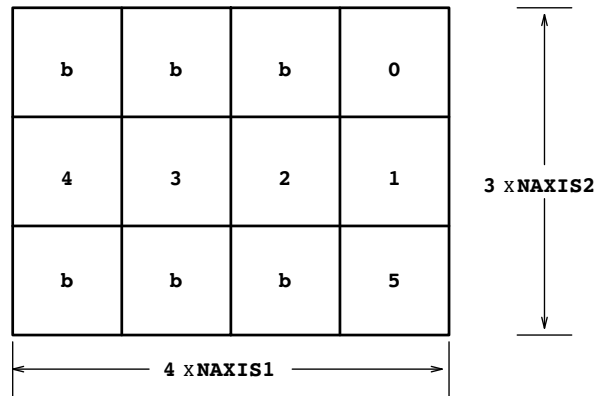


Figure 5.3-2: The *DIRBE* pixel numbering scheme in the quadrilateralized spherical cube projection.

4 3 2 1  
5

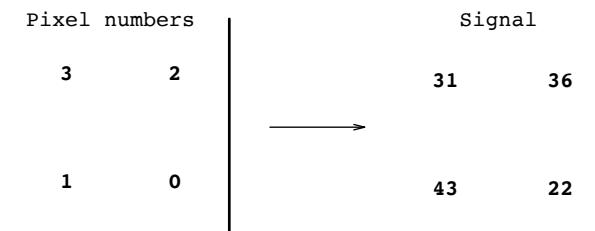
In the following equivalent arrangement, b denotes blank areas and  $NAXIS1 = NAXIS2 = 256$ :



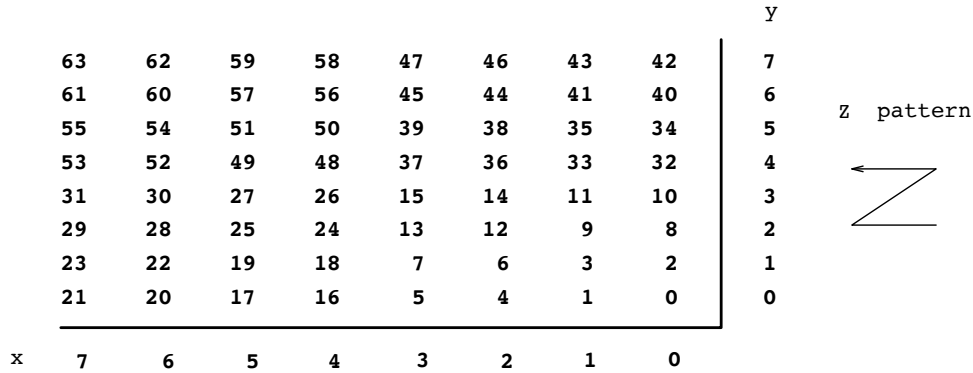
*COBE* data can be displayed on this unfolded cube by arranging the pixels in a binary table as they are arranged in the primary array of this file. For example, consider a sky map that contains the following data in a FITS binary table:

Pixel number	Signal	Error	Ecliptic longitude	Ecliptic latitude
0	22	1	315°0	36°7
1	43	2	317.9	38.1
2	36	2	312.1	38.1
3	31	1	315.0	39.7
⋮	⋮	⋮	⋮	⋮

Then the signal values will be mapped into the sites of the corresponding pixel numbers given in face 0 (*i.e.*, the first plane) of the primary array with the following result:



This illustrates the quad-tree pixelization scheme in which pixel numbers begin in the lower right corner of a cube face and increase from right to left and bottom to top. This “Z” pattern is repeated throughout a face as shown below for the lower right corner of face 0:



The quad-tree pixel ordering scheme is related to rasterized rectangular array positions as follows. The location within a face is specified by the  $2^{(PIXINDEX-1)}$  least significant bits. The most significant bits identify the cube face as described below. The even least significant bits (0, 2, . . . ,  $2(PIXINDEX - 2)$ ) specify the x, or horizontal, raster position, and the odd bits (1, 3, . . . ,  $2(PIXINDEX) - 3$ ) specify the y position. Changing the pixel resolution thus simply requires adding or deleting pairs of least significant bits; each pair represents a resolution change in the x and y face coordinates by a factor of 2.

For example, for a PIXINDEX value of 4, the quad-tree pixel 24 (in binary) is

$$\begin{array}{cccccc}
 0 & 1 & 1 & 0 & 0 & 0 \\
 y & x & y & x & y & x
 \end{array}$$

Extracting the even and odd least significant bits gives

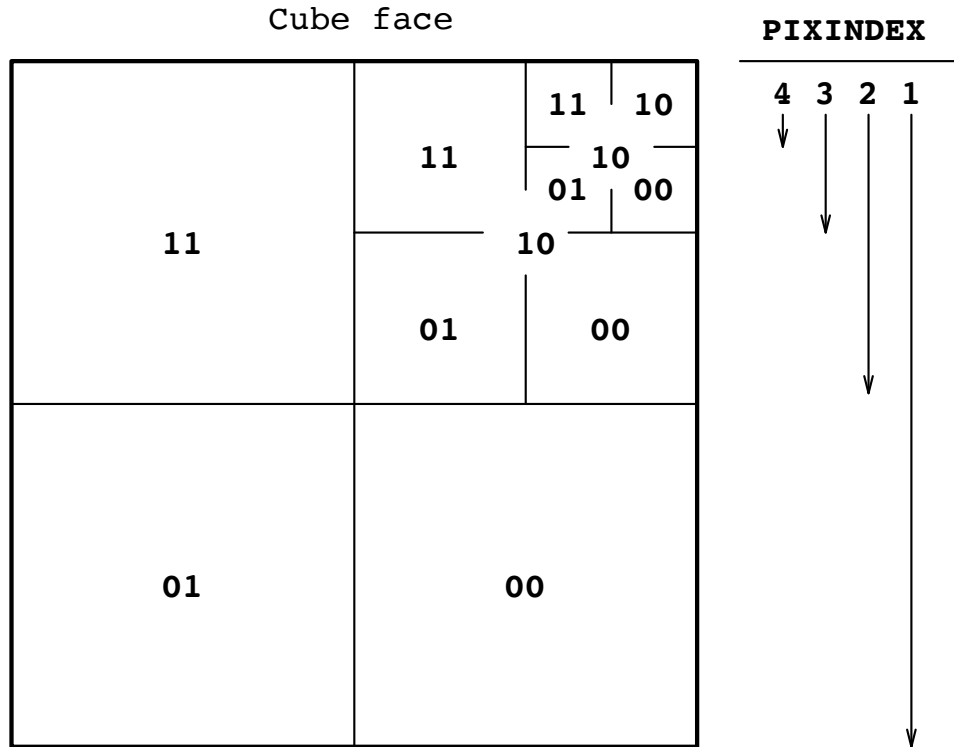
$$\begin{array}{l}
 y = 010 = 2 \\
 x = 100 = 4
 \end{array}$$

Thus, writing the pixel numbers in binary form clarifies the mapping hierarchy:

									Row
	111111	111110	111011	111010	101111	101110	101011	101010	7
	111101	111100	111001	111000	101101	101100	101001	101000	6
	110111	110110	110011	110010	100111	100110	100011	100010	5
	110101	110100	110001	110000	100101	100100	100001	100000	4
	011111	011110	011011	011010	001111	001110	001011	001010	3
	011101	011100	011001	011000	001101	001100	001001	001000	2
	010111	010110	010011	010010	000111	000110	000011	000010	1
	010101	010100	010001	010000	000101	000100	000001	000000	0
Bit #	543210	543210	543210	543210	543210	543210	543210	543210	
Column	7	6	5	4	3	2	1	0	

The separating lines above show how the hierarchy is built up.

As illustrated below, a cube face is bisected ( $PIXINDEX - 1$ ) times to reach the pixel resolution. In the following picture, a face at a  $PIXINDEX$  of 4 is depicted:



The face index is specified in the Most Significant Bits, that is, in bits  $2(PIXINDEX - 1)$  through  $2 PIXINDEX$ . Thus for pixel 24 on face 0 the binary number would be

$$\begin{array}{cccccccc} 0 & 0 & 0 & & 0 & 1 & 1 & 0 & 0 & 0 & & , \\ | & \text{Face} & | & \text{Pixel number} & | & & & & & & & \end{array}$$

whereas for pixel number 24 on face 5 the binary number would be

$$\begin{array}{cccccccc} 1 & 0 & 1 & & 0 & 1 & 1 & 0 & 0 & 0 & & . \\ | & \text{Face} & | & \text{Pixel number} & | & & & & & & & \end{array}$$

The pixel numbers run sequentially from 0 on face 0 to  $(NAXIS1 \times NAXIS2 \times NAXIS3) - 1$  on face 5. The last pixel number in a face is  $(\text{facenumber} + 1) \times 2^{[2(PIXINDEX-1)]} - 1$ . The first pixel number in a face is 0 for face 0, and 1 plus the last pixel number in the previous face for the other faces. Thus, for a  $PIXINDEX$  value of 4, pixel 24 on face 5, would be number 344 (binary 101011000 = decimal 344) with respect to the whole cube.

World coordinates such as ecliptic, equatorial, and Galactic are *not* linear across the *COBE* sky cube. The CSC is defined using the ecliptic J2000 reference frame. Cube face 0 is centered on the North ecliptic pole (NEP), faces 1 through 4 lie along the ecliptic plane (each spanning 90 degrees of ecliptic longitude), and face 5 is centered on the South ecliptic pole (SEP). Ecliptic longitude increases from face 1 to face 4. The vernal equinox lies at the center of face 1. Face 1 spans ecliptic longitudes from  $-45^\circ$  (*i.e.*,  $315^\circ$ ) to  $+45^\circ$ . The anti-vernal equinox point is at the center of face 3. Faces 1-4 include the ecliptic latitudes ranging from roughly  $-45^\circ$  to  $+45^\circ$ . Face 0 covers all ecliptic longitudes and latitudes around the North ecliptic pole down to approximately  $+45^\circ$ . Face 5 covers all ecliptic longitudes and latitudes around the South ecliptic pole up to approximately  $-45^\circ$ . The latitude ranges in each face are not exact because of the curvilinear nature of the coordinates on the CSC.

As shown in Figure 5.3-1, the North Galactic pole is on face 3 at J2000 ecliptic longitude  $179^\circ 32095$  and latitude  $29^\circ 811954$ , and the Galactic center is on face 4 at J2000 ecliptic longitude  $266^\circ 14097$  and

latitude  $-5^{\circ}52967943$ . The South Galactic pole is on face 1, and the Galactic anti-center is on face 2. Pixel numbers for these locations can be found in the `DIRBE_SKYMAP_INFO.FITS` binary table.

The North celestial pole is at ecliptic coordinates  $(90^{\circ}0, 66^{\circ}5607089)$  and is located on face 0.

## 5.4 Data Product Formats

With a few exceptions, noted below, the data products are given in FITS format to enable their use in a variety of computing environments. The FITS standards and conventions are specified in *Definition of the Flexible Image Transport System (FITS)* and *A User's Guide for the Flexible Image Transport System (FITS)*, both of which are available at [http://www.gsfc.nasa.gov/astro/fits/fits\\_home.html](http://www.gsfc.nasa.gov/astro/fits/fits_home.html). Appendix D.1 provides advice on how to read FITS data.

### 5.4.1 FITS Binary Table Extension

All of the *DIRBE* Sky Maps, the CIO, the DSZA and DCAF files, the Faint Source Model, the Solar System Objects Data, and the Photometric Standard Values are in FITS Binary Table extension format; they are not two-dimensional images. This format is reasonably compact and recognized by software that is readily available and in widespread use. In most cases, the rows of the FITS table correspond to pixels (*i.e.*, locations in the sky) and are organized in ascending pixel number order. Standard FITS-reading software provides the capability to select data from either a column of a FITS table (*e.g.*, intensity at a particular wavelength) or a row (*e.g.*, energy distribution at a particular direction). Thus, for example, it is straightforward to extract the 10-band spectral energy distribution in a particular pixel from the *DIRBE* Galactic Plane Maps file.

### 5.4.2 FITS Image Format

The Beam Profile Maps are stored as FITS images. A FITS-reading subroutine will return a two-dimensional array, and the FITS header provides coordinate information for the axes.

### 5.4.3 Native Binary Format

The Time-Ordered Data files are available in their original format: binary files of fixed record length. Since the data were processed on a VAX computer, floating point numbers do not conform to IEEE convention. The TOD file format is described in detail in a file called `DIRBE_TOD_RECORD_STRUCTURE.ASC`.

### 5.4.4 ASCII

System Spectral Response Functions, Color Correction Tables, and the *DIRBE* Beam Parameters table (Table 4.2-1) are provided in flat ASCII files to facilitate their incorporation into user programs.

## 5.5 Color Corrections

Following the *IRAS* convention (see the "*IRAS Catalogs and Atlases Explanatory Supplement*," p. VI-27), the *DIRBE* spectral intensity data,  $I_{\nu}$ , are expressed in MJy/sr at fixed nominal frequencies, assuming the source spectrum is  $\nu I_{\nu} = \text{constant}$  (*i.e.*, constant intensity per logarithmic frequency interval). Where this is not true, a color correction must be applied to obtain an accurate intensity. The color correction factor,  $K$ , is defined such that

$$I_{\nu_0}(\text{actual}) = I_{\nu_0}(\text{quoted})/K, \quad (5.1)$$

where  $I_{\nu_0}(\text{actual})$  is the actual specific intensity of the sky at frequency  $\nu_0$ ,  $I_{\nu_0}(\text{quoted})$  is the corresponding value given in a *DIRBE* data product, and  $\nu_0$  represents the frequency corresponding to one of the *DIRBE* band nominal wavelengths (1.25, 2.2, 3.5, 4.9, 12, 25, 60, 100, 140, or 240  $\mu\text{m}$ ). Thus,

$$K \equiv \frac{\int (I_\nu/I_{\nu_0})_{\text{actual}} R_\nu d\nu}{\int (\nu_0/\nu)_{\text{quoted}} R_\nu d\nu} \quad (5.2)$$

where  $(I_\nu/I_{\nu_0})_{\text{actual}}$  is the actual specific intensity of the sky normalized to the the intensity at frequency  $\nu_0$ , and  $R_\nu$  is the relative system response (see Table A.0-1 in Appendix A). Color correction factors applicable to a variety of source spectral shapes are given in Appendix B and in the ASCII file DIRBE\_COLOR\_CORRECTION\_TABLES.ASC.

## 5.6 Data Limitations

### 5.6.1 Photometric and Temporal Discontinuities in the Galactic Plane Maps

The *DIRBE* Galactic Plane Maps contain observations made during the six-month interval from 1990 January 1 to 1990 July 2 inclusive. There are photometric as well as temporal discontinuities in the maps at the two ecliptic longitudes,  $10^\circ$  and  $190^\circ$  (or at Galactic longitudes  $\ell \simeq 102^\circ$  and  $282^\circ$ ), where the data from January and July meet. The photometric discontinuity is due to the Earth's different orbital positions at those two times and reflects a path difference through the interplanetary dust cloud. The effect is strongest in the spectral region where the zodiacal emission is brightest. Table 5.6-1 gives representative magnitudes of the discontinuities at  $\ell \simeq 102^\circ$ . The discontinuities are smaller at  $\ell \simeq 282^\circ$  and are not readily discernible at wavelengths other than those listed.

Table 5.6-1: Photometric discontinuities at  $\ell \simeq 102^\circ$

Wavelength ( $\mu\text{m}$ )	$\Delta I_\nu$ MJy/sr
4.9	0.1
12	2.5
25	3.5
60	1.5

### 5.6.2 Exclusion of Solar System Objects: Gaps in Sky Coverage

In order to avoid contaminating the Weekly Sky Maps with light from moving objects, data obtained when the *DIRBE* pointed near certain solar system objects were excluded when the maps were produced. The “exclusion zones” around these objects were large enough to make their stray light contributions negligible (see §4.4). The exclusion zones were circles  $10^\circ$  and  $1.5^\circ$  in radius around the Moon and Jupiter, respectively; around Mars, Uranus, and Neptune, data from  $7 \times 7$  pixel ( $\sim 2.5 \times 2.5$ ) square regions were censored;  $3 \times 3$  pixel exclusion zones were applied to the asteroids Ceres, Pallas, Vesta, and Juno. Comets Okazaki–Levy–Rudenko (1989R), Austin (1989C1), and Levy (1990C) were extended sources and had exclusion zones as large as  $50 \times 50$  pixels at 12 and 25  $\mu\text{m}$  (bands 5 and 6) and  $20 \times 20$  pixels in most other bands during those times when the comets were brightest, and  $9 \times 9$  pixels at other times. The CIO (or the Time–Ordered Data product) should be consulted for photometric observations of the excluded objects.

Since Saturn, Uranus and Neptune moved slowly across the sky, their exclusion left holes in the Weekly Sky Maps (near the Galactic center on cube face 4). Although faster moving objects, such as the Moon and Mars, did not leave holes in the maps, their locations are often betrayed by discrete patches in which the noise is relatively high because fewer photometric samples were included in the weekly averages.

### 5.6.3 Extrapolated Values

In the  $\varepsilon = 90^\circ$  and Galactic Plane Maps, the quoted intensity values in some pixels were calculated by extrapolation (see §5.2.4). Other pixels observed at  $\varepsilon = 90^\circ$  at the beginning or end of the cryogenic



mission are of lower quality because the baseline available for interpolation is relatively short. A data quality flag identifies the affected data. The FITS headers (see Appendix D) explain how to interpret the data quality flags.

#### 5.6.4 Regions Where the Statistical Noise is Relatively High

Since the photometry errors reported in the Sky Map data products are standard deviations of the mean measured values, any effect that reduces the number of measurements increases the statistical error. Such effects and others that cause noise enhancements in the maps are the following:

**Elective exclusion of data** – Data deemed to be of low quality were excluded for a variety of reasons (see §4.7). Data deleted for the following reasons led to regions of relatively high noise in the maps:

- observations made while the Moon, planets, or comets (especially the Moon and Jupiter) were in close proximity to the *DIRBE* line of sight
- data obtained while the spacecraft was in the SAA
- unusually noisy 60  $\mu\text{m}$  (band 7) data
- high focal plane temperatures, *e.g.*, caused by Earth rising over the Sun–Earth shield or *FIRAS* calibrations
- data at 4.9 and 60  $\mu\text{m}$  (bands 4 and 7) taken while the *FIRAS* external calibrator was moving

**Detectors turned off** – Gaps in sky coverage resulted when the 1.25 – 100  $\mu\text{m}$  (band 1 – 8) detectors were turned off for instrument offset testing (see §3.3.2). These gaps gave rise to localized noisy regions in the  $\varepsilon = 90^\circ$  Sky Maps. Regions observed at solar elongation angles near  $90^\circ$  during the time intervals 90110–90135 and 90217–90242 were potentially affected.

**Uneven depth of sky coverage** – As illustrated in Figure 3.1-1(b), the number of observations made per pixel varied over the sky. The depth of coverage is reflected in the photometric noise given in the Annual Average Sky Maps.

**Short-term gain fluctuations** – Primarily at 12 – 100  $\mu\text{m}$  (bands 5–8), short-term fluctuations in the detector gains (see §4.5.3.1), when not fully corrected, contributed to the dispersion of the photometric measurements and sometimes led to noisy patches in the maps. For example, the effect of residual, uncorrected PIRE at 100  $\mu\text{m}$  is concentrated near the Galactic plane. Also, SAA-induced and IRS-induced gain changes tended to be less well corrected at times when the *COBE* spacecraft was exiting the SAA; the affected regions of the sky in these cases moved slowly as the *DIRBE* viewing swath precessed.

**Large brightness gradients** – Unresolved sky brightness structures contribute to the dispersion in the photometric measurements averaged in a map pixel because the *DIRBE* beam centroid location and position angle vary from sample to sample. The effect is most severe in parts of the sky that contain strong point sources or brightness gradients.

#### 5.6.5 Negative Intensities at 140 $\mu\text{m}$ and 240 $\mu\text{m}$

In regions of low signal-to-noise ratio in the 140 and 240  $\mu\text{m}$  maps, some of the quoted pixel intensities are negative. Coaddition of the data obtained over a period of weeks may be required to achieve a positive detection in a faint region at these wavelengths. Some negative pixel intensity values remain in the Annual Average Sky Maps.

#### 5.6.6 Point Source Photometry from the Maps

*As a rule, it is recommended that the DIRBE Calibrated Individual Observations (or Time-Ordered Data), not the Sky Maps, be used to determine the fluxes of point sources.* Because of the manner in which the sky was scanned and intensity values were assigned to pixels, the “point spread function”

applicable to the *DIRBE* Sky Maps is not the same as the beam profile. In particular, the observations averaged to derive a pixel intensity were made at various beam centroid locations (scattered around the nominal pixel center coordinates) and position angles or, equivalently, approach directions. Over a period of months, a typical point source was observed after being approached from a variety of directions, which may or may not have been uniformly distributed over all possible directions. Since over the course of a week the viewing perspective did not change much, point source photometry in the Weekly Sky Maps is particularly susceptible to any bias associated with approach from a limited range of directions. No compensation was made for the point spread functions applicable to individual map pixels because the *DIRBE* maps were intended to provide information about the diffuse sky brightness and not about point sources.

For those who wish to disregard the advice given above and use the *DIRBE* Sky Maps to determine the flux of a point source, it is recommended that the peak pixel intensity in a map rather than an integral over the point spread function be used; a better signal-to-noise ratio will be obtained in this case even if the  $\varepsilon = 90^\circ$  Sky Maps, Galactic Plane Maps, or Annual Average Sky Maps, which average over many approach angles, are used. From the peak brightness, subtract an estimate of the background brightness and multiply by the beam solid angle (see Table 4.2-1) to estimate the source flux. The fluxes of bright  $2.2 \mu\text{m}$  sources estimated using peak intensities from the Galactic Plane Maps or the Annual Average Sky Maps were found to be systematically 6 – 9% ( $\pm 1\%$  rms) lower than those based upon sightings in the Time-Ordered Data in which the beam crossed the source at the location of peak response. A similar, though smaller (3%  $\pm 1\%$  rms), effect was found at  $4.9 \mu\text{m}$ .

### 5.6.7 Annual Average Sky Maps

Although the Annual Average Sky Maps maximize the signal-to-noise ratio, the Weekly Sky Maps were coadded before the time-dependent zodiacal light component was removed. The variable zodiacal signal, coupled with non-uniform sky coverage, produced spurious features in the Annual Average Sky Maps which are particularly evident at  $4.9 - 100 \mu\text{m}$  (bands 4–8). At wavelengths where the zodiacal emission is weak, the artifacts are less significant and the Annual Average Sky Maps resemble corresponding  $\varepsilon = 90^\circ$  Sky Maps. The 140 and  $240 \mu\text{m}$  Annual Average Sky Maps are particularly useful because the zodiacal component is weak at these wavelengths and the signal-to-noise ratio improvement enables detection of otherwise undetectable faint emission at high Galactic latitudes.

### 5.6.8 $4.9 \mu\text{m}$ Data Excluded from Maps

When the *FIRAS* external calibrator was moved into the *FIRAS* sky horn, the  $4.9 \mu\text{m}$  (band 4) signal exhibited high-frequency (microphonic) noise. Since the noise lasted at most 75 seconds (see §4.7.8), all  $4.9 \mu\text{m}$  data obtained for 75 s following each calibrator move were excluded from the *DIRBE* Sky Maps, though not from the Time-Ordered Data. Table 5.6-2 lists the dates and times when the calibrator was moved.

### 5.6.9 JFET-off Test Periods

Observations made during the two JFET-off test periods are of limited quality and quantity (see §3.3.2). As noted in Tables 3.1-2 and 5.7-1, the tests were conducted during mission weeks 24, 39, and 40.

## 5.7 The Project Data Sets

This section gives a detailed description of the contents of each of the *DIRBE* Project Data Sets.

### 5.7.1 Time-ordered Data

Time-Ordered Data covering the entire cryogenic mission, from 89345 to 90264, are provided in the 41 files listed in Table 5.7-1. Each fixed record length file gives the complete set of data for one week in

Table 5.6-2: *FIRAS* external calibration times

Day Number	Date and Time (UT)
90049	1990 Feb 18 02:38
90079	1990 Mar 20 16:52
90110	1990 Apr 20 19:13
90138	1990 May 18 23:32
90181	1990 Jun 30 13:48
90220	1990 Aug 8 05:54
90229	1990 Aug 17 13:58
90234	1990 Aug 22 14:40
90239	1990 Aug 27 16:22
90244	1990 Sep 1 13:40
90248	1990 Sep 5 15:56
90253	1990 Sep 10 22:54
90257	1990 Sep 14 10:35
90262	1990 Sep 19 10:16

its native VAX binary format. The record length is 10240 bytes. Each record contains the data for a 32-second *DIRBE* “Major Frame.”

In the normal Science Data Mode (SDM; see §2.2.6), each of the 16 *DIRBE* detectors was sampled at  $\frac{1}{8}$ -second intervals, yielding 256 samples per detector per Major Frame. The SDM Time-Ordered photometric data were calibrated using the same algorithms as those applied to the sky map data and are given in units of MJy/sr. However, not all of the Time-Ordered Data records represent nominal SDM skyward-looking data: data obtained in the various calibration modes (see §2.2.6) and during special test periods (see §3.3.2) are included as well; these records are uncalibrated and essentially in their original telemetry form. Pointing information is stored in each record as an array of attitude quaternions, the usage of which is described in §5.7.1.2. There is also a great deal of ancillary spacecraft, environmental and operational information in each record.

Refer to Table 3.1-2 for a summary of weekly sky coverage, and the *DIRBE* Cold Mission Events Log (Appendix C) for a chronological record of non-survey mode activities. Table 5.7-2 summarizes the key fields present in each Time-Ordered Data record. The record contents are described in greater detail in an ASCII file called `DIRBE_TOD_RECORD_STRUCTURE.ASC`.

### 5.7.1.1 Time Convention

In the Time-Ordered Data and other *DIRBE* data products, time ( $T_{81}$ ) is given in International Atomic Time (TAI) seconds since 1981 January 1 00:00:00 UTC. The 1981.0 fiducial point was adopted to facilitate comparison of the *DIRBE* data with the *IRAS* Zodiacal Observation History File. As a reference point,  $T_{81} = 283996806.0000$  at 1990 January 1 00:00:00 UTC.

### 5.7.1.2 Using Quaternions

Quaternions, which allow the spacecraft attitude information to be stored compactly (Wertz 1978, Appendix D), can be translated into more familiar coordinates as follows:

**Associate a quaternion value with each of the 256 observations in the Major Frame.** While the detector data were stored every  $\frac{1}{8}$ th of a second (at half minor frame intervals), the 4-component quaternions were stored only every 4 seconds. The time associated with the first quaternion is the Major frame time ( $T_{81}$ ) minus 0.3125 s. The quaternion components should be individually interpolated to the half minor frame times. A cubic spline fit through two preceding and two succeeding quaternions was employed for this purpose in the *DIRBE* processing software.

Table 5.7-1: Time-Ordered Data files

File	Week	Time interval (yyddd)	File name suffix <sup>a</sup>	Start time <sup>b</sup>	Stop time <sup>b</sup>	Records
1	4	89345 – 89351	961081620	282182409.549	282787209.549	18721
2	5	89352 – 89358	961081630	282787209.549	283392009.549	18732
3	6	89359 – 89365	961081640	283392009.549	283996809.549	18749
4	7	90001 – 90007	961091019	283996809.549	284601609.554	18742
5	8	90008 – 90014	961091029	284601609.554	285206409.554	18762
6	9	90015 – 90021	961091039	285206409.554	285811209.554	18723
7	10	90022 – 90028	961091048	285811209.554	286416009.554	18594
8	11	90029 – 90035	961091058	286416009.554	287020809.554	18750
9	12	90036 – 90042	961091108	287020809.554	287625609.558	18759
10	13	90043 – 90049	961091117	287625609.558	288230409.560	18759
11	14	90050 – 90056	961091127	288230409.560	288835209.577	18700
12	15	90057 – 90063	961101651	288835209.577	289440009.581	18720
13	16	90064 – 90070	961101700	289440009.581	290044809.585	18737
14	17	90071 – 90077	961101710	290044809.585	290649609.587	18750
15	18	90078 – 90084	961101719	290649609.587	291254409.589	18713
16	19	90085 – 90091	961101728	291254409.589	291859209.589	18744
17	20	90092 – 90098	961101738	291859209.589	292464009.587	18755
18	21	90099 – 90105	961101747	292464009.587	293068809.585	18733
19	22	90106 – 90112	961101756	293068809.585	293673609.585	18754
20	23	90113 – 90119	961101806	293673609.585	294278409.585	18712
21	24	90120 – 90126 <sup>c</sup>	961101815	294278409.585	294883209.588	18734
22	25	90127 – 90133	961101823	294883209.588	295488009.597	18748
23	26	90134 – 90140	961101833	295488009.597	296092809.599	18704
24	27	90141 – 90147	961141119	296092809.599	296697609.607	18676
25	28	90148 – 90154	961141129	296697609.607	297302409.611	18770
26	29	90155 – 90161	961141139	297302409.611	297907209.622	18755
27	30	90162 – 90168	961141148	297907209.622	298512009.626	18537
28	31	90169 – 90175	961141158	298512009.626	299116809.623	18668
29	32	90176 – 90182	961151326	299116809.623	299721609.620	18673
30	33	90183 – 90189	961151335	299721609.620	300326409.620	18719
31	34	90190 – 90196	961151344	300326409.620	300931209.620	18760
32	35	90197 – 90203	961151353	300931209.620	301536009.626	18725
33	36	90204 – 90210	961151402	301536009.626	302140809.626	18690
34	37	90211 – 90217	961151412	302140809.626	302745609.635	18748
35	38	90218 – 90224	961151421	302745609.635	303350409.635	18724
36	39	90225 – 90231 <sup>c</sup>	961151430	303350409.635	303955209.645	18591
37	40	90232 – 90238 <sup>c</sup>	961151439	303955209.645	304560009.648	18719
38	41	90239 – 90245	961151448	304560009.648	305164809.655	18606
39	42	90246 – 90252	961151457	305164809.655	305769609.661	18755
40	43	90253 – 90259	961151506	305769609.661	306374409.667	18756
41	44	90260 – 90264	961151515	306374409.667	306754537.671	11782

<sup>a</sup> File names are of the form BPC\_DTOCI.CAL\_INTNS\_#####, where ##### is the tabulated suffix.

<sup>b</sup> T81 (see §5.7.1.1).

<sup>c</sup> Coverage reduced due to JFET-off test.

Table 5.7-2: Key fields in the Time-Ordered Data record

Name	First Byte	Description																																		
ATT_QUAT	108	the 4-component attitude quaternions (best available solution) corresponding to eight 4-second intervals starting at the middle of the first “half minor frame.” <sup>a</sup> Each quaternion component is a 32-bit floating point number.																																		
T81_time	245	64-bit floating point Major Frame start time in International Atomic Time (TAI) seconds since 1981 January 1 00:00:00 UTC. The time in the middle of the first half minor frame is T81_time - 0.3125 s.																																		
DADRBSI2	512	<p>Calibrated detector data in an array corresponding to 16 detectors <math>\times</math> 256 half minor frame samples, in the detector sampling order specified by DAMEPS (see below). Each datum is compressed into a signed 2-byte integer with the following bit structure:</p> <p style="text-align: center;">(MSB) s n n n n x x x x x x x x x x (LSB)</p> <p>One of two formulas must be used to reconstruct values, <math>R</math>, in MJy/sr. If DADRBSI2 is positive (<i>i.e.</i>, <math>s</math> is set to 0), then <math>R = X2^N M/f(b)</math>, where <math>X</math> is the integer represented by bits 0 - 10 (the <math>x</math>'s), <math>N</math> is the integer represented by bits 11 - 14 (the <math>n</math>'s), <math>M</math> is the smallest detectable non-zero signal (0.5) at maximum gain (<math>16 \times 27.12</math>; <i>i.e.</i>, <math>M = 0.5/(16 \times 27.12)</math>), and <math>f(b)</math> is the applicable wavelength band-dependent scale factor from the table below. If DADRBSI2 is negative (<i>i.e.</i>, <math>s</math> is set to 1) and has a value greater than or equal to -28358, take the absolute value,<sup>b</sup> extract the <math>N</math> and <math>X</math> (15 least significant) bits, and then calculate <math>R = -X2^N M/f(b)</math>.</p> <table border="1" style="margin-left: auto; margin-right: auto;"> <thead> <tr> <th>b</th> <th>f(b)</th> </tr> </thead> <tbody> <tr><td>1A</td><td>3.0</td></tr> <tr><td>1B</td><td>2.4</td></tr> <tr><td>1C</td><td>1.9</td></tr> <tr><td>2A</td><td>2.6</td></tr> <tr><td>2B</td><td>0.86</td></tr> <tr><td>2C</td><td>0.74</td></tr> <tr><td>3A</td><td>3.2</td></tr> <tr><td>3B</td><td>1.1</td></tr> <tr><td>3C</td><td>0.90</td></tr> <tr><td>4</td><td>3.1</td></tr> <tr><td>5</td><td>0.88</td></tr> <tr><td>6</td><td>0.64</td></tr> <tr><td>7</td><td>0.20</td></tr> <tr><td>8</td><td>0.29</td></tr> <tr><td>9</td><td>0.013</td></tr> <tr><td>10</td><td>0.026</td></tr> </tbody> </table> <p>The roundoff error associated with compression and reconstruction is less than or equal to 0.05% (<math>1\sigma</math>) or <math>0.0006/f(b)</math> MJy/sr, whichever is greater.</p> <p>DADRBSI2 values less than -28358 are given when the data have no scientific utility. One may add 11985 to such values and interpret them as described in Table 4.7-1.</p>	b	f(b)	1A	3.0	1B	2.4	1C	1.9	2A	2.6	2B	0.86	2C	0.74	3A	3.2	3B	1.1	3C	0.90	4	3.1	5	0.88	6	0.64	7	0.20	8	0.29	9	0.013	10	0.026
b	f(b)																																			
1A	3.0																																			
1B	2.4																																			
1C	1.9																																			
2A	2.6																																			
2B	0.86																																			
2C	0.74																																			
3A	3.2																																			
3B	1.1																																			
3C	0.90																																			
4	3.1																																			
5	0.88																																			
6	0.64																																			
7	0.20																																			
8	0.29																																			
9	0.013																																			
10	0.026																																			

DAMEPS	9232	<p>32-byte array giving the detector sampling order for the <i>previous</i> Major Frame. The bytes at array positions <math>2N - 1</math> and <math>2N</math>, where <math>N = 1, 2, \dots, 16</math>, correspond, respectively, to the high (<math>\times 16</math>) and low (<math>\times 1</math>) gain (see §2.2.5) MUX entry port addresses for the <math>N</math>th process sampled by the MUX. The byte values are related to detector numbers as follows:</p> <table border="1" data-bbox="727 453 1149 1024"> <thead> <tr> <th>Band</th> <th>Byte <math>2N - 1</math> (high gain)</th> <th>Byte <math>2N</math> (low gain)</th> </tr> </thead> <tbody> <tr><td>1A</td><td>16</td><td>0</td></tr> <tr><td>2A</td><td>17</td><td>1</td></tr> <tr><td>3A</td><td>18</td><td>2</td></tr> <tr><td>1B</td><td>19</td><td>3</td></tr> <tr><td>2B</td><td>20</td><td>4</td></tr> <tr><td>3B</td><td>21</td><td>5</td></tr> <tr><td>1C</td><td>22</td><td>6</td></tr> <tr><td>2C</td><td>23</td><td>7</td></tr> <tr><td>3C</td><td>24</td><td>8</td></tr> <tr><td>4</td><td>25</td><td>9</td></tr> <tr><td>5</td><td>26</td><td>10</td></tr> <tr><td>6</td><td>27</td><td>11</td></tr> <tr><td>7</td><td>28</td><td>12</td></tr> <tr><td>8</td><td>29</td><td>13</td></tr> <tr><td>9</td><td>30</td><td>14</td></tr> <tr><td>10</td><td>31</td><td>15</td></tr> </tbody> </table> <p>For example, DADBRSCI2 values (<math>N, 1 : 256</math>) where <math>N = 1</math> correspond to MUX process 1. Thus, if bytes <math>2N - 1</math> (<math>= 1</math>) and <math>2N</math> (<math>= 2</math>) have values of 23 and 7, respectively, then the table above shows that the first 256 DADBRSCI2 values refer to data from detector 2C. A similar algorithm can be used to assign detector numbers to each of the 16 processes for which detector data are given in DADBRSCI2.</p>	Band	Byte $2N - 1$ (high gain)	Byte $2N$ (low gain)	1A	16	0	2A	17	1	3A	18	2	1B	19	3	2B	20	4	3B	21	5	1C	22	6	2C	23	7	3C	24	8	4	25	9	5	26	10	6	27	11	7	28	12	8	29	13	9	30	14	10	31	15
Band	Byte $2N - 1$ (high gain)	Byte $2N$ (low gain)																																																			
1A	16	0																																																			
2A	17	1																																																			
3A	18	2																																																			
1B	19	3																																																			
2B	20	4																																																			
3B	21	5																																																			
1C	22	6																																																			
2C	23	7																																																			
3C	24	8																																																			
4	25	9																																																			
5	26	10																																																			
6	27	11																																																			
7	28	12																																																			
8	29	13																																																			
9	30	14																																																			
10	31	15																																																			
PCSV	9512	<p>an 8-byte array, called the “Pipeline Compressed State Vector,” of which only the second byte will be useful in most research applications. Byte 2 indicates “external” factors that influence the data quality and should be interpreted as follows:</p> <table border="1" data-bbox="521 1409 1357 1856"> <thead> <tr> <th>External factor (Bits)</th> <th>Value</th> <th>Interpretation</th> </tr> </thead> <tbody> <tr> <td rowspan="2">Fill data flag (0-1)</td> <td>01</td> <td>some minor frames missing</td> </tr> <tr> <td>11</td> <td>all minor frames missing</td> </tr> <tr> <td rowspan="2">Attitude control (2-3)</td> <td>01</td> <td>spacecraft slewing</td> </tr> <tr> <td>10</td> <td>special pointing</td> </tr> <tr> <td rowspan="3">Attitude solution (4-5)</td> <td>11</td> <td>coarse aspect (non-definitive)</td> </tr> <tr> <td>10</td> <td>coarse aspect (definitive)</td> </tr> <tr> <td>00</td> <td><i>DIRBE</i> fine aspect (definitive)</td> </tr> <tr> <td rowspan="4"><i>COBE</i> location† (6-7)</td> <td>00</td> <td>okay (or not checked, for backward compatibility)</td> </tr> <tr> <td>01</td> <td>in NVAB horn</td> </tr> <tr> <td>10</td> <td>in SVAB horn</td> </tr> <tr> <td>11</td> <td>in the SAA</td> </tr> </tbody> </table> <p>† location relative to SAA and radiation belts 16 seconds after the Major Frame start time. <i>Data when the spacecraft was in the SAA were of suspect quality and should not be used for scientific investigations.</i></p>	External factor (Bits)	Value	Interpretation	Fill data flag (0-1)	01	some minor frames missing	11	all minor frames missing	Attitude control (2-3)	01	spacecraft slewing	10	special pointing	Attitude solution (4-5)	11	coarse aspect (non-definitive)	10	coarse aspect (definitive)	00	<i>DIRBE</i> fine aspect (definitive)	<i>COBE</i> location† (6-7)	00	okay (or not checked, for backward compatibility)	01	in NVAB horn	10	in SVAB horn	11	in the SAA																						
External factor (Bits)	Value	Interpretation																																																			
Fill data flag (0-1)	01	some minor frames missing																																																			
	11	all minor frames missing																																																			
Attitude control (2-3)	01	spacecraft slewing																																																			
	10	special pointing																																																			
Attitude solution (4-5)	11	coarse aspect (non-definitive)																																																			
	10	coarse aspect (definitive)																																																			
	00	<i>DIRBE</i> fine aspect (definitive)																																																			
<i>COBE</i> location† (6-7)	00	okay (or not checked, for backward compatibility)																																																			
	01	in NVAB horn																																																			
	10	in SVAB horn																																																			
	11	in the SAA																																																			

DAOMS	9623	operating mode for the Major Frame encoded in a single byte. 0 $\Rightarrow$ Science Data Mode (SDM). <i>Always check this field before decoding the data.</i>
-------	------	--

<sup>a</sup> the 32-second Major Frame is divided into 128 minor frames (or 256 half minor frames), each lasting 0.25 s. In SDM, each detector's output was sampled once per half minor frame (*i.e.*, at  $\frac{1}{8}$ -second intervals).

<sup>b</sup> This assumes that twos complement representation is used for integers, as is the case on a VAX/VMS machine such as the one used to prepare the data product.

**Construct a matrix of the following form:**

$$\mathbf{A} = \begin{pmatrix} Q_{44} + Q_{11} - Q_{22} - Q_{33} & 2(Q_{12} - Q_{34}) & 2(Q_{13} + Q_{24}) \\ 2(Q_{12} + Q_{34}) & Q_{44} - Q_{11} + Q_{22} - Q_{33} & 2(Q_{23} - Q_{14}) \\ 2(Q_{13} - Q_{24}) & 2(Q_{23} + Q_{14}) & Q_{44} - Q_{11} - Q_{22} + Q_{33} \end{pmatrix}$$

where  $Q_{ij} = q_i q_j$  and  $(q_1, q_2, q_3, q_4)$  is the quaternion. (The quaternion components appear in order from  $q_1$  first to  $q_4$  last in the Time-Ordered Data files.)

Matrix  $\mathbf{A}$  enables transformation from coordinates fixed in the spacecraft reference frame to epoch 2000.0 geocentric equatorial coordinates.

**Transform the DIRBE boresight vector coordinates to equatorial coordinates.** The boresight vector in spacecraft coordinates is

$$\mathbf{V} = \begin{pmatrix} -0.86708729 \\ 0.43196023 \\ -0.24813300 \end{pmatrix}.$$

Thus the instantaneous DIRBE line of sight coordinates,  $\mathbf{D} = \mathbf{AV}$ .  $\mathbf{D}$  is related to epoch 2000 Right Ascension ( $RA$ ) and Declination ( $DEC$ ) as follows:

$$\mathbf{D} = \begin{pmatrix} \cos RA \cos DEC \\ \sin RA \cos DEC \\ \sin DEC \end{pmatrix},$$

where  $RA$  and  $DEC$  are in radians.

### 5.7.1.3 Standard MUX Sequence

During routine operations, the DIRBE detectors were sampled in the order specified in the second column of Table 3.2-1. Users of the Time-Ordered Data should check their decoding results for the DAMEPS field against the standard sequence. One should obtain the standard MUX sequence in most cases.

### 5.7.1.4 Notes on the Use of Polarization Data in the TOD

The intensities in the polarization and photometry channels are all independently celestially stabilized in the same fashion. To preserve the values of the ratios of the intensities in the 'B' and 'C' channels relative to the photometric ('A') channels, the absolute calibration applied to the polarization data in the TOD is handled differently than that of the photometry: the calibration factors and beam solid angles are fixed to the same values used for the corresponding photometric channels.

To calculate the polarizations in the 'B' and 'C' channels, the measured intensities in each channel are iteratively fitted to an expression of the form:

$$S_{\lambda, B \text{ or } C} = Q \cos 2\Theta + U \sin 2\Theta \quad (5.3)$$

where

$$S_{\lambda,B} = 1 - \frac{(I_{\lambda,B}/I_{\lambda,A}) (\Omega_{\lambda,A}/\Omega_{\lambda,B})}{K_{\lambda,B}},$$

$$S_{\lambda,C} = \frac{(I_{\lambda,C}/I_{\lambda,A}) (\Omega_{\lambda,A}/\Omega_{\lambda,C})}{K_{\lambda,C}} - 1,$$

$K_{\lambda,B}$  and  $K_{\lambda,C}$  are the polarization coefficients listed in Table 5.7-3, and  $\Omega$  is the beam solid angle (see Table 4.2-1).

Table 5.7-3: Polarization coefficients

$\lambda$ ( $\mu\text{m}$ )	$K_{\lambda,B}$	$\sigma_{K_{\lambda,B}}^a$	$K_{\lambda,C}$	$\sigma_{K_{\lambda,C}}^a$
1.25	0.784	0.002	0.630	0.002
2.2	0.359	0.002	0.303	0.002
3.5	0.317	0.002	0.279	0.002

<sup>a</sup> standard deviation of the mean

The quantity  $S_{\lambda,B}$  or  $C$  is the fractional signal in the ‘B’ or ‘C’ channel relative to ‘A’, after both channels are placed on the same relative photometric scale via the scaling factors  $K_{\lambda,B}$  or  $C$  ( $\Omega_{\lambda,B}$  or  $C/\Omega_{\lambda,A}$ ). The polarization coefficients,  $K$ , are derived from observations of unpolarized point sources corrected for channel-to-channel differences in detector responsivity. The solid angle ratio ( $\Omega_{\lambda,B}$  or  $C/\Omega_{\lambda,A}$ ) compensates for variations in the beam profile.

To compute the Stokes parameters  $Q$  and  $U$  from the ‘B’ and ‘C’ channel intensities, the orientations of the polarizers,  $\Theta$ , must be known, but polarizer orientations are not provided in the TOD. The orientations must be calculated from the time of observation via the attitude solution and spacecraft angular velocity, both of which are provided.

### 5.7.2 Calibrated Individual Observations and Associated Pixel Index Files

The Calibrated Individual Observations (CIO) files tabulate the calibrated individual  $\frac{1}{8}$ th-second sky survey data samples taken during each day of the cryogenic mission. The CIO files are much more convenient to use than the TOD product, and, in nearly all applications, can be substituted for the TOD. Relative to the TOD, the CIO files

- contain only science survey-mode data;
- omit selected low-quality data;
- present the data in wavelength band, rather than MUX-sequence, order;
- give pointing information in terms of pixel numbers instead of attitude quaternions; and
- are in standard FITS, rather than native (VAX) binary format.

The CIO database is organized into 285 pairs of files, one pair per day, where a “pair” consists of a data file and its associated pixel index file. The data pertaining to observations made between 0h UT and 23:59:59.999 UT, inclusive, are given in a single data file. Within each daily file, the observations are arranged in order of ascending *DIRBE* pixel number, and, whenever a given pixel is observed multiple times, the data for that pixel are given in chronological order.

The Pixel Index files are also organized in ascending pixel number order, and can be used to determine which pixels were observed on a given day. For each pixel, the CIO Pixel Index file lists the number of the last row in the corresponding CIO data file that contains information on that pixel. The number of the *first* row containing data on a given pixel can be derived by adding 1 to the *LastRow* value tabulated in the previous record; data pertaining to the first pixel listed in the Index table begins in row 1 of the data table.



For example, the first four entries in the Pixel Index file for day 89345 indicate that the last CIO data file rows containing data on pixels 20, 21, 22, and 23 are 6, 19, 20, and 30, respectively. According to the algorithm given above, the first rows containing data on these pixels are 1, 7, 20, and 21. In other words, the data pertaining to pixel 20 can be found in rows 1 through 6, the data on pixel 21 in rows 7 through 19, etc.

Tables 5.7-4 and 5.7-5 summarize the contents of the Calibrated Individual Observations and CIO Pixel Index files, respectively. The FITS headers give more detailed information about the individual data fields. Sample CIO and CIO Pixel Index FITS headers are listed in Appendix D. Users of the CIO data products will also need to be familiar with some or all of the information presented in the remainder of this section.

### 5.7.2.1 Reconstruction of Time Strings

Either one of the following methods could be used to extract a time-ordered data string from a CIO file:

1. ingest an entire day's worth of data, and then sort on the time field; or
2. for a given pixel, use the `Next_obs` (`Prev_obs`) field to locate the table row containing the next (previous) observation in the time sequence, and continue recursively until the desired time string has been selected.

Since non-survey mode and SAA crossing data are removed from the CIO dataset, the observations to which `Next_obs` and `Prev_obs` point are not always separated in time by  $\pm\frac{1}{8}$ th second from the current observation; gaps exist in the time sequence. Data in the `Time` field can be used to check for gaps.

### 5.7.2.2 Reconstitution of Attack Vector Values

Attack Vector values, `AttackV`, are represented as two-byte integers in the CIO files. Physical values will be reconstituted by generic FITS-reading software according to a transformation of the form  $\text{physical value} = \text{TSCAL} \times \text{stored value} + \text{TZERO}$ . In the FITS files, `TSCAL` is assigned the value  $2^{-15}$ , and `TZERO` is set to 0.

An offset *not* taken into account by `TZERO` should be added to the reconstituted `AttackV` values to compensate for a bug in the software used to calculate the integers recorded in the FITS files. Table 5.7-6 indicates how the offset should be applied. The correction will be applied automatically by the *COBE* analysis software (see §D.1; version 3.0 or higher).

### 5.7.2.3 Determination of Sky Coordinates

The tabulated `Pixel_no` corresponds to a position within the boundary of a resolution 9 ( $0^\circ 32$  square) CSC pixel (see §5.3). More accurate positions can be calculated if one uses the tabulated `PSubPos` and `PSbSbPos` data to reconstruct a resolution 15 quad-sphere "super pixel number," defined as follows:

$$\text{super pixel number} = 4096 \times \text{Pixel\_no} + 16 \times \text{PSubPos} + \text{PSbSbPos}. \quad (5.4)$$

Appendix D.1 lists programs that can be used to compute sky coordinates from input resolution 9 or resolution 15 CSC pixel numbers; a different program is required for each resolution. A resolution 15 pixel is a roughly  $20''$  square.

"Super pixel number" positions correspond to the nominal attitude, which was derived from the ensemble of data from all three  $2.2 \mu\text{m}$  detectors. However, as indicated in Table 4.2-1, the beam centroid of each individual detector can be offset by up to a few arcminutes from this nominal position due to differences in the beam profiles. Thus, in order to derive precise sky coordinates, detector-dependent corrections must be applied to the super pixel number coordinates. The correction calculation should go as follows.

1. Convert the super pixel number to an ecliptic J2000 3-vector line of sight (LOS) using the `SUPERCENPIX` routine;

Table 5.7-4: Columns in the Calibrated Individual Observations FITS tables

n	TTYEn <sup>a</sup>	Description
1	Pixel_no	<i>DIRBE pixel number</i> (signed 32-bit integer) Pixel number in the CSC projection (see §5.3).
2	PSubPos	<i>Pixel sub-position</i> (8-bit byte) Location of the line of sight within pixel Pixel_no.
3	PSbSbPos	<i>Pixel sub-sub-position</i> (8-bit byte) Location of the line of sight within sub-pixel PSubPos.
4	Time	<i>Time</i> (64-bit floating point) Time of observation in atomic (TAI) seconds elapsed since 1981 January 1 00:00:00 UTC <sup>b</sup> .
5	Next_obs	<i>Pointer to next observation</i> (32-bit integer) Number of the row in this table containing data on the next observation in the time sequence. Nominally the next survey-mode observation was made at Time + $\frac{1}{8}$ th sec.
6	Prev_obs	<i>Pointer to previous observation</i> (32-bit integer) Number of the row in this table containing data on the previous observation in the time sequence. Nominally the preceding survey-mode observation was made at Time - $\frac{1}{8}$ th sec.
7	Phot1A	<i>Intensities</i> , in MJy/sr, reported for a single, $\frac{1}{8}$ th second sample: (all 32-bit floating point) 1.25 $\mu\text{m}$ full (Band 1A) intensity 1.25 $\mu\text{m}$ polarized light (Band 1B) intensity 1.25 $\mu\text{m}$ polarized light (Band 1C) intensity 2.2 $\mu\text{m}$ full (Band 2A) intensity 2.2 $\mu\text{m}$ polarized light (Band 2B) intensity 2.2 $\mu\text{m}$ polarized light (Band 2C) intensity 3.5 $\mu\text{m}$ full (Band 3A) intensity 3.5 $\mu\text{m}$ polarized light (Band 3B) intensity 3.5 $\mu\text{m}$ polarized light (Band 3C) intensity 4.9 $\mu\text{m}$ (Band 4) intensity 12 $\mu\text{m}$ (Band 5) intensity 25 $\mu\text{m}$ (Band 6) intensity 60 $\mu\text{m}$ (Band 7) intensity 100 $\mu\text{m}$ (Band 8) intensity 140 $\mu\text{m}$ (Band 9) intensity 240 $\mu\text{m}$ (Band 10) intensity
8	Phot1B	
9	Phot1C	
10	Phot2A	
11	Phot2B	
12	Phot2C	
13	Phot3A	
14	Phot3B	
15	Phot3C	
16	Phot04	
17	Phot05	
18	Phot06	
19	Phot07	
20	Phot08	
21	Phot09	
22	Phot10	
23	LOS2VelV	<i>Angle between DIRBE line of sight and spacecraft orbital velocity vector</i> (signed 16-bit integer)
24	ApprVec	<i>Approach Vector</i> (8-bit byte) Observations were classified as “forward-looking,” and assigned Approach Vector value 1, if the line of sight was aligned within 90° of the direction of spacecraft motion; otherwise the observation was “backward-looking” and the Approach Vector was assigned the value 2.
25	AttackV	<i>Attack Vector</i> (vector of 3 signed 16-bit integers) A vector whose three components specify the rate of change (derivative with respect to time) of the <i>DIRBE</i> boresight unit vector.
26	AtV_Azim	<i>Azimuth of the Attack Vector</i> (signed 16-bit integer) Azimuth relative to a fiducial zero angle defined by the cross product of the <i>DIRBE</i> spin axis and boresight vectors.
27	SolElong	<i>Solar elongation angle, <math>\varepsilon</math></i> (signed 16-bit integer) Angle between the spacecraft-Sun vector and the <i>DIRBE</i> line of sight.
28	Moon2LOS	<i>Angle between spacecraft-Moon vector and DIRBE line of sight</i> (signed 16-bit integer) When Moon2LOS $\leq 10^\circ$ the observations are potentially contaminated by lunar stray light.

29	MoonAzim	<i>Azimuth of the Moon</i> (signed 16-bit integer) Azimuth of the projection of the spacecraft–Moon vector onto the plane normal to the <i>DIRBE</i> line of sight relative to the fiducial zero angle defined above (see description of <i>AtV_Azim</i> ).
30	Jup2LOS	<i>Angle between spacecraft–Jupiter vector and DIRBE line of sight</i> (signed 16-bit integer) When $\text{Jup2LOS} \leq 1.5$ the observations are potentially contaminated by stray light from Jupiter.
31	RadZone	<i>Radiation zone flag</i> (8-bit byte) Flag indicates if the spacecraft was within the South Atlantic Anomaly (SAA), North Van Allen Belt (NVAB) or South Van Allen Belt (SVAB) at the time of observation.
32	XSNoise	<i>Excess noise flag</i> (signed 16-bit integer) Flags indicate whether exceptionally noisy data were recorded during the 32-second long Major Frame that included this observation. Each of the 16 bits corresponds to one <i>DIRBE</i> detector.
33	OA_Flags	<i>Orbit and attitude flags</i> (8-bit byte) Miscellaneous orbit and attitude information.

<sup>a</sup> FITS keyword giving the label or heading for field (*i.e.*, table column) *n*.

<sup>b</sup> T81 (see §5.7.1.1).

Table 5.7-5: Columns in the CIO Pixel Index FITS tables

<i>n</i>	TTYPEn <sup>a</sup>	Description
1	Pixel_no	<i>DIRBE pixel number</i> (signed 32-bit integer) Pixel number in the CSC projection.
2	LastRow	<i>Last row number</i> (signed 32-bit integer) Number of the last row in the corresponding CIO data table that contains data on this pixel.

<sup>a</sup> FITS keyword giving the label or heading for field (*i.e.*, table column) *n*.

Table 5.7-6: Offset corrections for Attack Vectors in CIO files

If the physical value $\text{AttackV} \times \text{TSCAL}^a$ is	Then add
value $\geq \text{TSCAL}$	$0.5 \times \text{TSCAL}$
value $\leq -\text{TSCAL}$	$-0.5 \times \text{TSCAL}$
0.0	0.0

<sup>a</sup>  $\text{TSCAL} = 2^{-15}$

2. look up (or read from the ASCII file `DIRBE_BEAM_CHARACTERISTICS_P3B.ASC`) the in-scan and cross-scan beam centroid offsets corresponding to the detector of interest, and convert them to units of radians;

3. normalize the tabulated Attack Vector data (`AttackV`) by dividing each component by the magnitude,

$$\sqrt{\text{AttackV}(1)^2 + \text{AttackV}(2)^2 + \text{AttackV}(3)^2},$$

and call the normalized vector `NATV`; and

4. calculate the components of the new line of sight vector, `LOS'`, as follows:

$$\text{LOS}'(1) = \text{LOS}(1) + \text{ISCO} \times \text{NATV}(1) + \text{XSCO} \times [\text{LOS}(2) \times \text{NATV}(3) - \text{LOS}(3) \times \text{NATV}(2)],$$

$$\text{LOS}'(2) = \text{LOS}(2) + \text{ISCO} \times \text{NATV}(2) + \text{XSCO} \times [\text{LOS}(3) \times \text{NATV}(1) - \text{LOS}(1) \times \text{NATV}(3)],$$

and

$$\text{LOS}'(3) = \text{LOS}(3) + \text{ISCO} \times \text{NATV}(3) + \text{XSCO} \times [\text{LOS}(1) \times \text{NATV}(2) - \text{LOS}(2) \times \text{NATV}(1)],$$

where `ISCO` and `XSCO` are the in-scan and cross-scan beam offsets, respectively. The components of `LOS'` are direction cosines, in ecliptic J2000 coordinates, corresponding to the centers of the individual detector beams.

Users of the polarization data are advised to apply the 'A' channel centroid offsets to the 'A', 'B' and 'C' channels when making polarization maps. Failure to do this could lead to incorrect B/A and C/A intensity ratios.

Bear in mind that the *DIRBE* attitude solution has a  $1\sigma$  uncertainty of  $1'5$ . As a rule, in the absence of independent information, it would be *inappropriate to quote positions to greater than arcminute precision*.

#### 5.7.2.4 Quality Flags

Individual observations that failed to pass certain quality tests are replaced in the CIO files by sentinel values  $\leq -16385$ . However, some data known to be of low quality, such as observations affected by stray light from the Moon or Jupiter, were not explicitly flagged. Information given in the fields `Moon2LOS` and `Jup2LOS` can be used to cull out unflagged but low-quality data. Data rejection is recommended whenever (a) `Moon2LOS`  $\leq 10^\circ$ , (b) `Jup2LOS`  $\leq 1^\circ5$ , or (c) the `XNoise` flag is set for the detector of interest. Even if the CIO data are filtered as suggested, a few anomalies will remain, especially in Bands 7 and 8 (60 and 100  $\mu\text{m}$ ).

#### 5.7.2.5 Polarization Data in the CIO Files

The information in §5.7.1.4 on *Polarization Data in the TOD* also pertains to the CIO, with the exception that the polarizer orientation can be readily calculated from the Attack Vector and pixel number data provided in the CIO.

To compute the Stokes parameters  $Q$  and  $U$  from the 'B' and 'C' channel intensities using equation (5.3), the orientations of the 'C' channel polarizers,  $\Theta$ , must be known. By *DIRBE* convention,  $\Theta$  is defined as the angle between the polarizer axes and the local meridian (*i.e.*, a great circle drawn through the spacecraft and the North and South ecliptic poles). Noting that the transmission axes of the 'C' channel polarizers are aligned with the direction of scan motion,  $\Theta$  can be calculated as follows:

1. Compute the ecliptic longitude and latitude,  $(\lambda, \beta)$ , in radians, from the pixel number, `Pixel_no` (see §5.3)

2. Calculate

$$\text{att}_x = \text{AttackV}(1) \cos(\lambda) + \text{AttackV}(2) \sin(\lambda),$$

$$\text{att}_y = \text{AttackV}(2) \cos(\lambda) - \text{AttackV}(1) \sin(\lambda),$$

$$\text{colatitude} = \frac{\pi}{2} - \beta,$$

and

$$x' = \text{att\_x} \cos(\text{colatitude}) - \text{AttackV}(3) \sin(\text{colatitude})$$

3. Finally, calculate

$$\Theta = \arctan(\text{atty}/x'),$$

such that  $\Theta$  is in the range  $[-90^\circ, +90^\circ]$ .

Close to the solar elongation extrema,  $\varepsilon = 64^\circ$  and  $124^\circ$ , the ‘C’ channel transmission axis is nearly aligned with the local meridian, and  $\Theta \simeq 0$ . When  $\varepsilon \sim 94^\circ$ , the scan direction is perpendicular to the local meridian and  $\Theta \simeq \pm 90^\circ$ .

Further information about the *DIRBE* polarization algorithm can be found in Chapter 4. For a summary of polarization results, see Berriman *et al.* (1994).

### 5.7.3 Weekly Sky Maps

The Weekly Sky Maps give weekly-averaged intensity values for the 10 *DIRBE* photometric bands, plus the Stokes Q and U parameters at 1.25, 2.2 and 3.5  $\mu\text{m}$ . There are 41 Weekly Sky Map files, one per week of optimized operation in the cryogenic mission (see Table 3.1-2).

The files are FITS binary tables. Each table row corresponds to a *DIRBE* pixel. Table 5.7-7 describes the FITS table columns. More complete documentation is provided in the FITS headers (see Appendix D for a sample header listing).

The following two sections are relevant only to the (obsolete) Pass 2B versions of the Weekly Sky Maps. In the Pass 3B versions, non-zero FITS TZER0 keywords are included in the `DeltaT` and `SolElong` fields to align the data properly with respect to the  $\Delta Time$  and  $\varepsilon$  bins, and to allow for negative  $\Delta Time$  values. Standard FITS ingest software should correctly interpret the Pass 3B data files.

#### 5.7.3.1 Note on Reconstitution of $\Delta Time$ Values (Pass 2B only)

The  $\Delta Time$  field is unique in that it must be interpreted as a scaled signed byte (*i.e.*, as a number in the range  $-128$  to  $+127$  linearly transformed into a value of  $\Delta Time$ ). Unfortunately, because the FITS standard accommodates only *unsigned* bytes (which have values ranging from 0 to 255), generic FITS-reading software will not interpret the  $\Delta Time$  values properly. Compliance with the FITS standard was intended and an alternate encoding scheme may be applied if new versions of the Weekly Sky Maps are produced. In the meantime the *COBE* analysis software mentioned in §D.1 (version 3.0 or higher) will correctly unpack the  $\Delta Time$  field. The FORTRAN program `dirbe_wk_read` included in Appendix D illustrates how the data should be treated.

Additional information about the  $\Delta Time$  field is given below.

Table 5.7-7: Columns in the Weekly Sky Map FITS tables

n	TTYpEn <sup>a</sup>	Description
1	Pixel_no	<i>DIRBE pixel number</i> (signed 32-bit integer) Pixel number in the CSC projection (see §5.3).
2	PSubPos	<i>Pixel sub-position</i> (byte) Gives the small but potential offset between the centroid position of the samples included in the weekly average and the pixel center coordinates (see §5.3).
3	Displace	<i>Displacement means</i> (vector of 4 bytes) The centroid position given by Pixel_no and PSubPos is based upon the attitude solution, and thus upon band 2 (2.2 $\mu\text{m}$ ; see §4.3). Although the <i>DIRBE</i> map-making software compensates for the relative locations of the beams associated with the other bands (see §4.2.2), PSubPos is technically applicable only to band 2. Displace gives offsets analogous to PSubPos for the four bands that have the greatest beam offsets.
4	Time	<i>Time</i> (64-bit floating point) Average of the times at which the pixel was observed during the week given in International Atomic Time (TAI) seconds elapsed since 1981 January 1 00:00:00 UTC <sup>b</sup> .
5	DeltaT	$\Delta$ <i>Time</i> (vector of 10 bytes) Since the number of measurements included in a weekly average was photometric band-dependent, the Time value is only an approximation to the average time the pixel was observed at a particular wavelength. A more accurate time for each band is Time plus the value of DeltaT for that band.
6	SolElong	<i>Solar elongation angle, <math>\varepsilon</math></i> (signed 16-bit integer) Average of the solar elongation angles at which the pixel was observed during the week. The comment made about the accuracy of Time under DeltaT also applies to SolElong.
7	Photomet	<i>Photometry</i> (vector of 10 32-bit floating point values) Average intensity observed for the pixel over the week, in units of MJy/sr. The 10 values correspond to the 10 <i>DIRBE</i> bands in order of increasing wavelength.
8	Stokes	<i>Stokes parameters</i> (vector of 6 32-bit floating point values) Stokes Q and U parameters given as (Q,U) pairs for wavelengths in the order 1.25, 2.2 and 3.5 $\mu\text{m}$ . The Stokes parameters for each band are averages of the individual Qs and Us, weighted according to their uncertainties. Since more stringent data selection criteria were used for the polarimetry than for the photometry, average fields such as Time, DeltaT, and SolElong do not strictly apply to the polarization fields. However, because the Stokes parameters vary only weakly with time and $\varepsilon$ , the quoted weekly-averaged values may be assumed to apply.
9	NumRecs	<i>Number of records</i> (signed 16-bit integer) Number of times the pixel was observed this week in at least one photometric band. (Observations made contemporaneously at multiple wavelengths count once.)
10	WtNumObs	<i>Weighted number of observations</i> (vector of 10 bytes) Effective number of observations contributing to the weekly averaged intensities ( <i>i.e.</i> , sum of the weights assigned to the individual measurements). The band-dependent values are given in order of increasing wavelength.

11	StdDev	<i>Photometry standard deviation</i> (vector of 10 bytes) Standard deviations of the mean intensities for the 10 <i>DIRBE</i> bands given in ascending wavelength order and encoded. The FITS header describes how to decode the stored values.
12	StokesSD	<i>Stokes parameter standard deviations</i> (vector of 6 bytes) Standard deviations of the mean Stokes parameter values given in the same order as the Stokes parameters and encoded. The FITS header describes how to decode the stored values.
13	SSOFlag	<i>Solar system object flag</i> (byte) Indicates which solar system object exclusion zones (see §5.6.2), if any, intersect the pixel at some time during the week. See FITS header for interpretation instructions.
14	FracUsed	<i>Fraction of data used</i> (vector of 3 bytes) Percentage of available data used to calculate the weekly average values in all intensity bands, band 1B (1.25 $\mu\text{m}$ ), and band 7 (60 $\mu\text{m}$ ), respectively.
15	StokQual	<i>Stokes parameter quality flag</i> (vector of 6 bytes) Set of flags, one per Stokes parameter, indicating factors that affect the quality of the quoted values. See FITS header for interpretation instructions.

<sup>a</sup> FITS keyword giving the label or heading for field (*i.e.*, table column) *n*.

<sup>b</sup> T81 (see §5.7.1.1).

### 5.7.3.2 Note on Reconstitution of “Binned” Quantities (Pass 2B only)

As a space-saving measure  $\Delta Time$  and mean  $\epsilon$  values are not given to full precision in the Weekly Sky Maps. In particular, to represent a  $\Delta Time$  value in a single byte, the true value was assigned to one of 128 bins, each lasting 4725 seconds (one week divided by 128); analogously, to cast a solar elongation value into a two-byte integer, the true value was assigned to one of 32767 bins, each about a hundredth of a degree wide.

Generic FITS-reading software is supposed to apply a transformation of the form physical value = TSCAL  $\times$  stored value + TZERO, where TSCAL and TZERO come from the FITS header. Values of 0 were mistakenly assigned to TZERO for the DeltaT and SolElong fields; the values that *should* have been assigned, which correspond to half the respective bin intervals, are given in Table 5.7-8. The COBE analysis software (see §D.1; version 3.0 or higher) compensates for the error in the data files by adding the tabulated offset values. The FORTRAN program `dirbe_wk_read` included in Appendix D illustrates how the data should be treated.

Table 5.7-8: Offset values for Weekly Sky Map fields

Field	Offset
DeltaT	$0.5 \times 4725 \text{ sec}$
SolElong	$0.5 \times [360 / (2^{15} - 1)] \text{ deg}$

### 5.7.4 DIRBE Calibrated Annual File and Associated Pixel Index File

The *DIRBE* Calibrated Annual File (DCAF) is a reorganized form of the Weekly Sky Maps designed to facilitate access to the weekly-averaged intensities seen in individual pixels as a function of time. Those who wish to study or model time-variable signals, such as zodiacal light, will find this organization convenient.

The columns of the DCAF FITS binary table are exactly the same as those in the Weekly Sky Maps (see Table 5.7-7). The rows are organized differently, however. Whereas the Weekly Sky Maps contain only one weekly-averaged row entry per pixel, the DCAF contains multiple row entries per pixel,

each corresponding to a week of the cryogenic mission. As in the Weekly Maps, the data are given in ascending *DIRBE* pixel number order; the DCAF data for individual pixels are given in chronological order.

Because of its relatively large size, the DCAF dataset is presented in six files, one for each of the six faces of the *COBE* sky cube. Figures 5.3-1 and 5.3-2 show the relationships between pixel numbers, Galactic coordinates, and cube faces. Table 5.7-9 gives the range of ecliptic coordinates covered by each cube face. The *DIRBE* sky scan strategy (see §2.3.4) was such that pixels above  $|\beta| \sim 60^\circ$  were typically observed during each week of the mission, while pixels closer to the ecliptic plane were typically seen during only about half of the mission. Thus, the FACE0 and FACE5 DCAF files are about twice as large as the others.

Table 5.7-9: Ecliptic coordinate ranges covered by CSC cube faces

Cube face number	Range of		
	Pixel numbers	Ecliptic longitude ( $^\circ$ ) <sup>a</sup>	Ecliptic latitude ( $^\circ$ ) <sup>a</sup>
0	0 – 65535	0 – 360	+45 – +90
1	65536 – 131071	315 – 45	–45 – +45
2	131072 – 196607	45 – 135	–45 – +45
3	196608 – 262143	135 – 225	–45 – +45
4	262144 – 327679	225 – 315	–45 – +45
5	327680 – 393215	0 – 360	–45 – –90

<sup>a</sup> The ecliptic coordinate ranges are approximate.

A separate DCAF Pixel Index table is provided for each cube face. Table 5.7-10 lists the fields in a DCAF index table. One can use the tabulated **LastRow** to determine which rows (*i.e.*, range of row numbers) in the corresponding DCAF data file contain data on a specific pixel. To calculate “**FirstRow**,” the number of the first row in the range, add 1 to the **LastRow** value listed for the previous pixel; for the first listed pixel, “**FirstRow**” is equal to 1. (This calculation is illustrated in an example given in §5.7.2.) Once a range of row numbers has been specified, a FITS reader can be used to extract only the desired data, thus expediting data selection.

Sample DCAF and DCAF Pixel Index FITS headers are listed in Appendix D. The FITS headers give more detailed information about the individual data fields.

Table 5.7-10: Columns in the DCAF Pixel Index FITS tables

n	TTYPE <sup>n</sup>	Description
1	Pixel_no	<i>DIRBE pixel number</i> (signed 32-bit integer) Pixel number in the CSC projection.
2	LastRow	<i>Last row number</i> (signed 32-bit integer) Number of the last row in the corresponding DCAF data table that contains data on this pixel.
3	WksObs	<i>Weeks observed flag</i> (6 8-bit byte) Each bit set to 1 corresponds to a week during the cryogenic mission when the pixel was observed.

<sup>a</sup> FITS keyword giving the label or heading for field (*i.e.*, table column) n.

### 5.7.5 $\varepsilon = 90^\circ$ Sky Maps

The  $\varepsilon = 90^\circ$  Sky Maps are provided in 10 FITS binary table files, one per *DIRBE* intensity band. Both the file names and the FITS headers indicate to which band the data apply. Each row of the FITS table corresponds to a *DIRBE* pixel. However, for reasons described in §5.2.6, there are sometimes two entries, and hence two table rows, for a pixel. Table 5.7-11 describes the FITS table columns. More complete documentation is provided in the FITS headers (see Appendix D for a sample header listing).



Table 5.7-11: Columns in the  $\varepsilon = 90^\circ$  Sky Map FITS tables

n	TTYPE <sup>a</sup>	Description
1	Pixel_no	<i>DIRBE pixel number</i> (signed 32-bit integer) Pixel number in the CSC projection (see §5.3).
2	Time	<i>Time</i> (64-bit floating point) Effective time of observation at $\varepsilon = 90^\circ$ in International Atomic Time (TAI) seconds elapsed since 1981 January 1 00:00:00 UTC. <sup>b</sup>
3	Photomet	<i>Photometry</i> (32-bit floating point) Interpolated $\varepsilon = 90^\circ$ intensity in MJy/sr.
4	EfNumObs	<i>Effective number of observations</i> (signed 16-bit integer) Approximate number of observations of the pixel over the mission (see FITS header for details).
5	StdDev	<i>Photometry standard deviation</i> (byte) Standard deviation of the interpolated intensity (Photomet) encoded as described in the FITS header.
6	FitQual	<i>Fit quality flag</i> (byte) Information about quality and type of interpolation to $\varepsilon = 90^\circ$ . Bit values indicate various conditions (see FITS header for details).
7	FitChiSq	<i>Fit <math>\chi^2</math></i> (byte) $\chi^2$ per degree of freedom for the interpolation.

<sup>a</sup> FITS keyword giving the label or heading for field (*i.e.*, table column) n.

<sup>b</sup> T81 (see §5.7.1.1). The quoted time, which is based on an interpolation of the observation times to  $\varepsilon = 90^\circ$ , is not the same as the time at which the pixel center crossed  $\varepsilon = 90^\circ$ . However the difference between these two times was typically less than 1 hour.

### 5.7.6 Galactic Plane Maps ( $\varepsilon = 90^\circ$ )

The Galactic Plane Maps, which were designed to facilitate analysis of the Galaxy, are subsets of the  $\varepsilon = 90^\circ$  Sky Maps described in the previous section. Photometric data for all 10 *DIRBE* bands are given in a single 6 MB file. Each row of this FITS binary table corresponds to a *DIRBE* pixel. Table 5.7-12 describes the FITS table columns. More complete documentation is provided in the FITS header, which is listed in Appendix D.

Three versions of the Galactic Plane Maps file were produced. *The Pass 3B version supersedes both the initial DIRBE data product, which was released in July 1993 and prepared with an early version of the DIRBE data reduction software, and the Pass 2B version.* Over time, the calibration and map-making algorithms were refined. Early improvements compensated for the effect of photon-induced responsivity enhancement at 100  $\mu\text{m}$  (see §3.4.2) and made beam offset corrections (see §4.2.2). Additional calibration changes, especially in the 1.25 – 12  $\mu\text{m}$  bands, were introduced when the Pass 3B version was created.

With the following minor exceptions, the Pass 2B and 3B versions of the Galactic Plane Maps FITS file are identical in format to the Initial Product:

- the PHOT\_QUALITY compression factor, N, used for the 12 and 25  $\mu\text{m}$  bands (5 and 6) is 3 in the Initial Product and 4 in later versions, and
- the Pass 2B and 3B versions include a flag in bits 4–7 of the first PHOT\_QUALITY byte indicating if an “outlier” weekly-average sample was excluded in the interpolation to  $\varepsilon = 90^\circ$ .

The following section applies only to the (obsolete) Pass 2B version of the Galactic Plane Maps. Non-zero values are assigned to the FITS TZERO keywords in the Pass 3B version, and standard FITS ingest software should calculate the right ecliptic and Galactic coordinates.

Table 5.7-12: Columns in the Galactic Plane Maps FITS table

n	TTYPEn <sup>a</sup>	Description
1	Pixel_no	<i>DIRBE pixel number</i> (signed 32-bit integer) Pixel number in the CSC projection (see §5.3). Corresponding pixel center sky coordinates are given in columns 5,6,7 and 8.
2	Photomet	<i>Photometry</i> (vector of 10 32-bit floating point values) Intensity values for the 10 <i>DIRBE</i> photometric bands, in MJy/sr, listed in order of increasing wavelength.
3	PhotQual	<i>Quality of photometry</i> (vector of 10 signed 16-bit integers) Information about the quality of the photometric data. The first (least significant) byte indicates various conditions that affected the quality of the interpolation to $\varepsilon = 90^\circ$ ; the standard deviation of the intensity is encoded in the second (most significant) byte. The 10 <i>PhotQual</i> values correspond respectively to the 10 <i>Photomet</i> values. See FITS header for interpretation instructions.
4	TIME	<i>Time</i> (64-bit floating point value) Effective time of observation at $\varepsilon = 90^\circ$ in International Atomic Time (TAI) seconds elapsed since 1981 January 1 00:00:00 UTC. <sup>b</sup>
5	EcLon	<i>Ecliptic longitude</i> (signed 16-bit integer) J2000 ecliptic longitude of the CSC pixel center in degrees.
6	EcLat	<i>Ecliptic latitude</i> (signed 16-bit integer) J2000 ecliptic latitude of the CSC pixel center in degrees.
7	GaLon	<i>Galactic longitude</i> (signed 16-bit integer) Galactic longitude of the CSC pixel center in degrees.
8	GaLat	<i>Galactic latitude</i> (signed 16-bit integer) Galactic latitude of the CSC pixel center in degrees.

<sup>a</sup> FITS keyword giving the label or heading for field (*i.e.*, table column) n.<sup>b</sup> T81 (see §5.7.1.1). The quoted time, which is based on an interpolation of the observation times to  $\varepsilon = 90^\circ$ , is not the same as the time at which the pixel center crossed  $\varepsilon = 90^\circ$ . However the difference between these two times was typically less than 1 hour.

### 5.7.6.1 Note on Quoted Coordinate Values (Pass 2B only)

Pixel center coordinates are represented as two-byte integers in the Galactic Plane Maps. Physical values will be reconstituted by generic FITS-reading software according to a transformation of the form  $\text{physical value} = \text{TSCAL} \times \text{stored value} + \text{TZERO}$ . For all of the sky coordinates (`EcLon`, `EcLat`, `GaLon`, and `GaLat`), TSCAL was assigned the value  $360/(2^{15} - 1)$ , corresponding to about a hundredth of a degree, in the FITS header. In each case TZERO was set to 0.

An offset *not* taken into account by TZERO should be added to the reconstituted coordinates to compensate for a bug in the software used to generate the integers recorded in the FITS file. Table 5.7-13 describes how the offset should be applied. The correction will automatically be applied by the COBE analysis software (see §D.1; version 3.0 or higher). The FORTRAN program `dirbe_gp_read` included in Appendix D also illustrates how the data should be treated.

Table 5.7-13: Offset values for Galactic Plane Map coordinates<sup>a</sup>

If the physical value in degrees is	Then add
value $\geq 360/(2^{15} - 1)$	$0.5 \times [360/(2^{15} - 1)]$
value $\leq -360/(2^{15} - 1)$	$-0.5 \times [360/(2^{15} - 1)]$
$-360/(2^{15} - 1) < \text{value} < 360/(2^{15} - 1)$	0.0

<sup>a</sup> Corrections applicable to `EcLon`, `EcLat`, `GaLon`, and `GaLat`.

## 5.7.7 Annual Average Sky Maps

The Annual Average Sky Maps are provided in 10 FITS binary table files, one per *DIRBE* intensity band. Both the file names and the FITS headers indicate to which band the data apply. Each row of the FITS table corresponds to a *DIRBE* pixel. Table 5.7-14 describes the FITS table columns. More complete documentation is provided in the FITS headers (see Appendix D for a sample header listing).

## 5.8 The Analyzed Science Data Sets

The Analyzed Science Data Sets (ASDS) are high-level products derived from reductions of the lower-level *DIRBE* data. Some of these data sets are by-products of the processing pipeline.

### 5.8.1 *DIRBE* Sky and Zodi Atlas and associated Pixel Index File

In many applications, the DSZA can be used instead of the DCAF. Most of the information in the DCAF is included in the DSZA, and the latter product also includes estimates of the zodiacal light intensity which can be compared directly with, or subtracted from, the *DIRBE* measurements. Using the DSZA, one can readily compare the apparent time variability of the sky, as observed by the *DIRBE* with that of the *DIRBE* IPD model (Kelsall *et al.* 1998), or construct sky maps like the ZSMA maps using different data selection criteria (*e.g.*, maps based on data obtained during different weeks in the cryogenic mission).

The DSZA is accompanied by a pixel index and organized in the same fashion as the DCAF (see §5.7.4). Table 5.8-1 lists the columns in the DSZA binary table. The data in columns 1–9 are identical to those in corresponding columns of the DCAF; the calculated zodiacal light intensity is given in column 10. The fields in the DSZA pixel index files are the same as those in the DCAF pixel index files (see Table 5.7-10). More detailed descriptions of the individual fields can be found in the FITS headers.

### 5.8.2 Zodi-Subtracted Mission Average Maps (ZSMA)

Like the Annual Average Sky Maps (see §5.7.7), the ZSMA Maps are provided in ten FITS binary tables, one each at 1.25, 2.2, 3.5, 4.9, 12, 25, 60, 100, 140 and 240  $\mu\text{m}$ . The map wavelength is recorded both in the FITS header and the file name. Each row of the FITS table corresponds to a *DIRBE* pixel.

Table 5.7-14: Columns in the Annual Average Sky Map FITS tables

n	TTYPE <sup>a</sup>	Description
1	Pixel_no	<i>DIRBE pixel number</i> (signed 32-bit integer) Pixel number in the CSC projection (see §5.3).
2	PSubPos	<i>Pixel sub-position</i> (byte) Gives the small offset between the centroid position of the samples included in the annual average and the pixel center coordinates (see §5.3).
3	Time	<i>Time</i> (64-bit floating point) Average of the times at which the pixel was observed during the entire cryogenic mission given in International Atomic Time (TAI) seconds elapsed since 1981 January 1 00:00:00 UTC. <sup>b</sup>
4	Photomet	<i>Photometry</i> (32-bit floating point) Average intensity observed for the pixel over the entire cryogenic mission, in MJy/sr.
5	StdDev	<i>Photometry standard deviation</i> (32-bit floating point) Standard deviation of the mean intensity ( <b>Photomet</b> ) in MJy/sr.
6	WtNumObs	<i>Weighted number of observations</i> (16-bit integer) Sum of the weekly weighted numbers of observations used to calculate the mean intensity, <b>Photomet</b> .
7	SumNRecs	<i>Total number of observations</i> (32-bit integer) Total number of times the pixel was observed during the mission, regardless of the weights assigned to the observations.

<sup>a</sup> FITS keyword giving the label or heading for field (*i.e.*, table column) n.

<sup>b</sup> T81 (see §5.7.1.1). Note that the quoted time does not necessarily correspond to the time of an actual observation.

Only one ZL-subtracted intensity value, representing an average over the cryogenic mission, is given per pixel.

Table 5.8-2 describes the data fields in the Zodi-Subtracted Mission Average maps. More detailed information is contained in the FITS header.

### 5.8.3 Photometric Standard Values Table

Photometric data obtained on 92 standard objects which were judged not to vary in brightness at a particular wavelength over the course of the cold mission were used to stabilize the *DIRBE* photometric system in the celestial calibration stage of the *DIRBE* data reduction pipeline (see Chapter 4). The Photometric Standard Values Table lists mission-averaged flux densities (in Jy) for the selected objects. The quoted flux densities assume a source spectrum characterized by  $\nu F_\nu = \text{constant}$  (see § 5.5); a color correction (see Appendix B) must be applied to determine the true flux density if the source spectrum differs from the assumed energy distribution. Nominal wavelengths for the 10 *DIRBE* bands are 1.25, 2.2, 3.5, 4.9, 12, 25, 60, 100, 140 and 240  $\mu\text{m}$ . The bandwidths and system responses at each wavelength are described in § 2.2.2, and the response functions are tabulated in Appendix A and provided as a data product (see § 5.9).

Like the other calibrated *DIRBE* products, the Photometric Standard Values Table quotes flux densities whose absolute calibration at each wavelength is based upon measurements of a single source (see § 4.5.3). The *DIRBE* point source photometry agrees with that of Engelke (1992) and Cohen *et al.* (1992, 1995) at 2.2  $\mu\text{m}$  and 12  $\mu\text{m}$  (*IRAS*) to within the absolute calibration uncertainties of the different systems.

The quoted flux densities were derived as follows. For individual sightings of the standard objects in the time-ordered data, a local background intensity and a background-subtracted flux density were calculated using the algorithm described in § 4.5.3.2. At each wavelength, the background-subtracted flux densities were then averaged over the cold mission. The quoted error is the standard deviation of

Table 5.8-1: Columns in the DIRBE Sky and Zodi Atlas

n	TTYpEn <sup>a</sup>	Description
1	Pixel_no	<i>DIRBE pixel number</i> (signed 32-bit integer) Pixel number in the CSC projection (see §5.3).
2	Time	<i>Time</i> (64-bit floating point) Average of the times at which the pixel was observed during the week given in International Atomic Time (TAI) seconds elapsed since 1981 January 1 00:00:00 UTC <sup>b</sup> .
3	DeltaT	$\Delta$ <i>Time</i> (vector of 10 bytes) Since the number of measurements included in a weekly average was photometric band-dependent, the <i>Time</i> value is only an approximation to the average time the pixel was observed at a particular wavelength. A more accurate time for each band is <i>Time</i> plus the value of <i>DeltaT</i> for that band.
4	SolElong	<i>Solar elongation angle, <math>\varepsilon</math></i> (signed 16-bit integer) Average of the solar elongation angles at which the pixel was observed during the week. The comment made about the accuracy of <i>Time</i> under <i>DeltaT</i> also applies to <i>SolElong</i> .
5	Photomet	<i>Photometry</i> (vector of 10 32-bit floating point values) Average intensity observed for the pixel over the week, in units of MJy/sr. The 10 values correspond to the 10 <i>DIRBE</i> bands in order of increasing wavelength.
6	NumRecs	<i>Number of records</i> (signed 16-bit integer) Number of times the pixel was observed this week in at least one photometric band. (Observations made contemporaneously at multiple wavelengths count once.)
7	WtNumObs	<i>Weighted number of observations</i> (vector of 10 bytes) Number of observations that survived robust averaging and quality constraints and were used to form the average intensity values given in the <i>Photomet</i> field. Listed in order of increasing wavelength.
8	StdDev	<i>Photometry standard deviation</i> (vector of 10 bytes) Standard deviations of the mean weekly intensities for the 10 <i>DIRBE</i> bands given in ascending wavelength order and encoded. The FITS header describes how to decode the stored values.
9	SSOFlag	<i>Solar system object flag</i> (byte) Indicates which solar system object exclusion zones (see §5.6.2), if any, intersect the pixel at some time during the week. See FITS header for interpretation instructions.
10	ZL	<i>Zodiacal Light</i> (vector of 10 32-bit floating point values) Brightness of the zodiacal light, in units of MJy/sr, as computed from the <i>DIRBE</i> IPD Model for the time of observation ( <i>Time</i> + <i>DeltaT</i> ) and pixel coordinates. The 10 values correspond to the 10 <i>DIRBE</i> bands in order of increasing wavelength.

<sup>a</sup> FITS keyword giving the label or heading for field (*i.e.*, table column) n.<sup>b</sup> T81 (see §5.7.1.1).

Table 5.8-2: Columns in the Zodi-Subtracted Mission Average Maps

n	TTYPE <sup>a</sup>	Description
1	Pixel_no	<i>DIRBE pixel number</i> (signed 32-bit integer) Pixel number in the CSC projection (see §5.3).
2	Resid	<i>Residual intensity</i> (32-bit floating point) Unweighted average of weekly ZL-subtracted intensity values over the entire cryogenic mission, in MJy/sr.
3	NumObs	<i>Number of Observations</i> (signed 32-bit integer) The total number of individual photometric measurements included in the average.
4	NumWks	<i>Number of weeks</i> (8-bit byte) The number of weekly averaged intensity values used to compute the mission averaged residual intensity. This number varies with location in the sky.
5	StdDev	<i>Standard deviation</i> (32-bit floating point) Standard deviation of the mean ZL-subtracted intensity ( <b>Resid</b> ) in MJy/sr.

<sup>a</sup> FITS keyword giving the label or heading for field (*i.e.*, table column) n.

the mean flux density value; it *does not include the absolute calibration uncertainty*. When values of 0.0 are given for the flux density and error at a particular wavelength, they indicate that the object was not an approved calibration source at that wavelength.

To have been selected as an approved calibration object, a source had to satisfy the following criteria: little ( $\lesssim 2\%$ ) or no variability was seen in the photometry over the course of the cold mission; and the signal-to-noise ratio for a typical sighting was  $\geq 20$  for 1.25 - 4.9  $\mu\text{m}$ , or  $\geq 10$  for 12 - 240  $\mu\text{m}$ . The histograms in Figure 5.8-1 show the calibrator flux density ranges at the 10 *DIRBE* wavelengths; the labels tell how many sources qualified as calibrators. Few sources qualified at the longer wavelengths.

A background intensity value, in MJy/sr, is provided in the Photometric Standard Values Table at each wavelength for which the object was approved as a calibrator. The background values can be used to assess the source-to-background contrast if the beam solid angles given in Table 4.2-1 are used to convert the intensity units from MJy/sr to Jy/beam. Note that the listed background intensity is an average over individual sightings within the mission; the intensity actually detected varied as a function of time as the source was seen along different lines of sight through the interplanetary dust.

The coordinates of the objects are given in the equatorial (epoch 1950), Galactic, and geocentric ecliptic (epoch 2000) systems, and the data are tabulated in order of increasing Right Ascension. Figures 5.8-2 and 5.8-3 show the locations of the calibration sources in Galactic and ecliptic coordinates, respectively. Objects at ecliptic latitudes  $|\beta| \gtrsim 65^\circ$  are visible throughout the entire mission; the visibility decreases at lower latitudes. Most of the source positions provided for 1.25 - 25  $\mu\text{m}$  calibrators are taken from the SAO Bright Star Catalog (available from the Astronomical Data Center at <ftp://adc.gsfc.nasa.gov/pub/adc/archives/catalogs/5/5050/>). *IRAS* Point Source Catalog (PSC; see <http://www.gsfc.nasa.gov/astro/iras/psc.html>) positions were used for some circumstellar dust sources that did not appear in the SAO catalog. At the longer wavelengths (60 - 240  $\mu\text{m}$ ), source positions were taken from (in order of preference) the *IRAS* PSC, the *IRAS* Small Scale Structure Catalog (see <http://www.gsfc.nasa.gov/astro/iras/sss.html>), or the *DIRBE* time-ordered data themselves. In the latter cases, positional errors may be as large as a few arcminutes.

As a rule, but with some exceptions, stellar objects are referred to by a constellation designation (*e.g.*, YY Psc); Sharpless numbers are used for H II regions (*e.g.*, S 140); and NGC or Messier numbers are used for galaxies (*e.g.*, NGC 253).

Table 5.8-3 describes the format of the Photometric Standard Values Table.

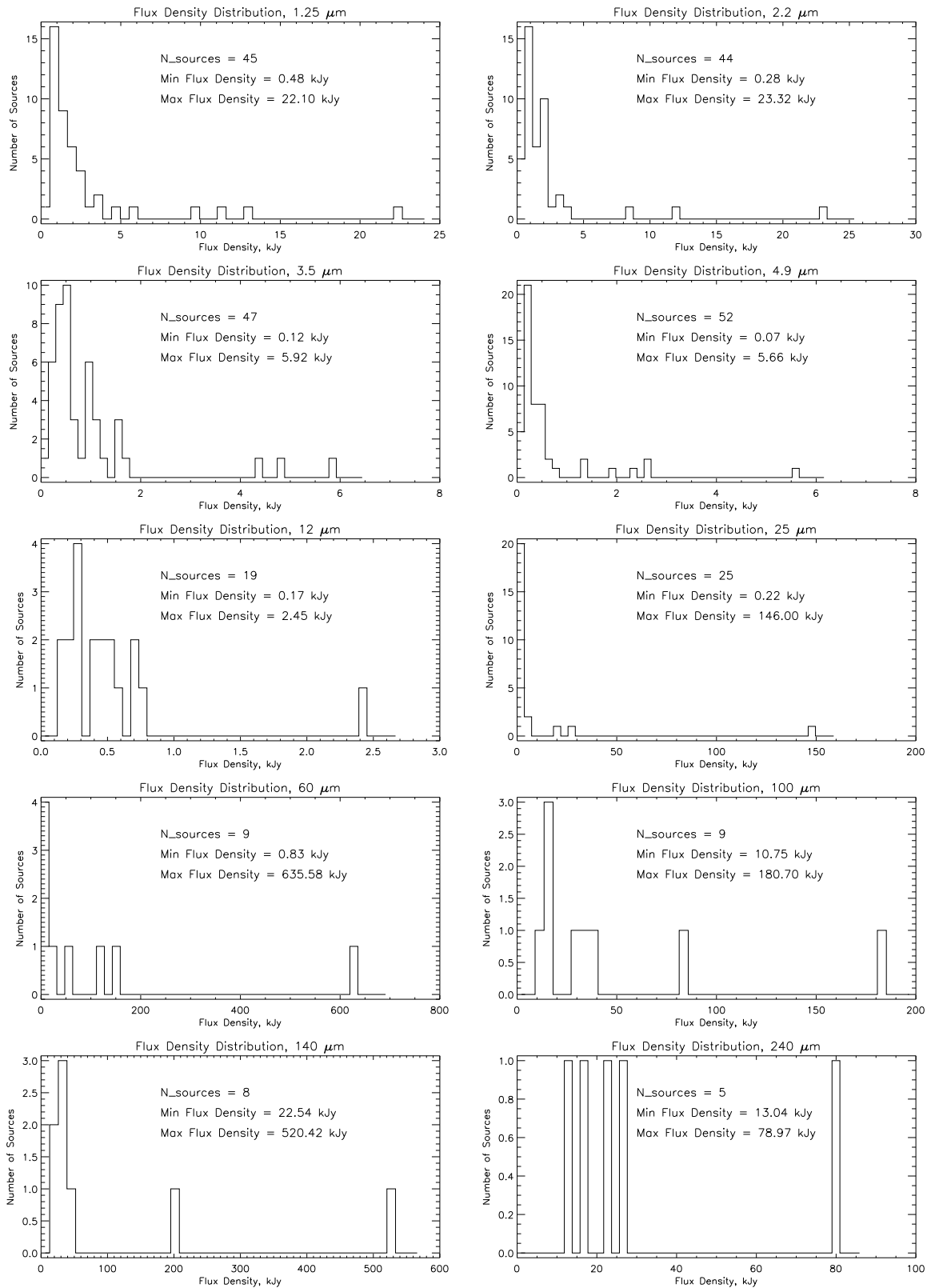


Figure 5.8-1: Histograms of the flux densities of sources used as relative calibrators for each of the ten DIRBE bands.

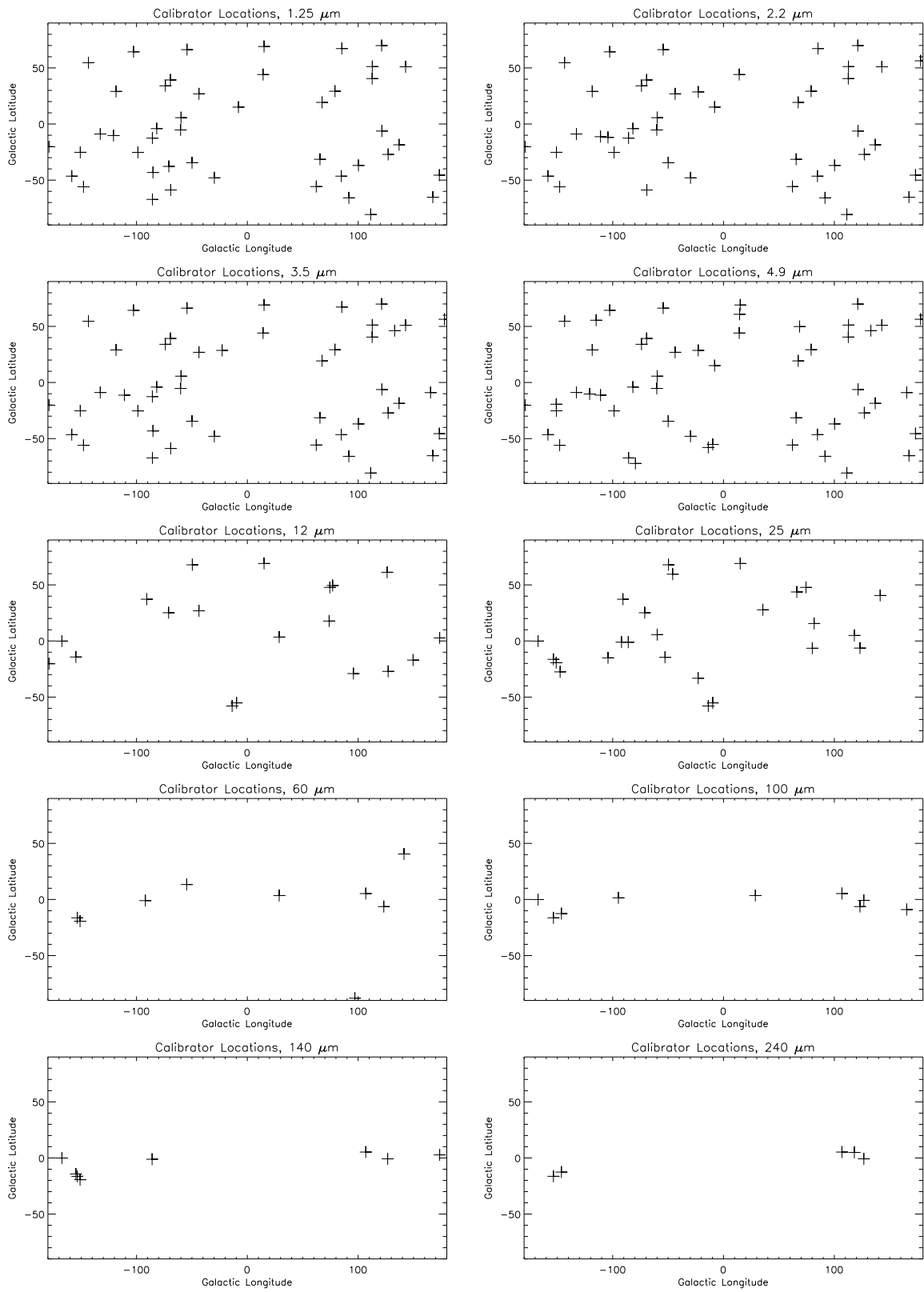


Figure 5.8-2: Locations of the relative calibration sources in Galactic coordinates.



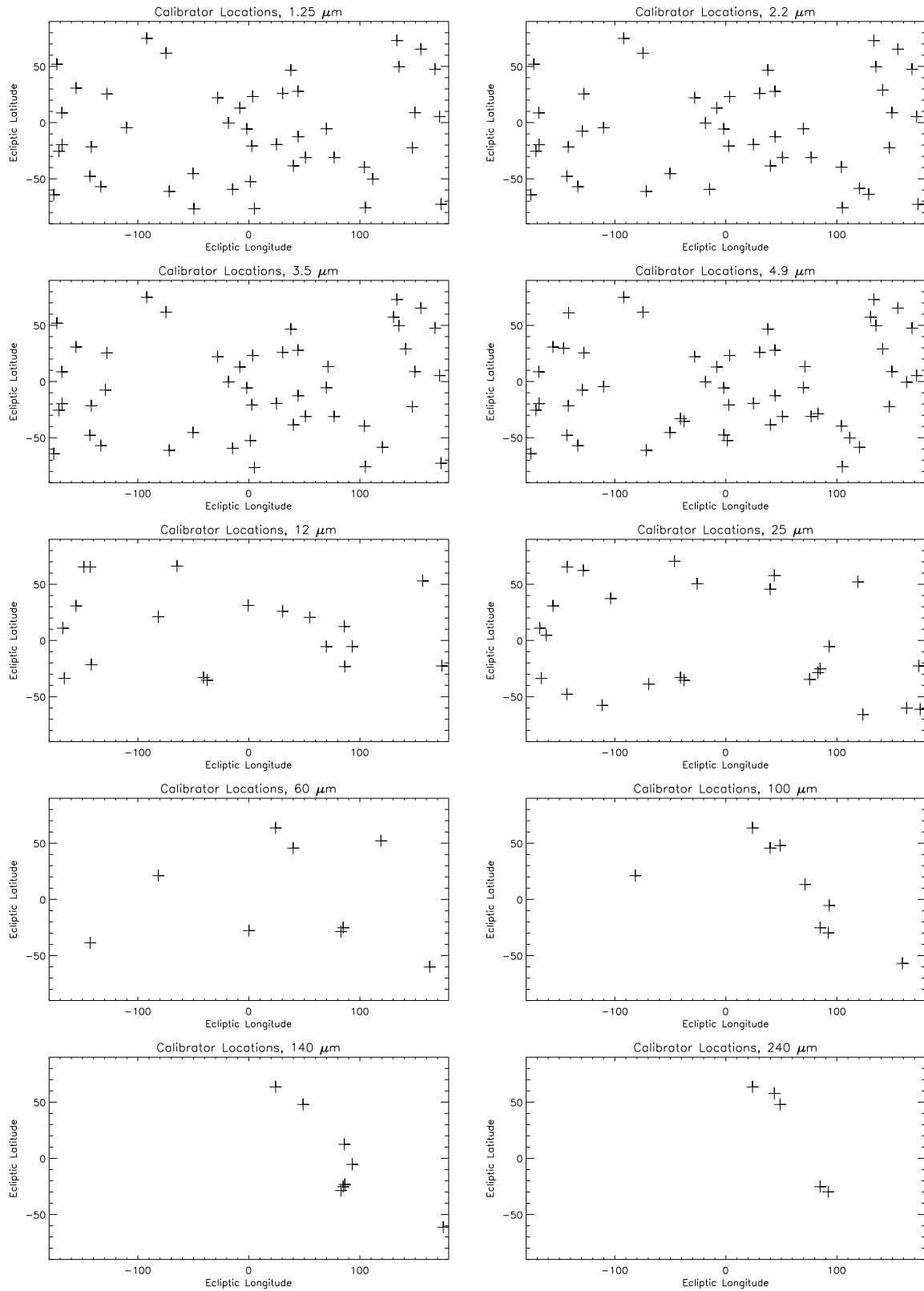


Figure 5.8-3: Locations of the relative calibration sources in geocentric ecliptic coordinates.

Table 5.8-3: Columns in the Photometric Standard Values Table

n	TTYPE <sup>n</sup> <sup>a</sup>	Description
1	Name	<i>Object name</i> (32-bit character) Name of the calibration object.
2	ObjIndex	<i>Object index</i> (signed 16-bit integer) DIRBE object index number.
3	Pixel_No	<i>DIRBE pixel number</i> (signed 32-bit integer) DIRBE pixel in which the object is located.
4	RA1950	<i>Right Ascension</i> (32-bit floating point) Right Ascension of the object, epoch 1950, in decimal hours.
5	DEC1950	<i>Declination</i> (32-bit floating point) Declination of the object, epoch 1950, in decimal degrees.
6	GallLon	<i>Galactic longitude</i> (32-bit floating point) Galactic longitude, $\ell_{II}$ , of the object, in decimal degrees.
7	GallLat	<i>Galactic latitude</i> (32-bit floating point) Galactic latitude, $b_{II}$ , of the object, in decimal degrees.
8	EclLon	<i>Ecliptic longitude</i> (32-bit floating point) Ecliptic longitude of the object, epoch 2000, in decimal degrees.
9	EclLat	<i>Ecliptic latitude</i> (32-bit floating point) Ecliptic latitude of the object, epoch 2000, in decimal degrees.
10	Photomet	<i>Average photometry</i> (10 32-bit floating point) Mission-averaged background-subtracted flux densities, in units of Jy, listed in order of increasing wavelength from 1.25 to 240 $\mu\text{m}$ . Flux densities are quoted at the nominal wavelength for a source with $\nu F_\nu = \text{constant}$ (a color correction is required if the true source spectrum differs from the assumed shape).
11	StdDev	<i>Standard deviation</i> (10 32-bit floating point) Standard deviation of the mean flux density quoted in the corresponding <i>Average photometry</i> field, in Jy ( <i>i.e.</i> , one value per wavelength band, listed in order of increasing wavelength).
12	NumObs	<i>Total number of observations</i> (10 32-bit integer) The total number of individual observations used to derive the flux density quoted in the corresponding <i>Average photometry</i> field ( <i>i.e.</i> , one value per wavelength band, listed in order of increasing wavelength).
13	AvgBkgd	<i>Average background</i> (10 32-bit floating point) Average background intensity, in MJy/sr, at each wavelength, listed in order of increasing wavelength.

<sup>a</sup> FITS keyword giving the label or heading for field (*i.e.*, table column) n.

### 5.8.4 Solar System Object Data

The Solar System Object Dataset provides flux densities and other data pertaining to individual passages of solar system objects through the *DIRBE* field of view during the period of cryogenic operation, from 11 December 1989 to 21 September 1990. The data are given in FITS tables, one for each of the following objects: Mars, Jupiter, Saturn, Uranus, Ceres, Pallas, and Vesta. Due to their low solar elongation angles, Mercury and Venus were not visible to the *DIRBE*, the Moon saturated the *DIRBE* detectors, and other solar system objects were generally below the source detection thresholds discussed below. Each table contains one record per object passage, and the sightings are organized chronologically. The FITS table columns are described in Table 5.8-5.

An object was considered to have been detected, and a table entry was made, only if a point source signal was evident in the time-ordered data. A zero-sum filtered data stream was checked for signals in at least two detectors in excess of specified detection thresholds. The filter-weighted signal was obtained by multiplying 9 consecutive  $\frac{1}{8}$ -second data samples by the factors -1, -1, -1, 2, 2, 2, -1, -1, -1 and summing the result. The detection thresholds used were equivalent to the point source flux density values listed in Table 5.8-4. Where confusion noise is negligible, the detection thresholds correspond to signal-to-noise ratios of about 20 for detectors 1A-4, 8 for detectors 5-7, and 10 for detectors 8-10.

Table 5.8-4: Solar System Object Detection Thresholds

Wavelength ( $\mu\text{m}$ )	1.25	2.2	3.5	4.9	12	25	60	100	140	240
Detector	1A	2A	3A	4	5	6	7	8	9	10
Threshold (Jy)	140	120	78	96	130	270	380	590	40000	20000

Positional criteria were used to further guard against the inclusion of low quality data. First, at the time of the object's closest approach to the center of the field of view, its ephemeris position was required to lie within  $\pm 10'$  of the *DIRBE* boresight position in the in-scan direction, and within  $\pm 18'$  in the cross-scan direction. Second, any data obtained while the *DIRBE* boresight passed within  $60'$  of either a *DIRBE* approved calibration object or another solar system object were excluded. Objects other than these, which could potentially contaminate the photometry, were *not* checked for positional coincidence.

Source photometry was calculated from the time-ordered data as follows:

1. A 15-point string of data was extracted, centered on the time of the object's closest approach to the center of the field of view;
2. a linear (for Bands 1-4) or quadratic (for Bands 5-10) function was fitted to the off-source region of the data string (typically the first 6 and the last 6 data samples) and used as a background model;
3. according to the cross-scan position of the object, a beam profile response template (*i.e.*, response as a function of in-scan position) was selected. The beam templates were derived from the normalized beam profile maps described in §5.9.1);
4. the portion of the background-subtracted intensity profile corresponding to the passage of the source through the beam – typically the 3 central data points – were fitted to the beam template times a constant factor. This factor is the point source flux density in instrument DN's.
5. Finally, this measure of the flux density was scaled by the appropriate celestial and absolute calibration coefficients (see §4.5.3), yielding the flux density value, in Jy, which is given in the `Photomet` field in the Solar System Object Dataset.

According to our convention, the quoted flux density corresponds to that of a source having a spectral shape  $\nu F_\nu = \text{constant}$ . Thus a color correction (see Appendix B) must be applied to obtain the true flux density if the real spectrum has a different shape, as is typically the case.

The photometry from a particular detector was considered unreliable if there were large residuals about the background or beam template fits, or if the object passed close to the “edge” of the beam,

where pointing error would result in a large uncertainty in the adopted beam template. In such cases, a sentinel value (-16000.) is recorded in the `Photomet` and `PhotErr` fields for the affected detector.

Positions of Mars, Jupiter, Saturn and Uranus were computed using the method of van Flandern and Pulkkinen (1979). Coordinates for the asteroids (Pallas, Ceres, Vesta) were calculated with a routine provided by M. A'Hearn (University of Maryland), using the orbital elements listed in Table 5.8-6.

### 5.8.5 Faint Source Model (FSM)

The *DIRBE* Faint Source Model, which was used by Arendt *et al.* (1998) to subtract (faint) stellar emission from the *DIRBE* sky maps as part of the search for the cosmic infrared background, is available as a data product. A detailed description of the Faint Source Model, and warnings with which the user should be familiar, can be found in Appendix F.

For each step along a line of sight, the FSM was used to compute an intensity and a variance in intensity at 1.25, 2.2, 3.5, 4.9, 12 and 25  $\mu\text{m}$ . Assuming Poisson statistics, the variances are proportional to the number of sources in each volume element. The intensities and variances are integrated over distance, source type, and Galactic structure component (see Appendix F). The square root of the total variance for each line of sight gives the  $1\sigma$  uncertainty assigned to the intensity in the corresponding *DIRBE* pixel. As shown in Table 5.8-7, the predicted intensities and their associated uncertainties are recorded in the FSM data product. There are six FSM FITS binary tables, one per wavelength. Each file is 5 MB in size.

## 5.9 Ancillary Data Sets

Machine-readable files containing important calibration information given in the *Explanatory Supplement* are included among the *DIRBE* data products.

### 5.9.1 Beam Profile Maps

Beam Profile Maps are provided in 16 FITS image files, one for each of the *DIRBE* detectors. Both the file names and the FITS headers indicate to which band the data apply. A sample FITS header is given in Appendix D. Each map is a 225 (in-scan)  $\times$  181 (cross-scan) pixel array with 0.4' pixel spacing in the cross-scan direction and 0.375' sampling in the scan direction.<sup>2</sup> The array values give the beam response normalized to unity at the peak.

Beam profiles for 10 of the detectors (bands 1A–4) were found to vary slightly over time, while those for bands 5–10 were taken to be constant throughout the cryogenic mission. Three separate beam profiles are given for the short-wavelength bands, one applicable to the time interval 89345 – 90176, another to 90176 – 90232, and a third to 90232 – 90264. The beam solid angles are listed in Table 4.2-1 and given in the FITS headers. The tabulated solid angles were used in the *DIRBE* data reduction software to convert the detected flux per beam into intensity in MJy/sr.

### 5.9.2 Spectral Response Functions

The *DIRBE* System Spectral Response functions depicted in Figure 2.2-2 and tabulated in Appendix A are also provided in an ASCII file called `DIRBE_SYSTEM_SPECTRAL_RESPONSE_TABLE.ASC`.

An early version of the file reported wavelengths to the nearest hundredth of a micron and contained what appeared to be duplicate entries at 1.00, 1.04, 1.09 and 1.16  $\mu\text{m}$ . A new version of the table released in March 1997 quotes wavelengths to the nearest 0.001  $\mu\text{m}$  and does not contain duplicate entries. The responsivity values are the same in both versions of the table.

### 5.9.3 Color Correction Tables

Color correction factors applicable to spectral energy distributions of the following forms are tabulated in Appendix B and provided in an ASCII file called `DIRBE_COLOR_CORRECTION_TABLES.ASC`:  $I_\nu \propto$

<sup>2</sup>The now-obsolete Pass 2B Beam Profile Maps were more coarsely sampled.

Table 5.8-5: Contents of Solar System Object Dataset

n	TTYEn <sup>a</sup>	Description
1	Time	<i>Time of closest approach</i> ( 64-bit floating point) Time of the object's closest approach to the center of the field of view, in TAI seconds since 1981 January 1 00:00:00 UTC <sup>b</sup> .
2	Pixel_No	<i>DIRBE pixel number</i> (signed 32-bit integer) Pixel in the CSC projection (see §5.3) in which the object is located at the time recorded in the Time field.
3	RA1950	<i>Right Ascension</i> (32-bit floating point) Coordinate of the object at the time recorded in the Time field, in hours, epoch 1950.
4	DEC1950	<i>Declination</i> (32-bit floating point) Coordinate of the object at the time recorded in the Time field, in decimal degrees, epoch 1950.
5	GalLon	<i>Galactic longitude</i> (32-bit floating point) Coordinate of the object at the time recorded in the Time field, in decimal degrees.
6	GalLat	<i>Galactic latitude</i> (32-bit floating point) Coordinate of the object at the time recorded in the Time field, in decimal degrees.
7	EclLon	<i>Ecliptic longitude</i> (32-bit floating point) Coordinate of the object at the time recorded in the Time field, in decimal degrees, epoch 2000.
8	EclLat	<i>Ecliptic latitude</i> (32-bit floating point) Coordinate of the object at the time recorded in the Time field, in decimal degrees, epoch 2000.
9	SolElong	<i>Solar Elongation</i> (32-bit floating point) Solar Elongation angle of the object at time recorded in the Time field, in decimal degrees
10	Distance	<i>Geocentric distance</i> (32-bit floating point) Distance of the object from Earth at the time recorded in the Time field, in Astronomical Units.
11	HelioDist	<i>Heliocentric distance</i> (32-bit floating point) Distance of the object from the Sun at the time recorded in the Time field, in Astronomical Units.
12	Photomet	<i>Flux density</i> (vector of 10 32-bit floating point values) Flux density of the object in the ten <i>DIRBE</i> total intensity wavelength bands, in Jy, listed in order of increasing wavelength from 1.25 to 240 $\mu\text{m}$ . Color corrections may be required (see text).
13	PhotErr	<i>Photometric uncertainty</i> (vector of 10 32-bit floating point values) Estimated error in the flux density, in Jy. Calculated as the quadrature sum of (1) the rms deviation of the time-ordered data from the baseline and beam template fits, and (2) the error due to uncertainty in the beam template associated with cross-scan pointing error.

<sup>a</sup> FITS keyword giving the label or heading for field (*i.e.*, table column) n.<sup>b</sup> T81 (see §5.7.1.1).

Table 5.8-6: Orbital elements used to calculate asteroid ephemerides

	Pallas	Ceres	Vesta
Perihelion date (yrs)	1986.244072	1986.074926	1989.314116
Perihelion distance (AU)	2.1201106	2.552557	2.1473662
Eccentricity	0.2347	0.0780	0.0906
Argument of perihelion (deg)	309.796	71.274	150.175
Ascending Node (deg)	173.323	80.702	104.015
Inclination to Ecliptic (deg)	34.804	10.607	7.139
Epoch (yrs)	1989.751	1989.751	1989.751
Equinox (yrs)	2000.0	2000.0	2000.0

Table 5.8-7: Columns in the Faint Source Model FITS tables

n	TTYPE <sup>n</sup>	Description
1	Pixel_no	<i>DIRBE pixel number</i> (signed 32-bit integer) Pixel number in the CSC projection (see §5.3).
2	Photomet	<i>Photometry</i> (32-bit floating point value) Faint Source Model intensity in MJy/sr.
3	StdDev	<i>Standard deviation</i> (32-bit floating point value) Standard deviation of the intensity ( <i>Photomet</i> ) in MJy/sr.

<sup>a</sup> FITS keyword giving the label or heading for field (*i.e.*, table column) n.

$\nu^n$ , where  $n = -3.0, -2.5, -2.0, \dots, +3.0$ ; and  $I_\nu \propto \nu^n B_\nu(T)$ , where  $n = 0.0, 0.5, \dots, 2.0$ , temperature  $T$  is in the range [10K, 20000K], and  $B_\nu(T)$  is the Planck function.



## Chapter 6

# References

- Arendt, R. G., Odegard, N., Weiland, J. L., Sodroski, T. J., Hauser, M. G., Dwek, E., Kelsall, T., Moseley, S. H., Silverberg, R. F., Leisawitz, D., Mitchell, K., & Reach, W. T. 1998, *ApJ*, submitted.
- A User's Guide for the Flexible Image Transport System (FITS)*, version 3.1, 1994, NASA/Science Office of Standards and Technology, available at [http://www.gsfc.nasa.gov/astro/fits/fits\\_home.html](http://www.gsfc.nasa.gov/astro/fits/fits_home.html).
- Berriman, G.B., Boggess, N.W., Hauser, M.G., Kelsall, T., Lisse, C.M., Moseley, S.H., Reach, W.T., & Silverberg, R.F. 1994, *ApJ*, **431**, L63.
- Boggess, N. W., Mather, J. C., Weiss, R., Bennett, C. L., Cheng, E. S., Dwek, E., Gulkis, S., Hauser, M. G., Janssen, M. A., Kelsall, T., Meyer, S. S., Moseley, S. H., Murdock, T. L., Shafer, R. A., Silverberg, R. F., Smoot, G. F., Wilkinson, D. T., & Wright, E. L. 1992, *ApJ*, **397**, 420.
- Campins, H., Rieke, G. H., & Lebofsky, M. J. 1985, *AJ*, **90**, 896.
- Chan, F. K. & O'Neill, E. M. 1975, *Feasibility Study of a Quadrilateralized Spherical Cube Earth Data Base*, Computer Sciences Corp., EPRF Tech. Rpt. 2-75, available from the National Technical Information Service, US Department of Commerce.
- Cohen, M., Walker, R. G., Barlow, M. J., & Deacon, J. R. 1992, *AJ*, **104**, 1650.
- Cohen, M., Witteborn, F. C., Walker, R. G., Bregman, J. D., and Wooden, D. H. 1995, *AJ*, **110**, 275.
- Definition of the Flexible Image Transport System (FITS)*, version 1.1, 1995, NASA/Science Office of Standards and Technology, available at [http://www.gsfc.nasa.gov/astro/fits/fits\\_home.html](http://www.gsfc.nasa.gov/astro/fits/fits_home.html).
- Engelke, C. W. 1992, *AJ*, **104**, 1248.
- Forrest, W. J., McCarthy, J. F., & Houck, J. R. 1980, *ApJ*, **240**, 37.
- Gezari, D. Y., Schmitz, M., Pitts, P. S., & Mead, J. M. 1993, *Catalog of Infrared Observations*, Third Edition, NASA Ref. Pub. 1294.
- Greisen, E. W. & Calabretta, M. 1993, *Representations of Celestial Coordinates in FITS*, Draft FITS proposal, NRAO.
- Gulkis, S., Lubin, P. M., Meyer, S. S., & Silverberg, R. F. 1990, *Sci. Amer.*, **262**, 132.



- Hanel, R., Crosby, D., Herath, L., Vanous, D., Collins, D., Creswick, H., Harris, C., & Rhodes, M. 1980, *Appl. Optics*, **19**, 1391.
- Hauser, M. G., Arendt, R. G., Kelsall, T., Dwek, E., Odegard, N., Weiland, J. L., Freudenreich, H. T., Reach, W. T., Silverberg, R. F., Moseley, S. H., Pei, Y. C., Mather, J. C., Smoot, G. F., Wilkinson, D. T., & Wright, E. L. 1998, *ApJ*, submitted.
- Heaney, J. B., Stewart, K. P., Boucarut, R. A., Alley, P. W., & Korb, A. R. 1986, *SPIE*, **619**, 142.
- Hildebrand, R. H., Loewenstein, R. F., Harper, D. A., Orton, G. S., & Keene, J. 1985, *Icarus*, **64**, 64.
- Hoaglin, D. C., Mosteller, F., & Tukey, J. W., eds. 1983, *Understanding Robust And Exploratory Data Analysis* (New York: John Wiley & Sons).
- IRAS Catalogs and Atlases Explanatory Supplement* 1988, Beichman, C. A., Neugebauer, G., Habing, H. J., Clegg, P. E., & Chester, T. J., eds. (Washington, DC: GPO).
- Kelsall, T., Weiland, J. L., Franz, B. A., Reach, W. T., Arendt, R. G., Dwek, E., Freudenreich, H. T., Hauser, M. G., Moseley, S. H., Odegard, N. P., & Silverberg, R. F. 1998, *ApJ*, submitted.
- Magner, T. J. 1987, *Opt. Eng.*, **26**, 264.
- Mather, J. C. 1982, *Opt. Eng.*, **21**, 769.
- Neugebauer, G., Habing, H. J., Van Duinen, R., Aumann, H. H., Beichman, C. A., Baud, B., Beintema, D. A., Boggess, N., Clegg, P. E., & De Jong, T. 1984, *ApJ*, **278**, L1.
- O'Neill, E. M. & Laubscher, R. E. 1976, *Extended Studies of a Quadrilateralized Spherical Cube Earth Data Base*, Computer Sciences Corp., EPRF Tech. Rpt. 3-76 available from the National Technical Information Service, US Department of Commerce.
- Pearl, J. C., Conrath, B. J., Hanel, R. A., Pirraglia, J. A., & Coustenis, A. 1990, *Icarus*, **84**, 12.
- Rieke, G. H., Lebofsky, M. J., & Low, F. J. 1985, *AJ*, **90**, 900.
- van Flandern, T. C., & Pulkkinen, K. F. 1979, *ApJS*, **41**, 391.
- Wertz, J. R., ed. 1978, *Spacecraft Attitude Determination and Control* (Dordrecht: D. Reidel).
- White, R. A. & Mather, J. C. 1991, "Databases from Cosmic Background Explorer (COBE)," in *Databases and On-Line Data in Astronomy*, ed. M. Albrecht & D. Egret (Dordrecht: Kluwer), pp. 29-34.
- White, R. A. & Stemwedel, S. W. 1992, "The Quadrilateralized Spherical Cube and Quad-Tree for All Sky Data," in *Astronomical Data Analysis Software and Systems I*, vol. 25, ed. D.M. Worrall, C. Biemesderfer, & J. Barnes, pp. 379-381.

## Appendix A

# *DIRBE* System Spectral Response

Table A.0-1 gives the normalized System Spectral Responses for the 10 *DIRBE* photometric bands. The uncertainties per measurement are estimated to be 1% or less.















7.837	0.00	0.00	0.00	0.00	0.03	0.00	0.00	0.00	0.00	0.00
7.898	0.00	0.00	0.00	0.00	0.03	0.00	0.00	0.00	0.00	0.00
7.960	0.00	0.00	0.00	0.00	0.04	0.00	0.00	0.00	0.00	0.00
8.022	0.00	0.00	0.00	0.00	0.15	0.00	0.00	0.00	0.00	0.00
8.085	0.00	0.00	0.00	0.00	0.21	0.00	0.00	0.00	0.00	0.00
8.148	0.00	0.00	0.00	0.00	0.25	0.00	0.00	0.00	0.00	0.00
8.212	0.00	0.00	0.00	0.00	0.29	0.00	0.00	0.00	0.00	0.00
8.276	0.00	0.00	0.00	0.00	0.32	0.00	0.00	0.00	0.00	0.00
8.341	0.00	0.00	0.00	0.00	0.35	0.00	0.00	0.00	0.00	0.00
8.406	0.00	0.00	0.00	0.00	0.38	0.00	0.00	0.00	0.00	0.00
8.471	0.00	0.00	0.00	0.00	0.41	0.00	0.00	0.00	0.00	0.00
8.538	0.00	0.00	0.00	0.00	0.45	0.00	0.00	0.00	0.00	0.00
8.604	0.00	0.00	0.00	0.00	0.50	0.00	0.00	0.00	0.00	0.00
8.671	0.00	0.00	0.00	0.00	0.54	0.00	0.00	0.00	0.00	0.00
8.739	0.00	0.00	0.00	0.00	0.59	0.00	0.00	0.00	0.00	0.00
8.807	0.00	0.00	0.00	0.00	0.63	0.00	0.00	0.00	0.00	0.00
8.876	0.00	0.00	0.00	0.00	0.68	0.00	0.00	0.00	0.00	0.00
8.946	0.00	0.00	0.00	0.00	0.71	0.00	0.00	0.00	0.00	0.00
9.016	0.00	0.00	0.00	0.00	0.72	0.00	0.00	0.00	0.00	0.00
9.086	0.00	0.00	0.00	0.00	0.71	0.00	0.00	0.00	0.00	0.00
9.157	0.00	0.00	0.00	0.00	0.71	0.00	0.00	0.00	0.00	0.00
9.228	0.00	0.00	0.00	0.00	0.72	0.00	0.00	0.00	0.00	0.00
9.301	0.00	0.00	0.00	0.00	0.72	0.00	0.00	0.00	0.00	0.00
9.373	0.00	0.00	0.00	0.00	0.73	0.00	0.00	0.00	0.00	0.00
9.446	0.00	0.00	0.00	0.00	0.73	0.00	0.00	0.00	0.00	0.00
9.520	0.00	0.00	0.00	0.00	0.73	0.00	0.00	0.00	0.00	0.00
9.595	0.00	0.00	0.00	0.00	0.70	0.00	0.00	0.00	0.00	0.00
9.669	0.00	0.00	0.00	0.00	0.67	0.00	0.00	0.00	0.00	0.00
9.745	0.00	0.00	0.00	0.00	0.65	0.00	0.00	0.00	0.00	0.00
9.821	0.00	0.00	0.00	0.00	0.61	0.00	0.00	0.00	0.00	0.00
9.898	0.00	0.00	0.00	0.00	0.57	0.00	0.00	0.00	0.00	0.00
9.975	0.00	0.00	0.00	0.00	0.53	0.00	0.00	0.00	0.00	0.00
10.05	0.00	0.00	0.00	0.00	0.53	0.00	0.00	0.00	0.00	0.00
10.13	0.00	0.00	0.00	0.00	0.55	0.00	0.00	0.00	0.00	0.00
10.21	0.00	0.00	0.00	0.00	0.57	0.00	0.00	0.00	0.00	0.00
10.29	0.00	0.00	0.00	0.00	0.59	0.00	0.00	0.00	0.00	0.00
10.37	0.00	0.00	0.00	0.00	0.61	0.00	0.00	0.00	0.00	0.00
10.45	0.00	0.00	0.00	0.00	0.64	0.00	0.00	0.00	0.00	0.00
10.53	0.00	0.00	0.00	0.00	0.65	0.00	0.00	0.00	0.00	0.00
10.62	0.00	0.00	0.00	0.00	0.64	0.00	0.00	0.00	0.00	0.00
10.70	0.00	0.00	0.00	0.00	0.62	0.00	0.00	0.00	0.00	0.00
10.78	0.00	0.00	0.00	0.00	0.61	0.00	0.00	0.00	0.00	0.00
10.87	0.00	0.00	0.00	0.00	0.59	0.00	0.00	0.00	0.00	0.00
10.95	0.00	0.00	0.00	0.00	0.58	0.00	0.00	0.00	0.00	0.00
11.04	0.00	0.00	0.00	0.00	0.59	0.00	0.00	0.00	0.00	0.00

11.12	0.00	0.00	0.00	0.00	0.64	0.00	0.00	0.00	0.00	0.00
11.21	0.00	0.00	0.00	0.00	0.69	0.00	0.00	0.00	0.00	0.00
11.30	0.00	0.00	0.00	0.00	0.74	0.00	0.00	0.00	0.00	0.00
11.39	0.00	0.00	0.00	0.00	0.78	0.00	0.00	0.00	0.00	0.00
11.47	0.00	0.00	0.00	0.00	0.83	0.00	0.00	0.00	0.00	0.00
11.56	0.00	0.00	0.00	0.00	0.84	0.00	0.00	0.00	0.00	0.00
11.65	0.00	0.00	0.00	0.00	0.84	0.00	0.00	0.00	0.00	0.00
11.75	0.00	0.00	0.00	0.00	0.84	0.00	0.00	0.00	0.00	0.00
11.84	0.00	0.00	0.00	0.00	0.84	0.00	0.00	0.00	0.00	0.00
11.93	0.00	0.00	0.00	0.00	0.83	0.00	0.00	0.00	0.00	0.00
12.02	0.00	0.00	0.00	0.00	0.84	0.00	0.00	0.00	0.00	0.00
12.12	0.00	0.00	0.00	0.00	0.87	0.00	0.00	0.00	0.00	0.00
12.21	0.00	0.00	0.00	0.00	0.90	0.00	0.00	0.00	0.00	0.00
12.31	0.00	0.00	0.00	0.00	0.94	0.00	0.00	0.00	0.00	0.00
12.40	0.00	0.00	0.00	0.00	0.97	0.00	0.00	0.00	0.00	0.00
12.50	0.00	0.00	0.00	0.00	1.00	0.00	0.00	0.00	0.00	0.00
12.60	0.00	0.00	0.00	0.00	0.98	0.00	0.00	0.00	0.00	0.00
12.70	0.00	0.00	0.00	0.00	0.97	0.00	0.00	0.00	0.00	0.00
12.80	0.00	0.00	0.00	0.00	0.95	0.00	0.00	0.00	0.00	0.00
12.90	0.00	0.00	0.00	0.00	0.94	0.00	0.00	0.00	0.00	0.00
13.00	0.00	0.00	0.00	0.00	0.91	0.00	0.00	0.00	0.00	0.00
13.10	0.00	0.00	0.00	0.00	0.86	0.00	0.00	0.00	0.00	0.00
13.20	0.00	0.00	0.00	0.00	0.80	0.00	0.00	0.00	0.00	0.00
13.30	0.00	0.00	0.00	0.00	0.75	0.00	0.00	0.00	0.00	0.00
13.41	0.00	0.00	0.00	0.00	0.69	0.00	0.00	0.00	0.00	0.00
13.51	0.00	0.00	0.00	0.00	0.64	0.00	0.00	0.00	0.00	0.00
13.62	0.00	0.00	0.00	0.00	0.72	0.00	0.00	0.00	0.00	0.00
13.72	0.00	0.00	0.00	0.00	0.78	0.00	0.00	0.00	0.00	0.00
13.83	0.00	0.00	0.00	0.00	0.83	0.00	0.00	0.00	0.00	0.00
13.94	0.00	0.00	0.00	0.00	0.87	0.00	0.00	0.00	0.00	0.00
14.05	0.00	0.00	0.00	0.00	0.91	0.00	0.00	0.00	0.00	0.00
14.16	0.00	0.00	0.00	0.00	0.91	0.00	0.00	0.00	0.00	0.00
14.27	0.00	0.00	0.00	0.00	0.91	0.00	0.00	0.00	0.00	0.00
14.38	0.00	0.00	0.00	0.00	0.90	0.00	0.00	0.00	0.00	0.00
14.49	0.00	0.00	0.00	0.00	0.89	0.00	0.00	0.00	0.00	0.00
14.61	0.00	0.00	0.00	0.00	0.86	0.00	0.00	0.00	0.00	0.00
14.72	0.00	0.00	0.00	0.00	0.82	0.00	0.00	0.00	0.00	0.00
14.83	0.00	0.00	0.00	0.00	0.79	0.00	0.00	0.00	0.00	0.00
14.95	0.00	0.00	0.00	0.00	0.79	0.00	0.00	0.00	0.00	0.00
15.07	0.00	0.00	0.00	0.00	0.78	0.00	0.00	0.00	0.00	0.00
15.18	0.00	0.00	0.00	0.00	0.76	0.00	0.00	0.00	0.00	0.00
15.30	0.00	0.00	0.00	0.00	0.73	0.00	0.00	0.00	0.00	0.00
15.42	0.00	0.00	0.00	0.00	0.71	0.00	0.00	0.00	0.00	0.00
15.54	0.00	0.00	0.00	0.00	0.71	0.01	0.00	0.00	0.00	0.00
15.66	0.00	0.00	0.00	0.00	0.74	0.02	0.00	0.00	0.00	0.00

15.79	0.00	0.00	0.00	0.00	0.76	0.04	0.00	0.00	0.00	0.00
15.91	0.00	0.00	0.00	0.00	0.79	0.05	0.00	0.00	0.00	0.00
16.03	0.00	0.00	0.00	0.00	0.83	0.08	0.00	0.00	0.00	0.00
16.16	0.00	0.00	0.00	0.00	0.90	0.16	0.00	0.00	0.00	0.00
16.29	0.00	0.00	0.00	0.00	0.95	0.21	0.00	0.00	0.00	0.00
16.41	0.00	0.00	0.00	0.00	0.97	0.34	0.00	0.00	0.00	0.00
16.54	0.00	0.00	0.00	0.00	0.77	0.45	0.00	0.00	0.00	0.00
16.67	0.00	0.00	0.00	0.00	0.52	0.55	0.00	0.00	0.00	0.00
16.80	0.00	0.00	0.00	0.00	0.41	0.67	0.00	0.00	0.00	0.00
16.93	0.00	0.00	0.00	0.00	0.29	0.79	0.00	0.00	0.00	0.00
17.06	0.00	0.00	0.00	0.00	0.16	0.85	0.00	0.00	0.00	0.00
17.20	0.00	0.00	0.00	0.00	0.03	0.89	0.00	0.00	0.00	0.00
17.33	0.00	0.00	0.00	0.00	0.02	0.92	0.00	0.00	0.00	0.00
17.47	0.00	0.00	0.00	0.00	0.01	0.93	0.00	0.00	0.00	0.00
17.60	0.00	0.00	0.00	0.00	0.00	0.91	0.00	0.00	0.00	0.00
17.74	0.00	0.00	0.00	0.00	0.00	0.88	0.00	0.00	0.00	0.00
17.88	0.00	0.00	0.00	0.00	0.00	0.84	0.00	0.00	0.00	0.00
18.02	0.00	0.00	0.00	0.00	0.00	0.82	0.00	0.00	0.00	0.00
18.16	0.00	0.00	0.00	0.00	0.00	0.88	0.00	0.00	0.00	0.00
18.30	0.00	0.00	0.00	0.00	0.00	0.94	0.00	0.00	0.00	0.00
18.44	0.00	0.00	0.00	0.00	0.00	1.00	0.00	0.00	0.00	0.00
18.59	0.00	0.00	0.00	0.00	0.00	0.99	0.00	0.00	0.00	0.00
18.73	0.00	0.00	0.00	0.00	0.00	0.93	0.00	0.00	0.00	0.00
18.88	0.00	0.00	0.00	0.00	0.00	0.87	0.00	0.00	0.00	0.00
19.03	0.00	0.00	0.00	0.00	0.00	0.81	0.00	0.00	0.00	0.00
19.18	0.00	0.00	0.00	0.00	0.00	0.68	0.00	0.00	0.00	0.00
19.33	0.00	0.00	0.00	0.00	0.00	0.56	0.00	0.00	0.00	0.00
19.48	0.00	0.00	0.00	0.00	0.00	0.46	0.00	0.00	0.00	0.00
19.63	0.00	0.00	0.00	0.00	0.00	0.51	0.00	0.00	0.00	0.00
19.78	0.00	0.00	0.00	0.00	0.00	0.60	0.00	0.00	0.00	0.00
19.94	0.00	0.00	0.00	0.00	0.00	0.69	0.00	0.00	0.00	0.00
20.09	0.00	0.00	0.00	0.00	0.00	0.70	0.00	0.00	0.00	0.00
20.25	0.00	0.00	0.00	0.00	0.00	0.64	0.00	0.00	0.00	0.00
20.41	0.00	0.00	0.00	0.00	0.00	0.60	0.00	0.00	0.00	0.00
20.57	0.00	0.00	0.00	0.00	0.00	0.58	0.00	0.00	0.00	0.00
20.73	0.00	0.00	0.00	0.00	0.00	0.63	0.00	0.00	0.00	0.00
20.89	0.00	0.00	0.00	0.00	0.00	0.66	0.00	0.00	0.00	0.00
21.05	0.00	0.00	0.00	0.00	0.00	0.70	0.00	0.00	0.00	0.00
21.22	0.00	0.00	0.00	0.00	0.00	0.75	0.00	0.00	0.00	0.00
21.38	0.00	0.00	0.00	0.00	0.00	0.80	0.00	0.00	0.00	0.00
21.55	0.00	0.00	0.00	0.00	0.00	0.80	0.00	0.00	0.00	0.00
21.72	0.00	0.00	0.00	0.00	0.00	0.69	0.00	0.00	0.00	0.00
21.89	0.00	0.00	0.00	0.00	0.00	0.59	0.00	0.00	0.00	0.00
22.06	0.00	0.00	0.00	0.00	0.00	0.53	0.00	0.00	0.00	0.00
22.23	0.00	0.00	0.00	0.00	0.00	0.57	0.00	0.00	0.00	0.00

22.41	0.00	0.00	0.00	0.00	0.00	0.61	0.00	0.00	0.00	0.00
22.58	0.00	0.00	0.00	0.00	0.00	0.66	0.00	0.00	0.00	0.00
22.76	0.00	0.00	0.00	0.00	0.00	0.74	0.00	0.00	0.00	0.00
22.93	0.00	0.00	0.00	0.00	0.00	0.83	0.00	0.00	0.00	0.00
23.11	0.00	0.00	0.00	0.00	0.00	0.83	0.00	0.00	0.00	0.00
23.29	0.00	0.00	0.00	0.00	0.00	0.78	0.00	0.00	0.00	0.00
23.48	0.00	0.00	0.00	0.00	0.00	0.73	0.00	0.00	0.00	0.00
23.66	0.00	0.00	0.00	0.00	0.00	0.70	0.00	0.00	0.00	0.00
23.84	0.00	0.00	0.00	0.00	0.00	0.68	0.00	0.00	0.00	0.00
24.03	0.00	0.00	0.00	0.00	0.00	0.67	0.00	0.00	0.00	0.00
24.22	0.00	0.00	0.00	0.00	0.00	0.79	0.00	0.00	0.00	0.00
24.41	0.00	0.00	0.00	0.00	0.00	0.90	0.00	0.00	0.00	0.00
24.60	0.00	0.00	0.00	0.00	0.00	0.95	0.00	0.00	0.00	0.00
24.79	0.00	0.00	0.00	0.00	0.00	0.94	0.00	0.00	0.00	0.00
24.98	0.00	0.00	0.00	0.00	0.00	0.93	0.00	0.00	0.00	0.00
25.18	0.00	0.00	0.00	0.00	0.00	0.77	0.00	0.00	0.00	0.00
25.38	0.00	0.00	0.00	0.00	0.00	0.62	0.00	0.00	0.00	0.00
25.57	0.00	0.00	0.00	0.00	0.00	0.48	0.00	0.00	0.00	0.00
25.77	0.00	0.00	0.00	0.00	0.00	0.35	0.00	0.00	0.00	0.00
25.98	0.00	0.00	0.00	0.00	0.00	0.24	0.00	0.00	0.00	0.00
26.18	0.00	0.00	0.00	0.00	0.00	0.18	0.00	0.00	0.00	0.00
26.38	0.00	0.00	0.00	0.00	0.00	0.14	0.00	0.00	0.00	0.00
26.59	0.00	0.00	0.00	0.00	0.00	0.09	0.00	0.00	0.00	0.00
26.80	0.00	0.00	0.00	0.00	0.00	0.08	0.00	0.00	0.00	0.00
27.01	0.00	0.00	0.00	0.00	0.00	0.07	0.00	0.00	0.00	0.00
27.22	0.00	0.00	0.00	0.00	0.00	0.08	0.00	0.00	0.00	0.00
27.43	0.00	0.00	0.00	0.00	0.00	0.08	0.00	0.00	0.00	0.00
27.64	0.00	0.00	0.00	0.00	0.00	0.07	0.00	0.00	0.00	0.00
27.86	0.00	0.00	0.00	0.00	0.00	0.05	0.00	0.00	0.00	0.00
28.08	0.00	0.00	0.00	0.00	0.00	0.04	0.00	0.00	0.00	0.00
28.30	0.00	0.00	0.00	0.00	0.00	0.03	0.00	0.00	0.00	0.00
28.52	0.00	0.00	0.00	0.00	0.00	0.02	0.00	0.00	0.00	0.00
28.74	0.00	0.00	0.00	0.00	0.00	0.02	0.00	0.00	0.00	0.00
28.97	0.00	0.00	0.00	0.00	0.00	0.01	0.00	0.00	0.00	0.00
29.19	0.00	0.00	0.00	0.00	0.00	0.01	0.00	0.00	0.00	0.00
29.42	0.00	0.00	0.00	0.00	0.00	0.00	0.00	0.00	0.00	0.00
29.65	0.00	0.00	0.00	0.00	0.00	0.00	0.00	0.00	0.00	0.00
29.88	0.00	0.00	0.00	0.00	0.00	0.00	0.00	0.00	0.00	0.00
30.11	0.00	0.00	0.00	0.00	0.00	0.00	0.00	0.00	0.00	0.00
30.35	0.00	0.00	0.00	0.00	0.00	0.00	0.01	0.00	0.00	0.00
30.59	0.00	0.00	0.00	0.00	0.00	0.00	0.01	0.00	0.00	0.00
30.83	0.00	0.00	0.00	0.00	0.00	0.00	0.01	0.00	0.00	0.00
31.07	0.00	0.00	0.00	0.00	0.00	0.00	0.01	0.00	0.00	0.00
31.31	0.00	0.00	0.00	0.00	0.00	0.00	0.01	0.00	0.00	0.00
31.55	0.00	0.00	0.00	0.00	0.00	0.00	0.01	0.00	0.00	0.00

31.80	0.00	0.00	0.00	0.00	0.00	0.00	0.01	0.00	0.00	0.00
32.05	0.00	0.00	0.00	0.00	0.00	0.00	0.02	0.00	0.00	0.00
32.30	0.00	0.00	0.00	0.00	0.00	0.00	0.02	0.00	0.00	0.00
32.55	0.00	0.00	0.00	0.00	0.00	0.00	0.02	0.00	0.00	0.00
32.81	0.00	0.00	0.00	0.00	0.00	0.00	0.02	0.00	0.00	0.00
33.06	0.00	0.00	0.00	0.00	0.00	0.00	0.02	0.00	0.00	0.00
33.32	0.00	0.00	0.00	0.00	0.00	0.00	0.02	0.00	0.00	0.00
33.58	0.00	0.00	0.00	0.00	0.00	0.00	0.02	0.00	0.00	0.00
33.84	0.00	0.00	0.00	0.00	0.00	0.00	0.02	0.00	0.00	0.00
34.11	0.00	0.00	0.00	0.00	0.00	0.00	0.02	0.00	0.00	0.00
34.37	0.00	0.00	0.00	0.00	0.00	0.00	0.02	0.00	0.00	0.00
34.64	0.00	0.00	0.00	0.00	0.00	0.00	0.01	0.00	0.00	0.00
34.91	0.00	0.00	0.00	0.00	0.00	0.00	0.01	0.00	0.00	0.00
35.18	0.00	0.00	0.00	0.00	0.00	0.00	0.01	0.00	0.00	0.00
35.46	0.00	0.00	0.00	0.00	0.00	0.00	0.01	0.00	0.00	0.00
35.74	0.00	0.00	0.00	0.00	0.00	0.00	0.01	0.00	0.00	0.00
36.02	0.00	0.00	0.00	0.00	0.00	0.00	0.00	0.00	0.00	0.00
36.30	0.00	0.00	0.00	0.00	0.00	0.00	0.00	0.00	0.00	0.00
36.58	0.00	0.00	0.00	0.00	0.00	0.00	0.00	0.00	0.00	0.00
36.87	0.00	0.00	0.00	0.00	0.00	0.00	0.00	0.00	0.00	0.00
37.15	0.00	0.00	0.00	0.00	0.00	0.00	0.00	0.00	0.00	0.00
37.44	0.00	0.00	0.00	0.00	0.00	0.00	0.00	0.00	0.00	0.00
37.74	0.00	0.00	0.00	0.00	0.00	0.00	0.00	0.00	0.00	0.00
38.03	0.00	0.00	0.00	0.00	0.00	0.00	0.03	0.00	0.00	0.00
38.33	0.00	0.00	0.00	0.00	0.00	0.00	0.06	0.00	0.00	0.00
38.63	0.00	0.00	0.00	0.00	0.00	0.00	0.09	0.00	0.00	0.00
38.93	0.00	0.00	0.00	0.00	0.00	0.00	0.11	0.00	0.00	0.00
39.23	0.00	0.00	0.00	0.00	0.00	0.00	0.13	0.00	0.00	0.00
39.54	0.00	0.00	0.00	0.00	0.00	0.00	0.16	0.00	0.00	0.00
39.85	0.00	0.00	0.00	0.00	0.00	0.00	0.19	0.00	0.00	0.00
40.16	0.00	0.00	0.00	0.00	0.00	0.00	0.22	0.00	0.00	0.00
40.47	0.00	0.00	0.00	0.00	0.00	0.00	0.24	0.00	0.00	0.00
40.79	0.00	0.00	0.00	0.00	0.00	0.00	0.27	0.00	0.00	0.00
41.11	0.00	0.00	0.00	0.00	0.00	0.00	0.30	0.00	0.00	0.00
41.43	0.00	0.00	0.00	0.00	0.00	0.00	0.34	0.00	0.00	0.00
41.75	0.00	0.00	0.00	0.00	0.00	0.00	0.37	0.00	0.00	0.00
42.08	0.00	0.00	0.00	0.00	0.00	0.00	0.39	0.00	0.00	0.00
42.41	0.00	0.00	0.00	0.00	0.00	0.00	0.42	0.00	0.00	0.00
42.74	0.00	0.00	0.00	0.00	0.00	0.00	0.45	0.00	0.00	0.00
43.07	0.00	0.00	0.00	0.00	0.00	0.00	0.48	0.00	0.00	0.00
43.41	0.00	0.00	0.00	0.00	0.00	0.00	0.50	0.00	0.00	0.00
43.75	0.00	0.00	0.00	0.00	0.00	0.00	0.53	0.00	0.00	0.00
44.09	0.00	0.00	0.00	0.00	0.00	0.00	0.56	0.00	0.00	0.00
44.44	0.00	0.00	0.00	0.00	0.00	0.00	0.59	0.00	0.00	0.00
44.78	0.00	0.00	0.00	0.00	0.00	0.00	0.62	0.00	0.00	0.00

45.13	0.00	0.00	0.00	0.00	0.00	0.00	0.65	0.00	0.00	0.00
45.49	0.00	0.00	0.00	0.00	0.00	0.00	0.67	0.00	0.00	0.00
45.84	0.00	0.00	0.00	0.00	0.00	0.00	0.69	0.00	0.00	0.00
46.20	0.00	0.00	0.00	0.00	0.00	0.00	0.70	0.00	0.00	0.00
46.56	0.00	0.00	0.00	0.00	0.00	0.00	0.72	0.00	0.00	0.00
46.92	0.00	0.00	0.00	0.00	0.00	0.00	0.73	0.00	0.00	0.00
47.29	0.00	0.00	0.00	0.00	0.00	0.00	0.74	0.00	0.00	0.00
47.66	0.00	0.00	0.00	0.00	0.00	0.00	0.75	0.00	0.00	0.00
48.03	0.00	0.00	0.00	0.00	0.00	0.00	0.76	0.00	0.00	0.00
48.41	0.00	0.00	0.00	0.00	0.00	0.00	0.77	0.00	0.00	0.00
48.78	0.00	0.00	0.00	0.00	0.00	0.00	0.78	0.00	0.00	0.00
49.17	0.00	0.00	0.00	0.00	0.00	0.00	0.79	0.00	0.00	0.00
49.55	0.00	0.00	0.00	0.00	0.00	0.00	0.80	0.00	0.00	0.00
49.94	0.00	0.00	0.00	0.00	0.00	0.00	0.81	0.00	0.00	0.00
50.33	0.00	0.00	0.00	0.00	0.00	0.00	0.83	0.00	0.00	0.00
50.72	0.00	0.00	0.00	0.00	0.00	0.00	0.84	0.00	0.00	0.00
51.12	0.00	0.00	0.00	0.00	0.00	0.00	0.85	0.00	0.00	0.00
51.52	0.00	0.00	0.00	0.00	0.00	0.00	0.86	0.00	0.00	0.00
51.92	0.00	0.00	0.00	0.00	0.00	0.00	0.87	0.00	0.00	0.00
52.32	0.00	0.00	0.00	0.00	0.00	0.00	0.88	0.00	0.00	0.00
52.73	0.00	0.00	0.00	0.00	0.00	0.00	0.89	0.00	0.00	0.00
53.14	0.00	0.00	0.00	0.00	0.00	0.00	0.89	0.00	0.00	0.00
53.56	0.00	0.00	0.00	0.00	0.00	0.00	0.89	0.00	0.00	0.00
53.98	0.00	0.00	0.00	0.00	0.00	0.00	0.89	0.00	0.00	0.00
54.40	0.00	0.00	0.00	0.00	0.00	0.00	0.90	0.00	0.00	0.00
54.82	0.00	0.00	0.00	0.00	0.00	0.00	0.90	0.00	0.00	0.00
55.25	0.00	0.00	0.00	0.00	0.00	0.00	0.91	0.00	0.00	0.00
55.68	0.00	0.00	0.00	0.00	0.00	0.00	0.92	0.00	0.00	0.00
56.12	0.00	0.00	0.00	0.00	0.00	0.00	0.94	0.00	0.00	0.00
56.56	0.00	0.00	0.00	0.00	0.00	0.00	0.96	0.00	0.00	0.00
57.00	0.00	0.00	0.00	0.00	0.00	0.00	0.97	0.00	0.00	0.00
57.44	0.00	0.00	0.00	0.00	0.00	0.00	0.98	0.00	0.00	0.00
57.89	0.00	0.00	0.00	0.00	0.00	0.00	0.98	0.00	0.00	0.00
58.35	0.00	0.00	0.00	0.00	0.00	0.00	0.99	0.00	0.00	0.00
58.80	0.00	0.00	0.00	0.00	0.00	0.00	0.99	0.00	0.00	0.00
59.26	0.00	0.00	0.00	0.00	0.00	0.00	0.99	0.00	0.00	0.00
59.72	0.00	0.00	0.00	0.00	0.00	0.00	0.99	0.00	0.00	0.00
60.19	0.00	0.00	0.00	0.00	0.00	0.00	1.00	0.00	0.00	0.00
60.66	0.00	0.00	0.00	0.00	0.00	0.00	1.00	0.00	0.00	0.00
61.13	0.00	0.00	0.00	0.00	0.00	0.00	1.00	0.00	0.00	0.00
61.61	0.00	0.00	0.00	0.00	0.00	0.00	1.00	0.00	0.00	0.00
62.09	0.00	0.00	0.00	0.00	0.00	0.00	1.00	0.00	0.00	0.00
62.58	0.00	0.00	0.00	0.00	0.00	0.00	1.00	0.00	0.00	0.00
63.07	0.00	0.00	0.00	0.00	0.00	0.00	0.97	0.00	0.00	0.00
63.56	0.00	0.00	0.00	0.00	0.00	0.00	0.95	0.00	0.00	0.00

64.06	0.00	0.00	0.00	0.00	0.00	0.00	0.93	0.00	0.00	0.00
64.56	0.00	0.00	0.00	0.00	0.00	0.00	0.90	0.00	0.00	0.00
65.06	0.00	0.00	0.00	0.00	0.00	0.00	0.88	0.00	0.00	0.00
65.57	0.00	0.00	0.00	0.00	0.00	0.00	0.84	0.01	0.00	0.00
66.08	0.00	0.00	0.00	0.00	0.00	0.00	0.80	0.01	0.00	0.00
66.60	0.00	0.00	0.00	0.00	0.00	0.00	0.77	0.03	0.00	0.00
67.12	0.00	0.00	0.00	0.00	0.00	0.00	0.73	0.04	0.00	0.00
67.64	0.00	0.00	0.00	0.00	0.00	0.00	0.69	0.06	0.00	0.00
68.17	0.00	0.00	0.00	0.00	0.00	0.00	0.66	0.08	0.00	0.00
68.70	0.00	0.00	0.00	0.00	0.00	0.00	0.62	0.10	0.00	0.00
69.24	0.00	0.00	0.00	0.00	0.00	0.00	0.58	0.11	0.00	0.00
69.78	0.00	0.00	0.00	0.00	0.00	0.00	0.55	0.13	0.00	0.00
70.32	0.00	0.00	0.00	0.00	0.00	0.00	0.52	0.14	0.00	0.00
70.87	0.00	0.00	0.00	0.00	0.00	0.00	0.49	0.15	0.00	0.00
71.43	0.00	0.00	0.00	0.00	0.00	0.00	0.46	0.15	0.00	0.00
71.99	0.00	0.00	0.00	0.00	0.00	0.00	0.42	0.16	0.00	0.00
72.55	0.00	0.00	0.00	0.00	0.00	0.00	0.37	0.17	0.00	0.00
73.11	0.00	0.00	0.00	0.00	0.00	0.00	0.32	0.18	0.00	0.00
73.69	0.00	0.00	0.00	0.00	0.00	0.00	0.27	0.18	0.00	0.00
74.26	0.00	0.00	0.00	0.00	0.00	0.00	0.23	0.19	0.00	0.00
74.84	0.00	0.00	0.00	0.00	0.00	0.00	0.20	0.20	0.00	0.00
75.43	0.00	0.00	0.00	0.00	0.00	0.00	0.17	0.21	0.00	0.00
76.01	0.00	0.00	0.00	0.00	0.00	0.00	0.14	0.22	0.00	0.00
76.61	0.00	0.00	0.00	0.00	0.00	0.00	0.10	0.23	0.00	0.00
77.21	0.00	0.00	0.00	0.00	0.00	0.00	0.08	0.24	0.00	0.00
77.81	0.00	0.00	0.00	0.00	0.00	0.00	0.07	0.27	0.00	0.00
78.42	0.00	0.00	0.00	0.00	0.00	0.00	0.06	0.29	0.00	0.00
79.03	0.00	0.00	0.00	0.00	0.00	0.00	0.04	0.31	0.00	0.00
79.65	0.00	0.00	0.00	0.00	0.00	0.00	0.03	0.34	0.00	0.00
80.27	0.00	0.00	0.00	0.00	0.00	0.00	0.02	0.36	0.00	0.00
80.90	0.00	0.00	0.00	0.00	0.00	0.00	0.01	0.38	0.00	0.00
81.53	0.00	0.00	0.00	0.00	0.00	0.00	0.01	0.40	0.00	0.00
82.17	0.00	0.00	0.00	0.00	0.00	0.00	0.00	0.42	0.00	0.00
82.81	0.00	0.00	0.00	0.00	0.00	0.00	0.00	0.43	0.00	0.00
83.45	0.00	0.00	0.00	0.00	0.00	0.00	0.00	0.45	0.00	0.00
84.11	0.00	0.00	0.00	0.00	0.00	0.00	0.00	0.47	0.00	0.00
84.76	0.00	0.00	0.00	0.00	0.00	0.00	0.00	0.49	0.00	0.00
85.43	0.00	0.00	0.00	0.00	0.00	0.00	0.00	0.51	0.00	0.00
86.09	0.00	0.00	0.00	0.00	0.00	0.00	0.00	0.52	0.00	0.00
86.76	0.00	0.00	0.00	0.00	0.00	0.00	0.00	0.54	0.00	0.00
87.44	0.00	0.00	0.00	0.00	0.00	0.00	0.00	0.56	0.00	0.00
88.13	0.00	0.00	0.00	0.00	0.00	0.00	0.00	0.57	0.00	0.00
88.81	0.00	0.00	0.00	0.00	0.00	0.00	0.00	0.59	0.00	0.00
89.51	0.00	0.00	0.00	0.00	0.00	0.00	0.00	0.61	0.00	0.00
90.21	0.00	0.00	0.00	0.00	0.00	0.00	0.00	0.63	0.00	0.00

90.91	0.00	0.00	0.00	0.00	0.00	0.00	0.00	0.66	0.00	0.00
91.62	0.00	0.00	0.00	0.00	0.00	0.00	0.00	0.68	0.00	0.00
92.34	0.00	0.00	0.00	0.00	0.00	0.00	0.00	0.71	0.00	0.00
93.06	0.00	0.00	0.00	0.00	0.00	0.00	0.00	0.74	0.00	0.00
93.79	0.00	0.00	0.00	0.00	0.00	0.00	0.00	0.76	0.00	0.00
94.52	0.00	0.00	0.00	0.00	0.00	0.00	0.00	0.79	0.00	0.00
95.26	0.00	0.00	0.00	0.00	0.00	0.00	0.00	0.81	0.00	0.00
96.00	0.00	0.00	0.00	0.00	0.00	0.00	0.00	0.83	0.00	0.00
96.75	0.00	0.00	0.00	0.00	0.00	0.00	0.00	0.84	0.00	0.00
97.51	0.00	0.00	0.00	0.00	0.00	0.00	0.00	0.86	0.00	0.00
98.27	0.00	0.00	0.00	0.00	0.00	0.00	0.00	0.88	0.00	0.00
99.04	0.00	0.00	0.00	0.00	0.00	0.00	0.00	0.89	0.00	0.00
99.81	0.00	0.00	0.00	0.00	0.00	0.00	0.00	0.91	0.01	0.00
100.59	0.00	0.00	0.00	0.00	0.00	0.00	0.00	0.95	0.01	0.00
101.37	0.00	0.00	0.00	0.00	0.00	0.00	0.00	0.96	0.02	0.00
102.17	0.00	0.00	0.00	0.00	0.00	0.00	0.00	0.97	0.02	0.00
102.96	0.00	0.00	0.00	0.00	0.00	0.00	0.00	0.98	0.03	0.00
103.77	0.00	0.00	0.00	0.00	0.00	0.00	0.00	0.99	0.03	0.00
104.58	0.00	0.00	0.00	0.00	0.00	0.00	0.00	1.00	0.04	0.00
105.40	0.00	0.00	0.00	0.00	0.00	0.00	0.00	1.00	0.05	0.00
106.22	0.00	0.00	0.00	0.00	0.00	0.00	0.00	1.00	0.06	0.00
107.05	0.00	0.00	0.00	0.00	0.00	0.00	0.00	1.00	0.08	0.00
107.89	0.00	0.00	0.00	0.00	0.00	0.00	0.00	0.99	0.09	0.00
108.73	0.00	0.00	0.00	0.00	0.00	0.00	0.00	0.99	0.11	0.00
109.58	0.00	0.00	0.00	0.00	0.00	0.00	0.00	0.99	0.12	0.00
110.43	0.00	0.00	0.00	0.00	0.00	0.00	0.00	0.98	0.15	0.00
111.30	0.00	0.00	0.00	0.00	0.00	0.00	0.00	0.95	0.18	0.00
112.17	0.00	0.00	0.00	0.00	0.00	0.00	0.00	0.88	0.21	0.00
113.04	0.00	0.00	0.00	0.00	0.00	0.00	0.00	0.81	0.23	0.00
113.92	0.00	0.00	0.00	0.00	0.00	0.00	0.00	0.72	0.24	0.00
114.81	0.00	0.00	0.00	0.00	0.00	0.00	0.00	0.64	0.26	0.00
115.71	0.00	0.00	0.00	0.00	0.00	0.00	0.00	0.54	0.28	0.00
116.62	0.00	0.00	0.00	0.00	0.00	0.00	0.00	0.44	0.30	0.00
117.53	0.00	0.00	0.00	0.00	0.00	0.00	0.00	0.35	0.32	0.00
118.44	0.00	0.00	0.00	0.00	0.00	0.00	0.00	0.27	0.32	0.00
119.37	0.00	0.00	0.00	0.00	0.00	0.00	0.00	0.20	0.33	0.00
120.30	0.00	0.00	0.00	0.00	0.00	0.00	0.00	0.16	0.34	0.00
121.24	0.00	0.00	0.00	0.00	0.00	0.00	0.00	0.12	0.34	0.00
122.19	0.00	0.00	0.00	0.00	0.00	0.00	0.00	0.09	0.35	0.00
123.14	0.00	0.00	0.00	0.00	0.00	0.00	0.00	0.07	0.35	0.00
124.10	0.00	0.00	0.00	0.00	0.00	0.00	0.00	0.06	0.36	0.00
125.07	0.00	0.00	0.00	0.00	0.00	0.00	0.00	0.05	0.37	0.00
126.05	0.00	0.00	0.00	0.00	0.00	0.00	0.00	0.04	0.38	0.00
127.04	0.00	0.00	0.00	0.00	0.00	0.00	0.00	0.03	0.39	0.00
128.03	0.00	0.00	0.00	0.00	0.00	0.00	0.00	0.03	0.41	0.00













# Appendix B

## Color Correction Tables

Color correction factors,  $K$ , are given for a variety of assumed source spectral energy distributions in Tables B.0-1 to B.0-6. Null entries imply that  $K > 3$ . The correction factor should be divided into the quoted intensity to calculate an estimate of the actual intensity, as follows:

$$I_\nu(\text{actual}) = I_\nu(\text{quoted})/K.$$

Equation (5.2) in §5.5 specifies how a color correction factor can be derived for an arbitrary source spectrum.

Table B.0-1: Color correction factors for power law spectra of the form  $I_\nu \propto \nu^n$

n	DIRBE band									
	1	2	3	4	5	6	7	8	9	10
-3.00	1.03	1.02	1.03	0.99	1.09	0.71	0.89	0.97	1.14	1.10
-2.50	1.02	1.01	1.02	1.00	1.05	0.76	0.91	0.97	1.10	1.06
-2.00	1.01	1.01	1.01	1.00	1.02	0.83	0.93	0.98	1.06	1.03
-1.50	1.01	1.00	1.00	1.00	1.01	0.91	0.96	0.99	1.03	1.01
-1.00	1.00	1.00	1.00	1.00	1.00	1.00	1.00	1.00	1.00	1.00
-0.50	1.00	1.00	1.00	1.00	1.00	1.10	1.05	1.02	0.98	0.99
0.00	0.99	0.99	1.00	1.01	1.02	1.23	1.10	1.04	0.97	0.99
0.50	0.99	0.99	1.00	1.01	1.04	1.37	1.17	1.07	0.96	1.00
1.00	0.99	0.99	1.00	1.01	1.08	1.53	1.25	1.11	0.95	1.01
1.50	0.99	0.99	1.00	1.02	1.13	1.72	1.34	1.15	0.95	1.03
2.00	0.99	0.99	1.01	1.02	1.19	1.95	1.46	1.20	0.96	1.06
2.50	1.00	0.99	1.02	1.03	1.27	2.21	1.59	1.26	0.96	1.09
3.00	1.00	0.99	1.03	1.03	1.36	2.52	1.75	1.33	0.98	1.13

Table B.0-2: Color correction factors for spectra of the form  $I_\nu \propto B_\nu(T)$ 

T (K)	DIRBE band									
	1	2	3	4	5	6	7	8	9	10
10	–	–	–	–	–	–	–	1.35	1.61	1.01
12	–	–	–	–	–	1.38	2.25	1.14	1.31	0.97
14	–	–	–	–	–	0.76	1.57	1.03	1.17	0.96
16	–	–	–	–	–	0.53	1.25	0.98	1.09	0.96
18	–	–	–	–	–	0.42	1.07	0.95	1.04	0.96
20	–	–	–	–	–	0.36	0.96	0.94	1.01	0.96
22	–	–	–	–	–	0.33	0.90	0.93	0.99	0.97
24	–	–	–	–	–	0.31	0.86	0.93	0.97	0.97
26	–	–	–	–	–	0.30	0.83	0.93	0.96	0.98
28	–	–	–	–	–	0.30	0.82	0.94	0.96	0.98
30	–	–	–	–	–	0.29	0.81	0.94	0.95	0.98
32	–	–	–	–	–	0.30	0.81	0.95	0.95	0.99
34	–	–	–	–	–	0.30	0.81	0.96	0.95	0.99
36	–	–	–	–	–	0.30	0.82	0.96	0.94	1.00
38	–	–	–	–	–	0.31	0.82	0.97	0.94	1.00
40	–	–	–	–	–	0.31	0.83	0.98	0.94	1.00
42	–	–	–	–	–	0.32	0.84	0.98	0.94	1.00
44	–	–	–	–	–	0.33	0.85	0.99	0.94	1.01
46	–	–	–	–	–	0.34	0.86	1.00	0.94	1.01
48	–	–	–	–	–	0.35	0.87	1.00	0.94	1.01
50	–	–	–	–	–	0.36	0.88	1.01	0.94	1.01
55	–	–	–	–	–	0.38	0.90	1.02	0.94	1.02
60	–	–	–	–	–	0.41	0.93	1.04	0.94	1.02
65	–	–	–	2.65	–	0.44	0.96	1.05	0.94	1.02
70	–	–	–	2.31	–	0.46	0.98	1.06	0.94	1.02
75	–	–	–	2.06	–	0.49	1.00	1.07	0.94	1.03
80	–	–	–	1.87	–	0.52	1.02	1.07	0.94	1.03
85	–	–	–	1.73	–	0.55	1.04	1.08	0.94	1.03
90	–	–	–	1.61	2.67	0.58	1.06	1.09	0.94	1.03
95	–	–	–	1.52	2.34	0.61	1.08	1.09	0.94	1.03
100	–	–	–	1.45	2.09	0.64	1.10	1.10	0.94	1.03
110	–	–	–	1.34	1.74	0.70	1.12	1.11	0.95	1.04
120	–	–	–	1.26	1.51	0.76	1.15	1.12	0.95	1.04
130	–	–	–	1.20	1.35	0.81	1.17	1.12	0.95	1.04
140	–	–	–	1.16	1.24	0.86	1.19	1.13	0.95	1.04
150	–	–	–	1.12	1.16	0.91	1.21	1.13	0.95	1.04
160	–	–	–	1.10	1.10	0.95	1.22	1.14	0.95	1.04
170	–	–	2.93	1.08	1.05	1.00	1.24	1.14	0.95	1.04
180	–	–	2.61	1.06	1.02	1.04	1.25	1.14	0.95	1.04
190	–	–	2.36	1.05	0.99	1.07	1.26	1.15	0.95	1.05

200	–	2.87	2.16	1.04	0.97	1.11	1.27	1.15	0.95	1.05
210	–	2.62	2.00	1.03	0.96	1.14	1.28	1.15	0.95	1.05
220	–	2.41	1.87	1.02	0.95	1.17	1.29	1.15	0.95	1.05
230	–	2.25	1.76	1.02	0.94	1.20	1.29	1.16	0.95	1.05
240	–	2.11	1.67	1.01	0.93	1.23	1.30	1.16	0.95	1.05
250	–	1.99	1.59	1.01	0.93	1.26	1.31	1.16	0.95	1.05
260	–	1.89	1.53	1.00	0.93	1.28	1.31	1.16	0.95	1.05
270	–	1.81	1.47	1.00	0.93	1.30	1.32	1.16	0.95	1.05
280	–	1.73	1.42	1.00	0.93	1.32	1.32	1.16	0.95	1.05
290	–	1.67	1.38	1.00	0.93	1.34	1.33	1.17	0.95	1.05
300	–	1.61	1.34	1.00	0.93	1.36	1.33	1.17	0.95	1.05
320	–	1.52	1.28	0.99	0.93	1.40	1.34	1.17	0.95	1.05
340	–	1.45	1.23	0.99	0.94	1.43	1.35	1.17	0.95	1.05
360	–	1.39	1.19	0.99	0.94	1.46	1.35	1.17	0.95	1.05
380	–	1.34	1.16	0.99	0.95	1.48	1.36	1.17	0.95	1.05
400	–	1.30	1.14	0.99	0.95	1.51	1.36	1.17	0.95	1.05
420	–	1.26	1.11	0.99	0.96	1.53	1.37	1.18	0.95	1.05
440	–	1.23	1.10	0.99	0.97	1.55	1.37	1.18	0.95	1.05
460	–	1.21	1.08	0.99	0.97	1.56	1.38	1.18	0.95	1.05
480	–	1.19	1.07	0.99	0.98	1.58	1.38	1.18	0.95	1.05
500	–	1.17	1.06	0.99	0.99	1.60	1.38	1.18	0.95	1.05
550	2.48	1.13	1.04	0.99	1.00	1.63	1.39	1.18	0.95	1.05
600	2.10	1.10	1.02	0.99	1.01	1.66	1.40	1.18	0.95	1.05
650	1.85	1.08	1.01	0.99	1.03	1.68	1.40	1.18	0.95	1.05
700	1.67	1.07	1.00	1.00	1.04	1.70	1.40	1.19	0.95	1.05
750	1.54	1.05	1.00	1.00	1.05	1.72	1.41	1.19	0.95	1.05
800	1.45	1.04	1.00	1.00	1.05	1.73	1.41	1.19	0.95	1.05
850	1.37	1.04	0.99	1.00	1.06	1.75	1.41	1.19	0.95	1.05
900	1.31	1.03	0.99	1.00	1.07	1.76	1.42	1.19	0.95	1.05
950	1.27	1.02	0.99	1.00	1.08	1.77	1.42	1.19	0.95	1.05
1000	1.23	1.02	0.99	1.00	1.08	1.78	1.42	1.19	0.95	1.05
1100	1.17	1.01	0.99	1.00	1.09	1.79	1.42	1.19	0.95	1.05
1200	1.13	1.01	0.99	1.01	1.10	1.81	1.43	1.19	0.95	1.05
1300	1.10	1.00	0.99	1.01	1.11	1.82	1.43	1.19	0.95	1.05
1400	1.07	1.00	0.99	1.01	1.11	1.83	1.43	1.19	0.95	1.06
1500	1.06	1.00	0.99	1.01	1.12	1.84	1.43	1.19	0.96	1.06
2000	1.01	0.99	0.99	1.01	1.14	1.87	1.44	1.19	0.96	1.06
3000	0.99	0.99	1.00	1.02	1.15	1.89	1.44	1.20	0.96	1.06
5000	0.99	0.99	1.00	1.02	1.17	1.92	1.45	1.20	0.96	1.06
7000	0.99	0.99	1.01	1.02	1.17	1.93	1.45	1.20	0.96	1.06
9000	0.99	0.99	1.01	1.02	1.18	1.93	1.45	1.20	0.96	1.06
10000	0.99	0.99	1.01	1.02	1.18	1.93	1.45	1.20	0.96	1.06
12000	0.99	0.99	1.01	1.02	1.18	1.94	1.45	1.20	0.96	1.06
14000	0.99	0.99	1.01	1.02	1.18	1.94	1.45	1.20	0.96	1.06
16000	0.99	0.99	1.01	1.02	1.18	1.94	1.45	1.20	0.96	1.06
18000	0.99	0.99	1.01	1.02	1.18	1.94	1.45	1.20	0.96	1.06
20000	0.99	0.99	1.01	1.02	1.18	1.94	1.45	1.20	0.96	1.06



Table B.0-3: Color correction factors for spectra of the form  $I_\nu \propto \nu^{0.5} B_\nu(T)$ 

T (K)	DIRBE band									
	1	2	3	4	5	6	7	8	9	10
10	–	–	–	–	–	–	–	1.29	1.49	0.98
12	–	–	–	–	–	1.31	2.09	1.10	1.24	0.95
14	–	–	–	–	–	0.73	1.48	1.01	1.12	0.95
16	–	–	–	–	–	0.51	1.18	0.96	1.05	0.95
18	–	–	–	–	–	0.41	1.02	0.94	1.01	0.96
20	–	–	–	–	–	0.35	0.93	0.93	0.98	0.97
22	–	–	–	–	–	0.32	0.87	0.93	0.96	0.97
24	–	–	–	–	–	0.31	0.84	0.93	0.95	0.98
26	–	–	–	–	–	0.30	0.82	0.93	0.95	0.99
28	–	–	–	–	–	0.29	0.81	0.94	0.94	0.99
30	–	–	–	–	–	0.29	0.81	0.95	0.94	1.00
32	–	–	–	–	–	0.30	0.81	0.96	0.94	1.00
34	–	–	–	–	–	0.30	0.81	0.97	0.94	1.01
36	–	–	–	–	–	0.31	0.82	0.98	0.93	1.01
38	–	–	–	–	–	0.31	0.83	0.99	0.93	1.02
40	–	–	–	–	–	0.32	0.84	1.00	0.93	1.02
42	–	–	–	–	–	0.33	0.85	1.00	0.93	1.02
44	–	–	–	–	–	0.34	0.86	1.01	0.93	1.03
46	–	–	–	–	–	0.35	0.88	1.02	0.94	1.03
48	–	–	–	–	–	0.36	0.89	1.03	0.94	1.03
50	–	–	–	–	–	0.37	0.90	1.04	0.94	1.03
55	–	–	–	–	–	0.39	0.94	1.05	0.94	1.04
60	–	–	–	–	–	0.42	0.97	1.07	0.94	1.04
65	–	–	–	2.59	–	0.46	1.00	1.08	0.94	1.05
70	–	–	–	2.26	–	0.49	1.03	1.09	0.94	1.05
75	–	–	–	2.02	–	0.52	1.05	1.10	0.94	1.05
80	–	–	–	1.84	–	0.55	1.08	1.11	0.94	1.05
85	–	–	–	1.70	2.78	0.59	1.10	1.12	0.95	1.06
90	–	–	–	1.59	2.40	0.62	1.12	1.13	0.95	1.06
95	–	–	–	1.50	2.12	0.66	1.14	1.14	0.95	1.06
100	–	–	–	1.43	1.90	0.69	1.16	1.14	0.95	1.06
110	–	–	–	1.32	1.59	0.76	1.20	1.15	0.95	1.06
120	–	–	–	1.24	1.39	0.82	1.23	1.16	0.95	1.07
130	–	–	–	1.19	1.25	0.88	1.25	1.17	0.95	1.07
140	–	–	–	1.14	1.16	0.94	1.28	1.18	0.95	1.07
150	–	–	–	1.11	1.09	1.00	1.30	1.18	0.95	1.07
160	–	–	–	1.09	1.04	1.05	1.31	1.19	0.95	1.07
170	–	–	2.80	1.07	1.00	1.10	1.33	1.19	0.95	1.07
180	–	–	2.49	1.05	0.97	1.15	1.34	1.19	0.96	1.07
190	–	–	2.26	1.04	0.95	1.19	1.36	1.20	0.96	1.07

200	—	2.78	2.07	1.03	0.94	1.23	1.37	1.20	0.96	1.08
210	—	2.54	1.92	1.02	0.93	1.27	1.38	1.20	0.96	1.08
220	—	2.34	1.79	1.02	0.92	1.30	1.39	1.21	0.96	1.08
230	—	2.18	1.69	1.01	0.92	1.34	1.40	1.21	0.96	1.08
240	—	2.05	1.61	1.01	0.92	1.37	1.41	1.21	0.96	1.08
250	—	1.94	1.54	1.00	0.92	1.40	1.41	1.21	0.96	1.08
260	—	1.84	1.47	1.00	0.92	1.43	1.42	1.21	0.96	1.08
270	—	1.76	1.42	1.00	0.92	1.45	1.43	1.22	0.96	1.08
280	—	1.69	1.38	1.00	0.92	1.48	1.43	1.22	0.96	1.08
290	—	1.63	1.34	0.99	0.92	1.50	1.44	1.22	0.96	1.08
300	—	1.58	1.30	0.99	0.93	1.53	1.44	1.22	0.96	1.08
320	—	1.49	1.25	0.99	0.94	1.57	1.45	1.22	0.96	1.08
340	—	1.42	1.20	0.99	0.94	1.60	1.46	1.22	0.96	1.08
360	—	1.36	1.16	0.99	0.95	1.64	1.47	1.23	0.96	1.08
380	—	1.31	1.14	0.99	0.96	1.67	1.48	1.23	0.96	1.08
400	—	1.27	1.11	0.99	0.97	1.69	1.48	1.23	0.96	1.08
420	—	1.24	1.09	0.99	0.98	1.72	1.49	1.23	0.96	1.08
440	—	1.21	1.08	0.99	0.99	1.74	1.49	1.23	0.96	1.08
460	—	1.19	1.06	0.99	1.00	1.76	1.50	1.23	0.96	1.08
480	—	1.17	1.05	0.99	1.01	1.78	1.50	1.23	0.96	1.08
500	2.93	1.15	1.04	0.99	1.02	1.80	1.50	1.24	0.96	1.08
550	2.35	1.12	1.02	0.99	1.04	1.84	1.51	1.24	0.96	1.08
600	2.00	1.09	1.01	0.99	1.05	1.87	1.52	1.24	0.96	1.08
650	1.77	1.07	1.00	1.00	1.07	1.90	1.52	1.24	0.96	1.08
700	1.61	1.06	1.00	1.00	1.08	1.92	1.53	1.24	0.96	1.08
750	1.49	1.04	0.99	1.00	1.09	1.94	1.53	1.24	0.96	1.09
800	1.40	1.04	0.99	1.00	1.10	1.96	1.54	1.24	0.96	1.09
850	1.33	1.03	0.99	1.00	1.11	1.97	1.54	1.24	0.96	1.09
900	1.28	1.02	0.99	1.00	1.12	1.99	1.54	1.25	0.96	1.09
950	1.23	1.02	0.99	1.00	1.13	2.00	1.55	1.25	0.96	1.09
1000	1.20	1.01	0.99	1.01	1.14	2.01	1.55	1.25	0.96	1.09
1100	1.14	1.01	0.99	1.01	1.15	2.03	1.55	1.25	0.96	1.09
1200	1.10	1.00	0.99	1.01	1.16	2.05	1.55	1.25	0.96	1.09
1300	1.08	1.00	0.99	1.01	1.17	2.06	1.56	1.25	0.96	1.09
1400	1.06	1.00	0.99	1.01	1.17	2.07	1.56	1.25	0.96	1.09
1500	1.04	0.99	0.99	1.01	1.18	2.08	1.56	1.25	0.96	1.09
2000	1.00	0.99	1.00	1.02	1.20	2.11	1.57	1.25	0.96	1.09
3000	0.98	0.99	1.00	1.02	1.22	2.15	1.58	1.25	0.96	1.09
5000	0.98	0.99	1.01	1.02	1.24	2.17	1.58	1.25	0.96	1.09
7000	0.99	0.99	1.01	1.02	1.25	2.19	1.58	1.26	0.96	1.09
9000	0.99	0.99	1.01	1.02	1.25	2.19	1.59	1.26	0.96	1.09
10000	0.99	0.99	1.01	1.02	1.25	2.19	1.59	1.26	0.96	1.09
12000	0.99	0.99	1.01	1.02	1.26	2.20	1.59	1.26	0.96	1.09
14000	0.99	0.99	1.02	1.03	1.26	2.20	1.59	1.26	0.96	1.09
16000	0.99	0.99	1.02	1.03	1.26	2.20	1.59	1.26	0.96	1.09
18000	0.99	0.99	1.02	1.03	1.26	2.20	1.59	1.26	0.96	1.09
20000	0.99	0.99	1.02	1.03	1.26	2.20	1.59	1.26	0.96	1.09

Table B.0-4: Color correction factors for spectra of the form  $I_\nu \propto \nu B_\nu(T)$ 

T (K)	<i>DIRBE</i> band									
	1	2	3	4	5	6	7	8	9	10
10	–	–	–	–	–	–	–	1.24	1.40	0.96
12	–	–	–	–	–	1.25	1.95	1.07	1.18	0.94
14	–	–	–	–	–	0.70	1.39	0.98	1.07	0.95
16	–	–	–	–	–	0.49	1.12	0.95	1.01	0.95
18	–	–	–	–	–	0.40	0.98	0.93	0.98	0.96
20	–	–	–	–	–	0.35	0.90	0.92	0.96	0.98
22	–	–	–	–	–	0.32	0.85	0.92	0.95	0.99
24	–	–	–	–	–	0.30	0.82	0.93	0.94	1.00
26	–	–	–	–	–	0.30	0.81	0.94	0.93	1.00
28	–	–	–	–	–	0.29	0.80	0.95	0.93	1.01
30	–	–	–	–	–	0.29	0.80	0.96	0.93	1.02
32	–	–	–	–	–	0.30	0.81	0.97	0.93	1.03
34	–	–	–	–	–	0.30	0.82	0.98	0.93	1.03
36	–	–	–	–	–	0.31	0.83	1.00	0.93	1.04
38	–	–	–	–	–	0.32	0.84	1.01	0.93	1.04
40	–	–	–	–	–	0.32	0.86	1.02	0.93	1.05
42	–	–	–	–	–	0.33	0.87	1.03	0.93	1.05
44	–	–	–	–	–	0.34	0.89	1.04	0.93	1.05
46	–	–	–	–	–	0.35	0.90	1.05	0.94	1.06
48	–	–	–	–	–	0.37	0.92	1.06	0.94	1.06
50	–	–	–	–	–	0.38	0.93	1.07	0.94	1.06
55	–	–	–	–	–	0.41	0.97	1.09	0.94	1.07
60	–	–	–	3.00	–	0.44	1.01	1.10	0.94	1.07
65	–	–	–	2.54	–	0.48	1.05	1.12	0.95	1.08
70	–	–	–	2.21	–	0.51	1.08	1.13	0.95	1.08
75	–	–	–	1.98	–	0.55	1.11	1.15	0.95	1.08
80	–	–	–	1.80	2.95	0.59	1.14	1.16	0.95	1.09
85	–	–	–	1.66	2.50	0.63	1.17	1.17	0.95	1.09
90	–	–	–	1.56	2.17	0.67	1.20	1.18	0.95	1.09
95	–	–	–	1.47	1.92	0.71	1.22	1.18	0.95	1.09
100	–	–	–	1.40	1.73	0.75	1.24	1.19	0.96	1.10
110	–	–	–	1.30	1.46	0.82	1.28	1.20	0.96	1.10
120	–	–	–	1.23	1.28	0.90	1.32	1.21	0.96	1.10
130	–	–	–	1.17	1.17	0.97	1.35	1.22	0.96	1.10
140	–	–	–	1.13	1.09	1.03	1.38	1.23	0.96	1.11
150	–	–	–	1.10	1.03	1.10	1.40	1.24	0.96	1.11
160	–	–	–	1.08	0.99	1.16	1.42	1.24	0.96	1.11
170	–	–	2.67	1.06	0.96	1.22	1.44	1.25	0.97	1.11
180	–	–	2.38	1.05	0.94	1.27	1.46	1.25	0.97	1.11
190	–	2.99	2.16	1.03	0.92	1.32	1.47	1.26	0.97	1.11

200	—	2.70	1.98	1.03	0.92	1.37	1.49	1.26	0.97	1.11
210	—	2.46	1.84	1.02	0.91	1.41	1.50	1.26	0.97	1.11
220	—	2.28	1.73	1.01	0.91	1.46	1.51	1.27	0.97	1.11
230	—	2.12	1.63	1.01	0.91	1.50	1.52	1.27	0.97	1.11
240	—	2.00	1.55	1.00	0.91	1.53	1.53	1.27	0.97	1.11
250	—	1.89	1.48	1.00	0.91	1.57	1.54	1.27	0.97	1.12
260	—	1.80	1.43	1.00	0.91	1.60	1.55	1.28	0.97	1.12
270	—	1.72	1.38	0.99	0.92	1.63	1.56	1.28	0.97	1.12
280	—	1.65	1.33	0.99	0.92	1.66	1.56	1.28	0.97	1.12
290	—	1.59	1.30	0.99	0.93	1.69	1.57	1.28	0.97	1.12
300	—	1.54	1.27	0.99	0.94	1.72	1.57	1.28	0.97	1.12
320	—	1.45	1.21	0.99	0.95	1.76	1.59	1.29	0.97	1.12
340	—	1.39	1.17	0.99	0.96	1.81	1.60	1.29	0.97	1.12
360	—	1.33	1.14	0.99	0.97	1.85	1.60	1.29	0.97	1.12
380	—	1.29	1.11	0.99	0.99	1.88	1.61	1.29	0.97	1.12
400	—	1.25	1.09	0.99	1.00	1.91	1.62	1.29	0.97	1.12
420	—	1.22	1.07	0.99	1.01	1.94	1.63	1.30	0.97	1.12
440	—	1.19	1.06	0.99	1.02	1.97	1.63	1.30	0.97	1.12
460	—	1.17	1.05	0.99	1.04	1.99	1.64	1.30	0.97	1.12
480	—	1.15	1.04	0.99	1.05	2.01	1.64	1.30	0.97	1.12
500	2.76	1.13	1.03	0.99	1.06	2.04	1.65	1.30	0.97	1.12
550	2.23	1.10	1.01	0.99	1.08	2.08	1.66	1.30	0.97	1.12
600	1.91	1.08	1.00	1.00	1.10	2.12	1.66	1.30	0.97	1.12
650	1.69	1.06	0.99	1.00	1.12	2.15	1.67	1.31	0.98	1.12
700	1.55	1.05	0.99	1.00	1.14	2.18	1.68	1.31	0.98	1.12
750	1.44	1.04	0.99	1.00	1.15	2.20	1.68	1.31	0.98	1.12
800	1.35	1.03	0.98	1.00	1.16	2.22	1.69	1.31	0.98	1.12
850	1.29	1.02	0.98	1.01	1.17	2.24	1.69	1.31	0.98	1.12
900	1.24	1.01	0.98	1.01	1.19	2.26	1.69	1.31	0.98	1.12
950	1.20	1.01	0.98	1.01	1.19	2.27	1.70	1.31	0.98	1.12
1000	1.17	1.01	0.98	1.01	1.20	2.28	1.70	1.31	0.98	1.12
1100	1.12	1.00	0.99	1.01	1.22	2.31	1.70	1.31	0.98	1.13
1200	1.08	1.00	0.99	1.01	1.23	2.33	1.71	1.32	0.98	1.13
1300	1.06	0.99	0.99	1.01	1.24	2.34	1.71	1.32	0.98	1.13
1400	1.04	0.99	0.99	1.02	1.25	2.35	1.71	1.32	0.98	1.13
1500	1.03	0.99	0.99	1.02	1.26	2.37	1.72	1.32	0.98	1.13
2000	0.99	0.99	1.00	1.02	1.28	2.41	1.72	1.32	0.98	1.13
3000	0.98	0.99	1.01	1.02	1.31	2.45	1.73	1.32	0.98	1.13
5000	0.99	0.99	1.02	1.03	1.33	2.48	1.74	1.32	0.98	1.13
7000	0.99	0.99	1.02	1.03	1.34	2.49	1.74	1.32	0.98	1.13
9000	0.99	0.99	1.02	1.03	1.35	2.50	1.74	1.32	0.98	1.13
10000	0.99	0.99	1.02	1.03	1.35	2.50	1.74	1.32	0.98	1.13
12000	1.00	0.99	1.02	1.03	1.35	2.50	1.74	1.32	0.98	1.13
14000	1.00	0.99	1.02	1.03	1.35	2.51	1.75	1.32	0.98	1.13
16000	1.00	0.99	1.02	1.03	1.35	2.51	1.75	1.32	0.98	1.13
18000	1.00	0.99	1.02	1.03	1.35	2.51	1.75	1.32	0.98	1.13
20000	1.00	0.99	1.03	1.03	1.35	2.51	1.75	1.32	0.98	1.13

Table B.0-5: Color correction factors for spectra of the form  $I_\nu \propto \nu^{1.5} B_\nu(T)$ 

T (K)	DIRBE band									
	1	2	3	4	5	6	7	8	9	10
10	–	–	–	–	–	–	–	1.20	1.31	0.94
12	–	–	–	–	–	1.19	1.82	1.04	1.12	0.94
14	–	–	–	–	–	0.68	1.31	0.96	1.03	0.95
16	–	–	–	–	–	0.48	1.07	0.93	0.98	0.96
18	–	–	–	–	–	0.39	0.94	0.92	0.96	0.98
20	–	–	–	–	–	0.34	0.87	0.92	0.94	0.99
22	–	–	–	–	–	0.31	0.83	0.93	0.93	1.00
24	–	–	–	–	–	0.30	0.81	0.94	0.93	1.02
26	–	–	–	–	–	0.29	0.80	0.95	0.92	1.03
28	–	–	–	–	–	0.29	0.80	0.96	0.92	1.04
30	–	–	–	–	–	0.29	0.81	0.98	0.92	1.05
32	–	–	–	–	–	0.30	0.82	0.99	0.93	1.05
34	–	–	–	–	–	0.30	0.83	1.01	0.93	1.06
36	–	–	–	–	–	0.31	0.84	1.02	0.93	1.07
38	–	–	–	–	–	0.32	0.86	1.03	0.93	1.07
40	–	–	–	–	–	0.33	0.88	1.05	0.93	1.08
42	–	–	–	–	–	0.34	0.90	1.06	0.94	1.08
44	–	–	–	–	–	0.35	0.91	1.07	0.94	1.09
46	–	–	–	–	–	0.36	0.93	1.08	0.94	1.09
48	–	–	–	–	–	0.38	0.95	1.09	0.94	1.09
50	–	–	–	–	–	0.39	0.97	1.10	0.94	1.10
55	–	–	–	–	–	0.42	1.02	1.13	0.95	1.10
60	–	–	–	2.93	–	0.46	1.06	1.15	0.95	1.11
65	–	–	–	2.48	–	0.50	1.11	1.17	0.95	1.12
70	–	–	–	2.17	–	0.54	1.15	1.18	0.96	1.12
75	–	–	–	1.94	–	0.59	1.18	1.20	0.96	1.12
80	–	–	–	1.77	2.65	0.63	1.22	1.21	0.96	1.13
85	–	–	–	1.63	2.25	0.67	1.25	1.22	0.96	1.13
90	–	–	–	1.53	1.96	0.72	1.28	1.23	0.97	1.13
95	–	–	–	1.45	1.74	0.76	1.31	1.24	0.97	1.13
100	–	–	–	1.38	1.58	0.81	1.34	1.25	0.97	1.14
110	–	–	–	1.28	1.34	0.90	1.39	1.26	0.97	1.14
120	–	–	–	1.21	1.19	0.98	1.43	1.28	0.97	1.14
130	–	–	–	1.16	1.09	1.06	1.46	1.29	0.98	1.15
140	–	–	–	1.12	1.03	1.14	1.49	1.29	0.98	1.15
150	–	–	–	1.09	0.98	1.22	1.52	1.30	0.98	1.15
160	–	–	2.91	1.07	0.95	1.29	1.55	1.31	0.98	1.15
170	–	–	2.55	1.05	0.93	1.35	1.57	1.31	0.98	1.15
180	–	–	2.28	1.04	0.91	1.42	1.59	1.32	0.98	1.15
190	–	2.89	2.07	1.03	0.90	1.48	1.61	1.32	0.98	1.16

200	—	2.62	1.91	1.02	0.90	1.53	1.62	1.33	0.98	1.16
210	—	2.39	1.77	1.01	0.90	1.59	1.64	1.33	0.98	1.16
220	—	2.21	1.66	1.01	0.90	1.63	1.65	1.34	0.98	1.16
230	—	2.07	1.57	1.00	0.90	1.68	1.67	1.34	0.98	1.16
240	—	1.94	1.50	1.00	0.91	1.72	1.68	1.34	0.99	1.16
250	—	1.84	1.44	1.00	0.91	1.77	1.69	1.34	0.99	1.16
260	—	1.75	1.38	0.99	0.92	1.80	1.70	1.35	0.99	1.16
270	—	1.68	1.34	0.99	0.93	1.84	1.71	1.35	0.99	1.16
280	—	1.61	1.30	0.99	0.94	1.87	1.72	1.35	0.99	1.16
290	—	1.56	1.26	0.99	0.94	1.91	1.72	1.35	0.99	1.16
300	—	1.51	1.23	0.99	0.95	1.94	1.73	1.36	0.99	1.16
320	—	1.42	1.18	0.99	0.97	1.99	1.74	1.36	0.99	1.16
340	—	1.36	1.14	0.99	0.99	2.04	1.76	1.36	0.99	1.16
360	—	1.31	1.11	0.99	1.01	2.09	1.77	1.36	0.99	1.16
380	—	1.26	1.09	0.99	1.02	2.13	1.78	1.37	0.99	1.17
400	—	1.23	1.07	0.99	1.04	2.17	1.78	1.37	0.99	1.17
420	—	1.20	1.05	0.99	1.05	2.20	1.79	1.37	0.99	1.17
440	—	1.17	1.04	0.99	1.07	2.23	1.80	1.37	0.99	1.17
460	—	1.15	1.03	0.99	1.08	2.26	1.80	1.37	0.99	1.17
480	2.88	1.13	1.02	0.99	1.10	2.29	1.81	1.37	0.99	1.17
500	2.60	1.12	1.01	0.99	1.11	2.31	1.82	1.38	0.99	1.17
550	2.12	1.09	1.00	1.00	1.14	2.37	1.83	1.38	0.99	1.17
600	1.82	1.07	0.99	1.00	1.16	2.41	1.84	1.38	0.99	1.17
650	1.63	1.05	0.99	1.00	1.19	2.45	1.84	1.38	0.99	1.17
700	1.49	1.04	0.98	1.00	1.21	2.48	1.85	1.38	0.99	1.17
750	1.39	1.03	0.98	1.01	1.22	2.51	1.86	1.39	0.99	1.17
800	1.31	1.02	0.98	1.01	1.24	2.53	1.86	1.39	0.99	1.17
850	1.25	1.01	0.98	1.01	1.25	2.55	1.87	1.39	0.99	1.17
900	1.21	1.01	0.98	1.01	1.26	2.57	1.87	1.39	0.99	1.17
950	1.17	1.00	0.98	1.01	1.28	2.59	1.87	1.39	0.99	1.17
1000	1.14	1.00	0.98	1.01	1.29	2.61	1.88	1.39	0.99	1.17
1100	1.10	1.00	0.99	1.02	1.30	2.63	1.88	1.39	0.99	1.17
1200	1.06	0.99	0.99	1.02	1.32	2.65	1.89	1.39	0.99	1.17
1300	1.04	0.99	0.99	1.02	1.33	2.67	1.89	1.39	0.99	1.17
1400	1.03	0.99	1.00	1.02	1.34	2.69	1.90	1.39	0.99	1.17
1500	1.01	0.99	1.00	1.02	1.35	2.70	1.90	1.40	1.00	1.17
2000	0.99	0.99	1.01	1.03	1.38	2.75	1.91	1.40	1.00	1.17
3000	0.98	0.99	1.02	1.03	1.42	2.80	1.92	1.40	1.00	1.17
5000	0.99	0.99	1.03	1.03	1.44	2.83	1.93	1.40	1.00	1.17
7000	0.99	0.99	1.03	1.03	1.45	2.85	1.93	1.40	1.00	1.17
9000	1.00	0.99	1.03	1.04	1.46	2.86	1.93	1.40	1.00	1.17
10000	1.00	0.99	1.03	1.04	1.46	2.86	1.93	1.40	1.00	1.17
12000	1.00	0.99	1.03	1.04	1.46	2.87	1.93	1.40	1.00	1.17
14000	1.00	0.99	1.03	1.04	1.46	2.87	1.93	1.40	1.00	1.17
16000	1.00	0.99	1.04	1.04	1.47	2.87	1.93	1.40	1.00	1.17
18000	1.00	0.99	1.04	1.04	1.47	2.87	1.93	1.40	1.00	1.17
20000	1.01	0.99	1.04	1.04	1.47	2.87	1.94	1.40	1.00	1.17

Table B.0-6: Color correction factors for spectra of the form  $I_\nu \propto \nu^2 B_\nu(T)$ 

T (K)	<i>DIRBE</i> band									
	1	2	3	4	5	6	7	8	9	10
10	–	–	–	–	–	2.90	2.88	1.15	1.24	0.93
12	–	–	–	–	–	1.14	1.70	1.01	1.07	0.94
14	–	–	–	–	–	0.65	1.24	0.95	1.00	0.96
16	–	–	–	–	–	0.46	1.02	0.92	0.96	0.97
18	–	–	–	–	–	0.38	0.91	0.92	0.94	0.99
20	–	–	–	–	–	0.33	0.84	0.92	0.93	1.01
22	–	–	–	–	–	0.31	0.81	0.93	0.92	1.03
24	–	–	–	–	–	0.30	0.80	0.95	0.92	1.04
26	–	–	–	–	–	0.29	0.80	0.96	0.92	1.06
28	–	–	–	–	–	0.29	0.80	0.98	0.92	1.07
30	–	–	–	–	–	0.30	0.81	1.00	0.92	1.08
32	–	–	–	–	–	0.30	0.83	1.02	0.93	1.09
34	–	–	–	–	–	0.31	0.84	1.03	0.93	1.10
36	–	–	–	–	–	0.32	0.86	1.05	0.93	1.10
38	–	–	–	–	–	0.33	0.88	1.07	0.94	1.11
40	–	–	–	–	–	0.34	0.90	1.08	0.94	1.12
42	–	–	–	–	–	0.35	0.93	1.10	0.94	1.12
44	–	–	–	–	–	0.36	0.95	1.11	0.94	1.13
46	–	–	–	–	–	0.37	0.97	1.12	0.95	1.13
48	–	–	–	–	–	0.39	1.00	1.14	0.95	1.14
50	–	–	–	–	–	0.40	1.02	1.15	0.95	1.14
55	–	–	–	–	–	0.44	1.07	1.18	0.96	1.15
60	–	–	–	2.86	–	0.48	1.13	1.20	0.96	1.16
65	–	–	–	2.43	–	0.53	1.18	1.22	0.97	1.16
70	–	–	–	2.12	–	0.58	1.22	1.24	0.97	1.17
75	–	–	–	1.90	2.87	0.63	1.27	1.26	0.97	1.17
80	–	–	–	1.73	2.38	0.68	1.31	1.27	0.98	1.17
85	–	–	–	1.61	2.03	0.73	1.35	1.28	0.98	1.18
90	–	–	–	1.51	1.78	0.78	1.38	1.30	0.98	1.18
95	–	–	–	1.43	1.59	0.83	1.42	1.31	0.98	1.18
100	–	–	–	1.36	1.44	0.88	1.45	1.32	0.99	1.19
110	–	–	–	1.26	1.24	0.98	1.51	1.33	0.99	1.19
120	–	–	–	1.20	1.11	1.08	1.55	1.35	0.99	1.19
130	–	–	–	1.15	1.03	1.18	1.60	1.36	0.99	1.20
140	–	–	–	1.11	0.97	1.27	1.63	1.37	1.00	1.20
150	–	–	–	1.08	0.94	1.35	1.67	1.38	1.00	1.20
160	–	–	2.78	1.06	0.91	1.44	1.70	1.39	1.00	1.20
170	–	–	2.44	1.04	0.90	1.51	1.72	1.39	1.00	1.20
180	–	–	2.19	1.03	0.89	1.59	1.75	1.40	1.00	1.21
190	–	2.81	1.99	1.02	0.89	1.66	1.77	1.40	1.00	1.21

200	—	2.54	1.83	1.01	0.89	1.72	1.79	1.41	1.00	1.21
210	—	2.33	1.71	1.01	0.89	1.78	1.81	1.41	1.00	1.21
220	—	2.15	1.60	1.00	0.90	1.84	1.82	1.42	1.01	1.21
230	—	2.01	1.52	1.00	0.91	1.90	1.84	1.42	1.01	1.21
240	—	1.89	1.45	1.00	0.92	1.95	1.85	1.42	1.01	1.21
250	—	1.79	1.39	0.99	0.93	1.99	1.86	1.43	1.01	1.21
260	—	1.71	1.34	0.99	0.94	2.04	1.88	1.43	1.01	1.21
270	—	1.64	1.30	0.99	0.95	2.08	1.89	1.43	1.01	1.21
280	—	1.58	1.26	0.99	0.96	2.12	1.90	1.44	1.01	1.22
290	—	1.52	1.23	0.99	0.97	2.16	1.91	1.44	1.01	1.22
300	—	1.47	1.20	0.99	0.98	2.20	1.92	1.44	1.01	1.22
320	—	1.39	1.15	0.99	1.00	2.26	1.93	1.44	1.01	1.22
340	—	1.33	1.12	0.99	1.03	2.32	1.94	1.45	1.01	1.22
360	—	1.28	1.09	0.99	1.05	2.38	1.96	1.45	1.01	1.22
380	—	1.24	1.07	0.99	1.07	2.42	1.97	1.45	1.01	1.22
400	—	1.21	1.05	0.99	1.09	2.47	1.98	1.45	1.01	1.22
420	—	1.18	1.04	0.99	1.11	2.51	1.99	1.46	1.01	1.22
440	—	1.16	1.03	0.99	1.13	2.55	2.00	1.46	1.01	1.22
460	—	1.14	1.02	0.99	1.14	2.58	2.00	1.46	1.01	1.22
480	2.71	1.12	1.01	0.99	1.16	2.61	2.01	1.46	1.01	1.22
500	2.45	1.10	1.00	1.00	1.17	2.64	2.02	1.46	1.01	1.22
550	2.02	1.08	0.99	1.00	1.21	2.70	2.03	1.47	1.01	1.22
600	1.75	1.05	0.99	1.00	1.24	2.75	2.04	1.47	1.01	1.22
650	1.57	1.04	0.98	1.00	1.27	2.80	2.05	1.47	1.02	1.22
700	1.44	1.03	0.98	1.01	1.29	2.84	2.06	1.47	1.02	1.22
750	1.34	1.02	0.98	1.01	1.31	2.87	2.07	1.47	1.02	1.22
800	1.27	1.01	0.98	1.01	1.33	2.90	2.07	1.48	1.02	1.22
850	1.22	1.01	0.98	1.01	1.35	2.92	2.08	1.48	1.02	1.23
900	1.18	1.00	0.98	1.01	1.36	2.95	2.08	1.48	1.02	1.23
950	1.14	1.00	0.99	1.02	1.38	2.97	2.09	1.48	1.02	1.23
1000	1.12	1.00	0.99	1.02	1.39	2.99	2.09	1.48	1.02	1.23
1100	1.08	0.99	0.99	1.02	1.41	3.02	2.10	1.48	1.02	1.23
1200	1.05	0.99	0.99	1.02	1.43	3.04	2.10	1.48	1.02	1.23
1300	1.03	0.99	1.00	1.02	1.44	3.06	2.11	1.48	1.02	1.23
1400	1.01	0.99	1.00	1.03	1.45	3.08	2.11	1.49	1.02	1.23
1500	1.00	0.99	1.00	1.03	1.46	3.10	2.12	1.49	1.02	1.23
2000	0.98	0.99	1.02	1.03	1.50	3.15	2.13	1.49	1.02	1.23
3000	0.98	0.99	1.03	1.04	1.54	3.21	2.14	1.49	1.02	1.23
5000	0.99	0.99	1.04	1.04	1.57	3.25	2.15	1.49	1.02	1.23
7000	1.00	0.99	1.04	1.04	1.58	3.27	2.15	1.50	1.02	1.23
9000	1.00	0.99	1.04	1.04	1.59	3.28	2.16	1.50	1.02	1.23
10000	1.01	0.99	1.04	1.04	1.59	3.29	2.16	1.50	1.02	1.23
12000	1.01	0.99	1.05	1.04	1.60	3.29	2.16	1.50	1.02	1.23
14000	1.01	0.99	1.05	1.04	1.60	3.29	2.16	1.50	1.02	1.23
16000	1.01	0.99	1.05	1.04	1.60	3.30	2.16	1.50	1.02	1.23
18000	1.01	0.99	1.05	1.04	1.60	3.30	2.16	1.50	1.02	1.23
20000	1.01	0.99	1.05	1.04	1.60	3.30	2.16	1.50	1.02	1.23





## Appendix C

# *DIRBE* Cold Mission Events Log

Table C.0-1 is a log of events that affected the *DIRBE* from *COBE* launch through exhaustion of the cryogen.

Table C.0-1: Abridged on-orbit events log

Date	Time <sup>a</sup> (yy:ddd:hh:mm:ss)	Event
1989 November 18	89:322:14:34:04	<i>COBE</i> launch
November 19	89:323:14:11	<i>DIRBE</i> Power-on and configure
November 21	89:325:11:18	Dewar cover ejection (roll 4°)
November 21	89:325:14:30	Begin science telemetry format
November 22	89:326:05:32	ACS Gyro B failure
November 22	89:326:07:22	ACS Gyro B cross-strapped out
November 23	89:327:11:18–11:36	New ACS control mode; pitch-back 5–7°
November 23	89:327:14:10–17:55	<i>DIRBE</i> preliminary optimization
November 24	89:328:00:00	Initiate <i>DIRBE</i> nominal operations
November 25	89:329:14:10	Spin Rate 0.4 rpm
November 26	89:330:14:24	Spin Rate 0.6 rpm
November 26	89:330:20:12–20:15	Band 8 heater real-time test
November 27	89:331:11:29	Spin Rate 0.8 rpm
November 27	89:331:12:54–23:52	<i>DIRBE</i> onboard deglitcher on
November 28	89:332:21:00	Start of <i>DIRBE</i> optimization tests
November 29	89:333:06:06	End of <i>DIRBE</i> optimization tests
November 29	89:333:08:48	Interlocked-IRS linearity test (DIR567, TA086 equivalent)
November 29	89:333:10:42	IRS vs. sky linearity test
November 30	89:334:21:00–23:59	<i>FIRAS</i> MTM hits in Van Allen Belts (VABs)
December 1	89:335	<i>FIRAS</i> MTM hits in VABs all day
December 1	89:335:04:33:40	Analog gain calibration test
December 2	89:336:00:00	Band 8 overbias level raised to 168 DN
December 3	89:337:17:16	First Moon crossing predicted
December 9	89:343:00:00	Start commanding <i>FIRAS</i> MTM to position mode during SAA crossings
December 10	89:344:23:03–23:32	<i>DIRBE</i> shutter left closed (loss of lock during real-time IRS cal)
December 11	89:345:00:00–23:59	100 s duration IRS boost and band 8 overbias during anneal (one day only)
December 11	89:345:01:04	New <i>DIRBE</i> operating parameters loaded and start of new IRS calibration runs
December 12	89:346	First off-nominal pointing test (roll to 2 and 8°)
December 13	89:347:17:48	Momentum wheel speed reduced by 0.5%
December 17	89:351:00:00	Resume 100 s duration of IRS boost and band 8 overbias during annealing
December 17	89:351:22:51	Start of second off-nominal pointing test (roll to 8°)
December 18	89:352	First command triggering with new SAA contours
December 18	89:352:00:00–17:46	Second off-nominal pointing test (roll to 8 and 2°)
December 19	89:353	IRS boost at 3200 DN during anneal
December 19	89:353:11:30	Roll to 8° for <i>FIRAS</i> XCAL motion
December 19	89:353:11:48	<i>FIRAS</i> XCAL moved into horn (at roll 8°)
December 20	89:354	No band 8 overbiasing during anneal
December 20	89:354:09:55–11:20	Periodic IRS runs after hard SAA
December 21	89:355	Resume nominal annealing recipe (IRS boost 2800 DN, band 8 overbiasing 168 DN)
December 21	89:355:15:47	<i>FIRAS</i> XCAL removed from horn (at roll 8°)
December 27	89:361:06:16:28	Analog gain calibration test
December 27	89:361:14:40	Re-run differential linearity test
December 27	89:361:22:42	Re-run IRS vs. sky linearity test

1989	December 28	89:362:03:27	Re-run detector optimization with nominal biases and heaters
	December 29	89:363:03:22	Band 7 bias changed to .2V (67 DN) by real-time command
	December 30	89:364:01:56:20	Band 7 bias reset to .24V (81 DN)
1990	January 1	90:001:00:00	Install final annealing recipe: IRS boost for 100 s, no band 8 overbiasing
	January 10	90:010:17:16	<i>FIRAS</i> MTM hit at SAA entrance (see §3.5.3.1)
	January 12	90:012:22:19	<i>FIRAS</i> MTM hit at SAA entrance (see §3.5.3.1)
	January 13	90:013:18:57	<i>FIRAS</i> MTM hit at SAA entrance (see §3.5.3.1)
	January 14	90:014:22:18	<i>FIRAS</i> MTM hit at SAA entrance (see §3.5.3.1)
	January 15	90:015:22:18	<i>FIRAS</i> MTM hit at SAA entrance (see §3.5.3.1)
	January 16	90:016:20:14–21:43	Backup X-axis gyro used by ACS
	January 17	90:017:15:31–16:03	Test of ACS eclipse mode (engineering telemetry format)
	January 17	90:017:17:50	Momentum wheel speed increased by 0.5%
	January 18	90:018:14:15–16:09	Start of <i>FIRAS</i> calibration; roll 8° for XCAL insertion
	January 20	90:020:01:41–02:41	End of <i>FIRAS</i> calibration; roll 8° for XCAL stow
	January 22	90:018:34–18:50	Test of ACS eclipse mode (engineering telemetry format)
	January 24	90:024:~17:00	Test of ACS eclipse mode (engineering telemetry format)
	January 25	90:025:00:01:32	Analog gain calibration test
	January 26	90:026:18:27–18:45	Solar eclipse by the Moon; roll excursion to 3°5
	January 26	90:026:20:26–20:44	Solar eclipse by the Moon; roll excursion to 11°
	February 15	90:046	Jupiter enters <i>DIRBE</i> swath
	February 16	90:047:14:00	Start of <i>FIRAS</i> calibration; roll 8° for XCAL insertion
	February 18	90:049:01:42	End of <i>FIRAS</i> calibration; roll 8° for XCAL stow
	February 26	90:055:07:40:12	Analog gain calibration test
	March 4	90:063	Uranus enters <i>DIRBE</i> swath
	March 6	90:065:15:37–15:57	Real-time command procedure test
	March 7	90:066:15:37–15:57	Real-time command procedure test
	March 9	90:068	Neptune enters <i>DIRBE</i> swath
	March 15	90:074:22:08–22:22	<i>FIRAS</i> XCAL test
	March 16	90:075:14:38–14:58	<i>FIRAS</i> MTM Relay Test
	March 16	90:075:16:45–17:05	<i>FIRAS</i> MTM Relay Test
	March 18	90:077:09:41	Start of <i>FIRAS</i> calibration; roll 8° for XCAL insertion
	March 19	90:078	Saturn enters <i>DIRBE</i> swath
	March 20	90:079:16:44	End of <i>FIRAS</i> calibration: roll 8° for XCAL stow
	March 21	90:080	<i>FIRAS</i> initiates MTM power-off at every SAA entrance as normal operation
	March 26	90:085:14:00–22:00	Roll test at 1.5°
	March 27	90:086:14:00–20:38	Roll test at 1.0°
	March 28	90:087:08:59:40	Analog gain calibration test
	March 28	90:087:14:55–15:15	<i>FIRAS</i> MTM relay test
	March 28	90:087:16:30–16:50	<i>FIRAS</i> MTM relay test
	April 17	90:107	Start of <i>FIRAS</i> calibration; roll 8° for XCAL insertion
	April 20	90:110	Last <i>DIRBE</i> observations of Jupiter at 4.5° roll
	April 20	90:110	End of <i>FIRAS</i> calibration; roll 8° for XCAL stow
	April 20	90:110:20:28	Spacecraft roll commanded to 1.°75; actual roll 2°

1990	April 24	90:114	Last <i>DIRBE</i> observations of Jupiter at 2° roll
	April 28	90:118	Mars enters <i>DIRBE</i> swath
	April 30	90:120:13:56	Start of JFET-off test; bands 1 – 6 (1.25 – 25 μm) commanded off
	May 1	90:121:01:05	JFET-off test; 60 μm band (7) commanded off
	May 2	90:122:00:58	JFET-off test; 100 μm band (8) commanded off
	May 4	90:124	Uranus exits <i>DIRBE</i> swath
	May 5	90:125:08:20:43	Analog gain calibration test
	May 6	90:126:01:17–12:30	End of JFET-off test; all bands commanded on
	May 7	90:127	Earth limb over sunshade at 2° roll
	May 10	90:130	Neptune exits <i>DIRBE</i> swath
	May 12–14	90:132–134	<i>DIRBE</i> observes Comet Austin
	May 15	90:135:08:30	Spacecraft roll angle commanded to 4° (Sun angle 94° )
	May 15	90:135:08:40	Start of <i>FIRAS</i> calibration; roll 8° for XCAL insertion
	May 17	90:137	Start of eclipse season; first penumbra
	May 17	90:137:02:27:48	Shutter-closed CBM mode IRS cal (standard prime source cal)
	May 17	90:137:10:15:08	Start of eclipse season; first loss of Sun presence
	May 18	90:138:21:26	End of <i>FIRAS</i> calibration; roll 8° for XCAL stow
	May 19	90:139:~00:00	Spacecraft roll angle commanded to 3° (Sun angle 93° )
	May 21	90:141	Saturn exits <i>DIRBE</i> swath
	May 24–25	90:144–145	<i>DIRBE</i> observes Comet Austin
	May 29	90:149:~17:00	Spacecraft roll angle commanded to 2° (Sun angle 92° )
	June 9	90:160:00:00	Start of roll toggling at Earth limb; roll to 1° during limb passages
	June 11	90:162:13:28–15:12	One orbit of engineering mode telemetry for dewar and ACS analysis
	June 29	90:180	<i>DIRBE</i> operations includes 2-source CAL at each NVAB exit
	June 29	90:180:13:42	Start of <i>FIRAS</i> calibration; roll 8° for XCAL insertion
	June 30	90:181:13:38	End of <i>FIRAS</i> calibration; roll 8° for XCAL stow
	July 2	90:183:20:16:34	ACS pitch-back angle changed from 6° to 3°
	July 7	90:188	Primary and backup IRS sources interchanged (from this day on)
	July 9	90:190:01:48–02:11	Eclipse-mode voltage/current test
	July 10	90:191	First day of band 1B test; power-off 2 minutes every orbit
	July 11	90:192	Second day of band 1B test; power-off 2 minutes every orbit
	July 12	90:193	Third day of band 1B test; power-off 2 minutes every orbit
	July 12	90:193:~18:00	<i>FIRAS</i> Sky Horn temperature reduced from 6 to 4° K
	July 13	90:194	Fourth day of band 1B test; toggle power on/off every other orbit
	July 14	90:195	Spacecraft roll angle changed to 2.25, 1.25 during earth limb
	July 14	90:195	Fifth day of band 1B test; toggle power on/off every other orbit
	July 15	90:196	Sixth day of band 1B test; power-off 2 orbits per day
	July 16	90:197	Last day of band 1B test; power-off 2 orbits per day
	July 22	90:203:02:00–04:04	Eclipse of Sun by Moon; roll angle changed to 6°
	July 23	90:204:03:20–04:00	Interlocked IRS linearity test (DIR567, TA086 equivalent)
	July 25	90:206:01:32	Last ACS eclipse mode event
	July 26	90:207:11:00	Start of <i>FIRAS</i> Sky Horn Test
	July 27	90:208:06:00	End of <i>FIRAS</i> Sky Horn Test

1990	August 2	90:214:14:34	Start of <i>FIRAS</i> calibration; roll 8° for XCAL insertion
	August 8	90:220:05:10	End of <i>FIRAS</i> calibration; roll 8° for XCAL stow
	August 9	90:221:00:00	Start of <i>FIRAS</i> XCAL temp controller test
	August 10	90:222:17:12	End of <i>FIRAS</i> XCAL temp controller test
	August 11	90:223:03:20	IRS <i>vs.</i> sky linearity test (DIR668; fixed IRS with slow shutter flutter)
	August 12	90:224:16:08	IRS <i>vs.</i> sky linearity test (DIR667; IRS ramps with shutter flutter)
	August 13	90:225, once/3 orbits	Absolute differential linearity test (DIR669; IRS A and B fixed levels)
	August 14	90:226, once/3 orbits	Absolute differential linearity test (DIR669; IRS A and B fixed levels)
	August 15	90:227:12:43	JFET-off test; bands 1 through 6 powered off
	August 15	90:227:13:52	Start of first <i>FIRAS</i> MiniCAL
	August 16	90:228:01:33	JFET-off test; 60 $\mu\text{m}$ band (7) powered off
	August 17	90:229:01:29	JFET-off test; 100 $\mu\text{m}$ band (8) powered off
	August 21	90:233:01:40–11:11	End of JFET-off test; all channels powered on
	August 25	90:237	Uranus enters <i>DIRBE</i> swath
	August 29	90:241:21:58	Band 1B powered off in real-time (after start of Moon passage)
	August 30	90:242	Temporary IRS cal RTSs used (to reload standard RTSs)
	August 31	90:243	Standard IRS cal RTSs reloaded
	August 31	90:243	Neptune enters <i>DIRBE</i> swath
	September 1	90:244:21:49	Band 1B powered on in real-time (after end of Moon passage)
	September 1	90:244:22:00–23:05	Engineering telemetry format (dewar and ACS analysis)
	September 5	90:248, once/3 orbits	Absolute differential linearity test (DIR670; IRS A and B fixed levels)
	September 6	90:249, once/3 orbits	Absolute differential linearity test (DIR670; IRS A and B fixed levels)
	September 7	90:250, 3 times	Absolute differential linearity test (DIR669; IRS A and B fixed levels)
	September 7	90:250	Saturn enters <i>DIRBE</i> swath
	September 7	90:250:15:42	Start of <i>FIRAS</i> calibration; roll to 8° for XCAL insertion
	September 10	90:253:00:32	Band 1B powered off by real-time command after start of Moon passage
	September 10	90:253:22:39	End of <i>FIRAS</i> calibration; roll to 8° for XCAL stow
	September 15	90:258:07:45	Band 1B powered on by real-time command after end of Moon passage
	September 21	90:264:09:37	Dewar helium depleted
	September 21	90:264:09:51	Dewar over-temperature circuit tripped; <i>FIRAS</i> power disconnected

<sup>a</sup> Greenwich Mean Time (GMT).



# Appendix D

## Data Retrieval

### D.1 Reading the FITS Data

This Appendix lists sample headers for each of the *DIRBE* data products provided in FITS format and gives examples of Interactive Data Language (IDL) and FORTRAN programs that can be used to read the files.

A *COBE* analysis software package, coded primarily in IDL, and the *COBE Guest Investigator Software User's Guide* may be obtained via the *COBE* Home Page at [http://www.gsfc.nasa.gov/astro/cobe/cobe\\_home.html](http://www.gsfc.nasa.gov/astro/cobe/cobe_home.html) (click on “*COBE* analysis software” in the General Information section). The package contains data I/O, analysis, and display tools designed specifically to work with the *COBE* data products and is described in detail in the *User's Guide*.

Other software packages capable of reading FITS binary tables are publicly available. The *FITSIO* FORTRAN subroutines developed for this purpose by W. Pence *et al.* at the NASA/GSFC HEASARC are available from <http://heasarc.gsfc.nasa.gov/docs/software/fitsio/fitsio.html>. The *IDL Astronomy User's Library* developed by W. Landsman *et al.* of the NASA/GSFC UIT team has FITS I/O (and many other) capabilities and is available from <http://idlastro.gsfc.nasa.gov/homepage.html>.

#### D.1.1 FITS Headers for the *DIRBE* Data Products

##### D.1.1.1 Calibrated Individual Observations

Table D.1-1: Sample FITS headers for the Calibrated Individual Observations Pixel Index files

```
SIMPLE =                T / file does conform to FITS standard
BITPIX =                32 / number of bits per data pixel
NAXIS  =                0 / number of data axes
EXTEND =                T / FITS dataset may contain extensions
COMMENT  FITS (Flexible Image Transport System) format defined in Astronomy and
COMMENT  Astrophysics Supplement Series v44/p363, v44/p371, v73/p359, v73/p365.
COMMENT  Contact the NASA Science Office of Standards and Technology for the
COMMENT  FITS Definition document #100 and other FITS information.
DATE    = '11/04/97'    / FITS file creation date (dd/mm/yy)
DATE-MAP= '11/07/95'    / Date of original file creation (dd/mm/yy)
ORIGIN  = 'CDAC'       / Cosmology Data Analysis Center
TELESCOP= 'COBE'      / Cosmic Background Explorer satellite
INSTRUME= 'DIRBE'     / COBE instrument [DIRBE, DMR, FIRAS]
OBJECT  = 'DAILY-SKY' / part of sky given [e.g., ALL-SKY, WEEKLY-SKY,
COMMENT  /           DAILY-SKY, GAL-SLICE, FACE ...]
```



```

EQUINOX =                2000.0 / equinox of coords in following tables
REFERENC= 'COBE/DIRBE Explanatory Supplement,' /
REFERENC= 'ed. M.G. Hauser, T. Kelsall, D. Leisawitz, and J. Weiland,' /
REFERENC= 'COBE Ref. Pub. No. 97-A (Greenbelt,MD: NASA/GSFC),' /
REFERENC= 'available in electronic form from the NSSDC.' /
COMMENT
COMMENT      COBE specific keywords
DATE-BEG= '11/12/89'      / date of initial data represented (dd/mm/yy)
DATE-END= '11/12/89'      / date of final data represented (dd/mm/yy)
PIXRESOL=                9 / Quad tree pixel resolution [6, 9]
COMMENT
COMMENT      DIRBE specific keywords
PRODUCT = 'CIOINDEX_89345' / Pixel Index to DIRBE CIO, YYDDD=89345
VERSION = 'Pass 3B '      / Version of Data Reduction Software
COMMENT
COMMENT
END

XTENSION= 'BINTABLE'      / Extension type is Binary Table
BITPIX   =                8 / Binary data
NAXIS    =                2 / Data are in a table
NAXIS1   =                8 / Number of 8 bit bytes in each row
NAXIS2   =                171862 / Number of rows
PCOUNT   =                0 / Number of bytes of data following table
GCOUNT   =                1 / Group count (always 1 for bintable extensions)
TFIELDS  =                2 / Number of fields (columns) in the table
COMMENT
COMMENT
COMMENT -----
COMMENT *****
COMMENT      DIRBE Calibrated Individual Observations: Pixel Index
COMMENT      ----- Cryogenic Mission, day 345 of 1989 -----
COMMENT
COMMENT      This is the companion pixel index to the DIRBE Calibrated
COMMENT      Individual Observations (CIO) data file for day 345 of 1989.
COMMENT      The pixel index is intended to simplify and expedite data
COMMENT      retrieval for a user-selected subset of pixels in the CIO.
COMMENT      There is one row in the index table for each DIRBE pixel
COMMENT      (resolution 9) observed on this day. Pixels are listed in
COMMENT      ascending order. For each pixel, the pixel index table
COMMENT      identifies the LAST row number within the corresponding
COMMENT      CIO table which contains observations for that pixel.
COMMENT      *****
COMMENT      -----
COMMENT      =====
COMMENT      Coordinate Information (Spatial):
COMMENT      =====
COMMENT      -----
COMMENT      DIRBE Pixel number (resolution 9)
TTYPE1  = 'Pixel_no'      / pipeline fieldname = Pixel_no
TUNIT1  = ' '             /
TFORM1  = '1J '          /
COMMENT -----
COMMENT =====

```

```

COMMENT   Pixel Indexing Information:
COMMENT   =====
COMMENT   -----
COMMENT           Number of the last row within the corresponding CIO
COMMENT           binary table which contains information for this pixel number.
COMMENT           Row numbers are counted starting at 1.
COMMENT
TTYPE2   = 'LastRow '           / pipeline fieldname = last_data_record
TUNIT2   = '           '       /
TFORM2   = '1J           '     /
COMMENT   -----
END

```

Table D.1-2: Sample FITS headers for the Calibrated Individual Observations data files

```

SIMPLE   =                               T / file does conform to FITS standard
BITPIX   =                               32 / number of bits per data pixel
NAXIS    =                               0 / number of data axes
EXTEND   =                               T / FITS dataset may contain extensions
COMMENT  FITS (Flexible Image Transport System) format defined in Astronomy and
COMMENT  Astrophysics Supplement Series v44/p363, v44/p371, v73/p359, v73/p365.
COMMENT  Contact the NASA Science Office of Standards and Technology for the
COMMENT  FITS Definition document #100 and other FITS information.
DATE     = '11/04/97'                   / FITS file creation date (dd/mm/yy)
DATE-MAP= '11/07/95'                   / Date of original file creation (dd/mm/yy)
ORIGIN   = 'CDAC           '           / Cosmology Data Analysis Center
TELESCOP= 'COBE           '           / Cosmic Background Explorer satellite
INSTRUME= 'DIRBE          '           / COBE instrument [DIRBE, DMR, FIRAS]
OBJECT   = 'DAILY-SKY'                 / part of sky given [e.g., ALL-SKY, WEEKLY-SKY,
COMMENT                                     /           DAILY-SKY, GAL-SLICE, FACE ...]
EQUINOX  =                               2000.0 / equinox of coords in following tables
REFERENC= 'COBE/DIRBE Explanatory Supplement,' /
REFERENC= 'ed. M.G. Hauser, T. Kelsall, D. Leisawitz, and J. Weiland,' /
REFERENC= 'COBE Ref. Pub. No. 97-A (Greenbelt,MD: NASA/GSFC),' /
REFERENC= 'available in electronic form from the NSSDC.' /
COMMENT
COMMENT           COBE specific keywords
DATE-BEG= '11/12/89'                   / date of initial data represented (dd/mm/yy)
DATE-END= '11/12/89'                   / date of final data represented (dd/mm/yy)
PIXRESOL=                               9 / Quad tree pixel resolution [6, 9]
COMMENT
COMMENT           DIRBE specific keywords
PRODUCT  = 'CIO_89345'                 / Calibrated Individual Obs. for YYYYY = 89345
VERSION  = 'Pass 3B '                 / Version of Data Reduction Software
WAVE1    = '1.25 microns'              / nominal wavelength of Band 1
WAVE2    = '2.2 microns'               / nominal wavelength of Band 2
WAVE3    = '3.5 microns'               / nominal wavelength of Band 3
WAVE4    = '4.9 microns'               / nominal wavelength of Band 4
WAVE5    = '12. microns'               / nominal wavelength of Band 5
WAVE6    = '25. microns'              / nominal wavelength of Band 6
WAVE7    = '60. microns'               / nominal wavelength of Band 7

```

```

WAVE8   = '100. microns'      / nominal wavelength of Band 8
WAVE9   = '140. microns'      / nominal wavelength of Band 9
WAVE10  = '240. microns'      / nominal wavelength of Band 10
SOLELONG= 'ALL      '        / all available solar elongations included
APPVEC  = 'SEPARATE'         / data having different approach vectors
COMMENT                                / are not combined during processing
ZLREMOV =                    F / zodiacal foreground removal indicator
COMMENT                                / if 'T(true)', zodi foreground has been removed
COMMENT                                / if 'F(false)', observed sky brightness is given
COMMENT
COMMENT
END

```

```

XTENSION= 'BINTABLE'         / Extension type is Binary Table
BITPIX  =                    8 / Binary data
NAXIS   =                    2 / Data are in a table
NAXIS1  =                   109 / Number of 8 bit bytes in each row
NAXIS2  =                  474064 / Number of rows
PCOUNT  =                    0 / Number of bytes of data following table
GCOUNT  =                    1 / Group count (always 1 for bintable extensions)
TFIELDS =                   33 / Number of fields (columns) in the table
COMMENT
COMMENT
TIMVERSN= 'OGIP/93-003'      / GSFC Office of Guest Investigator Programs
COMMENT                                / (OGIP) memo in which the convention is
COMMENT                                / described
COMMENT                                The times reported in this file are International
COMMENT                                Atomic Time (TAI) seconds elapsed since
COMMENT                                00:00:00 UTC, 1 January 1981. Time information is
COMMENT                                recorded in a manner consistent with the convention specified
COMMENT                                in OGIP/93-003 with the understanding that time is counted
COMMENT                                in atomic seconds and the origin of time (MJDREF) is quoted
COMMENT                                in ephemeris MJD.
TIMESYS = '1981.00 '        / time system (same as IRAS)
MJDREFI =                   44605 / Integer portion of ephemeris MJD
COMMENT                                / corresponding to 0h UTC 1 Jan 1981
MJDREFF =                   0.00059240741 / Fractional portion of ephemeris MJD
COMMENT                                / corresponding to 0h UTC 1 Jan 1981
TIMEUNIT= 's                ' / unit for TSTART, TSTOP, TIMEZERO = seconds
TSTART  =                   282182405.000 / observation start time in TIMESYS system
TSTOP   =                   282268804.999 / observation stop time in TIMESYS system
COMMENT
COMMENT
COMMENT -----
COMMENT *****
COMMENT ---- DIRBE Calibrated Individual Observations ----
COMMENT ----- Cryogenic Mission, day 345 of 1989 -----
COMMENT
COMMENT Calibrated individual observations (i.e., 1/8th-second
COMMENT samples) of the sky as measured by each of the 16 DIRBE
COMMENT detectors during the specified day. Observations
COMMENT are sorted in order of increasing pixel number.
COMMENT It is possible to have multiple observations of a pixel
COMMENT within a day: these multiple observations are listed in

```

COMMENT consecutive rows within the table and are  
 COMMENT sorted in order of ascending observation time.  
 COMMENT Reconstruction of time-ordered data strings may be  
 COMMENT accomplished either through use of the TIME field  
 COMMENT or the PREV\_OBS/NEXT\_OBS fields.  
 COMMENT The companion Pixel Index to this day's data  
 COMMENT may be used to determine quickly which pixels were  
 COMMENT observed on this day and where data for specific pixels  
 COMMENT are located within this file.  
 COMMENT  
 COMMENT Although observations are sorted using the DIRBE  
 COMMENT (resolution 9) pixel number (PIXEL\_NO), the position  
 COMMENT of the boresight at the time of observation may be  
 COMMENT reconstructed to a precision of ~20 arcsec by using the  
 COMMENT additional pointing information provided in fields  
 COMMENT PSUBPOS and PSBSBPOS. See the COBE/DIRBE Explanatory  
 COMMENT Supplement description of this product (Chapter 5) for  
 COMMENT further details.  
 COMMENT  
 COMMENT Before using the photometric data, the user should examine  
 COMMENT the corresponding data quality flags. Observations  
 COMMENT which occurred within the SAA, non-sky-survey mode data,  
 COMMENT or time periods during which none of the DIRBE detectors met  
 COMMENT quality standards have already been excluded from this product.  
 COMMENT However, time periods during which data from some, but not all,  
 COMMENT detectors are of low quality are included. In many of  
 COMMENT these cases, the low quality detector data have been  
 COMMENT replaced with a sentinel value to guard against inadvertent  
 COMMENT use. There are some instances when low quality data have  
 COMMENT neither been removed nor sentinelized. These include:  
 COMMENT 1) intervals of excess noise for isolated detectors,  
 COMMENT such as Band 1b lunar effects, and the occasional  
 COMMENT microphonics noted especially in Bands 4 and 7.  
 COMMENT The XSNOISE detector flags are included to  
 COMMENT indicate affected observations.  
 COMMENT 2) observations contaminated by stray light from  
 COMMENT the Moon or Jupiter. The MOON2LOS and JUP2LOS  
 COMMENT fields can be used to eliminate these data.  
 COMMENT  
 COMMENT Unlike the higher level DIRBE data products  
 COMMENT (e.g., the DIRBE Weekly Maps, Calibrated Annual File,  
 COMMENT Maps at Solar Elongation Angle = 90 degrees,  
 COMMENT Galactic Plane Maps, Annual Average Maps),  
 COMMENT the Calibrated Individual Observations product INCLUDES  
 COMMENT data from those portions of the sky which contain  
 COMMENT Mars, Jupiter, Saturn, Uranus, Neptune, Juno, Vesta, Ceres,  
 COMMENT Pallas, or comets Austin, Levy, and Okazaki-Levy-Rudenko.  
 COMMENT The JUP2LOS field indicates when Jupiter was visible;  
 COMMENT locations of other objects can be computed using an  
 COMMENT external ephemeris.  
 COMMENT  
 COMMENT The foreground signal from Zodiacal dust has not been  
 COMMENT removed from the observations.  
 COMMENT \*\*\*\*\*

```

COMMENT -----
COMMENT =====
COMMENT Coordinate Information (Spatial and Temporal):
COMMENT =====
COMMENT -----
COMMENT      DIRBE Pixel number (resolution 9)
TTYPE1 = 'Pixel_no'      / pipeline fieldname = Pixel_no
TUNIT1 = '      '      /
TFORM1 = '1J      '      /
COMMENT -----
COMMENT      Sub-pixel containing the DIRBE line of sight
COMMENT      when the DIRBE pixel specified in
COMMENT      field "Pixel_no" is divided into 256
COMMENT      sub-pixels (16x16 grid) according
COMMENT      to standard quad-sphere rules
COMMENT      Range: [0 - 255]
TTYPE2 = 'PSubPos '      / pipeline fieldname = Pixel_subpos
TUNIT2 = '      '      /
TFORM2 = '1B      '      /
COMMENT -----
COMMENT      Sub-sub-pixel containing the DIRBE
COMMENT      line of sight when the DIRBE sub-pixel
COMMENT      specified in field "PSubPos"
COMMENT      is divided into 16 "sub-sub-pixels"
COMMENT      (4x4 grid) according to standard
COMMENT      quad-sphere rules. The sub-sub-
COMMENT      pixel number is stored in the 4
COMMENT      most significant bits. Bits 0-3
COMMENT      are not used.
COMMENT      Range: [0 - 15]
TTYPE3 = 'PSbSbPos'      / pipeline fieldname = Pixel_subsubpos
TUNIT3 = '      '      /
TFORM3 = '1B      '      /
TSCAL3 =      0.0625000 / divide by 16 to access bits 4-7
TZERO3 =      0.00 /
COMMENT -----
COMMENT -----
COMMENT      Time of observation in International Atomic Time (TAI)
COMMENT      seconds elapsed since 01-JAN-1981:00:00:00.000 UTC.
COMMENT      The reported time corresponds to the midpoint of the
COMMENT      1/8th second sample interval.
TTYPE4 = 'Time      '      / pipeline fieldname = Time
TUNIT4 = 's      '      /
TFORM4 = '1D      '      /
COMMENT -----
COMMENT      Number of the row within this FITS binary table which
COMMENT      contains the next observation in the time-ordered sequence.
COMMENT      Usually the time of the next observation is TIME + 1/8 sec,
COMMENT      but gaps in the time sequence do exist.
COMMENT      Next_obs is set to -1 if the time of the next observation
COMMENT      lies outside the time boundaries defined for this file.
TTYPE5 = 'Next_obs'      / pipeline fieldname = Next_obs
TUNIT5 = '      '      /
TFORM5 = '1J      '      /

```

```

COMMENT -----
COMMENT      Number of the row within this FITS binary table which contains
COMMENT      the previous observation in the time-ordered sequence.
COMMENT      Usually the time of the previous observation is
COMMENT      TIME - 1/8 sec, but gaps in the time sequence do exist.
COMMENT      Prev_obs is set to -1 if the time of the preceding observation
COMMENT      lies outside the time boundaries defined for this file.
TTYPE6 = 'Prev_obs'      / pipeline fieldname = Prev_obs
TUNIT6 = '      '      /
TFORM6 = '1J      '      /
COMMENT -----
COMMENT -----
COMMENT =====
COMMENT      DIRBE Sky Brightness and Polarization Information:
COMMENT =====
COMMENT -----
COMMENT      The following 16 columns tabulate the 1/8th second
COMMENT      photometric samples taken for the each of the 16
COMMENT      DIRBE detectors at the time of observation.
COMMENT      The photometric measurements
COMMENT      are given as spectral intensities, I(nu) in MJy/sr, and
COMMENT      are quoted at the nominal wavelength
COMMENT      for a source with nu*I(nu) = constant -- i.e.,
COMMENT      a color correction is required if the source
COMMENT      spectrum differs from nu*I(nu) = constant.
COMMENT      Data which have been replaced by flagged (sentinel) values
COMMENT      in processing have values .LE. -16375.
COMMENT
COMMENT      Photometry for band 1, channel A (1A: 1.25 um, full intensity)
TTYPE7 = 'Phot1A '      / pipeline fieldname = Photometry(1)
TUNIT7 = 'MJy/sr '      /
TFORM7 = '1E      '      /
COMMENT      Photometry for band 1, channel B (1B: 1.25 um, polarized light)
TTYPE8 = 'Phot1B '      / pipeline fieldname = Photometry(2)
TUNIT8 = 'MJy/sr '      /
TFORM8 = '1E      '      /
COMMENT      Photometry for band 1, channel C (1C: 1.25 um, polarized light)
TTYPE9 = 'Phot1C '      / pipeline fieldname = Photometry(3)
TUNIT9 = 'MJy/sr '      /
TFORM9 = '1E      '      /
COMMENT      Photometry for band 2, channel A (2A: 2.2 um, full intensity)
TTYPE10 = 'Phot2A '     / pipeline fieldname = Photometry(4)
TUNIT10 = 'MJy/sr '     /
TFORM10 = '1E      '     /
COMMENT      Photometry for band 2, channel B (2B: 2.2 um, polarized light)
TTYPE11 = 'Phot2B '     / pipeline fieldname = Photometry(5)
TUNIT11 = 'MJy/sr '     /
TFORM11 = '1E      '     /
COMMENT      Photometry for band 2, channel C (2C: 2.2 um, polarized light)
TTYPE12 = 'Phot2C '     / pipeline fieldname = Photometry(6)
TUNIT12 = 'MJy/sr '     /
TFORM12 = '1E      '     /
COMMENT      Photometry for band 3, channel A (3A: 3.5 um, full intensity)
TTYPE13 = 'Phot3A '     / pipeline fieldname = Photometry(7)

```

```

TUNIT13 = 'MJy/sr ' /
TFORM13 = '1E ' /
COMMENT Photometry for band 3, channel B (3B: 3.5 um, polarized light)
TTYPE14 = 'Phot3B ' / pipeline fieldname = Photometry(8)
TUNIT14 = 'MJy/sr ' /
TFORM14 = '1E ' /
COMMENT Photometry for band 3, channel C (3C: 3.5 um, polarized light)
TTYPE15 = 'Phot3C ' / pipeline fieldname = Photometry(9)
TUNIT15 = 'MJy/sr ' /
TFORM15 = '1E ' /
COMMENT Photometry for band 4 (4.9 um)
TTYPE16 = 'Phot04 ' / pipeline fieldname = Photometry(10)
TUNIT16 = 'MJy/sr ' /
TFORM16 = '1E ' /
COMMENT Photometry for band 5 (12 um)
TTYPE17 = 'Phot05 ' / pipeline fieldname = Photometry(11)
TUNIT17 = 'MJy/sr ' /
TFORM17 = '1E ' /
COMMENT Photometry for band 6 (25 um)
TTYPE18 = 'Phot06 ' / pipeline fieldname = Photometry(12)
TUNIT18 = 'MJy/sr ' /
TFORM18 = '1E ' /
COMMENT Photometry for band 7 (60 um)
TTYPE19 = 'Phot07 ' / pipeline fieldname = Photometry(13)
TUNIT19 = 'MJy/sr ' /
TFORM19 = '1E ' /
COMMENT Photometry for band 8 (100 um)
TTYPE20 = 'Phot08 ' / pipeline fieldname = Photometry(14)
TUNIT20 = 'MJy/sr ' /
TFORM20 = '1E ' /
COMMENT Photometry for band 9 (140 um)
TTYPE21 = 'Phot09 ' / pipeline fieldname = Photometry(15)
TUNIT21 = 'MJy/sr ' /
TFORM21 = '1E ' /
COMMENT Photometry for band 10 (240 um)
TTYPE22 = 'Phot10 ' / pipeline fieldname = Photometry(16)
TUNIT22 = 'MJy/sr ' /
TFORM22 = '1E ' /
COMMENT -----
COMMENT =====
COMMENT DIRBE Viewing Geometry and External Influences Information:
COMMENT =====
COMMENT -----
COMMENT Angle between DIRBE boresight (or line of sight, LOS) and
COMMENT spacecraft orbital velocity vector.
COMMENT Range = [0, 180] degrees
TTYPE23 = 'LOS2VelV' / pipeline fieldname = BS_re_Vel
TUNIT23 = 'deg ' /
TFORM23 = '1I ' /
TSCAL23 = 0.0109867 / bin size 360/(2**15 -1) degrees
TZERO23 = 0.00549333 / offset to bin center in degrees
COMMENT -----
COMMENT Approach Vector
COMMENT Divides observations into two groups:

```

```

COMMENT      those which are looking in the forward direction of
COMMENT      spacecraft motion, and those which are looking backwards
COMMENT      from the direction of spacecraft motion.
COMMENT      Approach Vector 1 (AV1):
COMMENT      Forward looking, i.e.,    0 .LE. LOS2VelV .LE.  90 deg
COMMENT      Approach Vector 2 (AV2):
COMMENT      Backward looking, i.e.,  90 .LT. LOS2VelV .LE. 180 deg
TTYPE24 = 'ApprVec '      / pipeline fieldname = Approach_vector
TUNIT24 = '      '      /
TFORM24 = '1B      '      /
COMMENT      -----
COMMENT      Attack Vector
COMMENT      A vector whose three components specify the rate of change
COMMENT      (derivative with respect to time) of the DIRBE boresight
COMMENT      unit vector (i.e. the rate of change of the direction
COMMENT      cosines in geocentric ecliptic coordinates).
COMMENT      The Attack Vector is computed from the cross product of
COMMENT      the spacecraft angular velocity vector (which includes both
COMMENT      orbital and spin components) and the boresight.
COMMENT      The Attack Vector points in the DIRBE scan direction
COMMENT      across the sky, and is normal to the leading edge of the
COMMENT      field of view (FOV). The length of this vector gives the
COMMENT      scan rate in radians/sec.
COMMENT      Nominal range for scan rate: .041 - .044 rad/sec
TTYPE25 = 'AttackV '      / pipeline fieldname = Attack_vector
TUNIT25 = '      '      /
TFORM25 = '3I      '      /
TDIM25  = '(3)      '      /
TSCAL25 =      0.0000305176 / bin size 1./(2**15) per second
TZERO25 =      0.00 / see ExSupp for offset to bin center in /sec
COMMENT      -----
COMMENT      Azimuth of the Attack Vector,
COMMENT      computed as a positive or negative rotation angle about
COMMENT      the DIRBE boresight in the plane normal to the boresight
COMMENT      vector (i.e., the plane of the field of view (FOV)).
COMMENT      Azimuth is measured with respect to the fiducial vector
COMMENT      defined by the cross product of the DIRBE spin axis and
COMMENT      boresight vectors, and is positive if the rotation sense
COMMENT      is the same as that of the spacecraft (i.e., azimuth =
COMMENT      +90 deg. points toward the spin axis, following the
COMMENT      right-hand sign convention).
COMMENT      Range = (-180, 180] degrees
COMMENT      Nominal range: [-2,+2] degrees
TTYPE26 = 'AtV_Azim'      / pipeline fieldname = FOV_Azimuth
TUNIT26 = 'deg      '      /
TFORM26 = '1I      '      /
TSCAL26 =      0.0109867 / bin size 360/(2**15 -1) degrees
TZERO26 =      0.00549333 / offset to bin center in degrees
COMMENT      -----
COMMENT      Solar elongation of observation,
COMMENT      i.e. angle between the vector from the spacecraft to the
COMMENT      center of the Sun and the DIRBE line of sight (boresight).
COMMENT      Nominal range = [64, 124] degrees
TTYPE27 = 'SolElong'      / pipeline fieldname = Sun_re_BS (word 1)

```



```

TUNIT27 = 'deg      ' /
TFORM27 = '1I      ' /
TSCAL27 =          0.0109867 / bin size 360/(2**15 -1) degrees
TZERO27 =          0.00549333 / offset to bin center in degrees
COMMENT -----
COMMENT      Angle between the vector from the spacecraft to the center
COMMENT      of the moon and the DIRBE line of sight (boresight).
COMMENT      Observations for which Moon2LOS .LE. 10 degrees are
COMMENT      potentially contaminated by lunar stray light.
TTYPER28 = 'Moon2LOS' / pipeline fieldname = Moon_re_BS (word 1)
TUNIT28 = 'deg      ' /
TFORM28 = '1I      ' /
TSCAL28 =          0.0109867 / bin size 360/(2**15 -1) degrees
TZERO28 =          0.00549333 / offset to bin center in degrees
COMMENT -----
COMMENT      Azimuth of the Moon
COMMENT      The vector from the spacecraft to the center of the Moon
COMMENT      is projected onto the plane normal to the boresight vector
COMMENT      (i.e., the plane of the field of view (FOV)).
COMMENT      The azimuth of this projected vector is then computed as a
COMMENT      positive or negative rotation angle about the DIRBE boresight.
COMMENT      Azimuth is measured with respect to the fiducial vector
COMMENT      defined by the cross product of the DIRBE spin axis and
COMMENT      boresight vectors, and is positive if the rotation sense
COMMENT      is the same as that of the spacecraft (i.e., azimuth =
COMMENT      +90 deg. points toward the spin axis, following the
COMMENT      right-hand sign convention). The AtV_Azim field gives
COMMENT      the relationship between the Attack Vector and the
COMMENT      zero azimuth fiducial.
COMMENT      Range = (-180, 180] degrees
TTYPER29 = 'MoonAzim' / pipeline fieldname = Moon_re_BS (word 2)
TUNIT29 = 'deg      ' /
TFORM29 = '1I      ' /
TSCAL29 =          0.0109867 / bin size 360/(2**15 -1) degrees
TZERO29 =          0.00549333 / offset to bin center in degrees
COMMENT -----
COMMENT      Angle between the vector from the spacecraft to the center
COMMENT      of Jupiter and the DIRBE line of sight (boresight).
COMMENT      Observations for which Jup2LOS .LE. 1.5 degrees are
COMMENT      potentially contaminated by stray light from Jupiter.
TTYPER30 = 'Jup2LOS ' / pipeline fieldname = Jupiter_re_BS (word 1)
TUNIT30 = 'deg      ' /
TFORM30 = '1I      ' /
TSCAL30 =          0.0109867 / bin size 360/(2**15 -1) degrees
TZERO30 =          0.00549333 / offset to bin center in degrees
COMMENT -----
COMMENT      Radiation Zone flag
COMMENT      Flag indicates if the spacecraft was within the
COMMENT      South Atlantic Anomaly (SAA), North Van Allen Belt (NVAB)
COMMENT      or South Van Allen Belt (SVAB) at the time of observation.
COMMENT      Radiation zone boundaries for the mission were defined
COMMENT      according to the number of radiation hits received as a
COMMENT      function of COBE subsatellite position. If the subsatellite
COMMENT      position at the time of observation was contained within

```

```

COMMENT      a zone's defined boundaries, then the flag for that zone
COMMENT      is set. Subsatellite position is updated every
COMMENT      32 seconds.
COMMENT      Observations occurring within the SAA
COMMENT      have already been eliminated; observations made within the
COMMENT      NVAB and SVAB remain in the dataset.
COMMENT      Bit 0 (LSB) = 1 if in NVAB ; 0 if clear of NVAB
COMMENT      Bit 1      = 1 if in SVAB ; 0 if clear of SVAB
COMMENT      Bit 2      = 1 if in SAA  ; 0 if clear of SAA
COMMENT      Bits 3-7 Not Used
TTYPE31 = 'RadZone '      / pipeline fieldname = Radiation_cont
TUNIT31 = '          '      /
TFORM31 = '1B          '   /
COMMENT      -----
COMMENT      Excess Noise Flags (per detector)
COMMENT      Flags indicating if exceptionally noisy data were recorded
COMMENT      by any of the 16 detectors during the 32-second
COMMENT      long Major Frame that included this observation.
COMMENT      Detector observations for which the flag is set
COMMENT      are unreliable and should not be used.
COMMENT      The 16-bit field is encoded so that each bit represents one
COMMENT      of the 16 detectors. Bits are assigned in detector order:
COMMENT      1A,1B,1C,2A,2B,2C,3A,3B,3C,4,5,6,7,8,9,10, where
COMMENT      Bit 0 (least significant bit) = 1 if Detector 1A excessively noisy
COMMENT      ... up through
COMMENT      Bit 15 (most significant bit) = 1 if Detector 10 excessively noisy
TTYPE32 = 'XSNoise '      / pipeline fieldname = Glitch_Flags
TUNIT32 = '          '      /
TFORM32 = '1I          '   /
COMMENT      -----
COMMENT      Orbit and Attitude Flags.
COMMENT      Miscellaneous orbit and attitude
COMMENT      information encoded into a single byte. The individual
COMMENT      bits are interpreted as follows, where Bit 0 is the
COMMENT      least significant bit:
COMMENT      Flags indicating attitude used
COMMENT      Bit 0 = 1 if non-definitive attitude
COMMENT      = 0 if definitive attitude used
COMMENT      Bit 1 = 1 if coarse attitude used
COMMENT      = 0 if fine attitude used
COMMENT      Bit 2 = 1 if merged attitude used
COMMENT      = 0 if external (UAX) attitude used
COMMENT      Flags describing attitude control
COMMENT      Bit 3 = 1 if spacecraft slewing
COMMENT      = 0 otherwise
COMMENT      Bit 4 = 1 during Special Pointing
COMMENT      = 0 otherwise
COMMENT      Node Flag
COMMENT      Bit 5 = 1 when spacecraft (NOT LOS) in ascending
COMMENT      portion of COBE orbit, i.e., moving
COMMENT      up towards North Ecliptic Pole
COMMENT      = 0 when spacecraft (NOT LOS) in descending
COMMENT      portion of COBE orbit, i.e., moving
COMMENT      down towards South Ecliptic Pole

```

```

COMMENT      Leading/Trailing Flag
COMMENT      Plane passing through Sun, Earth and ecliptic poles
COMMENT      divides sky into two halves:
COMMENT      Bit 6 = 1 when LOS is pointed to that half of sky
COMMENT      LEADING earth orbital motion
COMMENT      = 0 when LOS is pointed to that half of sky
COMMENT      TRAILING earth orbital motion
COMMENT      Bit 7 Not Used
TTYPE33 = 'OA_Flags'      / pipeline fieldname = ATT_Flags
TUNIT33 = '      '      /
TFORM33 = '1B      '      /
COMMENT      -----
END

```

### D.1.1.2 DIRBE Calibrated Annual File

Table D.1-3: Sample FITS headers for the *DIRBE* Calibrated Annual File Index files

```

SIMPLE =          T / file does conform to FITS standard
BITPIX =          32 / number of bits per data pixel
NAXIS  =          0 / number of data axes
EXTEND  =          T / FITS dataset may contain extensions
COMMENT  FITS (Flexible Image Transport System) format defined in Astronomy and
COMMENT  Astrophysics Supplement Series v44/p363, v44/p371, v73/p359, v73/p365.
COMMENT  Contact the NASA Science Office of Standards and Technology for the
COMMENT  FITS Definition document #100 and other FITS information.
DATE    = '09/04/97'      / FITS file creation date (dd/mm/yy)
DATE-MAP= '04/04/96'      / Date of original file creation (dd/mm/yy)
ORIGIN  = 'CDAC      '    / Cosmology Data Analysis Center
TELESCOP= 'COBE      '    / Cosmic Background Explorer satellite
INSTRUME= 'DIRBE      '    / COBE instrument [DIRBE, DMR, FIRAS]
OBJECT  = 'FACE0      '    / part of sky given [e.g., ALL-SKY, WEEKLY-SKY,
COMMENT  /          DAILY-SKY, GAL-SLICE, FACE ...]
EQUINOX =          2000.0 / equinox of coords in following tables
REFERENC= 'COBE/DIRBE Explanatory Supplement,' /
REFERENC= 'ed. M.G. Hauser, T. Kelsall, D. Leisawitz, and J. Weiland,' /
REFERENC= 'COBE Ref. Pub. No. 97-A (Greenbelt,MD: NASA/GSFC),' /
REFERENC= 'available in electronic form from the NSSDC.' /
COMMENT
COMMENT      COBE specific keywords
DATE-BEG= '11/12/89'      / date of initial data represented (dd/mm/yy)
DATE-END= '21/09/90'      / date of final data represented (dd/mm/yy)
PIXRESOL=          9 / Quad tree pixel resolution [6, 9]
COMMENT
COMMENT      DIRBE specific keywords
PRODUCT = 'DCAFINDEX_F0'  / Pixel Index file for DCAF, Face 0
VERSION  = 'Pass 3B      ' / Version of Data Reduction Software
COMMENT
COMMENT
END

```

```

XTENSION= 'BINTABLE'          / Extension type is Binary Table
BITPIX   =                    8 / Binary data
NAXIS    =                    2 / Data are in a table
NAXIS1   =                   14 / Number of 8 bit bytes in each row
NAXIS2   =                   65536 / Number of rows
PCOUNT   =                    0 / Number of bytes of data following table
GCOUNT   =                    1 / Group count (always 1 for bintable extensions)
TFIELDS  =                    3 / Number of fields (columns) in the table
COMMENT
COMMENT
COMMENT -----
COMMENT *****
COMMENT          DIRBE Calibrated Annual File, Face 0 : Pixel Index
COMMENT
COMMENT          This is the companion pixel index to the DIRBE
COMMENT          Calibrated Annual File (DCAF) for Face 0 of the COBE
COMMENT          Quadrilateralized Spherical Cube: i.e., the index to DCAF
COMMENT          data tabulated for DIRBE pixel numbers 0 - 65535.
COMMENT          The pixel index is intended to simplify and expedite data
COMMENT          retrieval for a user-selected subset of pixels in the
COMMENT          DCAF. There is one row in the index table for each DIRBE
COMMENT          pixel (resolution 9) on the cube face. Pixels are listed
COMMENT          in ascending order. For each pixel, the pixel index
COMMENT          table gives the number of the LAST row within the
COMMENT          corresponding DCAF table which contains observations for
COMMENT          that pixel, and specifies which mission weeks contain
COMMENT          observations for that pixel.
COMMENT *****
COMMENT -----
COMMENT =====
COMMENT          Coordinate Information (Spatial):
COMMENT =====
COMMENT -----
COMMENT          DIRBE Pixel number (resolution 9)
TTYPE1 = 'Pixel_no'          / pipeline fieldname = Pixel_no
TUNIT1 = '                  ' /
TFORM1 = '1J                ' /
COMMENT -----
COMMENT =====
COMMENT          Pixel Indexing Information:
COMMENT =====
COMMENT -----
COMMENT          Number of the last row within the corresponding DCAF
COMMENT          binary table which contains information for this pixel number.
COMMENT          Row numbers are counted starting at 1.
TTYPE2 = 'LastRow '          / pipeline fieldname = last_data_record
TUNIT2 = '                  ' /
TFORM2 = '1J                ' /
COMMENT -----
COMMENT          Mission week numbers for which data are available on this
COMMENT          pixel. Stored as a 6 byte (48 bit) vector, where each bit
COMMENT          corresponds to a specific week number in the mission.
COMMENT          Bit numbers start with 0 as the LSB in byte 1, 8 as the

```

```

COMMENT      LSB in byte 2, etc., and are related to mission week
COMMENT      numbers as follows:
COMMENT      Week number = bit number + 4
COMMENT      Thus, for example, if the LSB in byte 3 is set to 1, then
COMMENT      data are available for mission week 20. Week numbers range
COMMENT      from 4 to 44. A list of week numbers and their corresponding
COMMENT      times is provided in the Explanatory Supplement.
COMMENT
TTYPE3 = 'WksObs ' / pipeline fieldname = weeks_observed
TUNIT3 = ' ' /
TFORM3 = '6B ' /
TDIM3 = '(6) ' /
COMMENT -----
END

```

Table D.1-4: Sample FITS headers for the *DIRBE* Calibrated Annual File

```

SIMPLE = T / file does conform to FITS standard
BITPIX = 32 / number of bits per data pixel
NAXIS = 0 / number of data axes
EXTEND = T / FITS dataset may contain extensions
COMMENT FITS (Flexible Image Transport System) format defined in Astronomy and
COMMENT Astrophysics Supplement Series v44/p363, v44/p371, v73/p359, v73/p365.
COMMENT Contact the NASA Science Office of Standards and Technology for the
COMMENT FITS Definition document #100 and other FITS information.
DATE = '09/04/97' / FITS file creation date (dd/mm/yy)
DATE-MAP= '04/04/96' / Date of original file creation (dd/mm/yy)
ORIGIN = 'CDAC ' / Cosmology Data Analysis Center
TELESCOP= 'COBE ' / Cosmic Background Explorer satellite
INSTRUME= 'DIRBE ' / COBE instrument [DIRBE, DMR, FIRAS]
OBJECT = 'FACEO ' / part of sky given [e.g., ALL-SKY, WEEKLY-SKY,
COMMENT / DAILY-SKY, GAL-SLICE, FACE ...]
EQUINOX = 2000.0 / equinox of coords in following tables
REFERENC= 'COBE/DIRBE Explanatory Supplement,' /
REFERENC= 'ed. M.G. Hauser, T. Kelsall, D. Leisawitz, and J. Weiland,' /
REFERENC= 'COBE Ref. Pub. No. 97-A (Greenbelt,MD: NASA/GSFC),' /
REFERENC= 'available in electronic form from the NSSDC.' /
COMMENT
COMMENT COBE specific keywords
DATE-BEG= '11/12/89' / date of initial data represented (dd/mm/yy)
DATE-END= '21/09/90' / date of final data represented (dd/mm/yy)
PIXRESOL= 9 / Quad tree pixel resolution [6, 9]
COMMENT
COMMENT DIRBE specific keywords
PRODUCT = 'DCAF_F0 ' / DIRBE Calibrated Annual File, Face 0
VERSION = 'Pass 3B ' / Version of Data Reduction Software
WAVE1 = '1.25 microns' / nominal wavelength of Band 1
WAVE2 = '2.2 microns' / nominal wavelength of Band 2
WAVE3 = '3.5 microns' / nominal wavelength of Band 3
WAVE4 = '4.9 microns' / nominal wavelength of Band 4
WAVE5 = '12. microns' / nominal wavelength of Band 5

```

```

WAVE6  = '25.  microns'      / nominal wavelength of Band 6
WAVE7  = '60.  microns'      / nominal wavelength of Band 7
WAVE8  = '100. microns'      / nominal wavelength of Band 8
WAVE9  = '140. microns'      / nominal wavelength of Band 9
WAVE10 = '240. microns'      / nominal wavelength of Band 10
SOLELONG= 'ALL      '        / all available solar elongations included
APPVEC  = 'COMBINED'        / data having different approach vectors
COMMENT                                / are combined during processing
ZLREMOV =                    F / zodiacal foreground removal indicator
COMMENT                                / if 'T(true)', zodi foreground has been removed
COMMENT                                / if 'F(false)', observed sky brightness is given
COMMENT
COMMENT
END

XTENSION= 'BINTABLE'        / Extension type is Binary Table
BITPIX  =                    8 / Binary data
NAXIS   =                    2 / Data are in a table
NAXIS1  =                   131 / Number of 8 bit bytes in each row
NAXIS2  =                   2085580 / Number of rows
PCOUNT  =                    0 / Number of bytes of data following table
GCOUNT  =                    1 / Group count (always 1 for bintable extensions)
TFIELDS =                   15 / Number of fields (columns) in the table
COMMENT
COMMENT
TIMVERSN= 'OGIP/93-003'     / GSFC Office of Guest Investigator Programs
COMMENT                                / (OGIP) memo in which the convention is
COMMENT                                / described
COMMENT                                The times reported in this file are International
COMMENT                                Atomic Time (TAI) seconds elapsed since
COMMENT                                00:00:00 UTC, 1 January 1981. Time information is
COMMENT                                recorded in a manner consistent with the convention specified
COMMENT                                in OGIP/93-003 with the understanding that time is counted
COMMENT                                in atomic seconds and the origin of time (MJDREF) is quoted
COMMENT                                in ephemeris MJD.
TIMESYS = '1981.00 '        / time system (same as IRAS)
MJDREFI =                   44605 / Integer portion of ephemeris MJD
COMMENT                                / corresponding to 0h UTC 1 Jan 1981
MJDREFF =                   0.00059240741 / Fractional portion of ephemeris MJD
COMMENT                                / corresponding to 0h UTC 1 Jan 1981
TIMEUNIT= 's                ' / unit for TSTART, TSTOP, TIMEZERO = seconds
TSTART  =                   282185275.611 / observation start time in TIMESYS system
TSTOP   =                   306753235.358 / observation stop time in TIMESYS system
COMMENT
COMMENT
COMMENT -----
COMMENT *****
COMMENT ----- DIRBE Calibrated Annual File: Face 0 -----
COMMENT ----- Cryogenic Mission -----
COMMENT
COMMENT                                The DIRBE Calibrated Annual File (DCAF) combines the
COMMENT                                information contained in the 41 DIRBE Weekly Sky Maps
COMMENT                                into a merged all-sky version which is sorted by ascending
COMMENT                                DIRBE pixel number (resolution 9). Although the

```

information is identical to that given in the complete set of Weekly Sky Maps for the cryogenic mission, the data are organized differently, allowing more convenient access to the full range of temporal variations observed for each pixel. The DCAF table contains multiple row entries for each pixel, one row for each mission week for which photometric data are available. The multiple entries per pixel are stored in consecutive rows which are sorted in order of increasing observation time. A companion Pixel Index is provided to facilitate data selection and extraction.

Because of its relatively large size, the DCAF has been divided into six separate data files, each of which has its own Pixel Index. Each of the six data files corresponds to a face on the DIRBE skycube, and each is named according to the face number. The face number is also recorded in the OBJECT and PRODUCT keywords. There is no overlap in sky coverage between the files. Sky coverage is as follows:

Face No.	DIRBE Pixel No.s	Range(*) of Ecl. Longitude	Range(*) of Ecl. Latitude
0	0 - 65535	0 - 360 deg	+45 to +90 deg
1	65536 - 131071	315 - 45	-45 to +45
2	131072 - 196607	45 - 135	-45 to +45
3	196608 - 262143	135 - 225	-45 to +45
4	262144 - 327679	225 - 315	-45 to +45
5	327680 - 393215	0 - 360	-45 to -90

(\*) The ecliptic coordinate ranges are only approximate. A more complete description of the sky coverage for each face is provided in the DIRBE Explanatory Supplement, Chapter 5.

As with the DIRBE Weekly Sky Maps, the as-observed sky brightness is tabulated; the foreground signal from Zodiacal dust has not been removed.

\*\*\*\*\*  
-----  
=====  
Coordinate Information (Spatial and Temporal):  
=====  
-----

DIRBE Pixel number (resolution 9)  
TTYPE1 = 'Pixel\_no' / pipeline fieldname = Pixel\_no  
TUNIT1 = ' ' /  
TFORM1 = '1J' /

-----  
Sub-pixel containing the mean DIRBE LOS (line-of-sight)  
when pixel is divided into 256  
sub-pixels (16x16 grid) according to  
standard quad-sphere rules

```

TTYPE2 = 'PSubPos ' / pipeline fieldname = Pixel_subpos
TUNIT2 = ' ' /
TFORM2 = '1B ' /
COMMENT -----
COMMENT Sub-pixel number of the average line-of-sight
COMMENT for individual bands which are expected to
COMMENT have the largest offsets from the nominal position.
COMMENT Subpixels are specified as a 16x16 grid
COMMENT according to standard quad-sphere rules.
COMMENT Byte 1: Sub-pixel for Band 1A
COMMENT Byte 2: Sub-pixel for Band 4
COMMENT Byte 3: Sub-pixel for Band 7
COMMENT Byte 4: Sub-pixel for Band 8
TTYPE3 = 'Displace' / pipeline fieldname = Displacement_Means
TUNIT3 = ' ' /
TFORM3 = '4B ' /
TDIM3 = '(4) ' /
COMMENT -----
COMMENT Time in International Atomic Time (TAI) seconds
COMMENT elapsed since 01-JAN-1981:00:00:00.000 UTC.
COMMENT This is the average time of all observations of a pixel
COMMENT within the time interval TSTART to TSTOP,
COMMENT regardless of the weight assigned to a particular observation.
TTYPE4 = 'Time ' / pipeline fieldname = Time
TUNIT4 = 's ' /
TFORM4 = '1D ' /
COMMENT -----
COMMENT Difference between the average time of observation of the pixel
COMMENT for each photometric band, and the
COMMENT average time of all observations of the pixel (as given in the
COMMENT TIME field). Therefore, for each pixel:
COMMENT Average time of observation of Band x = TIME + (DeltaT for Band x).
COMMENT Given in the order: 1A,2A,3A,4,5,6,7,8,9,10.
COMMENT Range = [-7.0,+7.0) days
TTYPE5 = 'DeltaT ' / pipeline fieldname = Delta_times
TUNIT5 = 's ' /
TFORM5 = '10B ' /
TDIM5 = '(10) ' /
TSCAL5 = 4725.0 / bin size (7*24*60*60)/(2**7) seconds
TZER05 = -602437.5 / offset to bin center in secs for unsigned byte
COMMENT -----
COMMENT Mean solar elongation of observation, i.e.
COMMENT angle between the vector from the spacecraft to the center
COMMENT of the Sun and the DIRBE line-of-sight,
COMMENT averaged over all observations of the pixel.
COMMENT Nominal range = [64,124] degrees
TTYPE6 = 'SolElong' / pipeline fieldname = Elongation
TUNIT6 = 'deg ' /
TFORM6 = '1I ' /
TSCAL6 = 0.0109867 / bin size 360/(2**15 -1) degrees
TZER06 = 0.00549333 / offset to bin center in degrees
COMMENT -----
COMMENT =====
COMMENT DIRBE Sky Brightness and Polarization Information:

```



```

COMMENT =====
COMMENT -----
COMMENT      Robust average of the week's photometric measurements
COMMENT      for the bands in the following order:
COMMENT      1A,2A,3A,4,5,6,7,8,9,10. The photometric measurements
COMMENT      are given as spectral intensities, I(nu) in MJy/sr, and
COMMENT      are quoted at the nominal wavelength
COMMENT      for a source with nu*I(nu) = constant -- i.e.,
COMMENT      a color correction is required if the source
COMMENT      spectrum differs from nu*I(nu) = constant.
COMMENT      Data which have been replaced by flagged values
COMMENT      in processing have values .LE. -16375.
TTYPE7 = 'Photomet'      / pipeline fieldname = Photometry
TUNIT7 = 'MJy/sr '      /
TFORM7 = '10E '        /
TDIM7  = '(10) '       /
COMMENT -----
COMMENT      Stokes parameters Q and U for Band 1, Q and U
COMMENT      for Band 2, and Q and U for Band 3.
COMMENT      Range = (-2.0,2.0)
COMMENT      Nominal range = (-1.0,1.0)
COMMENT      Three possible cases arise in
COMMENT      storing the Stokes parameters for each band.
COMMENT      Bits 5 and 6 of the Polarization_quality_flag
COMMENT      field (StokQual) indicate which case applies:
COMMENT      Case 1:
COMMENT      Stokes parameters were calculated for the B and C
COMMENT      channels and the averages over both channels are
COMMENT      stored.
COMMENT      Case 2:
COMMENT      Stokes parameters were calculated for the B channel only.
COMMENT      Case 3:
COMMENT      Stokes parameters were calculated for the C channel only.
COMMENT      Indeterminate quantities are set to a flagged value .LE. -16375.
TTYPE8 = 'Stokes '      / pipeline fieldname = Polarization
TUNIT8 = ' '            /
TFORM8 = '6E '         /
TDIM8  = '(6) '        /
COMMENT -----
COMMENT      Number of observations of the pixel for this week
COMMENT      that contained at least one valid photometric measurement.
TTYPE9 = 'NumRecs '     / pipeline fieldname = Num_rec
TUNIT9 = ' '           /
TFORM9 = '1I '         /
COMMENT -----
COMMENT      Number of observations which survived robust averaging
COMMENT      and quality constraints to form the photometric averages
COMMENT      supplied for each band in the 'Photomet' field.
COMMENT      Given in the order: 1A,2A,3A,4,5,6,7,8,9,10.
TTYPE10 = 'WtNumObs'    / pipeline fieldname = Weighted_num_obs
TUNIT10 = ' '          /
TFORM10 = '10B '       /

```

```

TDIM10 = '(10)      ' /
TSCAL10 =           0.50 / bin size 0.5
TZERO10 =           0.0 /
COMMENT -----
COMMENT      Standard deviation of the mean, in MJy/sr, for the
COMMENT      10 photometric measures, given in
COMMENT      the following order: 1A,2A,3A,4,5,6,7,8,9,10.
COMMENT
COMMENT      The contents B of the Standard_Deviation fields
COMMENT      are given on a uniform logarithmic scale,
COMMENT      spanning 4 decades, having been calculated
COMMENT      from the standard deviations S (in MJy/sr) as follows:
COMMENT      if S <= 10**(-N)           then B = 0
COMMENT      if 10**(-N) < S < 10**(-N+4) then B = IFIX((N+log10(S))*254./4.)+1
COMMENT      if S >= 10**(-N+4)         then B = 255
COMMENT      where the value of N is band-dependent, and given below.
COMMENT
COMMENT      Conversely, the standard deviations
COMMENT      can be reconstructed by:
COMMENT      S <= 10**(-N)           if B = 0
COMMENT      S = 10**(4*(B-0.5)/254. - N) if 1 <= B <= 254
COMMENT      S >= 10**(-N+4)         if B = 255
COMMENT      (The maximum error on the reconstructed value is 1.8 %)
COMMENT
COMMENT      The values of N are:
COMMENT      Bands 1A, 2A, 3A, 4:  N = 4
COMMENT      Bands 5, 6:         N = 3
COMMENT      Bands 7, 8:         N = 2
COMMENT      Band 9:             N = 0
COMMENT      Band 10:            N = 1
COMMENT
COMMENT      Range of S = [10**(-N),10**(-N+4)]
TTYPE11 = 'StdDev ' / pipeline filename = Standard_Deviation
TUNIT11 = 'MJy/sr ' /
TFORM11 = '10B ' /
TDIM11 = '(10) ' /
COMMENT -----
COMMENT      Standard deviation of the mean, in dimensionless units,
COMMENT      for Stokes parameters Q and U for Band 1,
COMMENT      Q and U for Band 2, and Q and U for Band 3.
COMMENT
COMMENT      The contents B of the Stokes_Standard_Deviation fields
COMMENT      are given on a uniform logarithmic scale,
COMMENT      spanning 4 decades, having been calculated
COMMENT      from the standard deviations S (dimensionless) as follows:
COMMENT      if S <= 10**(-4)           then B = 0
COMMENT      if 10**(-4) < S < 1       then B = IFIX((4+log10(S))*254./4.)+1
COMMENT      if S >= 1                 then B = 255
COMMENT
COMMENT      Conversely, the standard deviations
COMMENT      can be reconstructed by:
COMMENT      S <= 10**(-4)           if B = 0
COMMENT      S = 10**(4*(B-0.5)/254. - 4) if 1 <= B <= 254

```

```

COMMENT      S >= 1                      if B = 255
COMMENT      (The maximum error on the reconstructed value is 1.8 %)
COMMENT
COMMENT
COMMENT      Range of S = [0.0001,1.0]
TTYPE12 = 'StokesSD'          / pipeline fieldname = Stokes_Standard_Deviation
TUNIT12 = '          '        /
TFORM12 = '6B          '      /
TDIM12  = '(6)          '     /
COMMENT      -----
COMMENT      Solar System Objects Flag
COMMENT      A one-byte flag which is used to signal
COMMENT      which solar-system objects' exclusion
COMMENT      zones intersect this pixel during
COMMENT      part or all of the time period
COMMENT      covered by the observations.
COMMENT      Data intersected by an exclusion zone
COMMENT      are not included in the photometric
COMMENT      or polarimetric averages.
COMMENT      If set, bits indicate intersection with
COMMENT      the exclusion zone of the following objects:
COMMENT      (Least significant bit = bit 0)
COMMENT      bit 0 --- Moon
COMMENT      bit 1 --- Mars
COMMENT      bit 2 --- Jupiter
COMMENT      bit 3 --- Saturn
COMMENT      bit 4 --- Uranus
COMMENT      bit 5 --- Neptune
COMMENT      bit 6 --- asteroids and comets
COMMENT      bit 7 --- spare
TTYPE13 = 'SSOFlag '          / pipeline fieldname = Pixel_Quality_Flag, byte 3
TUNIT13 = '          '        /
TFORM13 = '1B          '      /
COMMENT      -----
COMMENT      Fraction of Data Used
COMMENT      Three-byte flag indicating the fraction
COMMENT      of available data used in the generation
COMMENT      of the weekly averages.
COMMENT      Byte 1 : Average % of all the
COMMENT      available data that was used in
COMMENT      the construction of the averaged
COMMENT      observations for Bands 1A, 2A, 3A,
COMMENT      4, 5, 6, 8, 9, and 10
COMMENT      Range = [0,100%]
COMMENT      Byte 2 : Percent of the available Band 1B data
COMMENT      that was used.
COMMENT      Range = [0,100%]
COMMENT      Byte 3 : Percent of the available Band 7 data
COMMENT      that was used.
COMMENT      Range = [0,100%]
TTYPE14 = 'FracUsed'          / pipeline fieldname = Pixel_Quality_Flag,byte 4-
TUNIT14 = '          '        /
TFORM14 = '3B          '      /
TDIM14  = '(3)          '     /

```

```

TSCAL14 =          0.392 / bin size 100./(2**8 - 1) %
TZERO14 =          0.0 /
COMMENT -----
COMMENT      Six-byte Flag indicating the quality of
COMMENT      data in each set of polarization ratios ( 1B/1A,
COMMENT      1C/1A...,3C/3A), used to find the Stokes parameters.
COMMENT      If any of bits 0 through 4 are set, then the
COMMENT      values of the Stokes parameters
COMMENT      found from these ratios may be subject to error
COMMENT      beyond the formal uncertainties.
COMMENT      One byte per polarization ratio, given in the order
COMMENT      (1B/1A,1C/1A,2B/2A,2C/2A,3B/3A,3C/3A).
COMMENT      Each bit, if set, is interpreted as follows:
COMMENT      Least Significant Bit = Bit 0
COMMENT      Bit 0: Only one ratio available.
COMMENT      Bit 1: Only two ratios available.
COMMENT      Bit 2: Between 3 and 9 ratios available.
COMMENT      Bit 3: Distribution of data such that the
COMMENT      Robust fitting used to deduce Stokes
COMMENT      parameters failed to converge.
COMMENT      Bit 4: Moon is within 25 degrees of boresight
COMMENT      for at least one of the polarization
COMMENT      ratios.
COMMENT      Bit 5: No ratios for 'C' channel: polarization
COMMENT      found from channel 'B' alone.
COMMENT      Bit 6: No ratios for 'B' channel: polarization
COMMENT      found from channel 'C' alone.
COMMENT      Bit 7: Processing of ratios failed to produce a value
COMMENT      of Q or U, or else set them to flag values.
TTYPE15 = 'StokQual'      / pipeline fieldname = Polarization_Quality_Flag
TUNIT15 = '      '      /
TFORM15 = '6B      '      /
TDIM15  = '(6)      '      /
COMMENT -----
END

```

### D.1.1.3 Weekly Sky Maps

Table D.1-5: Sample Weekly Sky Map FITS header

```

SIMPLE =          T / file does conform to FITS standard
BITPIX =          32 / number of bits per data pixel
NAXIS  =          0 / number of data axes
EXTEND =          T / FITS dataset may contain extensions
COMMENT FITS (Flexible Image Transport System) format defined in Astronomy and
COMMENT Astrophysics Supplement Series v44/p363, v44/p371, v73/p359, v73/p365.
COMMENT Contact the NASA Science Office of Standards and Technology for the
COMMENT FITS Definition document #100 and other FITS information.
DATE   = '11/02/97'      / FITS file creation date (dd/mm/yy)
DATE-MAP= '28/03/96'      / Date of original file creation (dd/mm/yy)
ORIGIN = 'CDAC      '      / Cosmology Data Analysis Center

```

```

TELESCOP= 'COBE      ' / Cosmic Background Explorer satellite
INSTRUME= 'DIRBE    ' / COBE instrument [DIRBE, DMR, FIRAS]
OBJECT   = 'WEEKLY-SKY' / part of sky given [e.g., ALL-SKY, WEEKLY-SKY,
COMMENT   /           DAILY-SKY, GAL-SLICE, FACE ...]
EQUINOX  =           2000.0 / equinox of coords in following tables
REFERENC= 'COBE/DIRBE Explanatory Supplement,' /
REFERENC= 'ed. M.G. Hauser, T. Kelsall, D. Leisawitz, and J. Weiland,' /
REFERENC= 'COBE Ref. Pub. No. 97-A (Greenbelt,MD: NASA/GSFC),' /
REFERENC= 'available in electronic form from the NSSDC.' /
COMMENT
COMMENT          COBE specific keywords
DATE-BEG= '11/12/89' / date of initial data represented (dd/mm/yy)
DATE-END= '17/12/89' / date of final data represented (dd/mm/yy)
PIXRESOL=           9 / Quad tree pixel resolution [6, 9]
COMMENT
COMMENT          DIRBE specific keywords
PRODUCT  = 'WEEKMAP4' / Weekly Averaged Map for Mission Week 4
VERSION  = 'Pass 3B ' / Version of Data Reduction Software
WAVE1   = '1.25 microns' / nominal wavelength of Band 1
WAVE2   = '2.2 microns' / nominal wavelength of Band 2
WAVE3   = '3.5 microns' / nominal wavelength of Band 3
WAVE4   = '4.9 microns' / nominal wavelength of Band 4
WAVE5   = '12. microns' / nominal wavelength of Band 5
WAVE6   = '25. microns' / nominal wavelength of Band 6
WAVE7   = '60. microns' / nominal wavelength of Band 7
WAVE8   = '100. microns' / nominal wavelength of Band 8
WAVE9   = '140. microns' / nominal wavelength of Band 9
WAVE10  = '240. microns' / nominal wavelength of Band 10
SOLELONG= 'ALL      ' / all available solar elongations included
APPVEC  = 'COMBINED' / data having different approach vectors
COMMENT / are combined during processing
ZLREMOV =           F / zodiacal foreground removal indicator
COMMENT / if 'T(true)', zodi foreground has been removed
COMMENT / if 'F(false)', observed sky brightness is given
COMMENT
COMMENT
END

XTENSION= 'BINTABLE' / Extension type is Binary Table
BITPIX  =           8 / Binary data
NAXIS   =           2 / Data are in a table
NAXIS1  =           131 / Number of 8 bit bytes in each row
NAXIS2  =          214125 / Number of rows
PCOUNT  =           0 / Number of bytes of data following table
GCOUNT  =           1 / Group count (always 1 for bintable extensions)
TFIELDS =           15 / Number of fields (columns) in the table
COMMENT
COMMENT
TIMVERSN= 'OGIP/93-003' / GSFC Office of Guest Investigator Programs (OGIP)
COMMENT / memo in which the convention is described
COMMENT The times reported in this file are International
COMMENT Atomic Time (TAI) seconds elapsed since
COMMENT 00:00:00 UTC, 1 January 1981. Time information is
COMMENT recorded in a manner consistent with the convention specified

```

```

COMMENT          in OGIP/93-003 with the understanding that time is counted
COMMENT          in atomic seconds and the origin of time (MJDREF) is quoted
COMMENT          in ephemeris MJD.
TIMESYS = '1981.00 ' / time system (same as IRAS)
MJDREFI =          44605 / Integer portion of ephemeris MJD
COMMENT          / corresponding to 0h UTC 1 Jan 1981
MJDREFF =          0.00059240741 / Fractional portion of ephemeris MJD
COMMENT          / corresponding to 0h UTC 1 Jan 1981
TIMEUNIT= 's      ' / unit for TSTART, TSTOP, TIMEZERO = seconds
TSTART  =          282185275.611 / observation start time in TIMESYS system
TSTOP   =          282787015.111 / observation stop time in TIMESYS system
COMMENT
COMMENT
COMMENT -----
COMMENT *****
COMMENT          Weekly Averaged Sky Map -- Mission Week 4
COMMENT          Photometry, Polarization and ancillary data averaged over
COMMENT          one week's worth of observations, covering the dates
COMMENT          11-Dec-1989 to 17-Dec-1989 (inclusive).
COMMENT          The foreground signal from Zodiacal dust remains in the map.
COMMENT *****
COMMENT -----
COMMENT =====
COMMENT          Coordinate Information (Spatial and Temporal):
COMMENT =====
COMMENT -----
COMMENT          DIRBE Pixel number (resolution 9)
TTYPE1  = 'Pixel_no' / pipeline fieldname = Pixel_no
TUNIT1  = '      '   /
TFORM1  = '1J      ' /
COMMENT -----
COMMENT          Sub-pixel containing the mean DIRBE LOS (line-of-sight)
COMMENT          when pixel is divided into 256
COMMENT          sub-pixels (16x16 grid) according to
COMMENT          standard quad-sphere rules
TTYPE2  = 'PSubPos ' / pipeline fieldname = Pixel_subpos
TUNIT2  = '      '   /
TFORM2  = '1B      ' /
COMMENT -----
COMMENT          Sub-pixel number of the average line-of-sight
COMMENT          for individual bands which are expected to
COMMENT          have the largest offsets from the nominal position.
COMMENT          Subpixels are specified as a 16x16 grid
COMMENT          according to standard quad-sphere rules.
COMMENT          Byte 1: Sub-pixel for Band 1A
COMMENT          Byte 2: Sub-pixel for Band 4
COMMENT          Byte 3: Sub-pixel for Band 7
COMMENT          Byte 4: Sub-pixel for Band 8
TTYPE3  = 'Displace' / pipeline fieldname = Displacement_Means
TUNIT3  = '      '   /
TFORM3  = '4B      ' /
TDIM3   = '(4)     ' /
COMMENT -----
COMMENT          Time in International Atomic Time (TAI) seconds

```

```

COMMENT      elapsed since 01-JAN-1981:00:00:00.000 UTC.
COMMENT      This is the average time of all observations of a pixel
COMMENT      within the time interval TSTART to TSTOP,
COMMENT      regardless of the weight assigned to a particular observation.
TTYPE4 = 'Time      '          / pipeline fieldname = Time
TUNIT4 = 's        '          /
TFORM4 = '1D      '          /
COMMENT      -----
COMMENT      Difference between the average time of observation of the pixel
COMMENT      for each photometric band, and the
COMMENT      average time of all observations of the pixel (as given in the
COMMENT      TIME field). Therefore, for each pixel:
COMMENT      Average time of observation of Band x = TIME + (DeltaT for Band x).
COMMENT      Given in the order: 1A,2A,3A,4,5,6,7,8,9,10.
COMMENT      Range = [-7.0,+7.0) days
TTYPE5 = 'DeltaT   '          / pipeline fieldname = Delta_times
TUNIT5 = 's        '          /
TFORM5 = '10B     '          /
TDIM5  = '(10)    '          /
TSCAL5 =              4725.0 / bin size (7*24*60*60)/(2**7) seconds
TZERO5 =              -602437.5 / offset to bin center in secs for unsigned byte
COMMENT      -----
COMMENT      Mean solar elongation of observation, i.e.
COMMENT      angle between the vector from the spacecraft to the center
COMMENT      of the Sun and the DIRBE line-of-sight,
COMMENT      averaged over all observations of the pixel.
COMMENT      Nominal range = [64,124] degrees
TTYPE6 = 'SolElong'          / pipeline fieldname = Elongation
TUNIT6 = 'deg        '          /
TFORM6 = '1I        '          /
TSCAL6 =              0.0109867 / bin size 360/(2**15 -1) degrees
TZERO6 =              0.00549333 / offset to bin center in degrees
COMMENT      -----
COMMENT      =====
COMMENT      DIRBE Sky Brightness and Polarization Information:
COMMENT      =====
COMMENT      -----
COMMENT      Robust average of the week's photometric measurements
COMMENT      for the bands in the following order:
COMMENT      1A,2A,3A,4,5,6,7,8,9,10. The photometric measurements
COMMENT      are given as spectral intensities, I(nu) in MJy/sr, and
COMMENT      are quoted at the nominal wavelength
COMMENT      for a source with nu*I(nu) = constant -- i.e.,
COMMENT      a color correction is required if the source
COMMENT      spectrum differs from nu*I(nu) = constant.
COMMENT      Data which have been replaced by flagged values
COMMENT      in processing have values .LE. -16375.
TTYPE7 = 'Photomet'          / pipeline fieldname = Photometry
TUNIT7 = 'MJy/sr   '          /
TFORM7 = '10E     '          /
TDIM7  = '(10)    '          /
COMMENT      -----
COMMENT      Stokes parameters Q and U for Band 1, Q and U
COMMENT      for Band 2, and Q and U for Band 3.

```

```

COMMENT      Range = (-2.0,2.0)
COMMENT      Nominal range = (-1.0,1.0)
COMMENT      Three possible cases arise in
COMMENT      storing the Stokes parameters for each band.
COMMENT      Bits 5 and 6 of the Polarization_quality_flag
COMMENT      field (StokQual) indicate which case applies:
COMMENT      Case 1:
COMMENT      Stokes parameters were calculated for the B and C
COMMENT      channels and the averages over both channels are
COMMENT      stored.
COMMENT      Case 2:
COMMENT      Stokes parameters were calculated for the B channel only.
COMMENT      Case 3:
COMMENT      Stokes parameters were calculated for the C channel only.
COMMENT      Indeterminate quantities are set to a flagged value .LE. -16375.
COMMENT
TTYPES      = 'Stokes '          / pipeline fieldname = Polarization
TUNIT8      = '          '        /
TFORM8      = '6E          '      /
TDIM8       = '(6)          '     /
COMMENT     -----
COMMENT      Number of observations of the pixel for this week
COMMENT      that contained at least one valid photometric measurement.
TTYPE9      = 'NumRecs '        / pipeline fieldname = Num_rec
TUNIT9      = '          '        /
TFORM9      = '1I          '      /
COMMENT     -----
COMMENT      Number of observations which survived robust averaging
COMMENT      and quality constraints to form the photometric averages
COMMENT      supplied for each band in the 'Photomet' field.
COMMENT      Given in the order: 1A,2A,3A,4,5,6,7,8,9,10.
TTYPE10     = 'WtNumObs'        / pipeline fieldname = Weighted_num_obs
TUNIT10     = '          '        /
TFORM10     = '10B          '     /
TDIM10      = '(10)          '   /
TSCAL10     =          0.50 / bin size 0.5
TZERO10     =          0.0 /
COMMENT     -----
COMMENT      Standard deviation of the mean, in MJy/sr, for the
COMMENT      10 photometric measures, given in
COMMENT      the following order: 1A,2A,3A,4,5,6,7,8,9,10.
COMMENT
COMMENT      The contents B of the Standard_Deviation fields
COMMENT      are given on a uniform logarithmic scale,
COMMENT      spanning 4 decades, having been calculated
COMMENT      from the standard deviations S (in MJy/sr) as follows:
COMMENT      if S <= 10**(-N)          then B = 0
COMMENT      if 10**(-N) < S < 10**(-N+4) then B = IFIX((N+log10(S))*254./4.)+1
COMMENT      if S >= 10**(-N+4)        then B = 255
COMMENT      where the value of N is band-dependent, and given below.
COMMENT
COMMENT      Conversely, the standard deviations
COMMENT      can be reconstructed by:

```



```

COMMENT      S <= 10**(-N)                if B = 0
COMMENT      S = 10**(4*(B-0.5)/254. - N) if 1 <= B <= 254
COMMENT      S >= 10**(-N+4)              if B = 255
COMMENT      (The maximum error on the reconstructed value is 1.8 %)
COMMENT
COMMENT
COMMENT      The values of N are:
COMMENT      Bands 1A, 2A, 3A, 4:  N = 4
COMMENT      Bands 5, 6:          N = 3
COMMENT      Bands 7, 8:          N = 2
COMMENT      Band 9:              N = 0
COMMENT      Band 10:             N = 1
COMMENT
COMMENT      Range of S = [10**(-N),10**(-N+4)]
TTYPE11 = 'StdDev ' / pipeline fieldname = Standard_Deviation
TUNIT11 = 'MJy/sr ' /
TFORM11 = '10B ' /
TDIM11 = '(10) ' /
COMMENT
COMMENT      -----
COMMENT      Standard deviation of the mean, in dimensionless units,
COMMENT      for Stokes parameters Q and U for Band 1,
COMMENT      Q and U for Band 2, and Q and U for Band 3.
COMMENT
COMMENT      The contents B of the Stokes_Standard_Deviation fields
COMMENT      are given on a uniform logarithmic scale,
COMMENT      spanning 4 decades, having been calculated
COMMENT      from the standard deviations S (dimensionless) as follows:
COMMENT      if S <= 10**(-4)                then B = 0
COMMENT      if 10**(-4) < S < 1            then B = IFIX((4+log10(S))*254./4.)+1
COMMENT      if S >= 1                      then B = 255
COMMENT
COMMENT      Conversely, the standard deviations
COMMENT      can be reconstructed by:
COMMENT      S <= 10**(-4)                if B = 0
COMMENT      S = 10**(4*(B-0.5)/254. - 4) if 1 <= B <= 254
COMMENT      S >= 1                      if B = 255
COMMENT      (The maximum error on the reconstructed value is 1.8 %)
COMMENT
COMMENT      Range of S = [0.0001,1.0]
TTYPE12 = 'StokesSD' / pipeline fieldname = Stokes_Standard_Deviation
TUNIT12 = ' ' /
TFORM12 = '6B ' /
TDIM12 = '(6) ' /
COMMENT
COMMENT      -----
COMMENT      Solar System Objects Flag
COMMENT      A one-byte flag which is used to signal
COMMENT      which solar-system objects' exclusion
COMMENT      zones intersect this pixel during
COMMENT      part or all of the time period
COMMENT      covered by the observations.
COMMENT      Data intersected by an exclusion zone
COMMENT      are not included in the photometric
COMMENT      or polarimetric averages.

```

```

COMMENT      If set, bits indicate intersection with
COMMENT      the exclusion zone of the following objects:
COMMENT      (Least significant bit = bit 0)
COMMENT      bit 0 --- Moon
COMMENT      bit 1 --- Mars
COMMENT      bit 2 --- Jupiter
COMMENT      bit 3 --- Saturn
COMMENT      bit 4 --- Uranus
COMMENT      bit 5 --- Neptune
COMMENT      bit 6 --- asteroids and comets
COMMENT      bit 7 --- spare
TTYPE13 = 'SSOFlag' / pipeline fieldname = Pixel_Quality_Flag, byte 3
TUNIT13 = ' ' /
TFORM13 = '1B' /
COMMENT -----
COMMENT      Fraction of Data Used
COMMENT      Three-byte flag indicating the fraction
COMMENT      of available data used in the generation
COMMENT      of the weekly averages.
COMMENT      Byte 1 : Average % of all the
COMMENT      available data that was used in
COMMENT      the construction of the averaged
COMMENT      observations for Bands 1A, 2A, 3A,
COMMENT      4, 5, 6, 8, 9, and 10
COMMENT      Range = [0,100%]
COMMENT      Byte 2 : Percent of the available Band 1B data
COMMENT      that was used.
COMMENT      Range = [0,100%]
COMMENT      Byte 3 : Percent of the available Band 7 data
COMMENT      that was used.
COMMENT      Range = [0,100%]
TTYPE14 = 'FracUsed' / pipeline fieldname = Pixel_Quality_Flag,byte 4-
TUNIT14 = ' ' /
TFORM14 = '3B' /
TDIM14 = '(3)' /
TSCAL14 = 0.392 / bin size 100./(2**8 - 1) %
TZERO14 = 0.0 /
COMMENT -----
COMMENT      Six-byte Flag indicating the quality of
COMMENT      data in each set of polarization ratios ( 1B/1A,
COMMENT      1C/1A...,3C/3A), used to find the Stokes parameters.
COMMENT      If any of bits 0 through 4 are set, then the
COMMENT      values of the Stokes parameters
COMMENT      found from these ratios may be subject to error
COMMENT      beyond the formal uncertainties.
COMMENT      One byte per polarization ratio, given in the order
COMMENT      (1B/1A,1C/1A,2B/2A,2C/2A,3B/3A,3C/3A).
COMMENT      Each bit, if set, is interpreted as follows:
COMMENT      Least Significant Bit = Bit 0
COMMENT      Bit 0: Only one ratio available.
COMMENT      Bit 1: Only two ratios available.
COMMENT      Bit 2: Between 3 and 9 ratios available.
COMMENT      Bit 3: Distribution of data such that the
COMMENT      Robust fitting used to deduce Stokes

```

```

COMMENT          parameters failed to converge.
COMMENT          Bit 4: Moon is within 25 degrees of boresight
COMMENT          for at least one of the polarization
COMMENT          ratios.
COMMENT          Bit 5: No ratios for 'C' channel: polarization
COMMENT          found from channel 'B' alone.
COMMENT          Bit 6: No ratios for 'B' channel: polarization
COMMENT          found from channel 'C' alone.
COMMENT          Bit 7: Processing of ratios failed to produce a value
COMMENT          of Q or U, or else set them to flag values.
TTYPE15 = 'StokQual'      / pipeline fieldname = Polarization_Quality_Flag
TUNIT15 = '              ' /
TFORM15 = '6B           ' /
TDIM15  = '(6)          ' /
COMMENT -----
END

```

#### D.1.1.4 Solar Elongation = 90° Sky Map

Table D.1-6: Sample  $\varepsilon = 90^\circ$  Sky Map FITS header

```

SIMPLE =          T / file does conform to FITS standard
BITPIX =          32 / number of bits per data pixel
NAXIS  =          0 / number of data axes
EXTEND =          T / FITS dataset may contain extensions
COMMENT  FITS (Flexible Image Transport System) format defined in Astronomy and
COMMENT  Astrophysics Supplement Series v44/p363, v44/p371, v73/p359, v73/p365.
COMMENT  Contact the NASA Science Office of Standards and Technology for the
COMMENT  FITS Definition document #100 and other FITS information.
DATE    = '11/02/97'      / FITS file creation date (dd/mm/yy)
DATE-MAP= '04/04/96'      / Date of original file creation (dd/mm/yy)
ORIGIN  = 'CDAC   '      / Cosmology Data Analysis Center
TELESCOP= 'COBE   '      / Cosmic Background Explorer satellite
INSTRUME= 'DIRBE  '      / COBE instrument [DIRBE, DMR, FIRAS]
OBJECT  = 'ALL-SKY '      / part of sky given [e.g., ALL-SKY, WEEKLY-SKY,
COMMENT  /              DAILY-SKY, GAL-SLICE, FACE ...]
EQUINOX =          2000.0 / equinox of coords in following tables
REFERENC= 'COBE/DIRBE Explanatory Supplement,' /
REFERENC= 'ed. M.G. Hauser, T. Kelsall, D. Leisawitz, and J. Weiland,' /
REFERENC= 'COBE Ref. Pub. No. 97-A (Greenbelt,MD: NASA/GSFC),' /
REFERENC= 'available in electronic form from the NSSDC.' /
COMMENT
COMMENT  COBE specific keywords
DATE-BEG= '08/12/89'      / date of initial data represented (dd/mm/yy)
DATE-END= '25/09/90'      / date of final data represented (dd/mm/yy)
PIXRESOL=          9 / Quad tree pixel resolution [6, 9]
COMMENT
COMMENT  DIRBE specific keywords
PRODUCT = 'B1A_E90 '      / Band 1A map for solar elongation = 90 deg.
VERSION = 'Pass 3B '      / Version of Data Reduction Software
WAVE1   = '1.25 microns'  / nominal wavelength of Band 1

```

```

SOLELONG= '90 degrees'      / only solar elongations of 90 deg. represented
APPVEC  = 'COMBINED'       / data having different approach vectors
COMMENT                               / are combined during processing
ZLREMOV =                   F / zodiacal foreground removal indicator
COMMENT                               / if 'T(ue)', zodi foreground has been removed
COMMENT                               / if 'F(alse)', observed sky brightness is given
COMMENT
COMMENT
END

```

```

XTENSION= 'BINTABLE'       / Extension type is Binary Table
BITPIX  =                   8 / Binary data
NAXIS   =                   2 / Data are in a table
NAXIS1  =                   21 / Number of 8 bit bytes in each row
NAXIS2  =                   616474 / Number of rows
PCOUNT  =                   0 / Number of bytes of data following table
GCOUNT  =                   1 / Group count (always 1 for bintable extensions)
TFIELDS =                   7 / Number of fields (columns) in the table
COMMENT
COMMENT

```

```

TIMVERSN= 'OGIP/93-003'    / GSFC Office of Guest Investigator Programs (OGIP)
COMMENT                               / memo in which the convention is described
COMMENT                               The times reported in this file are International
COMMENT                               Atomic Time (TAI) seconds elapsed since
COMMENT                               00:00:00 UTC, 1 January 1981. Time information is
COMMENT                               recorded in a manner consistent with the convention specified
COMMENT                               in OGIP/93-003 with the understanding that time is counted
COMMENT                               in atomic seconds and the origin of time (MJDREF) is quoted
COMMENT                               in ephemeris MJD.
TIMESYS = '1981.00'       / time system (same as IRAS)
MJDREFI =                   44605 / Integer portion of ephemeris MJD
COMMENT                               / corresponding to 0h UTC 1 Jan 1981
MJDREFF =                   0.00059240741 / Fractional portion of ephemeris MJD
COMMENT                               / corresponding to 0h UTC 1 Jan 1981
TIMEUNIT= 's'             / unit for TSTART, TSTOP, TIMEZERO = seconds
TSTART  =                   282007138.349 / observation start time in TIMESYS system
TSTOP   =                   307119590.188 / observation stop time in TIMESYS system
COMMENT
COMMENT

```

```

COMMENT -----
COMMENT *****
COMMENT Sky Map Interpolated to Solar Elongation=90 deg -- 1.25 microns
COMMENT Photometric data for Band 1A (1.25 microns) interpolated
COMMENT to a fixed solar elongation of 90 degrees using
COMMENT Weekly-Averaged Sky Maps as the basis for the
COMMENT interpolation.
COMMENT This map represents the sky as it would be
COMMENT observed at an elongation of 90 deg.; i.e., signal from
COMMENT the interplanetary dust cloud has not been removed.
COMMENT Since the data represented here cover a time range
COMMENT of 10 months, it is possible for a pixel to have
COMMENT more than one entry.
COMMENT

```

```

COMMENT *****
COMMENT -----
COMMENT =====
COMMENT Coordinate Information (Spatial and Temporal):
COMMENT =====
COMMENT -----
COMMENT      DIRBE Pixel number (resolution 9)
TTYPE1 = 'Pixel_no'          / pipeline fieldname = Pixel_no
TUNIT1 = '          '        /
TFORM1 = '1J          '      /
COMMENT -----
COMMENT      Time in International Atomic Time (TAI) seconds elapsed
COMMENT      since 01-JAN-1981:00:00:00.000 UTC.
COMMENT      Computed time corresponding to observation of pixel
COMMENT      at solar elongation = 90 deg.
COMMENT      Note that some of the quoted times fall outside of the
COMMENT      boundaries during which actual observations were made. This
COMMENT      is because extrapolations have been permitted under a limited
COMMENT      set of circumstances, as indicated by the Fit Quality
COMMENT      Flag (FitQual).
TTYPE2 = 'Time          '    / pipeline fieldname = Time
TUNIT2 = 's            '    /
TFORM2 = '1D          '    /
COMMENT -----
COMMENT =====
COMMENT      DIRBE Sky Brightness Information:
COMMENT =====
COMMENT -----
COMMENT      Photometry for Band 1A, interpolated to solar elongation 90 deg.
COMMENT      The photometric measurements are given as
COMMENT      spectral intensities, I(nu) in MJy/sr, and
COMMENT      are quoted at the nominal wavelength
COMMENT      for a source with nu*I(nu) = constant -- i.e.,
COMMENT      a color correction is required if the source
COMMENT      spectrum differs from nu*I(nu) = constant.
COMMENT      Data which have been replaced by flagged values
COMMENT      in processing have values .LE. -16375.
TTYPE3 = 'Photomet'       / pipeline fieldname = Photometry
TUNIT3 = 'MJy/sr        ' / MegaJanskys/steradian
TFORM3 = '1E           ' /
COMMENT -----
COMMENT      Effective number of observations of the
COMMENT      pixel over the mission. This is an approximate
COMMENT      number, calculated from the average of the weekly
COMMENT      weighted numbers of observations for all detectors.
TTYPE4 = 'EfNumObs'      / pipeline fieldname = Effective_num_obs
TUNIT4 = '              ' /
TFORM4 = '1I           ' /
COMMENT -----
COMMENT      Standard Deviation
COMMENT      Relative or absolute standard deviation
COMMENT      of the interpolated/extrapolated
COMMENT      photometry, given in logarithmic bins.
COMMENT      Units = none (Bands 1 - 8)

```

```

COMMENT          = MJy/sr (Bands 9 and 10)
COMMENT          Range = [0,255]
COMMENT          The contents B of the Standard_Deviation
COMMENT          byte have been found from the relative
COMMENT          standard deviations  $R = \sigma(I)/ABS(I)$  (Bands
COMMENT          1 through 8) or absolute standard deviations R
COMMENT          (Bands 9 and 10) as follows:
COMMENT          N = 3: Bands 1 - 4, 7 and 8
COMMENT          N = 4: Bands 5 and 6
COMMENT          N = 1: Bands 9 and 10
COMMENT
COMMENT          if R <= 10**(-N)          then B = 0
COMMENT          if 10**(-N) < R < 10**(-N+4) then B = IFIX((N+log10(R))*254./4.)+1
COMMENT          if R >= 10**(-N+4)        then B = 255
COMMENT
COMMENT          Conversely, the standard deviations can be reconstructed by:
COMMENT          R <= 10**(-N)          if B = 0
COMMENT          R = 10**(4*(B-0.5)/254. - N) if 1 <= B <= 254
COMMENT          R >= 10**(-N+4)        if B = 255
COMMENT
COMMENT          StdDev = R * ABS(I) (Bands 1 - 8)
COMMENT          StdDev = R          (Bands 9, 10)
COMMENT          (The maximum error on the reconstructed value is 1.8 %)
COMMENT
TTYPE5 = 'StdDev ' / pipeline filename = Standard_Deviation
TUNIT5 = ' ' /
TFORM5 = '1B ' /
COMMENT -----
COMMENT          Fit Quality Flag
COMMENT          quality of interpolation to elongation = 90 deg.
COMMENT          Bit 0 = least significant bit
COMMENT
COMMENT          Bits 0-3: Indicator for solar system
COMMENT          object effects and interpolation
COMMENT          quality
COMMENT          0000: No special problems
COMMENT          0001: One or more weekly average(s)
COMMENT          had data removed due to solar
COMMENT          system object contamination.
COMMENT          0010: Only two points (weekly averages)
COMMENT          available for the interpolation. Expect
COMMENT          systematic error.
COMMENT          0100: Average value used rather than interpolated
COMMENT          value, for quality reasons.
COMMENT          1111: Interpolation impossible. Intensity set to
COMMENT          a flagged value (.LE. -16375.)
COMMENT
COMMENT          Bits 4-7: Interpolation type indicator:
COMMENT          0000: Interpolation
COMMENT          0001: Extrapolation from observations
COMMENT          which have elongations > 90 deg.
COMMENT          0010: Extrapolation from observations
COMMENT          which have elongations < 90 deg.
COMMENT          0100: One weekly average was flagged

```

```

COMMENT          as an outlier and not used in
COMMENT          the interpolation process.
COMMENT
TTYPE6 = 'FitQual' / pipeline fieldname = Interpolation_flag, Byte 1
TUNIT6 = '        ' /
TFORM6 = '1B      ' /
COMMENT -----
COMMENT          Fit Chi-squared per degree of freedom
COMMENT          Chi-squared per degree of freedom
COMMENT          for the fit used in the interpolation.
TTYPE7 = 'FitChiSq' / pipeline fieldname = Interpolation_flag, Byte 2
TUNIT7 = '        ' /
TFORM7 = '1B      ' /
TSCAL7 =          0.10 / bin size 0.1
TZERO7 =          0.0 /
COMMENT -----
END

```

#### D.1.1.5 Galactic Plane Maps

Table D.1-7: The Galactic Plane Maps FITS header

```

SIMPLE =          T / file does conform to FITS standard
BITPIX =          32 / number of bits per data pixel
NAXIS  =          0 / number of data axes
EXTEND =          T / FITS dataset may contain extensions
COMMENT  FITS (Flexible Image Transport System) format defined in Astronomy and
COMMENT  Astrophysics Supplement Series v44/p363, v44/p371, v73/p359, v73/p365.
COMMENT  Contact the NASA Science Office of Standards and Technology for the
COMMENT  FITS Definition document #100 and other FITS information.
DATE    = '11/02/97' / FITS file creation date (dd/mm/yy)
DATE-MAP= '29/08/96' / Date of original data file creation (dd/mm/yy)
ORIGIN  = 'CDAC    ' / Cosmology Data Analysis Center
TELESCOP= 'COBE   ' / Cosmic Background Explorer satellite
INSTRUME= 'DIRBE  ' / COBE instrument [DIRBE, DMR, FIRAS]
OBJECT  = 'GAL-SLICE' / part of sky given [e.g., ALL-SKY, WEEKLY-SKY,
COMMENT  /          DAILY-SKY, GAL-SLICE, FACE ...]
EQUINOX =          2000.0 / equinox of coords in following tables
REFERENC= 'COBE/DIRBE Explanatory Supplement,' /
REFERENC= 'ed. M.G. Hauser, T. Kelsall, D. Leisawitz, and J. Weiland,' /
REFERENC= 'COBE Ref. Pub. No. 97-A (Greenbelt,MD: NASA/GSFC),' /
REFERENC= 'available in electronic form from the NSSDC.' /
COMMENT
COMMENT
COMMENT          COBE specific keywords
DATE-BEG= '01/01/90' / date of initial data represented (dd/mm/yy)
DATE-END= '02/07/90' / date of final data represented (dd/mm/yy)
PIXRESOL=          9 / Quad tree pixel resolution [6, 9]
COMMENT
COMMENT
COMMENT          DIRBE specific keywords
PRODUCT = 'GPM    ' / Galactic Plane Maps

```

```

VERSION = 'Pass 3B '           / Version of Data Reduction Software
WAVE1   = '1.25 microns'      / nominal wavelength of Band 1
WAVE2   = '2.2 microns'      / nominal wavelength of Band 2
WAVE3   = '3.5 microns'      / nominal wavelength of Band 3
WAVE4   = '4.9 microns'      / nominal wavelength of Band 4
WAVE5   = '12. microns'      / nominal wavelength of Band 5
WAVE6   = '25. microns'      / nominal wavelength of Band 6
WAVE7   = '60. microns'      / nominal wavelength of Band 7
WAVE8   = '100. microns'     / nominal wavelength of Band 8
WAVE9   = '140. microns'     / nominal wavelength of Band 9
WAVE10  = '240. microns'     / nominal wavelength of Band 10
SOLELONG= '90 degrees'       / only solar elongations of 90 deg. represented
APPVEC  = 'COMBINED'         / data having different approach vectors
COMMENT / are combined during processing
ZLREMOV = F                   / zodiacal foreground removal indicator
COMMENT / if 'T(true)', zodi foreground has been removed
COMMENT / if 'F(false)', observed sky brightness is given
COMMENT
COMMENT
COMMENT
COMMENT
COMMENT
END

XTENSION= 'BINTABLE'         / Extension type is Binary Table
BITPIX  = 8                   / Binary data
NAXIS   = 2                   / Data are in a table
NAXIS1  = 80                  / Number of 8 bit bytes in each row
NAXIS2  = 73644               / Number of rows
PCOUNT  = 0                   / Number of bytes of data following table
GCOUNT  = 1                   / Group count (always 1 for bintable extensions)
TFIELDS = 8                   / Number of fields (columns) in the table
COMMENT
TIMVERSN= 'OGIP/93-003'      / GSFC Office of Guest Investigator Programs (OGIP)
COMMENT / memo in which the convention is described
COMMENT The times reported in this file are International
COMMENT Atomic Time (TAI) seconds elapsed since
COMMENT 00:00:00 UTC, 1 January 1981. Time information is
COMMENT recorded in a manner consistent with the convention specified
COMMENT in OGIP/93-003 with the understanding that time is counted
COMMENT in atomic seconds and the origin of time (MJDREF) is quoted
COMMENT in ephemeris MJD.
TIMESYS = '1981.00 '         / time system (same as IRAS)
MJDREFI = 44605              / Integer portion of ephemeris MJD
COMMENT / corresponding to 0h UTC 1 Jan 1981
MJDREFF = 0.00059240741     / Fractional portion of ephemeris MJD
COMMENT / corresponding to 0h UTC 1 Jan 1981
TIMEUNIT= 's'                / unit for TSTART, TSTOP, TIMEZERO = seconds
TSTART  = 283996977.572     / observation start time in TIMESYS system
TSTOP   = 299759964.990     / observation stop time in TIMESYS system
COMMENT
COMMENT
COMMENT -----
COMMENT *****
COMMENT Galactic-Plane Sky Maps --

```



```

COMMENT      Photometric data for 10 bands (1.25 - 240 microns),
COMMENT      interpolated to a fixed solar elongation of 90 degrees
COMMENT      using Weekly-averaged sky maps as the basis for the
COMMENT      interpolation.
COMMENT      Array contains data only for pixels whose Galactic
COMMENT      coordinates satisfy the conditions:
COMMENT      -10 < b < +10 deg for 30 < l < 330 deg
COMMENT      -15 < b < +15 deg for 330 < l < 360 and 0 < l < 30 deg
COMMENT      *****
COMMENT      -----
COMMENT      DIRBE Pixel number (resolution 9)
TTYPE1 = 'Pixel_no'          / pipeline fieldname = Pixel_no
TUNIT1 = '          '        /
TFORM1 = '1J          '      /
COMMENT      -----
COMMENT      Photometry
COMMENT      10 intensities, in increasing band number
COMMENT      order (1A,2A,3A,4,5,6,7,8,9,10),
COMMENT      interpolated to solar elongation 90 deg.
COMMENT      The photometric measurements are given as
COMMENT      spectral intensities, I(nu) in MJy/sr, and
COMMENT      are quoted at the nominal wavelength
COMMENT      for a source with nu*I(nu) = constant -- i.e.,
COMMENT      a color correction is required if the source
COMMENT      spectrum differs from nu*I(nu) = constant.
COMMENT      Data which have been replaced by flagged values
COMMENT      in processing have values .LE. -16375.
TTYPE2 = 'Photomet'         / pipeline fieldname = Photometry
TUNIT2 = 'MJy/sr '         / MegaJanskys/steradian
TFORM2 = '10E          '   /
TDIM2  = '(10)          '  /
COMMENT      -----
COMMENT      Data quality flag
COMMENT      Indicates quality of interpolation to elongation = 90 deg.
COMMENT      for each photometric measure.
COMMENT      Listed in increasing band number order: (1A,2A,3A,4,5,6,7,8,9,10)
COMMENT
COMMENT      Byte 1 (least significant byte):
COMMENT      Bit 0 = least significant bit
COMMENT      Bits 0-3: Indicator for input data
COMMENT      quality and interpolation quality:
COMMENT      0001: One or more weekly average(s)
COMMENT      had some data removed due to solar
COMMENT      system object contamination.
COMMENT      0010: Only two points (weekly averages)
COMMENT      available for the interpolation. Expect
COMMENT      systematic error.
COMMENT      0100: Average value used rather than interpolated
COMMENT      value, for quality reasons.
COMMENT      1111: Interpolation impossible. Photometry set
COMMENT      to a flagged value (.LE. -16375.)
COMMENT
COMMENT

```

```

COMMENT      Bits 4-7: Interpolation type indicator:
COMMENT      0000: Interpolation
COMMENT      0001: Extrapolation from above
COMMENT          ( > specified elongation)
COMMENT      0010: Extrapolation from below
COMMENT          ( < specified elongation)
COMMENT      0100: One weekly average was flagged
COMMENT          as an outlier and not used in
COMMENT          the interpolation process.
COMMENT
COMMENT
COMMENT      Byte 2 (most significant byte):
COMMENT      Relative or absolute standard deviation
COMMENT          on the interpolated/extrapolated
COMMENT          intensity for each band, given in
COMMENT          logarithmic binning.
COMMENT          Units = none   (Bands 1 - 8)
COMMENT                   = MJy/sr (Bands 9 and 10)
COMMENT          Range = [0,255]
COMMENT      The byte value B has been found from the
COMMENT      RELATIVE standard deviation  $R = \sigma(I)/ABS(I)$  (Bands 1 to 8)
COMMENT      or ABSOLUTE standard deviation  $R = \sigma(I)$  (Bands 9 and 10)
COMMENT      as follows:
COMMENT          N = 3: Bands 1 - 4, 7 and 8
COMMENT          N = 4: Bands 5 and 6
COMMENT          N = 1: Bands 9 and 10
COMMENT
COMMENT      if  $R \leq 10^{*-N}$  then B = 0
COMMENT      if  $10^{*-N} < R < 10^{*(-N+4)}$  then B = IFIX((N+log10(R))*254./4.)+1
COMMENT      if  $R \geq 10^{*(-N+4)}$  then B = 255
COMMENT
COMMENT      Conversely, the sigma value can be reconstructed by:
COMMENT       $R \leq 10^{*-N}$  if B = 0
COMMENT       $R = 10^{*(4*(B-0.5)/254. - N)}$  if  $1 \leq B \leq 254$ 
COMMENT       $R \geq 10^{*(-N+4)}$  if B = 255
COMMENT
COMMENT      sigma = R * ABS(I) (Bands 1 - 8)
COMMENT      sigma = R (Bands 9 and 10)
COMMENT      (The maximum error on the reconstructed value is 1.8 %)
TTYPE3 = 'PhotQual' / pipeline fieldname = Phot_quality
TUNIT3 = ' ' /
TFORM3 = '10I ' /
TDIM3 = '(10) ' /
COMMENT -----
COMMENT      Time in International Atomic Time (TAI) seconds
COMMENT      elapsed since 1-JAN-1981:00:00:00.000 UTC.
COMMENT      Computed time corresponding to observation
COMMENT      of pixel at solar elongation = 90 deg.
TTYPE4 = 'TIME ' / pipeline fieldname = Time
TUNIT4 = 's ' /
TFORM4 = '1D ' /
COMMENT -----

```

```

COMMENT      Ecliptic longitude of pixel center
COMMENT      range = [0,360) degrees
TTYPE5 = 'EcLon   ' / pipeline fieldname = Ecliptic_longitude
TUNIT5 = 'deg     ' /
TFORM5 = '1I     ' /
TSCAL5 =          0.0109867 / bin size 360/(2**15-1) degrees
TZERO5 =          0.00549333 / offset to bin center in degrees
COMMENT      -----
COMMENT      Ecliptic latitude of pixel center
COMMENT      range = [-90, 90] degrees
TTYPE6 = 'EcLat   ' / pipeline fieldname = Ecliptic_latitude
TUNIT6 = 'deg     ' /
TFORM6 = '1I     ' /
TSCAL6 =          0.0109867 / bin size 360/(2**15-1) degrees
TZERO6 =          0.00549333 / offset to bin center in degrees
COMMENT      -----
COMMENT      Galactic longitude of pixel center
COMMENT      range = [0,360) degrees
TTYPE7 = 'GaLon   ' / pipeline fieldname = Galactic_longitude
TUNIT7 = 'deg     ' /
TFORM7 = '1I     ' /
TSCAL7 =          0.0109867 / bin size 360/(2**15-1) degrees
TZERO7 =          0.00549333 / offset to bin center in degrees
COMMENT      -----
COMMENT      Galactic latitude of pixel center
COMMENT      range = [-90, 90] degrees
TTYPE8 = 'GaLat   ' / pipeline fieldname = Galactic_latitude
TUNIT8 = 'deg     ' /
TFORM8 = '1I     ' /
TSCAL8 =          0.0109867 / bin size 360/(2**15-1) degrees
TZERO8 =          0.00549333 / offset to bin center in degrees
COMMENT      -----
END

```

#### D.1.1.6 Annual Average Sky Maps

Table D.1-8: Sample Annual Average Sky Map FITS header

```

SIMPLE =          T / file does conform to FITS standard
BITPIX =          32 / number of bits per data pixel
NAXIS  =          0 / number of data axes
EXTEND  =          T / FITS dataset may contain extensions
COMMENT  FITS (Flexible Image Transport System) format defined in Astronomy and
COMMENT  Astrophysics Supplement Series v44/p363, v44/p371, v73/p359, v73/p365.
COMMENT  Contact the NASA Science Office of Standards and Technology for the
COMMENT  FITS Definition document #100 and other FITS information.
DATE    = '11/02/97' / FITS file creation date (dd/mm/yy)
DATE-MAP= '04/04/96' / Date of original file creation (dd/mm/yy)
ORIGIN  = 'CDAC   ' / Cosmology Data Analysis Center
TELESCOP= 'COBE   ' / Cosmic Background Explorer satellite
INSTRUME= 'DIRBE  ' / COBE instrument [DIRBE, DMR, FIRAS]

```

```

OBJECT = 'ALL-SKY ' / part of sky given [e.g., ALL-SKY, WEEKLY-SKY,
COMMENT / DAILY-SKY, GAL-SLICE, FACE ...]
EQUINOX = 2000.0 / equinox of coords in following tables
REFERENC= 'COBE/DIRBE Explanatory Supplement,' /
REFERENC= 'ed. M.G. Hauser, T. Kelsall, D. Leisawitz, and J. Weiland,' /
REFERENC= 'COBE Ref. Pub. No. 97-A (Greenbelt,MD: NASA/GSFC),' /
REFERENC= 'available in electronic form from the NSSDC.' /
COMMENT
COMMENT COBE specific keywords
DATE-BEG= '11/12/89' / date of initial data represented (dd/mm/yy)
DATE-END= '21/09/90' / date of final data represented (dd/mm/yy)
PIXRESOL= 9 / Quad tree pixel resolution [6, 9]
COMMENT
COMMENT DIRBE specific keywords
PRODUCT = 'B1A_AAM ' / Band 1A Annual Average Sky Map
VERSION = 'Pass 3B ' / Version of Data Reduction Software
WAVE1 = '1.25 microns' / nominal wavelength of Band 1
SOLELONG= 'ALL ' / all available solar elongations included
APPVEC = 'COMBINED' / data having different approach vectors
COMMENT / are combined during processing
ZLREMOV = F / zodiacal foreground removal indicator
COMMENT / if 'T(true)', zodi foreground has been removed
COMMENT / if 'F(false)', observed sky brightness is given
COMMENT
COMMENT
END

XTENSION= 'BINTABLE' / Extension type is Binary Table
BITPIX = 8 / Binary data
NAXIS = 2 / Data are in a table
NAXIS1 = 27 / Number of 8 bit bytes in each row
NAXIS2 = 393216 / Number of rows
PCOUNT = 0 / Number of bytes of data following table
GCOUNT = 1 / Group count (always 1 for bintable extensions)
TFIELDS = 7 / Number of fields (columns) in the table
COMMENT
COMMENT
TIMVERSN= 'OGIP/93-003' / GSFC Office of Guest Investigator Programs (OGIP)
COMMENT / memo in which the convention is described
COMMENT The times reported in this file are International
COMMENT Atomic Time (TAI) seconds elapsed since
COMMENT 00:00:00 UTC, 1 January 1981. Time information is
COMMENT recorded in a manner consistent with the convention specified
COMMENT in OGIP/93-003 with the understanding that time is counted
COMMENT in atomic seconds and the origin of time (MJDREF) is quoted
COMMENT in ephemeris MJD.
TIMESYS = '1981.00 ' / time system (same as IRAS)
MJDREFI = 44605 / Integer portion of ephemeris MJD
COMMENT / corresponding to 0h UTC 1 Jan 1981
MJDREFF = 0.00059240741 / Fractional portion of ephemeris MJD
COMMENT / corresponding to 0h UTC 1 Jan 1981
TIMEUNIT= 's ' / unit for TSTART, TSTOP, TIMEZERO = seconds
TSTART = 282185275.611 / observation start time in TIMESYS system
TSTOP = 306753235.358 / observation stop time in TIMESYS system

```

```

COMMENT
COMMENT
COMMENT -----
COMMENT *****
COMMENT     Annual Average Sky Map -- 1.25 microns
COMMENT     Mission-averaged photometric measurements and cumulative
COMMENT     sky coverage data for DIRBE Band 1A (1.25 microns).
COMMENT     The photometry is computed from the weighted average of all
COMMENT     available weekly-averaged maps for the entire mission,
COMMENT     up to the time when the cryogen supply was exhausted.
COMMENT     The foreground signal from Zodiacal dust remains in the map.
COMMENT *****
COMMENT -----
COMMENT =====
COMMENT Coordinate Information (Spatial and Temporal):
COMMENT =====
COMMENT -----
COMMENT     DIRBE Pixel number (resolution 9)
COMMENT     TTYPE1 = 'Pixel_no'           / pipeline fieldname = Pixel_no
COMMENT     TUNIT1 = '          '         /
COMMENT     TFORM1 = '1J          '       /
COMMENT -----
COMMENT     Sub-pixel containing the mean DIRBE LOS (line-of-sight)
COMMENT     when pixel is divided into 256
COMMENT     sub-pixels (16x16 grid) according to
COMMENT     standard quad-sphere rules.
COMMENT     TTYPE2 = 'PSubPos '           / pipeline fieldname = Pixel_subpos
COMMENT     TUNIT2 = '          '         /
COMMENT     TFORM2 = '1B          '       /
COMMENT -----
COMMENT     Time in International Atomic Time (TAI) seconds
COMMENT     elapsed since 01-JAN-1981:00:00:00.000 UTC.
COMMENT     This is the average time of all observations of a pixel
COMMENT     within the time interval TSTART to TSTOP,
COMMENT     regardless of the weight assigned to a particular observation.
COMMENT     For this product, not a physically meaningful quantity.
COMMENT     TTYPE3 = 'Time          '       / pipeline fieldname = Time
COMMENT     TUNIT3 = '          '         /
COMMENT     TFORM3 = '1D          '       /
COMMENT -----
COMMENT =====
COMMENT     DIRBE Sky Brightness Information:
COMMENT =====
COMMENT -----
COMMENT     Cumulative weighted average of the 1.25 micron photometry.
COMMENT     This average is calculated using the weighted number of
COMMENT     observations from each Weekly Averaged Map ( WtNumObs from
COMMENT     the Weekly Averaged Map) as the weight, such that
COMMENT     annual_average =
COMMENT         sum( weekly_average * weekly_weight )/ sum( weekly_weight )
COMMENT
COMMENT     The photometric measurement is given as a
COMMENT     spectral intensity, I(nu) in MJy/sr, and
COMMENT     is quoted at the nominal wavelength

```

```

COMMENT      for a source with nu*I(nu) = constant -- i.e.,
COMMENT      a color correction is required if the source
COMMENT      spectrum differs from nu*I(nu) = constant.
COMMENT      Data which have been replaced by flagged values
COMMENT      in processing have values .LE. -16375.
COMMENT
TTYPE4 = 'Photomet'          / pipeline fieldname = Photometry
TUNIT4 = 'MJy/sr '          /
TFORM4 = '1E '              /
COMMENT -----
COMMENT      The standard deviation of the (weighted) average photometry
COMMENT      values.
TTYPE5 = 'StdDev '          / pipeline fieldname = Standard_deviation
TUNIT5 = 'MJy/sr '          /
TFORM5 = '1E '              /
COMMENT -----
COMMENT      Sum of the weekly weighted number of observations that went into
COMMENT      forming the annual averages.
TTYPE6 = 'WtNumObs'         / pipeline fieldname = Weighted_num_obs
TUNIT6 = ' '                /
TFORM6 = '1I '              /
COMMENT -----
COMMENT      Sum of the total number of observations available, regardless
COMMENT      of assigned weight.
TTYPE7 = 'SumNRecs'         / pipeline fieldname = Sum_numrecs
TUNIT7 = ' '                /
TFORM7 = '1J '              /
COMMENT -----
END

```

#### D.1.1.7 Beam Profiles

Table D.1-9: Sample Beam Profile FITS header

```

SIMPLE =          T / file does conform to FITS standard
BITPIX =         -32 / REAL*4 data
NAXIS  =          3 / number of data axes
NAXIS1 =         225 / in-scan axis
NAXIS2 =         181 / cross-scan axis
NAXIS3 =          3 / time-period axis
DATE-MAP= '30/06/95' / Date of original data file creation (dd/mm/yy)
DATE    = '11/02/97' / FITS file creation date (dd/mm/yy)
ORIGIN  = 'CDAC'    / Cosmology Data Analysis Center
TELESCOP= 'COBE'   / Cosmic Background Explorer satellite
INSTRUME= 'DIRBE'  / COBE instrument [DIRBE, DMR, FIRAS]
OBJECT  = 'BEAM'   / DIRBE beam profile map
REFERENC= 'COBE/DIRBE Explanatory Supplement,' /
REFERENC= 'ed. M.G. Hauser, T. Kelsall, D. Leisawitz, and J. Weiland,' /
REFERENC= 'COBE Ref. Pub. No. 97-A (Greenbelt,MD: NASA/GSFC),' /
REFERENC= 'available in electronic form from the NSSDC.' /
COMMENT

```

```

COMMENT      COBE specific keywords
DATE-BEG= '11/12/89'      / date of initial data represented (dd/mm/yy)
DATE-END= '21/09/90'      / date of final data represented (dd/mm/yy)
COMMENT
COMMENT      DIRBE specific keywords
PRODUCT = 'BEAM1A'        / DIRBE Band 1A beam profile
VERSION = 'Pass 3B'       / Version of Data Reduction Software
WAVE1   = '1.25 microns'   / nominal wavelength of Band 1
SOLELONG= 'ALL'           / all available solar elongations used
APPVEC  = 'COMBINED'      / data having different approach vectors
COMMENT      / are combined during processing
COMMENT
COMMENT
COMMENT -----
COMMENT *****
COMMENT      Beam Profile -- DIRBE Band 1A.
COMMENT      This is an effective beam profile, which measures the
COMMENT      relative response of the DIRBE to a point source, including
COMMENT      the effects of sky-scanning and data-sampling rates.
COMMENT      Beam profiles are represented as two-dimensional
COMMENT      arrays which give the beam response as a
COMMENT      function of in-scan and cross-scan position.
COMMENT      In-scan position is defined as positive
COMMENT      toward the scan direction, and cross-scan position is
COMMENT      defined as positive toward the spacecraft spin-axis.
COMMENT      The origin (0,0) corresponds to the nominal boresight
COMMENT      position as defined from the attitude solution.
COMMENT
COMMENT      Beam profiles for Band 1A were noted to be
COMMENT      slightly time-dependent. Therefore, 3 beam profiles are
COMMENT      recorded here, covering the following time intervals (YYDDD):
COMMENT      beam #1: 89345 - 90175 (inclusive)
COMMENT      beam #2: 90176 - 90231 (inclusive)
COMMENT      beam #3: 90232 - 90264 (inclusive)
COMMENT
COMMENT      Beam #1 is normalized to a value of 1.0 at the
COMMENT      location of peak response. Beams #2 and #3
COMMENT      are normalized such that the beam profile solid angle
COMMENT      is constant during the cold mission, using the solid angle
COMMENT      found for Beam #1. The peak response of beams #2 and #3
COMMENT      differs from unity by less than 1%.
COMMENT
COMMENT      The beam solid angle for Band 1A used in the Pass3B data
COMMENT      processing is 1.198 e-04 sr.
COMMENT *****
COMMENT -----
CRVAL1 =          0.000000 / Value at origin (arcmin)
CRPIX1 =          113 / position of origin
CTYPE1 = 'INSCAN'      / in-scan coordinate; range +- 42 arcmin
CDEL1  =          0.375000 / in-scan sampling increment, arcmin per pixel
COMMENT -----
CRVAL2 =          0.000000 / Value at origin (arcmin)
CRPIX2 =           91 / position of origin
CTYPE2 = 'XSCAN'      / x-scan coordinate; range +- 36 arcmin

```

```

CDELTA2 =          0.400000 / x-scan sampling increment, arcmin per pixel
COMMENT  -----
CRVAL3  =          1 /
CRPIX3  =          1 /
CTYPE3  = 'BEAM-NO'      / beam number; range 1-3
CDELTA3 =          1 /
COMMENT  -----
END

```

### D.1.2 FORTRAN Access to the *DIRBE* Data Products

The *FITSIO* subroutines mentioned in §D.1 may be called from a FORTRAN program in order to read FITS-encoded data. The following examples illustrate how FORTRAN programs can be used to read the Solar Elongation = 90° Sky Maps and the *DIRBE\_SKYMAP\_INFO.FITS* file.

#### D.1.2.1 Access to the $\varepsilon = 90^\circ$ Sky Maps

```

program dirbe_e90_read

c -----
c A simple program to read the FITS binary table data from the
c DIRBE pixelized Solar Elongation = 90 degree Sky Maps. This
c program uses the FITSIO package developed by HEASARC at NASA GSFC.
c This program reads in the PHOTOMET field which contains the
c actual data. Also read in are the PIXEL_NO, TIME and STDDEV field.
c The STDDEV is then unpacked into the quantity SIGMA for each pixel
c for the given band.
c -----

implicit none

integer maxdim
parameter (maxdim = 20)

character*30 errtxt,extnam
character*30 ttype(maxdim), tform(maxdim), tunit(maxdim)
character*80 filename
character*80 comment
character*12 c_res

logical simple, extend, anyflg

integer iunit, status, bitpix, naxis, naxes(maxdim)
integer pcount, gcount
integer group, nelem, nrows
integer i, j, itemp, n, k
integer tfield, rwstat, bksize, vardat
integer colnum, frow, felem
integer hdu typ, inull

c

integer res, pixel(616474)
integer bandno
integer*2 stddev(616474)

```



```

real    photomet(616474), enull, sigma(616474)
real*8   time(616474)

status = 0
iunit = 15

c -----
c   open the existing  FITS file with readonly access
c -----
      rwstat = 0
      print *, 'Enter file name '
read(*,2000) filename
2000  format(a)
      print *, 'Enter Band number '
read(*,2001) bandno
2001  format(i)
      call ftopen(iunit, filename, rwstat, bksize, status)
      if (status .ne. 0) goto 1000

c -----
c   read in the required primary array keywords
c -----
      call ftghpr(iunit, maxdim, simple, bitpix, naxis, naxes,
%           pcount, gcount, extend, status)
      if (status .ne. 0) goto 1000

c -----
c   Get in the COBE specific field, RES which defines the resolution
c   of the data.  This is used to calculate the pixel numbers which
c   correspond to a specific face of the skycube.
c -----
      call ftgkey(iunit, 'PIXRESOL', c_res, comment, status)
      read(c_res, '(i1)') res
      print*, 'This file is at resolution: ',res

c -----
c   now move onto the binary table extension
c -----
      call ftmahd(iunit, 2, hdu typ, status)
      if (status .ne. 0) goto 1000

c -----
c   get the binary table parameters
c -----
      call ftghbn(iunit, maxdim, n rows, tfield, ttype, tform,
%           tunit, extnam, vardat, status)
      if (status .ne. 0) goto 1000

      print *, 'nrows: ',nrows

c -----
c   test that this is a DIRBE dataset, by looking at a few field names
c -----
      if (ttype(1) .ne. 'Pixel_no' .or.

```

```

%           ttype(3) .ne. 'Photomet' .or.
%           ttype(5) .ne. 'StdDev') then
    print *, 'This is not a DIRBE PDS/IP file'
    print *, 'ttype(1) = ', ttype(1)
    print *, 'ttype(3) = ', ttype(3)
    print *, 'ttype(5) = ', ttype(5)
    goto 1000
endif

c -----
c read in the pixel, photomet and photqual fields
c -----

write(6,*) 'reading in the data now'
do 100 frow = 1, nrows
    felem = 1
    nelelem = 1
    inull = 0

    colnum = 1
    call ftgcvj(iunit, colnum, frow, felem, nelelem, enull,
%           pixel(frow), anyflg, status)
%   if (status .ne. 0) write(6,*) '1frow:',frow,' status:',
%           status
%   if (status .ne. 0) goto 1000

    colnum = 2
    call ftgcvd(iunit, colnum, frow, felem, nelelem, enull,
%           time(frow), anyflg, status)
%   if (status .ne. 0) write(6,*) '1frow:',frow,' status:',
%           status
%   if (status .ne. 0) goto 1000

c -----
c note that for the photomet field and the phtoqual field we take
c 10 as the number of elements to read in.
c -----

    colnum = 3
    call ftgcve(iunit, colnum, frow, felem, nelelem, enull,
%           photomet(frow), anyflg, status)
%   if (status .ne. 0) write(6,*) '2frow:',frow,' status:',
%           status
%   if (status .ne. 0) goto 1000

    colnum = 5
    call ftgcvi(iunit, colnum, frow, felem, nelelem, enull,
%           stddev(frow), anyflg, status)
%   if (status .ne. 0) write(6,*) '3frow:',frow,' status:',
%           status
%   if (status .ne. 0) goto 1000

c -----
c extract the proper bytes from the PhotQual field
c -----

```

```

      N = 3
      I=bandno
      IF (I .GT. 8) N = 1
      IF (I .EQ. 5) N = 4
      IF (I .EQ. 6) N = 4
      IF (stddev(frow) .EQ. 0) THEN
        SIGMA(frow) = 10.0**(-N)
      ELSEIF (stddev(frow) .EQ. 255) THEN
        SIGMA(frow) = 10.0**(-N+4)
      ELSE
        SIGMA(frow) = 10.0**((stddev(frow) - 0.5)/63.5 - N)
      ENDIF

c -----
c NOTE, in the Initial Products AND some of the PDS the SIGMA's
c for Bands 1-8 are reported as relative SIGMA's while Bands 9
c and 10 are absolute SIGMA's.
c -----

      IF (I .LE. 8) SIGMA(frow) =
%         SIGMA(frow)*ABS(photomet(frow))
100    continue
      write(6,*) 'done reading in the data'

c -----
c now close the table and quit
c -----
      call ftclos(iunit, status)

      print *, 'next line is pixel,time,photomet,stddev(0-255),sigma'
      do j=1,10
        print *,pixel(j),time(j),photomet(j),stddev(j),sigma(j)
      end do

1000    if (status .le. 0) then
          print *, '*** Program completed successfully ***'
        else
c -----
c get the error description
c -----
          call ftgerr(status, errtxt)
          print *, '*** Error, program did not run successfully ***'
          print *, 'status =',status,': ',errtxt
        endif

      end

```

### D.1.2.2 Access to the Skymap Information Maps

program skyinfo

C A simple program to read in the primary data array from

```
C      the DIRBE_SKYMAP_INFO FITS file. The primary header is
C      also printed out in its entirety. The output array
C      PIXNUM is a 256,256,6 array where the third dimension
C      is the face number (i.e. 6 faces 0-5) and the first two
C      dimensions are the x and y positions. The value at any
C      given point is the pixel number at that point.
```

```
C      The orientation of the output is:
```

```
COMMENT          row  -----
COMMENT          n    |                |      n = NAXIS1 = NAXIS2
COMMENT          ^    |                |      n = 256
COMMENT          |    |                |
COMMENT          2    |                |
COMMENT          1    |                |
COMMENT          -----
COMMENT          1 2   -->      n
COMMENT                   column
```

```
integer iunit,status,bitpix,naxis,naxes(99),pcount,gcount
integer group,fpixel,nelem,i,j,rwstat,bksize
integer hdu typ,inull,nkeys,nmore
integer*4 pixnum(256,256,6)
logical simple,extend,anyflg
character*30 errtxt
character*80 fname,comm,record
```

```
status=0
```

```
iunit=15
```

```
C      open the existing FITS file with readonly access
```

```
rwstat=0
```

```
print *, 'Enter file name '
```

```
read(*,2000) fname
```

```
2000 format(a)
```

```
call ftopen(iunit,fname,rwstat,bksize,status)
```

```
C      read the required primary array keywords
```

```
call ftghpr(iunit,99,simple,bitpix,naxis,naxes,pcount,gcount,
```

```
& extend,status)
```

```
if (status .ne. 0)go to 99
```

```
C find out the number of keywords in the header
```

```
call ftghsp(iunit,nkeys,nmore,status)
```

```
C print out each keyword
```

```
do 10 i=1,nkeys
```

```
call ftgrec(iunit,i,record,status)
```

```
print *,record
```

```
10 continue
```

```
C      first, test to make sure this is a 3D array
```

```
if (naxis .ne. 3)then
```

```
print *, 'This program only works on a 3D FITS array'
```

```

        go to 100
    end if

C      read the raster
      inull=0
      group=0
      fpixel=1
      call ftg3dj(iunit,group,inull,naxes(1),naxes(2),naxes(1),
&      naxes(2),naxes(3),pixnum,anyflag,status)

C      now close the table and quit
      call ftclos(iunit,status)

99     if (status .le. 0)then
          print *,'*** Program completed successfully ***'
      else
C      get the error text description
          call ftgerr(status,errtxt)
          print *,'*** ERROR - program did not run successfully ***'
          print *,'status =',status,': ',errtxt
      end if

100    continue
      end

```

### D.1.2.3 Pixel Number to Coordinate Conversion

The following FORTRAN routines convert CSC pixel numbers (see §5.3) to longitude and latitude in the specified coordinate system (ecliptic, Galactic, or equatorial). The UIDL software described in §D.1.3 also has this capability. These routines apply only to Quadrilateralized Spherical Cubes of “resolution 9” or less. Standard *DIRBE* pixels are at resolution 9. The main program, `pix211`, is intended to be used as the basis for more comprehensive programs. Later in this section are listings of the `SUPER_CENPIX` and `SUPER_PIXNO` routines and associated subroutines, which work with “resolution 15” pixels.

```

      program pix211
!
! NAME:
!   pixel_2_uvec_2_lonlat
!
! PURPOSE:
!   Routine returns longitude and latitude pointing to center of
!   pixel given pixel number and resolution of the cube. The coordinate
!   system is an input. Note, all coordintes are at epoch=J2000.
!   Additionally the spherical quadrilateralized cube face ,x, y
!   positions can be returned.
!
! CALLING SEQUENCE:
!   pix211 (pixel, resolution, coord) > longitude,latitude
!
! INPUT:
!   pixel - Pixel number
!   resolution - Quad-cube resolution

```

```

!   coord - output coordinate system
!
!   OUTPUT:
!   vector - Longitude and latitude of center of pixel
!
!   SUBROUTINES CALLED:
!   PIXEL_VECTOR, FORWARD_CUBE, XYAXIS
!   UV211, CONV_E2G, CONV_E2Q
!
!   REVISION HISTORY
!
!       Implicit NONE
C
C   Arguments:
C
      character*1   COORD       ! Coordinate System
      integer*2    RESOLUTION   ! Quad-cube resolution
      integer*4    ISTAT       ! Status
      integer*4    UV211       ! Routine convert unit vector to lon/lat
      integer*4    PIXEL       ! Pixel number
      integer*4    X,Y,FACE    ! Face x,y coordinates for quad-cube,
                                ! where 0,0 is in bottom right hand
                                ! corner of face. There are 6 faces.
      real*4       VECTOR(3)    ! Temp. unit vector to center of pixel
      real*4       OVECTOR(3)   ! Unit vector to center of pixel
      real*4       PIXEL_VECTOR ! Routine computes unit vectors
      real*4       CONV_E2Q, CONV_E2G !Convert from ecliptic to galactic
                                !and ecliptic to equatorial
      real*4       longitude,latitude !output longitude and latitude

C
      print *, 'Enter pixel:'
      read(*,25) pixel
25  format(i8)
      print *, 'Enter resolution:'
      read(*,35) resolution
35  format(i2)
      call PIXEL_VECTOR(pixel,resolution,vector,x,y,face)
      print *, 'Enter output format: '
      print *, '(L=longitude/latitude, P=quad cube x,y,face positions)'
      read(*,45) coord
      if (coord .eq. 'P' .or. coord .eq. 'p') then
        print *, 'Face= ',face
        print *, 'X,Y= ',x,y
      else
        print *, 'Enter coordinate system ',
&          '(E=ecliptic,G=galactic,Q=Equatorial):'
      read(*,45) coord
45  format(A)
      if (coord .eq. 'G' .or. coord .eq. 'g')
&          call CONV_E2G(vector,ovector)
      if (coord .eq. 'Q' .or. coord .eq. 'q')
&          call CONV_E2Q(vector,ovector)
      if (coord .eq. 'E' .or. coord .eq. 'e') then

```

```

    ovector(1)=vector(1)
    ovector(2)=vector(2)
    ovector(3)=vector(3)
endif

    istat=UV2LL(ovector,longitude,latitude)
    print *,coord,' lat lon=',latitude,longitude
endif
end

*****
Subroutine conv_E2G(ivector,ovector)
C
C   Routine to convert ecliptic (celestial) coordinates at the given
C   epoch to galactic coordinates.
C
C   -----
C
C   Galactic Coordinate System Definition (from Zombeck, "Handbook of
C   Space Astronomy and Astrophysics", page 71):
C
C       North Pole:  12:49      hours right ascension (1950.0)
C                   +27.4      degrees declination   (1950.0)
C
C   Reference Point: 17:42:26.603 hours right ascension (1950.0)
C                   -28 55' 00.45 degrees declination  (1950.0)
C
C   -----
C
C   Implicit NONE
C
C   Arguments:
C
C       Real*4    IVECTOR(3)    ! Input coordinate vector
C       Real*4    OVECTOR(3)    ! Output coordinate vector
C
C   Program variables:
C
C       Real*8    T(3,3)        ! Galactic coordinate transformation matrix
C       Integer*2 I,J           ! Loop variables
C
C   Data T / -0.054882486d0, -0.993821033d0, -0.096476249d0, ! 1st column
+           0.494116468d0, -0.110993846d0, 0.862281440d0, ! 2nd column
+           -0.867661702d0, -0.000346354d0, 0.497154957d0/ ! 3rd column
C
C   Multiply vector by transpose of transformation matrix:
C
C   Do 200 I = 1,3
C       ovector(i) = 0.0
C       Do 100 J = 1,3
100          ovector(i) = ovector(i) + iverector(j)*T(j,i)
200      end do
C

```

```

    return
    end

*****
    Subroutine conv_E2Q(ivector,ovector)
C
C   Routine to convert from ecliptic coordinates to equatorial (celestial)
C   coordinates at the given epoch.
C
C   Implicit NONE
C
C   Arguments:
C
C       Real*4      IVECTOR(3)      ! Input coordinate vector
C       Real*4      OVECTOR(3)      ! Output coordinate vector
C
C   Program variables:
C
C       Real*8      T                ! Julian centuries since 1900.0
C       Real*4      EPOCH            ! Equatorial coordinate epoch
C       Real*8      EPSILON          ! Obliquity of the ecliptic
C
C   Set-up:
C
C       epoch=2000.
C       T = (epoch - 1900.d0) / 100.d0
C       epsilon = 23.452294d0 - 0.0130125d0*T - 1.63889d-6*T**2
C       +          + 5.02778d-7*T**3
C
C   Conversion:
C
C       ovector(1) = ivector(1)
C       ovector(2) = dcosd(epsilon)*ivector(2) - dsind(epsilon)*ivector(3)
C       ovector(3) = dcosd(epsilon)*ivector(3) + dsind(epsilon)*ivector(2)
C
C       return
C       end

C*****
c*   UV2LL
c*
c*   Function: Convert from unit three-vector to decimal latitude and
c*             longitude, in degrees. Longitude is between 0 and 360.
c*
c*   PROLOGUE:
c*
c*   INPUT DATA:  three-vector
c*
c*   OUTPUT DATA: latitude and longitude in degrees
c*
c*   INVOCATION:  status=UV2LL(vector,longitude,latitude)
c*
c*   INPUT PARAMETERS:
c*
c*

```



```

c*   Name           Type           Description
c*   ----           ----           -
c*
c*   vector         real*4(3)       coordinate vector
c*
c*   OUTPUT PARAMETERS:
c*
c*   Name           Type           Description
c*   ----           ----           -
c*
c*   longitude      real*4         in degrees
c*   latitude       real*4         in degrees
c*
c*   COMMON VARIABLES USED: none
c*
c*   SUBROUTINES CALLED:  none
c*
c*   FUNCTIONS CALLED:   none
c*
c*   PROCESSING METHOD:
c*
c*   BEGIN
c*
c*       Normalize input vector
c*       If pole:
c*           longitude = 0
c*       else
c*           calculate longitude
c*       endif
c*       Make sure longitude is positive
c*       Calculate latitude
c*       Return
c*
c*   END
c*****
c*
c*   Integer*4 Function UV2LL(vector,longitude,latitude)
c*
c*   Implicit NONE
c
c   Arguments:
c
c       Real*4      VECTOR(3)      ! coordinate vector
c       Real*4      LONGITUDE      ! in degrees
c       Real*4      LATITUDE       ! in degrees
c
c   Variables:
c
c       Real*4      V(3)           ! Normalized VECTOR
c       Real*4      NORM_INV       ! 1 / VECTOR norm
c
c   Normalize input vector:
c
c       norm_inv = sqrt(vector(1)**2 + vector(2)**2 + vector(3)**2)

```

```

    if (norm_inv .eq. 0) then
      print *, 'Unit vector normalization is 0'
      uv2ll = 0
      return
    else
      norm_inv = 1.0 / norm_inv
    endif

    v(1) = vector(1) * norm_inv
    v(2) = vector(2) * norm_inv
    v(3) = vector(3) * norm_inv

c
c   Conversion:
c
    if (v(2) .eq. 0.0 .and. v(1) .eq. 0.0) then
      longitude = 0.0
    else
      longitude = atan2d(v(2),v(1))
    endif
    if (longitude .lt. 0.0) longitude = longitude + 360.0

    latitude = atan2d(v(3),sqrt(v(1)**2+v(2)**2))

c
c   Done:
c
    uv2ll = 1
    return
end

*****
SUBROUTINE FORWARD_CUBE(X,Y,XI,ETA)
REAL*4 X,Y,XI,ETA
C
C INPUT: X,Y IN RANGE -1 TO +1 ARE DATABASE CO-ORDINATES
C
C OUTPUT: XI, ETA IN RANGE -1 TO +1 ARE TANGENT PLANE CO-ORDINATES
C
C BASED ON POLYNOMIAL FIT FOUND USING FCFIT.FOR
C
PARAMETER (NP=28)
REAL*4 P(NP)
DATA P/
1  -0.27292696, -0.07629969, -0.02819452, -0.22797056,
2  -0.01471565,  0.27058160,  0.54852384,  0.48051509,
3  -0.56800938, -0.60441560, -0.62930065, -1.74114454,
4   0.30803317,  1.50880086,  0.93412077,  0.25795794,
5   1.71547508,  0.98938102, -0.93678576, -1.41601920,
6  -0.63915306,  0.02584375, -0.53022337, -0.83180469,
7   0.08693841,  0.33887446,  0.52032238,  0.14381585/
XX=X*X
YY=Y*Y
XI=X*(1.+(1.-XX)*(
1  P(1)+XX*(P(2)+XX*(P(4)+XX*(P(7)+XX*(P(11)+XX*(P(16)+XX*P(22)))))) +
2  YY*( P(3)+XX*(P(5)+XX*(P(8)+XX*(P(12)+XX*(P(17)+XX*P(23)))))) +

```

```

3 YY*( P(6)+XX*(P(9)+XX*(P(13)+XX*(P(18)+XX*(P(24)))) ) +
4 YY*( P(10)+XX*(P(14)+XX*(P(19)+XX*(P(25)))) ) +
5 YY*( P(15)+XX*(P(20)+XX*(P(26))) +
6 YY*( P(21)+XX*(P(27) + YY*(P(28)))) ) ) )
ETA=Y*(1.+(1.-YY)*(
1 P(1)+YY*(P(2)+YY*(P(4)+YY*(P(7)+YY*(P(11)+YY*(P(16)+YY*(P(22)))))) ) +
2 XX*( P(3)+YY*(P(5)+YY*(P(8)+YY*(P(12)+YY*(P(17)+YY*(P(23)))))) ) +
3 XX*( P(6)+YY*(P(9)+YY*(P(13)+YY*(P(18)+YY*(P(24)))) ) +
4 XX*( P(10)+YY*(P(14)+YY*(P(19)+YY*(P(25)))) ) +
5 XX*( P(15)+YY*(P(20)+YY*(P(26))) +
6 XX*( P(21)+YY*(P(27) + XX*(P(28)))) ) ) )
RETURN
END

```

```

*****
SUBROUTINE XYAXIS(NFACE,XI,ETA,C)
C
C CONVERTS FACE NUMBER NFACE (0-5) AND XI, ETA (-1. - +1.)
C INTO A UNIT VECTOR C
C
REAL*4 C(3),XI,ETA,XI1,ETA1,NORM
C
C To preserve symmetry, the normalization sum must
C always have the same ordering (i.e. largest to smallest).
C
      XI1 = MAX(ABS(XI),ABS(ETA))
      ETA1 = MIN(ABS(XI),ABS(ETA))
      NORM = 1. / SQRT(1. + XI1**2 + ETA1**2)
C
GO TO (200,210,220,230,240,250), NFACE+1
200  C(3)=NORM !Transform face to sphere
      C(1)=-ETA*NORM
      C(2)=XI*NORM
      GO TO 300
210  C(1)=NORM
      C(3)=ETA*NORM
      C(2)=XI*NORM
      GO TO 300
220  C(2)=NORM
      C(3)=ETA*NORM
      C(1)=-XI*NORM
      GO TO 300
230  C(1)=-NORM
      C(3)=ETA*NORM
      C(2)=-XI*NORM
      GO TO 300
240  C(2)=-NORM
      C(3)=ETA*NORM
      C(1)=XI*NORM
      GO TO 300
250  C(3)=-NORM
      C(1)=ETA*NORM
      C(2)=XI*NORM
      GO TO 300

```

```

C
  300 CONTINUE
C
RETURN
END

*****

      Subroutine PIXEL_VECTOR(pixel,resolution,vector,jx,jy,face)
C
C   Routine to return unit vector pointing to center of pixel given pixel
C   number and resolution of the cube.
C
      Implicit NONE
C
C   Arguments:
C
      Integer*4      PIXEL          ! Pixel number
      Integer*2      RESOLUTION     ! Quad-cube resolution
      Real*4         VECTOR(3)     ! Unit vector to center of pixel
C
C   Variables:
C
      Integer*4      FACE           ! Face number
      Integer        JX,JY,IP,ID    ! Loop variables
      Real           X,Y           ! Face coordinates
      Real*4         SCALE
      Integer*4      PIXELS_PER_FACE ! Number of pixels on a single face
      Integer*4      FPIX          ! Pixel number within the face
      Real           XI,ETA        ! 'Database' coordinates
      Integer*4      ONE,TWO       ! Constants used to avoid integer
      ! overflow for large pixel numbers
      Integer*4      BIT_MASK      ! Bit mask to select the low order bit
C
      Parameter (ONE = 1)
      Parameter (TWO = 2)
      Parameter (BIT_MASK = 1)
C
      scale = 2**(resolution-1) / 2.0
      pixels_per_face = two**(two*(resolution-one))
C
      face = pixel/pixels_per_face      ! Note: Integer division truncates
      fpix = pixel - face*pixels_per_face
C
C   Break pixel number down into x and y bits:
C
      jx = 0
      jy = 0
      ip = 1
      do while (fpix .ne. 0)
         id = iand(bit_mask,fpix) ! = mod(fpix,2)
         fpix = ishft(fpix,-1)   ! = fpix / 2
         jx = id * ip + jx
         id = iand(bit_mask,fpix)

```

```

        fpix = ishft(fpix,-1)
        jy = id * ip + jy
        ip = ip * 2
    end do
C
    x = (jx - scale + 0.5) / scale
    y = (jy - scale + 0.5) / scale
    call FORWARD_CUBE(x,y,xi,eta)
    call XYAXIS(face,xi,eta,vector)
C
    return
end

```

\*\*\*\*\*

The following routines perform "resolution 15" pixel calculations. SUPER\_CENPIX accepts a resolution 15 pixel number as input and computes the corresponding line of sight unit vector; SUPER\_PIXNO performs the opposite transformation. The FORWARD\_CUBE subroutine, which is called by SUPER\_CENPIX, is listed above.

\*\*\*\*\*

```

SUBROUTINE AXISXY(C,NFACE,X,Y)
C
C CONVERTS UNIT VECTOR C INTO NFACE NUMBER (0-5) AND X,Y
C IN RANGE 0-1
C
REAL*4 C(3)
AC3=ABS(C(3))
AC2=ABS(C(2))
AC1=ABS(C(1))
IF(AC3.GT.AC2) THEN
    IF(AC3.GT.AC1) THEN
        IF(C(3).GT.0.) GO TO 100
GO TO 150
    ELSE
        IF(C(1).GT.0.) GO TO 110
GO TO 130
    ENDIF
ELSE
    IF(AC2.GT.AC1) THEN
        IF(C(2).GT.0.) GO TO 120
GO TO 140
    ELSE
        IF(C(1).GT.0.) GO TO 110
GO TO 130
    ENDIF
ENDIF
100 NFACE=0
ETA=-C(1)/C(3)
XI=C(2)/C(3)
GO TO 200
110 NFACE=1
XI=C(2)/C(1)

```

```

ETA=C(3)/C(1)
GO TO 200
120 NFACE=2
ETA=C(3)/C(2)
XI=-C(1)/C(2)
GO TO 200
130 NFACE=3
ETA=-C(3)/C(1)
XI=C(2)/C(1)
GO TO 200
140 NFACE=4
ETA=-C(3)/C(2)
XI=-C(1)/C(2)
GO TO 200
150 NFACE=5
ETA=-C(1)/C(3)
XI=-C(2)/C(3)
GO TO 200
C
200 CALL INCUBE(XI,ETA,X,Y)
X=(X+1.)/2.
Y=(Y+1.)/2.
RETURN
END

```

\*\*\*\*\*

```

SUBROUTINE INCUBE(ALPHA,BETA,X,Y)
C
C SEE CSC "EXTENDED STUDY ... NOTE THAT THE TEXT HAS TYPOS. I HAVE
C TRIED TO COPY THE FORTRAN LISTINGS
c*
c*   PROLOGUE:
c*
ch   Date       Version   SPR#   Programmer   Comments
ch   ----       -
ch
ch   08/20/90    6.7       7003   A.C.Rough    Minor modifications to improve
ch                                     efficiency
ch
C
REAL*4 ALPHA,BETA
      Real*4 GSTAR_1,M_G,C_COMB
PARAMETER GSTAR=1.37484847732,G=-0.13161671474,
1  M=0.004869491981,W1=-0.159596235474,C00=0.141189631152,
2  C10=0.0809701286525,C01=-0.281528535557,C11=0.15384112876,
3  C20=-0.178251207466,C02=0.106959469314,D0=0.0759196200467,
4  D1=-0.0217762490699
PARAMETER R0=0.577350269
AA=ALPHA**2
BB=BETA**2
A4=AA**2
B4=BB**2
ONMAA=1.-AA

```

```
ONMBB=1.-BB
```

```
gstar_1 = 1. - gstar
m_g      = m - g
c_comb   = c00 + c11*aa*bb
```

```
X = ALPHA *
+   (GSTAR +
+   AA * gstar_1 +
+   ONMAA * (BB * (G + (m_g)*AA +
+   ONMBB * (c_comb + C10*AA + C01*BB +
+   C20*A4 + C02*B4)) +
+   AA * (W1 - ONMAA*(DO + D1*AA))))
```

```
Y = BETA *
+   (GSTAR +
+   BB * gstar_1 +
+   ONMBB * (AA * (G + (m_g)*BB +
+   ONMAA * (c_comb + C10*BB + C01*AA +
+   C20*B4+C02*A4)) +
+   BB * (W1 - ONMBB*(DO + D1*BB))))
```

```
RETURN
END
```

```
*****
```

```
SUBROUTINE SPRCPX_SET
```

```
C
INTEGER*2 JX,JY
COMMON /SPRCPX/ JX(0:1023),JY(0:1023)
DATA JX(1023)/0/
C
SAVE /SPRCPX/
DO KPIX=0,1023
  JPIX=KPIX
  IX=0
  IY=0
  IP=1
  DO WHILE (JPIX.NE.0) !Break up the pixel number
    ID=MOD(JPIX,2) !By even and odd bits to get
    JPIX=JPIX/2 !IX and IY
    IX=ID*IP+IX
    ID=MOD(JPIX,2)
    JPIX=JPIX/2
    IY=ID*IP+IY
    IP=2*IP
  ENDDO
  JX(KPIX)=IX
  JY(KPIX)=IY
ENDDO
RETURN
END
```

```
*****
```

```

SUBROUTINE SUPER_CENPIX(NSUPER,C)
INTEGER*4 NSUPER !Input pixel number
REAL*4 C(3) !Output unit vector
PARAMETER IT28=2**28
C
INTEGER*2 IX,IY
COMMON /SPRCNPX/ IX(0:1023),IY(0:1023)
IF(IX(1023).NE.31) CALL SPRCNPX_SET
C
NFACE=NSUPER/IT28
N=MOD(NSUPER,IT28)
I=MOD(N,1024)
N=N/1024
J=MOD(N,1024)
K=N/1024
JX=1024*IX(K)+32*IX(J)+IX(I)
JY=1024*IY(K)+32*IY(J)+IY(I)
X=(JX-8191.5)/8192. !Database coordinates. Range
Y=(JY-8191.5)/8192. ! -1 -> 1 covers the square face
CALL FORWARD_CUBE(X,Y,XI,ETA) !Distort to tangent plane
C
C TWO ITERATIONS TO IMPROVE THE DISTORTION
C
CALL INCUBE(XI,ETA,XP,YP)
XI=XI-(XP-X)
ETA=ETA-(YP-Y)
CALL INCUBE(XI,ETA,XP,YP)
XI=XI-(XP-X)
ETA=ETA-(YP-Y)
CALL XYAXIS(NFACE,XI,ETA,C)
RETURN
END

```

\*\*\*\*\*

```

SUBROUTINE SUPER_PIXNO(C,NSUPER)
REAL*4 C(3) !Unit vector input
INTEGER*4 NSUPER !Output pixel number 1,...,6*2**28
PARAMETER IT14=16384,IT28=2**28
C
C PIXELIZES SPHERE TO 20" ACCURACY, EQUAL-AREA PIXELS USING
C QUADRILATERIZED SPHERICAL CUBE
C
INTEGER*4 NPIX,IX,IY,K,IP
SAVE /SPRBIT/
COMMON /SPRBIT/ IX(128),IY(128)
DATA IX(128) /0/
IF(IX(128).EQ.0) THEN !Set up the lookup tables
  DO I=1,128 !for converting x,y into
    J=I-1 !pixel numbers
    K=0
    IP=1
10    IF(J.EQ.0) THEN

```



```

IX(I)=K
IY(I)=2*K
      ELSE
ID=MOD(J,2)
J=J/2
K=IP*ID+K
IP=IP*4
GO TO 10
      ENDIF
    ENDDO
  ENDIF
CALL AXISXY(C,NFACE,X,Y)
I=IT14*X
J=IT14*Y
I=MIN(IT14-1,I) !Roundoff protection for cases very
J=MIN(IT14-1,J) !near an edge of the cube
IL=MOD(I,128)
IH=I/128
JL=MOD(J,128)
JH=J/128
NSUPER=NFACE*IT28+IX(IL+1)+IY(JL+1)+IT14*(IX(IH+1)+IY(JH+1))
RETURN
END

```

\*\*\*\*\*

```

SUBROUTINE XYAXIS(NFACE,XI,ETA,C)
C
C CONVERTS FACE NUMBER NFACE (0-5) AND XI, ETA (-1. - +1.)
C INTO A UNIT VECTOR C
c*
c*   PROLOGUE:
c*
c*   ch   Date       Version   SPR#    Programmer   Comments
c*   ch   ----       -
c*   ch
c*   ch 08/20/90     6.7       7003    A.C.Raugh    Minor modifications to improve
c*   ch                                     efficiency
c*   ch 03/06/92     9.4       9571    A.C.Raugh    Replaced algorithm with one
c*   ch                                     provided by Phil Keegstra (DMR)
c*   ch                                     to provide/use cube face symmetry
c*   ch
C
REAL*4 C(3),XI,ETA,XI1,ETA1,NORM
C
C To preserve symmetry, the normalization sum must
C always have the same ordering (i.e. largest to smallest).
C
      XI1 = MAX(ABS(XI),ABS(ETA))
      ETA1 = MIN(ABS(XI),ABS(ETA))
      NORM = 1. / SQRT(1. + XI1**2 + ETA1**2)
C
GO TO (200,210,220,230,240,250), NFACE+1
200  C(3)=NORM !Transform face to sphere

```

```

C(1)=-ETA*NORM
C(2)=XI*NORM
GO TO 300
210 C(1)=NORM
C(3)=ETA*NORM
C(2)=XI*NORM
GO TO 300
220 C(2)=NORM
C(3)=ETA*NORM
C(1)=-XI*NORM
GO TO 300
230 C(1)=-NORM
C(3)=ETA*NORM
C(2)=-XI*NORM
GO TO 300
240 C(2)=-NORM
C(3)=ETA*NORM
C(1)=XI*NORM
GO TO 300
250 C(3)=-NORM
C(1)=ETA*NORM
C(2)=XI*NORM
GO TO 300
C
300 CONTINUE
C
RETURN
END

```

### D.1.3 IDL Access to the *DIRBE* Data Products

The following example illustrates how the *IDL Astronomy User's Library* routines `headfits`, `readfits`, and `tbget` can be used to read the *DIRBE* Galactic Plane Maps FITS file. The *Library* can be obtained over the Web from the address given in §D.1.

```

IDL> filename = 'dirbe_galactic_plane_maps.fits' ; specify file name

IDL> mainhead = headfits(filename) ; read primary FITS header
; and store it in the string
; array "mainhead"

IDL> table = readfits(filename, exthead, /exten)
; read FITS binary table,
; store data in array "table"
; and extension header in string
; array "exthead"

IDL> phot = tbget(exthead, table, 'Photomet')
; store photometric data in
; array "phot." Dimensions of
; array are 10 (DIRBE bands) x
; number of pixels in map

```

The following example illustrates how the *COBE* analysis software (UIDL) can be used to read photometric data from the *DIRBE* 1.25  $\mu\text{m}$   $\varepsilon = 90^\circ$  Sky Map, represent the data as a  $1024 \times 512$  pixel Mollweide projection in Galactic coordinates, and save the image in a color Postscript file:

```
UIDL> datain, 'dirbe_band1_elongation90_skymap.fits', $ ; read in photometry and
UIDL> dsfield = 'photomet', data = data ; store in array "data"

UIDL> reproj, data, proj_map, proj = 'm', coord = 'g', psize = 'l' ; reproject data
; into new array
; "proj_map"

UIDL> psimage, proj_map, color = 3, output = 'dirbe_band1.ps' ; create a Postscript
; file called
; "dirbe_band1.ps"
; using default IDL
; color table 3
```

## D.2 Sample Data Plots and Dumps

The following tables list the data for pixel 42 (selected arbitrarily) from each of several representative FITS files <sup>1</sup> and may be used to check software designed to read the *DIRBE* data products. Tables D.2-1, D.2-2, D.2-3, and D.2-4 give excerpts from the Galactic Plane Maps file, Weekly Sky Map number 22, and the Annual Average and  $\varepsilon = 90^\circ$  Sky Maps, respectively.

Table D.2-1: Data for pixel 42 in the Galactic Plane Maps

File	DIRBE_GALACTIC_PLANE_MAPS.FITS									
Time (T81)	294533016.795 s									
Coordinates	Ecliptic					Galactic				
longitude	312°38					59°38				
latitude	36°65					-9°93				
Band	1A	2A	3A	4	5	6	7	8	9	10
$I_\nu$ (MJy/sr) <sup>a</sup>	0.879	0.695	0.403	0.693	17.438	31.831	11.093	12.054	12.291	10.530
$\sigma_{I_\nu}$ (MJy/sr) <sup>b</sup>	0.005	0.011	0.006	0.006	0.181	0.330	0.052	0.144	4.931	2.141
Quality flag (Hex)	00	00	00	00	00	00	00	00	00	00

<sup>a</sup> Photomet

<sup>b</sup> StdDev

Also to facilitate software validation, Figure D.2-1 shows a one-dimensional “slice” through the 25  $\mu\text{m}$   $\varepsilon = 90^\circ$  Sky Map at fixed ecliptic longitude. Specifically, photometric data obtained prior to mission week 30 at ecliptic longitudes between 84 and 85° are selected and plotted as a function of ecliptic latitude using the following IDL commands:

```
IDL> wk30_time = 2.979072e+08 ;1990 day 162 in seconds since 1981.00
IDL> early_times = where(t81 lt wk30_time)
IDL> eclon = eclon(early_times) & eclat = eclat(early_times)
IDL> phot = phot(early_times)
IDL> select = where((eclon lt 85) and (eclon gt 84))
IDL> !x.title = 'ECLIPTIC LATITUDE (degrees)'
IDL> !y.title = '25 micron INTENSITY (MJy/sr)'
IDL> !p.title = 'FIGURE D.2-1: FIXED ECLIPTIC LONGITUDE SCAN (84<L<85 deg)'
IDL> plot, eclat(select), phot(5, select), psym = 4, yrange = [0,80]
```

<sup>1</sup>Data processing “Pass 3B” versions

Table D.2-2: Data for pixel 42 in Weekly Sky Map 22

<b>File</b>	DIRBE_WK22_WEEKLY_AVERAGED_SKYMAP.FITS										
<b>Time (T81)</b>	293410493.389 s										
<b>PSubPos (Hex)</b>	C8										
<b>SolElong</b>	79°87										
<b>NumRecs</b>	14										
<b>SSOFlag (Hex)</b>	00										
<b>FracUsed (%)</b>	Overall 76.1			Band 1B 100.0				Band 7 71.4			
<b>Band</b>	1A	2A	3A	4	5	6	7	8	9	10	
$I_\nu$ (MJy/sr) <sup>a</sup>	0.892	0.734	0.416	0.830	19.617	34.749	11.365	12.046	10.631	2.529	
$\sigma_{I_\nu}$ (MJy/sr) <sup>b</sup>	0.013	0.030	0.017	0.012	0.031	0.061	0.129	0.343	10.369	5.113	
<b>WtNumObs</b>	8	13	11	9	13	12	10	6	13	11	
<b>DeltaT (hours)</b>	3.281	5.906	3.281	12.469	3.281	-0.656	4.594	-11.156	-1.969	5.906	
<b>Displace (Hex)</b>	C1			68			3F	6E			
<b>Polarization in band</b>						1		2		3	
						Q	U	Q	U	Q	U
<b>Stokes</b>						-16397	0.02	-16397	0.04	-16397	-0.06
<b>StokesSD</b>						0.	0.015	0.	0.038	0.	0.029
<b>StokQual (Hex) for band ratio</b>						1B/1A	1C/1A	2B/2A	2C/2A	3B/3A	3C/3A
						C0	40	C0	00	C0	00

<sup>a</sup> Photomet<sup>b</sup> StdDev

Table D.2-3: Data for pixel 42 in the Annual Average Sky Maps

<b>File</b>	DIRBE_BANDx_ANNUAL_AVERAGE_SKYMAP.FITS for $x = 1A, 2A, 3A, 4, \dots, 10$									
<b>Time (T81)</b>	295732488.424 s									
<b>SumNRecs</b>	303									
<b>PSubPos (Hex)</b>	3E									
<b>Band</b>	1A	2A	3A	4	5	6	7	8	9	10
$I_\nu$ (MJy/sr) <sup>a</sup>	0.903	0.723	0.419	0.735	18.0	32.1	10.9	11.5	15.7	11.4
$\sigma_{I_\nu}$ (MJy/sr) <sup>b</sup>	0.00719	0.00717	0.00455	0.0178	0.308	0.417	0.0895	0.0702	2.36	1.24
<b>WtNumObs</b>	202	213	210	223	211	205	186	154	222	221

<sup>a</sup> Photomet<sup>b</sup> StdDev

Table D.2-4: Data for pixel 42 in the Solar Elongation = 90° Sky Maps

<b>File</b>	DIRBE_BANDx_ELONGATION90_SKYMAP.FITS for $x = 1A, 2A, 3A, 4, \dots, 10$									
<b>Time (T81)</b>	294533016.795 s									
<b>EfNumObs</b>	40									
<b>Band</b>	1A	2A	3A	4	5	6	7	8	9	10
$I_\nu$ (MJy/sr) <sup>a</sup>	0.879	0.695	0.403	0.693	17.438	31.831	11.093	12.054	12.291	10.530
$\sigma_{I_\nu}$ (MJy/sr) <sup>b</sup>	0.005	0.011	0.006	0.006	0.018	0.033	0.052	0.144	4.931	2.141
<b>FitQual (Hex)</b>	00	00	00	00	00	00	00	00	00	00
$\chi^2$	0.8	0.3	0.6	0.4	0.5	3.3	1.9	0.2	0.1	0.4

<sup>a</sup> Photomet<sup>b</sup> StdDev

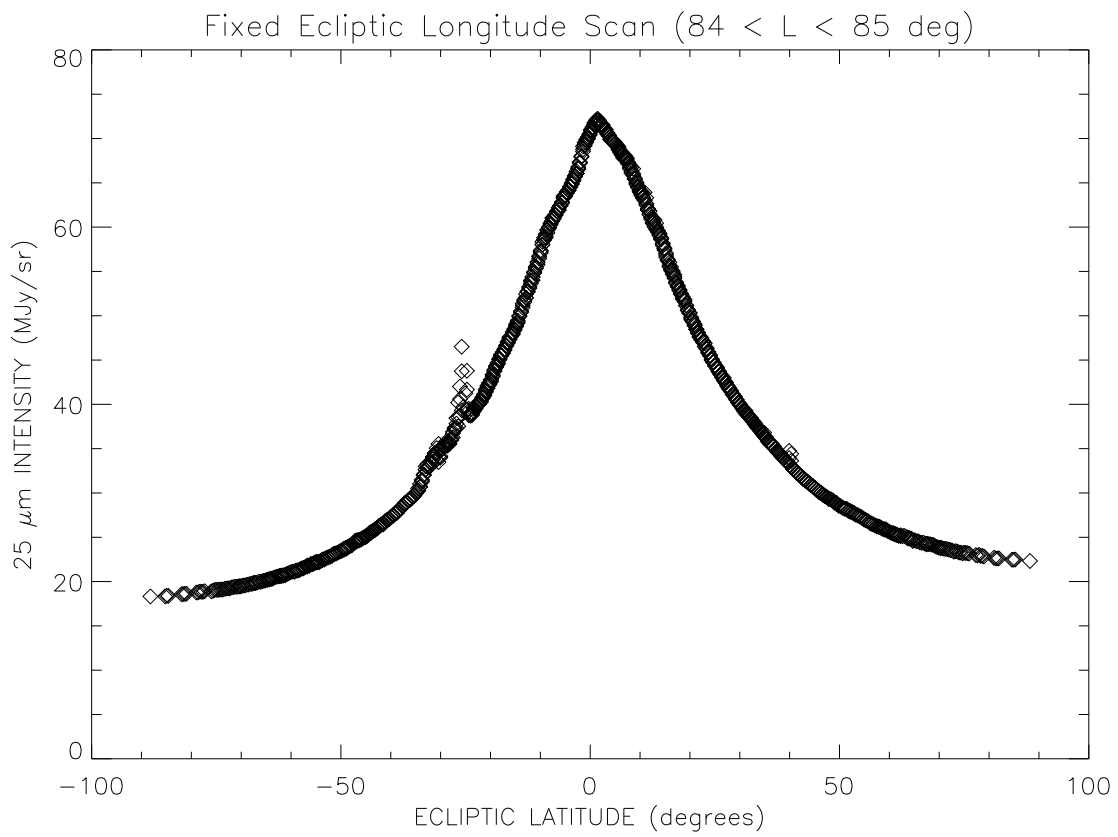


Figure D.2-1: A slice through the  $25 \mu\text{m}$   $\varepsilon = 90^\circ$  Sky Map at fixed ecliptic longitude.

## Appendix E

# Acronyms Used in this Document

Table E.0-1: Acronyms

Acronym	Definition
ACS	Attitude control system
AIPS	Astronomical Image Processing System
ANL	Annealing mode (of <i>DIRBE</i> operation)
APE	Analog processing electronics
ASCII	American Standard Code of Informational Interchange
ASDS	Analyzed Science Data Set (high-level data product)
AU	Astronomical Unit
AV	Approach Vector
BCC	Celestial_Calibration (software to determine calibration constants based upon celestial objects)
BCO	Select_Cal_Objects (software to search the data for object passages)
BEX_DO	Detector Offsets (internal use data set)
BEX_GC	Gain Coefficients (internal use data set)
BIB	Blocked Impurity Barrier
BIC_IRSCC	IRS Calibration Constants (internal use data set)
BIT_DO	Detector Offsets (internal use data set)
BLI	Linearize_Intensities (software to correct science data)
BMD_MA	Merged Archive (internal use data set)
BPW	Produce_Weekly_Maps (software)
BPW_WAF	Weekly Average File (data set)
CAL	Calibration mode
CBM	Continuous burst mode
CDAC	Cosmology Data Analysis Center
CGIF	<i>COBE</i> Guest Investigator Facility
CGIS	<i>COBE</i> Guest Investigator Support
CIB	Cosmic Infrared Background
CIO	Calibrated Individual Observations
CMB	Cosmic Microwave Background
COBE	Cosmic Background Explorer
CSC	<i>COBE</i> Quadrilateralized Spherical Cube
DCAF	<i>DIRBE</i> Calibrated Annual File
DEU	Digital Electronics Units
DGL	Deglitching setting
DIRBE	Diffuse Infrared Background Experiment
DMR	Differential Microwave Radiometers
DN	Data Numbers (uncalibrated photometry unit)
DO	Detector Offsets
DSZA	<i>DIRBE</i> Sky And Zodi Atlas
ETS	Electronic test signal mode
FIRAS	Far Infrared Absolute Spectrophotometer
FITS	Flexible Image Transport System
FOV	Field of view
FSM	Faint Source Model
FTIR	Fourier Transform Interferometer Radiometer
ftp	File Transfer Protocol
GI	Guest Investigator
GMT	Greenwich Mean Time

GPM	Galactic Plane Maps
GRT	Germanium Resistance Thermometer
GSFC	Goddard Space Flight Center
HEASARC	High Energy Astrophysics Science Archive Research Center
HCON	<i>IRAS</i> hours–confirmed observation
HMnF	Half Minor Frame
IDL	Interactive Data Language
IPAC	Infrared Processing and Analysis Center
IPD	Interplanetary Dust
IPDU	Instrument Power Distribution Unit
IR	Infrared
IRAS	Infrared Astronomical Satellite
IRIS	Voyager spectrometer
IRS	Internal Reference Source
IRSCC	IRS Calibration Constants
JFET	Junction Field-Effect Transistor
KAO	Kuiper Airborne Observatory
MF	Major frame
MGR	Mean Glitch Rate
MLI	Multilayer Insulating (blankets)
MLIF	Multilayer interference filter
MTM	Mirror Transport Mechanism
MUX	Multiplexor
NASA	National Aeronautics and Space Administration
NEP	North Ecliptic Pole
NGP	North Galactic Pole
NOST	NASA/OSSA Office of Standards and Technology
NVAB	North Van Allen Belt
OCLI	Optical Coating Laboratories, Inc., or generic term for similar product
OGIP	Office of Guest Investigator Programs
OSSA	Office of Space Science and Applications
PDS	Project Data Set
PIRE	Photon–Induced Responsivity Enhancement
PS	Postscript
RF	Radio frequency
RFI	Radio frequency interference
RMS	Root mean square
SAA	South Atlantic Anomaly
SD	Standard deviation
SDM	Science data mode
SNAP	Snapshot mode
SNG	Single channel mode
SOP	Satellite Operations Plan ( <i>IRAS</i> )
STM	Standby mode
SVAB	South Van Allen Belt
T81	TAI seconds elapsed since 1981 January 1 00:00:00 UTC
TAI	International Atomic Time
TDRSS	Tracking and Data Relay Satellite System
TFPR	Total Flux Photometric Reference
TOD	Time–Ordered Data
TSI	Time since IRS
UIT	Ultraviolet Imaging Telescope
UT	Universal Time
XCAL	External Calibrator ( <i>FIRAS</i> )
ZL	Zodiacal Light, including thermal emission and scattered light
ZOHF	<i>IRAS</i> Zodiacal Observation History File
ZSMA	Zodi–Subtracted Mission Average ( <i>ZSMA</i> ) Maps





# Appendix F

## The Faint Source Model

### F.1 Introduction

The *DIRBE* Faint Source Model (FSM) was created to simulate the unresolved Galactic emission of stars and other compact sources at wavelengths from 1.25 to 25  $\mu\text{m}$ . The emission predicted by the FSM was subtracted as a foreground component from the observed *DIRBE* intensities in an effort to determine the cosmic IR background (Arendt *et al.* 1998). The main requirements imposed on the FSM were (a) that it yield integrated surface brightnesses at the nominal *DIRBE* wavelengths, (b) that it provide maps of the surface brightness at *DIRBE* resolution, and (c) that it include an adjustable brightness cutoff, enabling exclusion of the brighter stars, which could be detected individually by the *DIRBE*.

The FSM is a statistical model which follows the basic form of the Wainscoat *et al.* (1992) and Cohen (1993, 1994, 1995) “SKY” models, including 5 structural components for the Galaxy (disk, spiral arms, molecular ring, bulge, and halo), 87 source types, each with a dispersion of absolute magnitudes, and interstellar extinction from dust in an exponential (in radius,  $R$ , and scale height,  $z$ ) disk. The formalism of the SKY model allows the FSM to predict source counts in stars per magnitude per steradian. With the application of a zero-magnitude flux to convert magnitudes to flux densities, the FSM transforms the source counts to integrated intensities, in MJy/sr, along each line of sight. Some of the relatively recent modifications to the SKY model (Cohen 1993, 1994, 1995) could also be used to improve the FSM, but many of these changes are either irrelevant at the *DIRBE* wavelengths, or are difficult to implement while maintaining fidelity to the SKY model. Some modifications to the Wainscoat *et al.* version of the SKY model (version 1.0) were included in the FSM, either out of necessity or to produce results that were better suited for comparison with the *DIRBE* data. These changes are as follows:

1. Since source count models cannot accurately represent the brightest point sources, which are unevenly distributed across the sky, the FSM was only integrated over stars fainter than those that were previously blanked from the *DIRBE* maps (see Table F.1-1). The value of the brightness limit at which the bright source blanking of the data stops and the Faint Source Model begins is not a significant source of uncertainty. Changes in the limits by 20% produce <5% changes in the Faint Source Model intensities.
2. The angular resolution of the model was increased; the sky brightness was calculated at the resolution of the *DIRBE* maps.
3. The halo is described by Wainscoat *et al.* (1992) only as an  $R^{1/4}$  law in projected surface brightness. Therefore we have adapted the formulation for the volume density presented by Young (1976) for use in the Faint Source Model. At high Galactic latitudes, the halo is the third most important component of the Faint Source Model after the disk and the spiral arms.
4. We omitted the extragalactic component of the SKY model, which contributes mainly at faint magnitudes at 25  $\mu\text{m}$  (Cohen 1994).

5. The position of the Sun was set at 18 pc North of the midplane of the Galactic disk. This was determined during preliminary trials, by requiring equal brightnesses at the north and south Galactic poles after subtraction of the FSM from the *DIRBE* maps in the near IR bands. This value is independently supported by analysis done with the SKY model (Cohen 1995), and by direct analysis of the *DIRBE* maps (Weiland *et al.* 1994).
6. For 3.5 and 4.9  $\mu\text{m}$  magnitudes, which are not represented in the Wainscoat *et al.* (1992) source table, we obtained approximate magnitudes for the various source types by extrapolating from the *J* magnitudes using  $V - J$ ,  $V - L$ , and  $V - M$  stellar colors from Johnson (1966).
7. Wainscoat *et al.* (1992) made adjustments to their model in certain Galactic latitude–longitude zones. These changes were not specified exactly in terms of magnitude and location, and thus could not be included in the FSM.
8. The FSM includes the split local spur as one of the spiral arm features, according to Cohen’s (1994) description.

Table F.1-1: Faint Source Model Parameters

Wavelength ( $\mu\text{m}$ )	Zero-Magnitude Flux Density (Jy)	Bright Source Cutoff (Jy)	Extinction ( $\tau \text{ kpc}^{-1}$ )
1.25	1547.	15	0.1610
2.2	612.3	15	0.0639
3.5	285.0	15	0.0331
4.9	153.5	15	0.0131
12	31.65	85	0.0274
25	12.23	110	0.0029

## F.2 Calibration

The SKY model as described in Wainscoat *et al.* (1992) is used to predict source counts as a function of magnitude. In order for the FSM to calculate intensities, the stellar magnitudes need to be converted to fluxes, using adopted values of the apparent flux density for a  $0^{\text{th}}$ -magnitude star at each *DIRBE* wavelength. The zero-magnitude flux densities used in the FSM (see Table F.1-1) were chosen to be consistent with the absolute calibration of the *DIRBE* data (see Chapter 4). The zero-magnitude flux density of the FSM at 2.2  $\mu\text{m}$  was reduced by a factor of 0.963 to account for differences between the color corrections of Sirius (which was used as the absolute calibrator) and those of K and M giants which dominate the emission of the FSM and have a CO absorption band partially within the 2.2  $\mu\text{m}$  *DIRBE* band. There exist uncertainties of 10 – 15% in the model arising from details of the absolute calibration of the model and the differences and treatment of the various broadband filter responses (Cohen 1993, private communication).

The extinction at each wavelength (specified as optical depth per kpc in the vicinity of the Sun) is listed in Table F.1-1. The extinction law was chosen to match that of Rieke & Lebofsky (1985), and normalized to  $A_V = 0.62 \text{ mag/kpc}$  (Wainscoat *et al.* 1992).

## F.3 Verification

To check the FSM, we compared the results of our calculations at 1.25 - 25  $\mu\text{m}$  to the average surface brightnesses, calculated using the SKY model, of 238 large zones covering the entire sky (Cohen 1993, private communication). Wainscoat *et al.* (1992) give a table and map of the zone boundaries. The Faint Source Model reproduces the mean intensities calculated with the SKY model to within  $\sim 5\%$  over most of the sky. The zones that are not well matched are all at low latitudes, below  $|b| = 20^\circ$ , except

a zone containing the LMC and another near the Taurus region. Cohen (1994) made adjustments for various localized features in the Galaxy, but no such adjustments were made in the FSM.

We also compared the star counts expected from the FSM with star counts from the prototype 2MASS survey in 7 fields at  $J$  and  $K_S$  (Skrutskie *et al.* 1996, private communication). The fields are all in the first Galactic longitude quadrant and span the latitude range  $8^\circ < b < 87^\circ$ . The FSM star counts are similar to the 2MASS star counts, although statistically significant differences were found in about half of the fields, mostly at magnitudes  $J > 12$  and  $K_S > 12$ . Because such faint stars contribute a small fraction of the total emission from these fields, the FSM predictions are consistent with the 2MASS observations in integrated brightness. This comparison is limited by the small sizes of the fields ( $0.122 - 6.9 \text{ deg}^2$ ) and the corresponding large statistical uncertainties in the star counts.

Discontinuities in the surface brightness of the FSM are due to the sharp edges (in galactocentric radius) in the geometric representation of the spiral arms. These edges are obscured at the resolution of the large zones used by Wainscoat *et al.* (1992). One edge of the local spur passes through the solar neighborhood and causes a discontinuity in the model at high Galactic latitudes.

## F.4 Comparison with the DIRBE Data

Residual maps generated by subtracting the FSM from the DIRBE data are presented by Arendt *et al.* (1998). At wavelengths  $\leq 3.5 \mu\text{m}$  and low Galactic latitudes ( $|b| < 10^\circ$ ), the FSM tends to overestimate the actual sky brightness, leading to negative residuals. A longitudinally anti-symmetric residual is present at the location of the Galactic bulge, which suggests that improvements could result if a bar-like model were used for the bulge (*e.g.*, Blitz & Spergel 1991, Weiland *et al.* 1994, Dwek *et al.* 1995, Freudenreich 1998). Some relatively large differences between the model and the data are found at locations where the Faint Source Model has omitted particular adjustments for specific disk and spiral arm features (Cohen 1994).

## F.5 Warnings

The FSM data product described in §5.8 incorporates the bright source limits listed in Table F.1-1. It will not properly represent the diffuse sky brightness if the bright stars are blanked at a different level, or if they are not blanked at all. Furthermore, the FSM is intended to be a reproduction of, rather than an improvement upon, the SKY model of Wainscoat *et al.* (1992). Its sole purpose was to enable subtraction of the contribution from faint stars to the near-IR sky brightness in order to search for the cosmic infrared background (Hauser *et al.* 1998). In other applications, one should not use the FSM as a substitute for the SKY model, which has been extensively compared with existing source counts.

## F.6 References

- Arendt, R. G., *et al.* 1994, *ApJ*, **425**, L85.  
 Blitz, L. & Spergel, D. N. 1991, *ApJ*, **379**, 631.  
 Cohen, M. 1993, *AJ*, **105**, 1860.  
 Cohen, M. 1994, *AJ*, **107**, 582.  
 Cohen, M. 1995, *ApJ*, **444**, 875.  
 Dwek, E., *et al.* 1995, *ApJ*, **445**, 716.  
 Freudenreich, H. T. 1998, *ApJ*, **492**, 495.  
 Johnson, H. L. 1966, *Ann. Rev. Astr. Ap.*, **4**, 193.  
 Rieke, G. H. & Lebofsky, M. J. 1985, *ApJ*, **288**, 618.  
 Wainscoat, R. J., Cohen, M., Volk, K., Walker, H. J., & Schwartz, D. E. 1992, *ApJS*, **83**, 111.  
 Weiland, J. L., *et al.* 1994, *ApJ*, **425**, L81.  
 Young, P. J. 1976, *AJ*, **81**, 807.



# Appendix G

## Related *COBE* Publications

The publications are organized into sections chronologically and sorted alphabetically by author name within each section.

### G.1 1982

**Optical Design of the Diffuse Infrared Background Experiment for NASA's Cosmic Background Explorer**, Miller, M.S., Evans, D.C., Moseley, H., & Ludwig, U.W., Instrumentation in Astronomy IV: SPIE March 1982, pp. 483–489.

### G.2 1983

**Principles of Stray Light Suppression and Conceptual Application to the Design of the Diffuse Infrared Background Experiment for NASA's Cosmic Background Explorer**, Evans, D.C., Generation, Measurement, and Control of Stray Radiation III: SPIE Jan 1983, pp. 82–87.

**Radiometric Accuracy of the Diffuse Infrared Background Experiment (DIRBE)**, Howell, B.J., & Wilson, M.E., Instrumentation in Astronomy V: Proceedings of Fifth meeting London, England, September 1983: SPIE pp. 284–294.

### G.3 1984

**APART PADE Analytical Evaluation of the Diffuse Infrared Background Experiment for NASA's Cosmic Background Explorer**, Evans, D.C., & Breault, R.P., Stray Radiation IV: SPIE August 1984, pp. 54–64.

**The Internal Reference Source (IRS) for the Diffuse Infrared Background Experiment (DIRBE)**, Silvergate, P., Cryogenic Optical Systems and Instruments: SPIE August 1984, pp. 191–198.

### G.4 1986

**Shutter Mechanism for Calibration of the Cryogenic Diffuse Infrared Background Experiment (DIRBE) Instrument**, Tyler, A., NASA Lewis Research Center: The 20th Aerospace Mechanics Symposium, May 1986, pp. 97–102.

## G.5 1987

**The Scatterometer for DIRBE**, Bolton, J. F., Stray Radiation V: SPIE 1987, pp. 174–179.

**The Diffuse Infrared Background Experiment (DIRBE) Optics Module Breadboard Alignment Methods and Results**, Magner, T. J., 1987, *Opt. Eng.*, **26**, 264.

## G.6 1990

**The Cosmic Background Explorer**, Gulkis, S., Lubin, P.M., Meyer, S.S., & Silverberg, R.F. 1990, *Sci. Amer.*, **262**, 132.

**The Diffuse Infrared Sky Brightness: Preliminary DIRBE Results**, Kelsall, T., Hauser, M., Moseley, H., Silverberg, R., Boggess, N., Cheng, E., Dwek, E., Mather, J., Murdock, T., Toller, G., Weiland, J., Wilkinson, D., Weiss, R., & Wright, E.L. 1990, *Bull. Amer. Phys. Soc.*, **35**, 972.

**COBE/Diffuse Infrared Background Experiment (DIRBE) Observations of Comet Austin (1981C1): Preliminary Results**, Lisse, C.M., Hauser, M.G., Kelsall, T., Moseley, S.H., Silverberg, R.F., Freudenreich H.T., Panitz, A.R., Patt, F.S., Spiesman, W.J., Toller, G.N., & Weiland, J.L. 1990, *Bull. Amer. Astron. Soc.*, **22**, 833.

**Early Results from the Cosmic Background Explorer (COBE)**, Mather, J.C., Hauser, M.G., Bennett, C.L., Boggess, N.W., Cheng, E.S., Eplee Jr., R.E., Freudenreich, H.T., Gulkis, S., Isaacman, R.B., Janssen, M., Kelsall, T., Lisse, C.M., Meyer, S.S., Moseley, S.H., Jr., Murdock, T.L., Shafer, R.A., Silverberg, R.F., Smoot, G.F., Spiesman, W.J., Toller, G.N., Weiland, J.L., Weiss, R., Wilkinson, D.T., & Wright, E.L., 1990, in *Proc. 29th Liege IAU Colloquium 123*, ESA SP-314, pp. 25–31.

**Status of DIRBE Observations of the Infrared Sky**, Silverberg, R.F., Hauser, M.G., Kelsall, T., Moseley, S.H., Toller, G., Weiland, J., Spiesman, W., Skard, J., Panitz, A., & Freudenreich, H. 1990, *Bull. Amer. Astron. Soc.*, **22**, 1324.

**The Diffuse Infrared Background Experiment (DIRBE) – Understanding Through Test and Simulation**, Wood, H.J., Cryogenic Optical Systems and Instruments IV: SPIE, July 1990, pp. 406–416.

COBE, Wright, E.L. 1990, *Ann. NY Acad. Sci.*, **647**, 190.

## G.7 1991

**The Cosmic Background Explorer (COBE): The Mission and Science Overview**, Boggess, N.W. 1991, in *IAU XXI Highlights Astron.*, ed. J. Bergeron, **9**, 273.

**COBE – The Software**, Cheng, E., November 7–9, 1991, in *Proc. First Annual Conference on Astronomical Data Analysis Software and Systems*, NOAO, Tucson, AZ.

**COBE/DIRBE Sky Map Trending**, Freedman, I., *et al.*, November 7–9, 1991, in *Proc. First Annual Conference on Astronomical Data Analysis Software and Systems*, NOAO, Tucson, AZ.

- COBE Astronomical Data Bases**, Freedman, I., *et al.*, November 7–9, 1991, in *Proc. First Annual Conference on Astronomical Data Analysis Software and Systems*, NOAO, Tucson, AZ.
- Detection of Glitches and Point Sources**, Freudenreich, H., *et al.*, November 7–9, 1991, in *Proc. First Annual Conference on Astronomical Data Analysis Software and Systems*, NOAO, Tucson, AZ.
- The Cosmic Infrared Background**, Hauser, M.G. 1991, in *IAU XXI Highlights Astron.*, ed. J. Bergeron, **9**, 291.
- Results of the COBE Mission**, Hauser, M.G. 1991, in *The Infrared and Submillimeter Sky After COBE*, Les Houches Conf. Proc., ed. M. Signore & C. Dupraz (Dordrecht: Kluwer), COBE Preprint No. 91–06.
- The Diffuse Infrared Background: COBE and Other Observations**, Hauser, M.G., Kelsall, T., Moseley, S.H., Jr., Silverberg, R.F., Murdock, T.L., Toller, G., Spiesman, W., & Weiland, J.L. 1991, in *After the First Three Minutes*, ed. S.S. Holt, C.L. Bennett, & V. Trimble (New York: AIP), AIP Conf. Proc. **222**, 161.
- Pattern Matching in COBE Spectral Analysis**, Isaacman, R., *et al.*, November 7–9, 1991, in *Proc. First Annual Conference on Astronomical Data Analysis Software and Systems*, NOAO, Tucson, AZ.
- COBE Observations of Comets**, Lisse, C.M., *et al.* 1991, in *Proc. International Conference on Asteroids, Comets, and Meteors*, *LPI Contrib.*, **765**, 139.
- Early Results from the Cosmic Background Explorer (COBE)**, Mather, J.C., Hauser, M.G., Bennett, C.L., Boggess, N.W., Cheng, E.S., Eplee, R.E., Jr., Freudenreich, H.T., Isaacman, R.B., Kelsall, T., Lisse, C.M., Moseley, S.H., Jr., Shafer, R.A., Silverberg, R.F., Spiesman, W.J., Toller, G.N., Weiland, J.L., Gulkis, S., Janssen, M., Lubin, P.M., Meyer, S.S., Weiss, R., Murdock, T.L., Smoot, G.F., Wilkinson, D.T., & Wright, E.L., 1991 COSPAR, *Adv. Space Res.*, **11**, 181.
- Some Noise Characteristics of DIRBE Photometry**, Mitchell, K.J., *et al.*, November 7–9, 1991, in *Proc. First Annual Conference on Astronomical Data Analysis Software and Systems*, NOAO, Tucson, AZ.
- Software Configuration Management and Quality Assurance in the Cosmic Background Explorer (COBE) Project**, Raugh, A.C., *et al.*, November 7–9, 1991, in *Proc. First Annual Conference on Astronomical Data Analysis Software and Systems*, NOAO, Tucson, AZ.
- DIRBE Project Pipeline Software System**, Skard, J.A., *et al.*, November 7–9, 1991, in *Proc. First Annual Conference on Astronomical Data Analysis Software and Systems*, NOAO, Tucson, AZ.
- An Overview of the Cosmic Background Explorer (COBE) and Its Observations: New Sky Maps of the Early Universe**, Smoot, G.F., March 1991, in Proc. NATO Advanced Study Institute, *The Infrared and Submillimetre Sky after COBE*, Les Houches.
- Display and Manipulation of COBE/DIRBE All-sky Data**, Toller, G.N., *et al.*, November 7–9, 1991, in *Proc. First Annual Conference on Astronomical Data Analysis Software and Systems*, NOAO, Tucson, AZ.



**Databases from the Cosmic Background Explorer (COBE)**, White, R.A. & Mather, J.C. 1991, in *Databases and On-line Data in Astronomy*, ed. M.A. Albrecht & D. Egret (Dordrecht: Kluwer), pp. 29–34.

**Preliminary Results from the FIRAS and DIRBE Experiments on COBE**, Wright, E.L. 1991, in *The Infrared and Submillimeter Sky After COBE*, Les Houches Conf. Proc., ed. M. Signore & C. Dupraz (Dordrecht: Kluwer), p. 231.

## G.8 1992

**The COBE Mission: Its Design and Performance Two Years After Launch**, Boggess, N.W., Mather, J.C., Weiss, R., Bennett, C.L., Cheng, E.S., Dwek, E., Gulkis, S., Hauser, M.G., Janssen, M.A., Kelsall, T., Meyer, S.S., Moseley, S.H., Murdock, T.L., Shafer, R.A., Silverberg, R.F., Smoot, G.F., Wilkinson, D.T., Wright, E.L. 1992, *ApJ*, **397**, 420.

**Scientific Results from COBE**, Bennett, C.L., Boggess, N.W., Cheng, E.S., Hauser, M.G., Kelsall, T., Mather, J.C., Moseley, S.H., Jr., Murdock, T.L., Shafer, R.A., Silverberg, R.F., Smoot, G.F., Weiss, R., Wright, E.L., 4–5 September 1992, in *Advances in Space Research*, COSPAR/IAF World Space Congress.

**Recent Results from COBE**, Bennett, C.L., Boggess, N.W., Cheng, E.S., Hauser, M.G., Mather, J.C., Smoot, G.F., Wright, E.L., July 5–10, 1992, in Proc. Third Teton Summer School, *The Evolution of Galaxies and their Environment*, ed. H.A. Thronson & J.M. Shull.

**An IDL-based Analysis Package for COBE and Other Skycube-formatted Astronomical Data**, Ewing, J.A., Isaacman, R., Gales, J.M., Chintala, S., Kryszak-Servin, P., & Galuk, K.G., November 2–4, 1992, in Proc. *Astronomical Data Analysis Software and Systems II*, Boston, MA.

**Cosmology from COBE**, Hauser, M.G., September 16–18, 1992, in Proc. *Surveys in Astronomy*, Caltech, Pasadena, CA.

**Scientific Results and the Use of Astronomical Databases in the COBE Project**, Isaacman, R., 14–16 September 1992, in Proc. *Second Conference on Astronomy with Large Data Bases*, Haguenau, France.

**COBE/DIRBE Infrared Observations of the Ecliptic Poles**, Murdock, T.L., Burdick, S.V., Hauser, M.G., Kelsall, T., Moseley, S.H., Jr., Silverberg, R.F., Toller, G.N., Stemwedel, S.W., & Freudenreich, H.T., 1992, *Bull. Amer. Astron. Soc.*, **23**, 1313.

**Anomalous On-orbit Behavior of the NASA Cosmic Background Explorer (COBE)** Dewar, Volz, S.M. & DiPirro, M.J. 1992, *Cryogenics*, **32**, 77.

**The COBE View of the Galaxy**, Wright, E.L., September 16–18, 1992, in Proc. *Surveys in Astronomy*, Caltech, Pasadena, CA.

## G.9 1993

**DIRBE Observations of Galactic Stellar Populations and Extinction**, Arendt, R.G., Hauser, M.G., Boggess, N., Dwek, E., Kelsall, T., Moseley, S.H., Murdock, T.L.,

Silverberg, R.F., Berriman, G.B., Weiland, J.L., Odegard, N., & Sodroski, T.J. 1993, in *Back to the Galaxy*, ed. S.S. Holt & F. Verter (New York: AIP), AIP Conf. Proc., **278**, 222.

**Polarimetry with the Diffuse Infrared Background Experiment Aboard COBE**, Berriman, G.B., Hauser, M.G., Boggess, N.W., Kelsall, T., Moseley, S.H., Silverberg, R.F., & Murdock, T.L. 1993, in *Back to the Galaxy*, ed. S.S. Holt & F. Verter (New York: AIP), AIP Conf. Proc., **278**, 214.

**DIRBE Evidence for a Warp in the Galaxy**, Freudenreich, H.T., Sodroski, T.J., Berriman, G.B., Dwek, E., Franz, B.A., Hauser, M.G., Kelsall, T., Moseley, S.H., Odegard, N.P., Silverberg, R.F., Toller, G.N., & Weiland, J.L. 1993, in *Back to the Galaxy*, ed. S.S. Holt & F. Verter (New York: AIP), AIP Conf. Proc., **278**, 485.

**COBE/DIRBE Observations of Infrared Emission from Stars and Dust**, Hauser, M.G. 1993, in *Back to the Galaxy*, ed. S.S. Holt & F. Verter (New York: AIP), AIP Conf. Proc., **278**, 201.

**Investigation of the Zodiacal Light from 1  $\mu\text{m}$  to 240  $\mu\text{m}$  Using COBE DIRBE Data**, Kelsall, T., Hauser, M.G., Berriman, G.B., Boggess, N.W., Moseley, S.H., Murdock, T.L., Silverberg, R.F., Spiesman, W.J., & Weiland, J.L., 1993, Proc. SPIE Conf. 2019, *Infrared Spaceborne Remote Sensing*, ed. M.S. Scholl (Bellingham: SPIE), 190.

**The Cosmic Background Explorer (COBE) Mission**, Mather, J.C., 1993, in Proc. SPIE Conf. 2019, *Infrared Spaceborne Remote Sensing*, ed. M.S. Scholl (Bellingham: SPIE).

**Scientific Results from COBE**, Mather, J.C., Hauser, M.G., Bennett, C.L., Boggess, N.W., Cheng, E.S., Kelsall, T., Moseley, S.H., Jr., Murdock, T.L., Shafer, R.A., Silverberg, R.F., Smoot, G.F., Weiss, R., & Wright, E.L., January 25–27, 1993, in Proc. *Unified Symmetry in the Small and in the Large*, Miami, FL.

**Design of the Diffuse Infrared Background Experiment (DIRBE) on COBE**, Silverberg, R.F., Hauser, M.G., Boggess, N.W., Kelsall, T., Moseley, S.H., & Murdock, T.L., 1993, Proc. SPIE Conf. 2019, *Infrared Spaceborne Remote Sensing*, ed. M.S. Scholl (Bellingham: SPIE), 180.

**Observations of the Large-scale Infrared Emission from the Galactic Plane Region by the Diffuse Infrared Background Experiment**, Sodroski, T.J., Arendt, R.G., Hauser, M.G., Boggess, N., Dwek, E., Kelsall, T., Moseley, S.H., Murdock, T.L., Silverberg, R.F., Berriman, G.B., Franz, B.A., Freudenreich, H.T., Lisse, C.M., Mitra, M., Odegard, N.P., Spiesman, W.J., Stemwedel, S.W., Toller, G.N., & Weiland, J.L., 1993, in Proc. SPIE Conf. 2019, *Infrared Spaceborne Remote Sensing*, ed. M.S. Scholl (Bellingham: SPIE).

**Large-scale Physical Conditions in the Interstellar Medium from DIRBE Observations**, Sodroski, T.J., Hauser, M.G., Dwek, E., Kelsall, T., Moseley, S.H., Silverberg, R.F., Boggess, N., Odegard, N., Weiland, J.L., & Franz, B. 1993, in *Back to the Galaxy*, ed. S.S. Holt & F. Verter (New York: AIP), AIP Conf. Proc., **278**, 218.

**DIRBE Observations of the Galactic Bulge**, Weiland, J.L., Hauser, M.G., Kelsall, T., Dwek, E., Moseley, S.H., Silverberg, R.F., Mitra, M., Odegard, N.P., Spiesman, W.J., Sodroski, T.J., Stemwedel, S.W., Freudenreich, H.T., & Lisse, C.M. 1993, in *Back to the Galaxy*, ed. S.S. Holt & F. Verter (New York: AIP), AIP Conf. Proc., **278**, 137.

**The COBE Experience**, Wright, E.L., 1993, in Proc. SPIE Conf. 2019, *Infrared Spaceborne Remote Sensing*, ed. M.S. Scholl (Bellingham: SPIE).

## G.10 1994

**COBE DIRBE Observations of Galactic Reddening and Stellar Populations**, Arendt, R.G., Berriman, G.B., Boggess, N., Dwek, E., Hauser, M.G., Kelsall, T., Moseley, S.H., Murdock, T.L., Odegard, N., Silverberg, R.F., Sodroski, T.J., & Weiland, J.L. 1994, *ApJ*, **425**, L85.

**COBE DIRBE Near-infrared Polarimetry of the Zodiacal Light: Initial Results**, Berriman, G.B., Boggess, N.W., Hauser, M.G., Kelsall, T., Lisse, C.M., Moseley, S.H., Reach, W.T., & Silverberg, R.F. 1994, *ApJ*, **431**, L63.

**DIRBE Evidence for a Warp in the Interstellar Dust Layer and Stellar Disk of the Galaxy**, Freudenreich, H.T., Berriman, G.B., Dwek, E., Hauser, M.G., Kelsall, T., Moseley, S.H., Silverberg, R.F., Sodroski, T.J., Toller, G.N., & Weiland, J.L. 1994, *ApJ*, **429**, L69.

**Infrared Observations of Comet Austin (1990V) by COBE Diffuse Infrared Background Experiment**, Lisse, C.M., Freudenreich, H.T., Hauser, M.G., Kelsall, T., Moseley, S.H., Reach, W.T., & Silverberg, R.F. 1994, *ApJ*, **432**, L71.

**Measurement of the Cosmic Microwave Background Spectrum by the COBE FIRAS Instrument**, Mather, J.C., Cheng, E.S., Cottingham, D.A., Eplee, R.E., Jr., Fixsen, D.J., Hewagama, T., Isaacman, R.B., Jensen, K.A., Meyer, S.S., Noerdlinger, P.D., Read, S.M., Rosen, L.P., Shafer, R.A., Wright, E.L., Bennett, C.L., Boggess, N.W., Hauser, M.G., Kelsall, T., Moseley, S.H., Jr., Silverberg, R.F., Smoot, G.F., Weiss, R., Wilkinson, D.T. 1994, *ApJ*, **420**, 439.

**Large-scale Characteristics of Interstellar Dust from COBE DIRBE Observations**, Sodroski, T.J., Bennett, C., Boggess, N., Dwek, E., Franz, B.A., Hauser, M.G., Kelsall, T., Moseley, S.H., Odegard, N., Silverberg, R.F., & Weiland, J.L. 1994, *ApJ*, **428**, 638.

**COBE DIRBE Observations of the Galactic Bulge**, Weiland, J.L., Arendt, R.G., Berriman, G.B., Dwek, E., Freudenreich, H.T., Hauser, M.G., Kelsall, T., Lisse, C.M., Mitra, M., Moseley, S.H., Odegard, N.P., Silverberg, R.F., Sodroski, T.J., Spiesman, W.J., & Stemwedel, S.W. 1994, *ApJ*, **425**, L81.

**Interpretation of the COBE FIRAS CMBR Spectrum**, Wright, E.L., Mather, J.C., Fixsen, D.J., Kogut, A., Shafer, R.A., Bennett, C.L., Boggess, N.W., Cheng, E.S., Silverberg, R.F., Smoot, G.F., Weiss, R. 1994, *ApJ*, **420**, 450.

## G.11 1995

**Morphology, Near-infrared Luminosity and the Mass of the Galactic Bulge from COBE DIRBE Observations**, Dwek, E., Arendt, R.G., Lisse, C.M., Sodroski, T.J., Weiland, J., Hauser, M.G., Kelsall, T., Moseley, S.H., & Silverberg, R.F. 1995, *ApJ*, **445**, 716.

**Infrared Background (Observations)**, Hauser, M.G. 1995, in *Extragalactic Background Radiation*, Space Telescope Science Institute Symp. Ser. 7, ed. D. Calzetti, M. Livio, & P. Madau (Cambridge: Cambridge Univ. Press), 135.

**The COBE DIRBE Search for the Cosmic Infrared Background**, Hauser, M.G. 1995, to be published in Proceedings of IAU Symp. 168, *Examining the Big Bang and Diffuse Background Radiations*, August 1995, The Hague.

**Observational Confirmation of a Circumsolar Dust Ring by the COBE Satellite**, Reach, W.T., Franz, B.A., Weiland, J.L., Hauser, M.G., Kelsall, T., Wright, E.L., Rawley, G., Stemwedel, S.W., & Spiesman, W.J. 1995, *Nature*, **374**, 521.

**The Ratio of  $H_2$  Column Density to  $^{12}\text{CO}$  Intensity in the Vicinity of the Galactic Center**, Sodroski, T.J., Odegard, N., Dwek, E., Hauser, M.G., Franz, B.A., Freedman, I., Wall, W.F., Berriman, G.B., Odenwald, S.F., Bennett, C.L., Reach, W.T., & Weiland, J.L. 1995, *ApJ*, **452**, 262.

**Near and Far Infrared Observations of Interplanetary Dust Bands from the COBE Diffuse Infrared Background Experiment**, Spiesman, W.J., Hauser, M.G., Kelsall, T., Lisse, C.M., Moseley, S.H., Reach, W.T., Silverberg, R.F., Stemwedel, S.W., & Weiland, J.L. 1995, *ApJ*, **442**, 662.

**COBE Guest Investigator Support Software User's Guide**, version 2.2, 1995 developed at the Cosmology Data Analysis Center on behalf of the COBE Science Working Group, ed. G. Rawley, available on line at [http://www.gsfc.nasa.gov/astro/cobe/cgis\\_docs.html](http://www.gsfc.nasa.gov/astro/cobe/cgis_docs.html)

**COBE Guest Investigator Support Software Catalog**, version 1.0, 1995 developed at the Cosmology Data Analysis Center on behalf of the COBE Science Working Group, ed. G. Rawley, available on line at [http://www.gsfc.nasa.gov/astro/cobe/cgis\\_docs.html](http://www.gsfc.nasa.gov/astro/cobe/cgis_docs.html)

## G.12 1996

**Subtraction of Galactic Stellar Emission from COBE/DIRBE Observations**, Arendt, R.G., Freudenreich, H.T., & Dwek, E. 1996, in *Unveiling the Cosmic Infrared Background*, ed. E. Dwek (New York: AIP), AIP Conf. Proc., **348**, 305.

**The Near-Infrared Scattering Properties of Interstellar Dust**, Berriman, G.B., Weiland, J.L., Lisse, C.M., Reach, W.T., Hauser, M.G., & Kelsall, T. 1996, in *Unveiling the Cosmic Infrared Background*, ed. E. Dwek (New York: AIP), AIP Conf. Proc., **348**, 292.

**The Effects of Dust and Metallicity Evolution on the Cosmic Infrared Background**, Dwek, E., & Varosi, F. 1996, in *Unveiling the Cosmic Infrared Background*, ed. E. Dwek (New York: AIP), AIP Conf. Proc., **348**, 237.

**Inversion of the DIRBE Photometry to Derive the Three-dimensional Distribution of the Interplanetary Dust**, Franz, B.A., Reach, W.T., Kelsall, T., & Weiland, J.L. 1996, in *Unveiling the Cosmic Infrared Background*, ed. E. Dwek (New York: AIP), AIP Conf. Proc., **348**, 296.

**The Shape and Color of the Galactic Disk**, Freudenreich, H.T. 1996, *ApJ*, **468**, 663.

**Searching for the Cosmic Infrared Background**, Hauser, M.G. 1996, in *Unveiling the Cosmic Infrared Background*, ed. E. Dwek (New York: AIP), AIP Conf. Proc., **348**, 11.

**Clustering of the Diffuse Infrared Light from the COBE DIRBE Maps I. C(0) and Limits on the Near-IR Background**, Kashlinsky, A., Mather, J.C., & Hauser, M.G. 1996, *ApJ*, **470**, 681.

**Clustering of DIRBE Light and IR Background**, Kashlinsky, A., Mather, J.C., Odenwald, S., & Hauser, M.G. 1996, in *Unveiling the Cosmic Infrared Background*, ed. E. Dwek (New York: AIP), AIP Conf. Proc., **348**, 115.

**An Overview of the DIRBE and FIRAS Data Products**, Leisawitz, D. 1996, in *Unveiling the Cosmic Infrared Background*, ed. E. Dwek (New York: AIP), AIP Conf. Proc., **348**, 287.

**EGBIRT and DESIRE: Measuring the CIBR at 3 AU**, Mather, J.C., & Beichman, C. 1996, in *Unveiling the Cosmic Infrared Background*, ed. E. Dwek (New York: AIP), AIP Conf. Proc., **348**, 271.

**Infrared Point Source Photometry With DIRBE: Instrument Gain Stabilization and Variable Star Monitoring**, Mitchell, K.J., Berriman, G.B., Kelsall, T., Richardson, D., Skard, J.A., & Stemwedel, S.W. 1996, in *Unveiling the Cosmic Infrared Background*, ed. E. Dwek (New York: AIP), AIP Conf. Proc., **348**, 301.

**A DIRBE 12 – 240 micron Survey for External Galaxies**, Odenwald, S., Newmark, J., & Smoot, G. 1996, in *Unveiling the Cosmic Infrared Background*, ed. E. Dwek (New York: AIP), AIP Conf. Proc., **348**, 318.

**DIRBE Observations of the Zodiacal Light**, Reach, W.T., Franz, B.A., Kelsall, T., & Weiland, J.L. 1996, in *Unveiling the Cosmic Infrared Background*, ed. E. Dwek (New York: AIP), AIP Conf. Proc., **348**, 37.

**A Three-dimensional Decomposition of the Infrared Emission from Dust in the Milky Way**, Sodroski, T.J., Arendt, R.G., Odegard, N., Weiland, J.L., Dwek, E., Hauser, M.G., & Kelsall, T. 1996, in *Unveiling the Cosmic Infrared Background*, ed. E. Dwek (New York: AIP), AIP Conf. Proc., **348**, 309.

**Near Infrared Background Correlations**, Veeraraghavan, S. 1996, in *Unveiling the Cosmic Infrared Background*, ed. E. Dwek (New York: AIP), AIP Conf. Proc., **348**, 122.

**COBE/DIRBE Observations of the Orion Constellation from the Near- to Far-infrared**, Wall, W.F., Reach, W.T., Hauser, M.G., Arendt, R.G., Weiland, J.L., Berriman, G.B., Bennett, C.L., Dwek, E., Leisawitz, D., Mitra, P.M., Odenwald, S.F., Sodroski, T.J., & Toller, G.N. 1996, *ApJ*, **456**, 566.

**The Interstellar Dust Contribution to the Diffuse Infrared Sky Brightness**, Weiland, J.L., Arendt, R.G., & Sodroski, T.J. 1996, in *Unveiling the Cosmic Infrared Background*, ed. E. Dwek (New York: AIP), AIP Conf. Proc., **348**, 74.

## G.13 1997

**Detection and Characterization of Cold Interstellar Dust and Polycyclic Aromatic Hydrocarbon Emission from COBE Observations**, Dwek, E., Arendt, R.G.,

Fixsen, D.J., Sodroski, T.J., Odegard, N., Weiland, J.L., Reach, W.T., Hauser, M.G., Kelsall, T., Moseley, S.H., Silverberg, R.F., Shafer, R.A., Ballester, J., Bazell, D., & Isaacman, R. 1997, *ApJ*, **475**, 565.